UNIVERSIDADE ESTADUAL DE CAMPINAS

Ruscaia Dias Teixeira

ANÁLISE FILOGENÉTICA DA FAMÍLIA TEIIDAE (SQUAMATA, REPTILIA), A ULTRA-ESTRUTURA DE ESPERMATOZÓIDE E A SUA UTILIDADE FILOGENÉTICA

Este exemplar corresponde à redação final da tese defendida pelo(a) candidato (a) Ruscaia Dias Teixeira

e aprovada pela Comissão Julgadora.

Tese apresentada ao Instituto de Biologia para obtenção do Título de Doutor em Biologia Celular e Estrutural na área de Biologia Celular.

Orientadora: Profa. Dra. Sônia Nair Báo

Co-orientador: Prof. Dr. Guarino Rinaldi Colli

FICHA CATALOGRÁFICA ELABORADA PELA BIBLIOTECA DO INSTITUTO DE BIOLOGIA – UNICAMP

T235a

Teixeira, Ruscaia Dias
Análise filogenética da família *Teiidae* (Squamata, Reptilia), a ultra-estrutura de espematozóide e a sua utilidade filogenética / Ruscaia Dias Teixeira.--
Campinas, SP: [s.n.], 2003.

Orientadora: Sônia Nair Báo
Co-orientador: Guarino Rinaldi Colli
Tese (Doutorado) – Universidade Estadual de Campinas . Instituto de Biologia.

1. Filogenia. 2. Répteis. 3. Evolução. 4. Espermatozóide. I. Bao, Sonia Nair. II. Colli, Guarino Rinaldi. III. Universidade Estadual de Campinas. Instituto de Biologia. IV.Título.

Campinas, 15 de julho de 2003

BANCA EXAMINADORA

Profa.Dra. Sônia Nair Báo (Orientadora)

Assinatura

Profa.Dra. Irani Quagio-Grassiotto

Assinatura

Prof.Dr. André Victor Lucci Freitas

Assinatura

Prof.Dr. Hussam El Dine Zaher

Assinatura

Prof.Dr. Marcos Di Bernardo

Assinatura

Profa.Dra. Mary Anne Heidi Dolder

Assinatura

Profa.Dra. Shirlei Maria Recco Pimentel

Assinatura

Pesquisa realizada junto ao Curso de Biologia Celular e Estrutural, do Instituto de Biologia, da Universidade Estadual de Campinas, Campinas, São Paulo, Brasil, sendo desenvolvido em três instituições:

1. Laboratório de Microscopia Eletrônica do Departamento de Biologia Celular, e Coleção Herpetológica do Departamento de Zoologia, Instituto de Ciências Biológicas da Universidade de Brasília (UnB), Brasília, DF, Brasil, sob orientação da Profa. Dra. Sônia Nair Báo (Depto de Biologia Celular, IB) e co-orientação do Prof. Dr. Guarino Rinaldi Colli (Depto de Zoologia, IB).

2. Department of Zoology and Entomology, University of Queensland, Brisbane, Australia, sob orientação do Dr. David Scheltinga.

3. Section of Amphibians and Reptiles, Carnegie Museum of Natural History, Pittsburgh, Pennsylvania, EUA, sob orientação do Dr. John J. Wiens (Programa Especial de Estágio no Exterior, CAPES).

O trabalho teve patrocínio financeiro das seguintes entidades:

- Conselho Nacional de Desenvolvimento Científico e Tecnológico (CNPq);
- Coordenação de Aperfeiçoamento de Pessoal de nível Superior (CAPES);
- Universidade de Brasília (UnB);
- Universidade Estadual de Campinas (UNICAMP)

Aos meus queridos pais, Wagner e Cida

e à minha irmã, Graziela.

Meus agradecimentos

- À professora Dra. Sônia Nair Báo, pelas suas inegáveis qualidades de orientadora e pesquisadora, e por toda sua amizade;
- Ao professor Dr. Guarino Rinaldi Colli, por ter me fornecido uma sólida base em sistemática filogenética, assim como um excelente exemplo de pesquisador.
- Ao Dr David Scheltinga e ao Dr. Barrie Jamieson, por suas pesquisas terem sido a fonte do tema da minha tese, por terem me fornecido uma grande conhecimento sobre ultra-estrutura de espermatozóide de Squamata, e pela carinhosa recepção durante meu estágio na University of Queensland, em Brisbane, Austrália.
- Ao Dr. John J. Wiens, por ter me dado a oportunidade de realizar parte da minha tese no Carnegie Museum of Natural History, em Pittsburgh, USA.
- Ao Gustavo H. C. Vieira, pela grande e sincera amizade e pelo imensurável apoio nas coletas e análises dos dados, principalmente nos momentos mais estressantes;
- À Líliam Giugliano e Leonora Tavares-Bastos, por terem me cedido as descrições sobre a ultra-estrutura de espermatozóide de *Ameiva ameiva* e *Tupinambis teguixin* e as micrografias de espermatozóide para a coleta dos dados morfométricos;
- Ao Ayrton K. Peres Júnior, pelo enorme apoio nas coletas de animais, análises de dados, concessão de alguns dados merísticos por ele coletados e por todo apoio aferido em todo o período de pós-graduação;

- À Helga C. Wiederhecker, pelas inúmeras horas ensinando-me a utilizar vários tipos de programas, pelas dicas esclarecedoras em relação a minha tese, e por todo apoio aferido em todo o meu período de pós-graduação;
- Ao Daniel O. Mesquita, por me ensinar a conduzir as análises estatísticas, pela ajuda na coleta de dados merísticos e por todo apoio aferido em todo o período de pós-graduação;
- À Fernanda Werneck, pela ajuda nas intermináveis coletas dos dados merísticos;
- Ao Frederico G. França, Adrian A. Garda, Renato G. Faria, Daniel Diniz, Gabriel Costa, pelo enorme apoio nas coletas de *Cnemidophorus* e *Kentropyx* e a Mariana Zatz, pelas inúmeras coletas de *Cercosaura*;
- À minha inesquecível amiga e roommate Ramona Walls por todo o apoio emocional durante minha estadia em sua casa, em Pittsburgh, possibilitando e favorecendo meus estudos nos EUA.
- Ao Patrick Stephens, pelos grandiosos ensinamentos de Sistemática Filogenética, e por toda amizade e apoio emocional durante meu trabalho no Carnegie Museum of Natural History;
- Ao Dr. Vitor Becker por todo companheirismo oferecido no decorrer do meu doutorado sanduíche no Carnegie Museum of Natural History;
- Aos demais professores do Departamento de Biologia Celular da UNICAMP, por transmitirem seus conhecimentos com tanto afinco e carinho.
- A todos meus amigos e familiares de Brasília e de Campinas que direta ou indiretamente me possibilitaram a realização com sucesso desta etapa da minha vida.

SUMÁRIO

RESUMO

Vários estudos têm sido realizados entre os lagartos da família Teiidae, utilizando diversas linhas de evidência morfológicas, sem resolver as relações filogenéticas entre os gêneros dentro das subfamílias Teiinae e Tupinambinae. A utilização de conjuntos de dados morfológicos tradicionais ainda não utilizados (hemipênis, língua e escamas), e dados morfológicos não tradicionais (a ultra-estrutura de espermatozóide) pode dar subsídio para a construção de uma árvore filogenética mais resolvida e provável para o grupo. A proposta do presente trabalho é buscar uma melhor compreensão das relações de parentesco entre os gêneros de teiídeos, avançar os conhecimentos do novo conjunto de dados morfológicos não tradicionais, a ultra-estrutura de espermatozóide, e avaliar a utilidade filogenética desta nova fonte de caracteres no nível genérico. Os estudos comparativos da ultra-estrutura de espermatozóide indicam altos níveis de variabilidade inter e intra-genérica, sugerindo o uso de espécies como táxons terminais, a fim de melhorar as estimativas da filogenia da família. Apesar da filogenia derivada dos conjuntos de dados morfológicos tradicionais e ultra-estrutura de espermatozóide apresentar muitas incongruências com os estudos prévios, ela reflete uma melhor estimativa da história filogenética da família devido ao grande número de caracteres empregados. Comparações do grau de congruência entre as filogenias derivadas pelo conjunto de dados morfológicos tradicionais e a ultra-estrutura de espermatozóide, indicam que a ultra-estrutura de espermatozóide é um bom indicador de filogenia da família Teiidae, apresentando poucas regiões conflitantes e de pouco suporte com a topologia baseada nos conjuntos de dados morfológicos tradicionais.

ABSTRACT

Several studies have attempted to clarify the relationship among the teiid genera, based on several types of morphological data sets. Therefore, the relationships among teiid genera are not completely solved. Increase the number of characters, using new sources of characters, the sperm ultrastructure, and additional traditional morphological characters such as hemipenis, scales, and tongue were included to possibly improve the resolution of Teiidae phylogenetic hypotheses. The proposals of this work are (1) to clarify the phylogenetic relationships of teiids, (2) to expand the knowledge on the new data set, sperm ultrastructure, investigating the level of variability in sperm ultrastructure, in order to reveal intergeneric stability of characters, and (3) to evaluate the usefulness of sperm ultrastructure characters in phylogenetic reconstruction at the generic level. Comparative studies among teiid genera indicate high levels of inter and intra generic levels of variability in sperm ultrastructure characters, suggesting a spliting of genera in species as terminals, in order to give more accurate estimates of phylogeny. Despite the fact that phylogeny derived from the combined data show high levels of incongruence with those of previous studies, it reflects favorably the evolutionary history of the family due to the high number of characters applied (those data sets used in the previous hypotheses, combined with meristic, tongue, hemipenis and sperm ultrastructural data), surely improving the estimates of teiid relationships. Sperm ultrastructure may be a good indicator of phylogeny, producing topologies with major areas in congruence with the traditional morphological phylogeny, having only few incongruent areas weakly supported by the traditional topology.

1 – INTRODUÇÃO

1.1 – IMPORTÂNCIA DAS ANÁLISES FILOGENÉTICAS

A análise filogenética fornece um referencial evolutivo, que permite uma maior eficiência no uso do conhecimento sobre as espécies e seus habitats, facilitando o gerenciamento do conhecimento biológico. Quando todo o conhecimento biológico sobre a vida é organizado ao redor de uma classificação filogenética, o armazenamento dessas informações torna-se mais eficiente e conseqüentemente facilita a recuperação dessas informações pelos cientistas e pela própria sociedade interessada. Enfim, através da análise filogenética, pode-se compreender os processos evolutivos como a especiação, extinção, adaptação e dessa forma inferir a história da evolução (Systematics Agenda 2000, 1994). Compreender os princípios e processos evolutivos é essencial à apreciação da diversidade biológica, já que esta biodiversidade é o resultado direto da evolução (Pough *et al.*, 1993).

Os Squamata representam o segundo maior grupo de tetrápodes viventes, existem duas vezes mais espécies de Squamata do que de mamíferos. Dentro do grupo, os lagartos podem ser distinguidos em termos coloquiais, mas não filogeneticamente, pois as serpentes e as cobras-de-duas-cabeças provavelmente derivaram desse grupo. Dessa forma, os lagartos constituem um grupo parafilético (não inclui todos os descendentes). Todavia, os lagartos, as serpentes e as cobras-de-duas-cabeças são muito distintos em sua ecologia e comportamento (Pough *et al.*, 1993).

Infelizmente, as relações filogenéticas entre as famílias e dentro das próprias famílias de Squamata são muito mal resolvidas (Estes & Pregill, 1988; Russel, 1988;

Schwenk, 1988; Maddison & Maddison, 1992). Como já foi dito anteriormente, um grande exemplo deste problema acontece com a família Teiidae, um dos membros de Squamata (Vanzolini & Valencia, 1965; Presch, 1970; 1974; MacLean, 1974; Rieppel, 1980; Veronese & Krause, 1997; Moro & Abdala, 2000).

1.2 – CONSIDERAÇÕES GERAIS DA FAMÍLIA TEIIDAE

A família Teiidae é um grupo estritamente do Novo Mundo, onde seus gêneros se distribuem do norte dos Estados Unidos até o norte da Patagônia (Cei & Scolaro, 1982; Wright, 1993). O grupo é muito antigo, sendo conhecido desde o Cretáceo superior na América do Norte e Ásia Central (Carrol, 1988).

Boulenger (1885) dividiu a família Teiidae em quatro grupos. O grupo I caracterizava-se pelo contato entre as duas escamas nasais e membros desenvolvidos. Este grupo foi denominado de Macroteiideios por Ruibal (1952) e de acordo com o nome, os lagartos desse grupo possuem comprimentos moderadamente longos. Os grupos II, III e IV ou microteíideos apresentam estas escamas separadas por uma escama fronto-nasal, além da tendência à redução dos membros, embora alguns representantes mantêm os membros normais.

Presch (1970), propôs a saída dos microteíideos com 28 gêneros da família Teiidae, para constituir a família Gymnophthalmidae. A família Teiidae passaria a ser constituída apenas pelos nove gêneros do grupo I (Macroteíideos): *Ameiva*, *Callopistes*, *Cnemidophorus*, *Crocodilurus*, *Dicrodon*, *Dracaena*, *Kentropyx*, *Teius*, e *Tupinambis*.

De acordo com a classificação mais recente feita por Estes *et al.* (1988) a família Teiidae é um membro da linha evolutiva dos lagartos Autarchoglossa e tem como grupo irmão à família Gymnophthalmidae.

As espécies pertencentes ao gênero *Cnemidophorus*, encontradas na América do Norte, passaram a pertencer a um novo gênero da família Teiidae, o gênero *Aspidoscelis* (Reeder *et al.*, 2002). As análises filogenéticas de Reeder et al. (2002), baseadas em aloenzimas, dados moleculares e dados morfológicos, indicam que o gênero *Cnemidophorus* não é monofilético, sendo o grupo *lemniscatus* mais aparentado com os gêneros *Ameiva* e *Kentropyx* do que com os *Cnemidophorus* existentes na América do Norte (grupos *deppii*, *sexlineatus*, and *tigris*). Desta forma, Reeder et al. (2002) sugerem que *Aspidoscelis* seja o gênero que acomode os *Cnemidophorus* da América do Norte, e que o gênero *Cnemidophorus* se aplique apenas aos *Cnemidophorus* do grupo *lemniscatus*.

1.2.1 – DISTRIBUIÇÃO GEOGRÁFICA DOS GÊNEROS DA FAMÍLIA TEIIDAE

Os gêneros da família Teiidae são restritos à América do Sul, com exceção de três gêneros que são encontrados na América do Norte e Central (*Cnemidophorus*, *Ameiva* e *Aspidoscelis*). Todos os gêneros são diurnos, terrestres ou semi-aquáticos, sendo encontrados ocasionalmente em arbustos (Presch, 1970).

Os lagartos do gênero *Ameiva* estão distribuídos nas regiões tropicais e temperadas da América do Sul, no sul do México e nas Antilhas. São insetívoros e terrestres, sendo encontrados em áreas abertas, não muito distantes de arbustos e outros tipos de coberturas vegetais (Rand & Humphrey, 1968).

Os lagartos do gênero *Callopistes* apresentam uma distribuição limitada às regiões secas do oeste dos Andes, do sul do Equador até a região central do Chile, também sendo encontrados no leste peruano. São formas insectívoras ou carnívoras, que vivem em ambientes abertos, em altitudes inferiores a 500 metros (Presch, 1970).

Os lagartos dos gêneros *Aspidoscelis* e *Cnemidophorus* ocorrem em áreas abertas, de vegetação espaçada, de preferência áreas expostas. São insetívoros, e terrestres, podendo ser encontrados em arbustos. O gênero *Aspidoscelis* compreende os grupos *deppii*, *sexlineatus*, and *tigris*, que ocupam regiões desérticas no sudoeste dos Estados Unidos. O gênero *"Cnemidophorus"* compreende o grupo *sexlineatus* que ocupam regiões tropicais e subtropicais da América do Sul e Central (Presch, 1970; Reeder *et al.*, 2002). Possuem espécies unissexual e bissexual (Zug *et al.*, 2001).

Os lagartos do gênero *Crocodilurus* são insetívoros, com distribuição restrita às regiões tropicais Guiano-Amazônicas (Vanzolini & Valencia, 1965). Possuem hábitos aquáticos, apresentando cauda achatada, igual a dos crocodilos, com um par de cristas dorsais, formadas por fileiras de escamas quilhadas. São encontrados em enseadas e áreas alagadas (Presch, 1970). Massary & Hoogmoed (2001) propuseram que o nome *C. amazonicus* (Spix, 1825), a designação mais antiga encontrada na literatura para o táxon formalmente conhecido como *C. lacertinus*, seria o nome mais correto para ser aplicado a este táxon.

As duas espécies do gênero *Dracaena* estão distribuídas de forma restrita na Bacia Amazônica, e no sul do Mato Grosso do Sul, Brasil (Vanzolini & Valencia, 1965; Avila-Pires, 1995). As espécies deste gênero habitam regiões alagadas e alimentam-se de

moluscos encontrados na água, passando a maior parte do tempo em galhos de arbustos (Vanzolini, 1961).

Os lagartos do gênero *Dicrodon* são restritos à costa oeste da América do Sul, encontrado desde o sudoeste do Equador ao Peru. São insetívoros, terrestres e vivem em buracos, nas áreas secas (Presch, 1970).

Os lagartos do gênero *Kentropyx* estão restritos a América do Sul. Estão distribuídos do sul da Venezuela até Tucuman, na Argentina, atingindo altitudes de até 1600m. São insetívoros, e semiterrestres, sendo achados no solo, folhagens caídas e pequenos arbustos. Vivem em florestas, mas podem ser achados em áreas abertas. É um grupo taxonomicamente bem definido, sendo o único gênero de Teiidae a apresentar escamas quilhadas com formato filóides (Magnusson, 1984; Gallagher Jr. *et al.*, 1986). O gênero possui espécies unissexual e bissexual (Zug *et al.*, 2001).

Os lagartos do gênero *Teius* são insetívoros, habitam áreas abertas e apresentam uma distribuição restrita ao sul da América do Sul, ocupando as regiões de clima subtropical e temperado (Presch, 1970). O gênero possui espécies unissexual e bissexual (Zug *et al.*, 2001).

Os lagartos do gênero *Tupinambis* são terrestres e onívoros, sendo os maiores representantes da família Teiidae e do Novo Mundo. Distribuem-se a leste dos Andes até o norte da Patagônia, sendo restritos à América do Sul (Presch, 1970; Cei & Scolaro, 1982; Peters & Orejas-Miranda, 1986).

1.3 – RELAÇÕES FILOGENÉTICAS DA FAMÍLIA TEIIDAE

Diversos trabalhos têm abordado a questão das relações filogenéticas entre os gêneros de Teiidae. Vanzolini & Valencia (1965) examinaram 16 caracteres morfológicos e reconheceram dois grupos dentro da família: um composto de *Cnemidophorus*, *Ameiva*, *Teius*, *Kentropyx* e *Dicrodon* (subfamília Teiinae) e outro composto por *Callopistes*, *Crocodilurus*, *Tupinambis* e *Dracaena* (subfamília Tupinambinae). Além disso, os autores postularam uma grande afinidade entre os pares *Ameiva-Cnemidophorus* e *Tupinambis-Dracaena*. Presh (1974) e Rieppel (1980) reconheceram os mesmos grupos dentro da família Teiidae, porém sem resolver completamente as relações filogenéticas dentro de cada um deles.

Apesar de vários estudos fenéticos e filogenéticos já terem sido feitos com a família Teiidae, utilizando características externas (Vanzolini & Valencia, 1965), cromossomos (Gorman, 1970), dados alimentares e de locomoção (MacLean, 1974), dados osteológicos (Boulenger, 1885; Presch, 1974; Veronese & Krause, 1997), e dados miológicos (Rieppel, 1980; Moro & Abdala, 2000), as relações filogenéticas entre os gêneros dentro das subfamílias Teiinae e Tupinambinae ainda continuam mal resolvidas.

Uma alternativa para melhorar a resolução das reconstruções filogenéticas da família Teiidae é aumentar o máximo possível o número de caracteres utilizados nas análises. Desta forma, uma boa opção é utilizar: (1) conjuntos de dados morfológicos tradicionais ainda não utilizados como, por exemplo, hemipênis, língua e escamas, e (2) conjunto de dados morfológicos não tradicionais, como por exemplo, a ultra-estrutura de espermatozóide.

1.4 – A ULTRA-ESTRUTURA DE ESPERMATOZÓIDE COMO UM NOVO CONJUNTO DE DADOS

O espermatozóide além de possuir uma grande importância no estudo dos mecanismos celulares de células reprodutivas e na própria reprodução, pode ser utilizado como um marcador ou indicador das relações de parentescos entre os organismos, informando as relações evolutivas entre eles e os padrões das mudanças evolutivas (Franzén, 1970). A ultra-estrutura de espermatozóide tem sido estudada em várias famílias de Squamata (Jamieson, 1995; Jamieson *et al.*, 1996; Oliver *et al.*, 1996; Teixeira *et al.*, 1999b, 1999c) e tem fornecido uma fonte de caracteres de valiosa utilidade para as análises filogenéticas, principalmente quando os grupos de caracteres morfológicos tradicionais não são esclarecedores (Teixeira *et al.*, 1999c).

De acordo com Teixeira *et al.* (1999b, 1999c), inferências filogenéticas feitas a partir da ultra-estrutura de espermatozóide, tanto entre os Squamata quanto entre anfisbenas apresentam resultados conflitantes com as hipóteses feitas a partir dos dados morfológicos. Essa heterogeneidade entre os conjuntos de caracteres ocorre, pois os caracteres evoluem em taxas diferentes. Uns evoluem mais rápidos que outros, resultando em histórias filogenéticas diferentes (Miyamoto & Fitch, 1995). Não é possível determinar o melhor conjunto de caracteres, em termos de qual fornece as verdadeiras relações filogenéticas. Entretanto, pode-se dizer que os caracteres da ultra-estrutura de espermatozóide são provavelmente mais cheios de "ruídos", contendo assim pouco sinal filogenético entre as famílias, devido a três deficiências: (1) o número de caracteres ultra-estruturais de espermatozóide é muito pequeno; (2) presença de altos níveis de variabilidade dentro das

famílias de Squamata; (3) a ultra-estrutura de espermatozóide de muitas famílias de Squamata ainda não foi descrita (Teixeira *et al.*, 1999b, 1999c).

Para tornar a ultra-estrutura de espermatozóide, um conjunto de caracteres ideal para a obtenção de inferências filogenéticas com melhores resultados, é necessário avançar os conhecimentos sobre essa nova opção de caracteres através de análises: (1) do grau de variabilidade inter e intragenérico, a fim de revelar o melhor nível taxonômico a ser utilizado nas análises filogenéticas e, (2) da existência de interdependência entre características, no intuito de selecionar apenas caracteres filogeneticamente independentes.

1.4.1 –VARIABILIDADE DA ULTRA-ESTRUTURA DE ESPERMATOZÓIDE

Nas análises filogenéticas, caracteres ideais são aqueles que variam entre as unidades terminais de uma análise, mas não variam dentro delas (Thiele, 1993). Como foi dito acima, as análises conduzidas por Teixeira *et al* (1999b, 1999c), mostraram que os altos níveis de variabilidade dentro dos táxons terminais (nível família nos casos citados), podem ter acarretado deficiências nas inferências filogenéticas derivadas da ultra-estrutura de espermatozóide, produzindo incongruências com os dados tradicionais morfológicos. Por esse motivo, avaliar o grau de variabilidade inter e intragenérico, torna-se de extrema importância, para uma melhor compreensão de qual nível taxonômico seria mais proveitoso para ser utilizado nos táxons terminais das análises filogenéticas. Por outro lado, a ocorrência de altos níveis de variabilidade na ultra-estrutura de espermatozóide entre os táxons terminais, torna esse conjunto de dados, uma fonte proveitosa de caracteres para as análises filogenéticas, já que os caracteres selecionados serão informativos em relação aos táxons terminais.

1.4.2 – INTERDEPENDÊNCIA DE CARACTERES

Os sistematas, que trabalham com conjuntos de dados morfológicos enfrentam um grande desafio na seleção dos caracteres quando se deparam com diferenças nas estruturas morfológicas. A grande dúvida é se uma diferença morfológica implica em um ou mais caracteres. A decisão em interpretar duas variáveis morfológicas como sendo apenas um caracter está baseada em um princípio da Sistemática, em que os caracteres utilizados nas análises filogenéticas precisam ser filogeneticamente independentes. Considerar duas

diferenças morfológicas como sendo dois caracteres nas análises, é postular duas novidades com histórias evolutivas diferentes. Existem custos para decidir que as diferenças morfológicas representam um caracter, assim como existem custos para decidir que as diferenças representam dois ou mais caracteres. O custo de combinar duas características morfológicas em apenas um caracter está no fato de enfraquecer o suporte de uma dada hipótese filogenética. No entanto, se as características morfológicas forem correlacionadas, o custo em tratá-las como dois caracteres distintos, pode dobrar a força de uma evidência evolutiva, inflando o suporte de sua hipótese filogenética por contar o caracter duas vezes. A correlação de características pode ser confirmada pela anatomia e pelo desenvolvimento das estruturas morfológicas. Por exemplo, a anatomia pode informar se duas características são realmente distintas ou não, se pertencerem à mesma região anatômica. O desenvolvimento também fornece informações sobre correlação, através do desenvolvimento integrado (alométrico ou isométrico) entre as duas características. No desenvolvimento alométrico, o crescimento das estruturas não é interdependente, enquanto no desenvolvimento isométrico, as estruturas crescem de forma coordenada, indicando interdependência (Zelditch *et al.*, 2000). Estruturas anatômicas interdependentes devem ser tratadas como um caracter, ao invés de serem tratadas como dois caracteres correlacionados.

No caso de novos caracteres morfológicos tradicionais ainda não utilizados em análises filogenéticas, como por exemplo, hemipênis, língua e escamas de teiídeos e a ultra-estrutura de espermatozóide, análises sobre interdependência das características é de extrema importância para a seleção de caracteres filogeneticamente independentes.

1.5 – CODIFICAÇÃO DE DADOS QUANTITATIVOS NAS ANÁLISES FILOGENÉTICAS

A maioria dos caracteres morfológicos apresenta variações quantitativas nas características, como, por exemplo, medidas de diferentes tamanhos, formatos ou contagens seriadas de estruturas homólogas, tendo os sistematas a opção de codificá-los quantitativamente ou qualitativamente (Thiele, 1993). Existem sistematas que manipulam os dados quantitativos sem codificá-los (Huey & Bennett, 1987; Swofford & Berlocher, 1987), gerando grandes dificuldades nas análises da evolução dos caracteres. Há também, sistematas que excluem os caracteres quantitativos devido à variação contínua ser teoricamente inadequada para as reconstruções filogenéticas (Pimentel & Riggins, 1987), ou devido à redução da precisão das análises filogenéticas pelo uso de tais caracteres (Campbell, 1986). Na maior parte das vezes, os autores rejeitam os caracteres quantitativos pela dificuldade em designar os estados de caracter, principalmente quando há variação contínua nos caracteres entre os táxons (Poe & Wiens, 2000). No entanto, os dados quantitativos são geralmente codificados como caracteres discretos de forma qualitativa ou quantitativa, em prol de facilitar comparações entre as variáveis quantitativas e qualitativas nos cladogramas (Kitching *et al.*, 1998).

Geralmente, existe muita confusão com a terminologia de diferentes tipos de caracteres morfológicos. Quatro termos indicam como uma característica é descrita: qualitativos, quantitativos, contínuos e discretos. De acordo com Thiele (1993), os caracteres quantitativos significam apenas as características descritas por escalas numéricas, isto é, por contagem (caracteres merísticos) ou medida (caracteres

morfométricos). Já, os caracteres qualitativos são apenas as características descritas por palavras. Os termos discretos e contínuos referem-se às propriedades matemáticas dos intervalos de valores numéricos utilizados para medir um atributo (Kitching *et al.*, 1998). Os caracteres contínuos são um subgrupo dos caracteres quantitativos, sendo aqueles descritos por números reais infinitamente divisíveis. Exemplos de caracteres contínuos: medida de um caracter morfométrico em um indivíduo, ou a média de valores de uma variável quantitativa (caracteres merísticos). Os caracteres discretos são valores estanques representados em intervalos independentes, ou seja, aqueles que estão limitados a um subconjunto de todos valores possíveis. Eles referem-se aos estados de caracter (0, 1), ou aos valores brutos de caracteres merísticos (20 vértebras, 25 dentes maxilares) (Wiens, 2001).

A codificação das variações quantitativas de forma qualitativa gera três grandes problemas muito comuns nas análises filogenéticas baseadas nos caracteres morfológicos: definições vagas dos caracteres e seus respectivos estados de caracteres, delimitações arbitrárias dos estados de caracteres, e ordenação dos estados de caracteres (Poe & Wiens, 2000; Wiens, 2001). Estes problemas são descritos a seguir:

I) A definição dos caracteres e a descrição dos estados de caracteres são extremamente vagas. Estados de caracteres são comumente descritos simplesmente como estreito X largo, pequeno X grande, ou curto X longo. A descrição dos estados de caracteres em pequeno e grande é algo subjetivo e não esclarece o que é uma estrutura pequena ou grande, sabendo que a variação pode ser contínua.

II) A delimitação dos estados de caracter torna-se arbitrária, quando valores arbitrários são utilizados como valores de corte para delimitar intervalos de valores, e conseqüentemente,

inferir estados de caracter para cada intervalo de valores (por exemplo, estado 0 = 1-3 escamas, estado 1 = 4-6 escamas, estado 0 = 20 - 60 cm, estado 1 = 70 – 110 cm). Neste caso, o uso de valores arbitrários na delimitação de intervalos de valores leva a três outros problemas pouco notados pelos sistematas. Primeiro, as variações dentro de cada intervalo de valores são ignoradas. Por exemplo, dado um caracter com estado 0 representando 11-14 vértebras e o estado 1 representando 15-20 vértebras, dois táxons com 11 e 14 vértebras seriam codificados como idênticos. Segundo, as diferenças dentro de cada intervalo podem ser maiores que entre os intervalos. A transformação de 11 para 14 vértebras é ignorada, mas a mudança de 14 para 15 recebe o peso máximo. Terceiro, o uso de valores de corte para criar intervalos de valores pode não indicar as diferenças das mudanças entre os estados de caracteres. Por exemplo, se um caracter é codificado com três estados (estado 0 = médias entre 0-2, estado 1 = médias entre 3-4, estado 2 = médias entre 11-15), uma análise que não dá pesos aos caracteres não reflete o grau de similaridade entre os estados 0 e 1 em relação ao estado 2.

III) A ordenação de estados de caracteres é outro grande problema. Para muitos caracteres que apresentam variações quantitativas, os sistematas geralmente assumem que as características similares, mas não idênticas entre os táxons podem ser agrupadas no mesmo estado de caracter.

De acordo com Wiens (2001), esses três problemas encontrados nas análises dos caracteres (definição dos estados dos caracteres, delimitação desses estados, e ordenação) podem ser potencialmente resolvidos, quando as características com natureza quantitativa são tratadas como variáveis quantitativas contínuas.

Geralmente, os métodos que codificam os caracteres quantitativamente podem ser descritos como métodos "gap-coding", que de forma resumida criam intervalos para codificação. Existem diversas variações: "simple gap-coding" (Mickevich & Johnson, 1976), "segment coding" (Colless, 1980), "divergence coding" (Thorpe, 1984), "generalized gap-coding" (Archie, 1985), "gap-weighting" (Thiele, 1993) e o "step matrix gap-weighting" (Wiens, 2001).

O método "step matrix gap-weighting" é uma modificação do método "gap-weighting" criado por Thiele (1993). No método "gap-weighting", as variáveis contínuas são tratadas quantitativamente, dando grandes pesos para grandes diferenças que ocorrem entre as médias dos valores das características dos táxons, e pesos pequenos para pequenas diferenças, através da seguinte equação:

$$Xs = (x - min/max - min)\ n$$

Onde x é a média do valor, Xs é o valor do dado padronizado e n é o máximo de estados ordenados permitido pelo programa de computador (32 para PAUP).

O método "step matrix gap-weighting" diferencia-se do "gap-weighting" atribuindo um estado de caracter para cada média com valor único, e custos para as transformações entre os estados de caracter, calculados por uma matriz de passos, baseados na diferença das médias dos valores entre cada par de táxons. O custo máximo entre os estados na matriz de passos é de 999 no MacClade e 1000 no PAUP. Para calcular os custos, dados padrões são calculados a partir de cada média, através da seguinte equação:

$$Xs = (x - min/max - min)\ 999$$

O custo das transformações entre cada estado de caracter é simplesmente a diferença entre os dados padrões (scores). Este método não é limitado quanto ao número de estados de caracteres como o "gap-weighting".

1.6 – COMBINAÇÃO DE DIFERENTES CONJUNTOS DE DADOS NAS ANÁLISES FILOGENÉTICAS

Existe um grande debate em sistemática se conjuntos de dados diferentes devem ser combinados ou analisados separadamente (de Queiroz *et al.*, 1995; Miyamoto & Fitch, 1995; Huelsenbeck *et al.*, 1996). Um fator que contribui imensamente para esse debate é o fato dos diferentes conjuntos de dados apresentarem topologias filogenéticas diferentes (Doyle, 1992). A possibilidade dos diferentes conjuntos de dados possuírem histórias filogenéticas diferentes tem sido um forte argumento contra combinação de tais conjuntos de dados nas análises filogenéticas (Bull *et al.*, 1993; de Queiroz, 1993). Por outro lado, o fato de conjuntos de dados diferentes apresentarem uma história filogenética em comum é uma importante suposição para análises combinadas (de Queiroz *et al.*, 1995; Miyamoto & Fitch, 1995). Alguns sistematas (i.e. de Queiroz, 1993) acusam a ocorrência de histórias evolutivas diferentes entre os conjuntos de dados, tentando justificar as incongruências encontradas entre as topologias, e acabam excluindo muitos táxons com a finalidade de esclarecer as áreas de conflito. Para Wiens (1998a), se as análises tiverem um grande número de táxons e caracteres, e o conflito entre as topologias envolver apenas alguns táxons (histórias filogenéticas parcialmente diferentes), a combinação dos conjuntos de dados com diferentes histórias filogenéticas não é um ato tão irracional como parece. Por um lado, parte da árvore combinada pode ficar mal conduzida devido à incongruência entre

as histórias filogenéticas. Por outro, a precisão das estimativas dos dados combinados pode aumentar consideravelmente nas áreas não afetadas pelas incongruências, graças ao grande número de caracteres utilizados. Devido a esta idéia, Wiens (1998a) propôs uma metodologia simples para lidar com conjuntos de dados com histórias filogenéticas diferentes. A metodologia consiste em (1) conduzir análises dos conjuntos de dados separadamente para maximizar a detecção de histórias diferentes; (2) combinar e analisar os diferentes conjuntos de dados, considerando a árvore combinada como a melhor estimativa, e (3) comparar as árvores separadas, considerando questionável as partes conflitantes fortemente suportadas. Esta abordagem baseia-se no argumento de que conflito entre clados fortemente suportados das árvores baseadas nos conjuntos de dados separados é um indicativo de histórias filogenéticas diferentes, enquanto que conflitos entre clados pouco suportados podem ser simplesmente erros não explicados ou aleatórios (Bull *et al.*, 1993; de Queiroz, 1993).

Quatro recomendações podem ser encontradas na literatura para lidar com conjuntos de dados que apresentam histórias filogenéticas diferentes: (1) nunca combiná-los (Miyamoto & Fitch, 1995), (2) sempre combiná-los (Kluge & Wolf, 1993; Chippindale & Wiens, 1994), (3) combiná-los, se não forem significativamente heterogêneos (Bull *et al.*, 1993; de Queiroz, 1993), e por fim (4) combina-los, dando atenção às diferenças na história filogenética (de Queiroz *et al.*, 1995; Wiens, 1998a).

Dada uma situação no qual há áreas incongruentes detectadas entre as topologias derivadas de diferentes conjuntos de dados, as histórias filogenéticas são parcialmente divergentes. Neste caso, os métodos que nunca combinam ou sempre combinam não são muito satisfatórios. Estudos empíricos (Wiens, 1998a) mostram que se os conjuntos de

dados não forem combinados, a precisão da análise diminui nas partes em que não houve conflito entre as histórias, devido ao reduzido número de caracteres. Se os dados forem sempre combinados, a análise vai ficar mal conduzida nas regiões de conflito. Se os conjuntos de dados forem considerados combináveis pelos testes de heterogeneidade, a análise combinada pode ficar mal conduzida nas áreas de conflito, e se não forem combináveis, a precisão vai ser reduzida nas partes com mesma história filogenética. Logo, combinar os conjuntos de dados de acordo com Wiens (1998a), considerando questionável as áreas bem suportadas em conflitos, não aumenta a precisão das áreas em conflito, mas melhora a precisão das regiões da árvore com a mesma história.

1.7 – OBJETIVOS

O presente trabalho tem três propostas: (1) buscar uma melhor compreensão das relações de parentesco entre os gêneros de teiídeos, utilizando conjuntos de dados morfológicos tradicionais e não tradicionais como a ultra-estrutura de espermatozóide; (2) avançar os conhecimentos sobre o novo conjunto de dados morfológicos não tradicionais, a ultra-estrutura de espermatozóide, e (3) avaliar a utilidade filogenética da ultra-estrutura de espermatozóide no nível de gêneros.

Assim sendo, o trabalho consiste de quatro etapas:

Etapa I: Estudo ultra-estrutural de espermatozóide da família Teiidae;

Etapa II: Coleta de novos dados morfológicos tradicionais (hemipênis, escamas e língua) ainda não utilizados;

Etapa III: Análises filogenéticas;

Etapa IV: Avaliação da utilidade filogenética da ultra-estrutura de espermatozóide.

Os objetivos propostos para cada etapa do trabalho são:

ETAPA I – ESTUDO ULTRA-ESTRUTURAL DE ESPERMATOZÓIDE

1. Descrever, através de microscopia eletrônica de transmissão, a ultra-estrutura de espermatozóide de representantes de cada gênero da família Teiidae: *Ameiva ameiva* (gênero *Ameiva*), *Aspidoscelis gularis gularis* (gênero *Aspidoscelis*), *Callopistes flavipunctatus* (gênero *Callopistes*), *Cnemidophorus ocellifer* (gênero *Cnemidophorus*), *Crocodilurus amazonicus* (gênero *Crocodilurus*), *Dicrodon guttulatum* (gênero *Dicrodon*), *Dracaena guianensis* (gênero *Dracaena*), *Kentropyx altamazonica* (gênero *Kentropyx*), *Teius oculatus* (gênero *Teius*), *Tupinambis teguixin*, *T. meriane*, *T. quadrilineatus*, e *T. duseni* (gênero *Tupinambis*).
2. Descrever a ultra-estrutura de espermatozóide de um representante da família Gymnophthalmidae, Cercosaura ocellata (gênero *Cercosaura*), através de microscopia eletrônica de transmissão, para servir como grupo externo nas análises filogenéticas;
3. Investigar o grau de variabilidade dos caracteres da ultra-estrutura de espermatozóide entre e dentro dos gêneros da família Teiidae;
4. Descrever caracteres qualitativos e quantitativos (morfométricos) do conjunto de dados ultra-estruturais de espermatozóide;

ETAPA II – DESCRIÇÃO E COLETA DE NOVOS CARACTERES MORFOLÓGICOS TRADICIONAIS

1. Preparar material de hemipenis dos 10 gêneros da família Teiidae e do gênero *Cercosaura*, e descrever os caracteres desse conjunto de dados morfológicos tradicionais;
2. Descrever a musculatura externa e interna da língua dos 10 gêneros da família Teiidae e do gênero *Cercosaura*, através de microscopia de luz, para a coleta de caracteres desse conjunto de dados morfológicos tradicionais;
3. Coletar dados merísiticos (escamas) dos 10 gêneros da família Teiidae e do gênero *Cercosaura*;
4. Levantamento na literatura dos dados osteológicos, miológicos, e morfológicos externos;

ETAPA III – ANÁLISES FILOGENÉTICAS

1. Conduzir uma análise filogenética dos lagartos da família Teiidae, utilizando como conjunto de caracteres a ultra-estrutura de espermatozóide dos 10 gêneros analisados;
2. Conduzir uma análise filogenética dos lagartos da família Teiidae, utilizando como conjunto de caracteres dados morfológicos tradicionais (escama, osso, musculatura externa e interna da língua, características externas e hemipênis);
3. Comparar as duas filogenias, visando analisar o grau de congruência;
4. Conduzir uma analise filogenética, baseada nos conjuntos de dados combinados, a fim de obter a melhor estimativa da filogenia da família.

ETAPA IV – UTILIDADE FILOGENÉTICA DA ULTRA-ESTRUTURA DE ESPERMATOZÓIDE

1. Comparar a filogenia baseada nos conjuntos de dados combinados com a filogenia baseada na ultra-estrutura de espermatozóide, a fim de verificar: (a) a performance da filogenia adquirida pela ultra-estrutura de espermatozóide e (b) a utilidade deste novo conjunto de dados nas reconstruções filogenéticas no nível taxonômico intergenérico.

A etapa I foi realizada no Laboratório de Microscopia Eletrônica, Departamento de Biologia Celular, IB, Universidade de Brasília, Brasil e no Department of Zoology and Entomology, University of Queensland, Brisbane, Australia. A etapa II foi realizada nas Coleções Herpetológicas do: Departamento de Zoologia, IB, Universidade de Brasília, Brasil; Museo Del Historia Natural San Marco, Lima, Peru; e Museu de História Natural, Santiago, Chile. A etapas III e IV foram realizadas no Carnegie Museum of Natural History, Pittsburgh, Pennsylvania, EUA.

2 – CAPÍTULOS

Com propósitos didáticos, a tese foi divida em dois capítulos. O primeiro capítulo consiste dos estudos ultra-estruturais de espermatozóide da família Teiidae (Etapa I), que resultou em três artigos publicados e um artigo a ser submetido. O segundo capítulo consiste das análises filogenéticas e da avaliação da utilidade filogenética da ultra-estrutura de espermatozóide (Etapas II, III e IV), que resultou um artigo a ser submetido.

2.1 – CAPÍTULO I

ESTUDO ULTRA-ESTRUTURAL DE ESPERMATOZÓIDE DOS LAGARTOS DA FAMÍLIA TEIIDAE

2.1.1 – ARTIGO PUBLICADO 1

GIUGLIANO, Liliam Gimenes; **TEIXEIRA, Ruscaia Dias**; COLLI, Guarino Rinaldi; BÁO, Sônia Nair. Ultrastructure of spermatozoa of the lizard *Ameiva ameiva*, with considerations on polymorphism within the family teiidae (Squamata). Journal of Morphology, EUA, v. 3, p. 264-271, 2002.

Este artigo fez parte do projeto de Iniciação Científica da estudante de Ciências Biológicas, Líliam Giugliano, desenvolvido no Programa Institucional de Bolsas de Iniciação Científica (PIBIC/UnB).

Ultrastructure of Spermatozoa of the Lizard *Ameiva ameiva*, With Considerations on Polymorphism Within the Family Teiidae (Squamata)

L.G. Giugliano,[1] R.D. Teixeira,[1,2] G.R. Colli,[3] and S.N. Báo[1]*

[1]*Departamento de Biologia Celular, Universidade de Brasília, Brasília, DF, Brasil*
[2]*Departamento de Biologia Celular, Universidade Estadual de Campinas, Campinas, SP, Brasil*
[3]*Departamento de Zoologia, Universidade de Brasília, Brasília, DF, Brasil*

ABSTRACT A detailed description of sperm ultrastructure of the lizard *Ameiva ameiva* (Teiidae) is provided. Mature spermatozoa are characterized by: a depressed acrosome at the anterior portion; a unilateral ridge at the anterolateral portion; an acrosome vesicle divided into cortex and medulla; medulla divided into two regions with different electron-densities; paracrystalline subacrosomal material with radial organization in transverse section; a pointed prenuclear perforatorium; a stopper-like perforatorium base plate that appears embedded in the subacrosomal material; the presence of an epinuclear lucent zone surrounded by its own membrane; a large nuclear rostrum; round nuclear shoulders; a nuclear space at the nucleus tip; a bilateral stratified laminar structure; a central dense body within the proximal centriole; a short midpiece; an axonemal midpiece axial component; peripheral fibers 3 and 8 grossly enlarged at the anterior portion of axoneme; columnar mitochondria with linear cristae; solid dense bodies arranged as rings or spirals; a triangular-shaped annulus in transverse section; a fibrous sheath into the midpiece; a thin zone of cytoplasm at the anterior portion of the principal piece; and a slight decrease in diameter of the principal piece immediately after the annulus. Comparisons with *Cnemidophorus sexlineatus* and *Micrablepharus maximiliani* failed to identify unique sperm ultrastructure traits of Teiidae or Teiioidea (Teiidae + Gymnophthalmidae). High levels of polymorphism between *Ameiva* and *Cnemidophorus*, two closely related genera of the family Teiidae, were detected, suggesting that extensive sampling within squamate families is essential if sperm ultrastructure data are to be used in phylogenetic analyses at this taxonomic level. J. Morphol. 253:264–271, 2002.

KEY WORDS: ultrastructure; spermatozoa; *Ameiva ameiva*; Teiidae; polymorphism

The ultrastructure of spermatozoa of squamate reptiles has recently been used as an independent source of characters for phylogenetic analyses (Jamieson, 1995b; Teixeira et al., 1999b,c). On the one hand, these studies have indicated that sperm ultrastructure data convey significant phylogenetic information (Teixeira et al., 1999b). On the other hand, phylogenetic analyses of squamate families based on sperm ultrastructure data have produced large numbers of shortest trees, leading to poorly resolved consensus trees that were incongruent with those produced from "traditional" morphological data, presumably due to high levels of intrafamilial polymorphism (Jamieson, 1995b; Teixeira et al., 1999b,c). Even though polymorphic characters are generally less reliable in inferring phylogenies, they contain significant phylogenetic structure (Wiens, 1995) and their exclusion from analyses may lead to reduced accuracy (Wiens and Servedio, 1997; Wiens, 1998b). Apparently, the best strategy to deal with polymorphic characters is to adequately describe and include frequency information in phylogenetic analysis (Wiens, 1995, 1998b, 1999; Wiens and Servedio, 1997). Further, in phylogenetic studies dealing with relationships of higher taxa, sampling multiple species within each higher taxon can greatly improve the chances of recovering accurate trees (Wiens, 1998a). If genera are the taxonomic units of phylogenetic analysis, between-species polymorphism within a given genus may lead to reduced accuracy in phylogenetic reconstruction. When conducting phylogenetic analyses at the family level, most characters chosen by researchers do not vary within families and polymorphic characters are often underrated. Because polymorphism within families might prove useful for phylogenetic analyses, the use of sperm ultrastructural data to investigate phylogenetic relationships among families of Squamata can greatly benefit from information on char-

Contract grant sponsor: Fundação de Apoio à Pesquisa do Distrito Federal-FAPDF; Contract grant number: 193.052/98; Contract grant sponsors: Programa Especial de Treinamento-PET/BIO, Coordenação de Aperfeiçoamento de Pessoal de Nível Superior-CAPES, Conselho Nacional de Desenvolvimento Científico e Tecnológico-CNPq; Contract grant number: 302343/88-1.

*Correspondence to: Sônia N. Báo, Departamento de Biologia Celular, Universidade de Brasília, 70919-970 Brasília, DF, Brasil. E-mail: snbao@unb.br

Published online 20 June 2002 in
Wiley InterScience (www.interscience.wiley.com)
DOI: 10.1002/jmor.10002

acter variability at the intrafamilial (i.e., generic) level.

Some datasets are clearly better than others for reconstructing phylogenetic relationships at particular levels of evolutionary divergence (Sites and Murphy, 1991; Hsiao et al., 1994; Simon et al., 1994; Soto-Adames et al., 1994; Hillis et al., 1996). Morphological data are used more often to investigate relationships at higher taxonomic levels (e.g., Estes and Pregill, 1988; Nielsen, 1998). For instance, the use of allozyme data has uncovered several cryptic species of neotropical lizards that can hardly be discerned by morphology (Cole et al., 1990, 1993; Cole and Dessauer, 1993). However, generalizations about the taxonomic rank at which a particular dataset is useful are difficult, given the arbitrariness of taxonomic assignments. Sperm ultrastructure data so far have been used to investigate squamate relationships at the family level, but it is still unclear at which level of the taxonomical hierarchy they will be most profitable for phylogenetic analyses.

The lizard family Teiidae is restricted to the New World, ranging from the northern United States to central Argentina and Chile and comprises nine genera (Presch, 1974, 1983). The mature spermatozoon of teiids has been described in detail only for *Cnemidophorus sexlineatus* (Newton and Trauth, 1992). Teixeira et al. (1999b) described the ultrastructure of the mature spermatozoa of *Micrablepharus maximiliani*, a member of the family Gymnophthalmidae, the sister-group of Teiidae (Estes et al., 1988). Herein we provide a detailed description of the ultrastructure of mature spermatozoa of the teiid lizard *Ameiva ameiva*, making comparisons with *C. sexlineatus* and *M. maximiliani*. Given that *Ameiva* is the sister taxon of *Cnemidophorus*, we also attempt to assess the degree of variability in sperm ultrastructure characters within close relatives of the family Teiidae.

MATERIALS AND METHODS

We obtained epididymal mature spermatozoa from an adult specimen of *Ameiva ameiva* L. collected at Minaçu, Goiás State, Brazil (13° 38′ S, 48° 15′ W) in February of 1997. We deposited the specimen at the Coleção Herpetológica da Universidade de Brasília (CHUNB 02120). We killed the specimen with a lethal injection of Tiopental®, removed the epididymides by dissection, placed them in a Petri dish with PBS, pH 7.2, and cut them into small pieces. We fixed epididymal tissue overnight at 4°C in a solution containing 2% glutaraldehyde, 2% paraformaldehyde, and 3% of sucrose in 0.1 M sodium cacodylate buffer pH 7.2. Subsequently, we washed tissues in 0.1 M sodium cacodylate buffer, pH 7.2, with 3% sucrose and postfixed them for 1 h in 1% osmium tetroxide, 0.8% potassium ferricyanide, and 5 mM $CaCl_2$ in sodium cacodylate buffer, pH 7.2. We dehydrated the material in a series of ascending concentrations of acetone (30–100%) and embedded it in Spurr's epoxy resin. We stained ultrathin sections with uranyl acetate and lead citrate and made observations with a Jeol® 100C transmission electron microscope. We made light microscopic observations of spermatozoa from glutaraldehyde-paraformaldehyde fixed smears under Nomarski contrast using a Zeiss® Axiophot microscope.

RESULTS

The spermatozoon of *Ameiva ameiva* is filiform and approximately 68 μm long, consisting of a head (acrosome complex and nucleus), a midpiece, and a tail (principal piece and endpiece) (Figs. 1, 2A). The head is short, approximately 15.4 μm in total length from light microscopy. The midpiece, a thick and short portion in the posterior segment of the head, is approximately 4.6 μm long, from transmission electron microscopy. The tail is approximately 48 μm long from light microscopy.

Acrosome Complex

The acrosome complex, located in the most anterior region of the head, caps the anterior part of the nucleus. The acrosome complex consists of the acrosome vesicle, the subacrosomal cone, and the perforatorium (Fig. 2B). In longitudinal section the acrosome complex is long and appears sharply attenuated in one plane, but flattened and spatulate in the plane at right angles to this (Fig. 2C). The acrosome is circular at its base, develops a unilateral electron-lucent ridge anteriorly, and becomes increasingly depressed in transverse section near the anterior tip (Fig. 2D–H). The acrosome vesicle is divisible into a cortex and medulla at its anterior portion (Fig. 2B,D,J,K). The cortex consists of a thin electron-lucent layer, which appears like a sleeve investment of the anterior extremity of the medulla. The latter consists of an external hollow cone, filled with a moderately electron-dense and uneven material, and an underlying strongly electron-dense structure that ensheathes the anterior end of the subacrosomal cone (Fig. 2J). The perforatorium, which originates from the apical part of the subacrosomal cone, has a pointed tip (Fig. 2B,K). The underlying subacrosomal material shows an uneven aspect in longitudinal section (Fig. 2B,C,J,K,L). However, in cross section this matrix is paracrystalline, with a radial arrangement around the nuclear tip (Fig. 2G). The epinuclear lucent zone, a narrow chamber that sits at the posterior portion of the subacrosomal cone and anterior end of the nucleus, is short, approximately 0.4 μm in diameter, and bounded by a membrane (Fig. 2E,L). The subacrosomal cone material is not closely associated with the inner membrane of the acrosome vesicle at its apical and anterolateral surface, where an electron-lucent layer separates these two caps, forming a unilateral ridge (Fig. 2L). An electron-dense structure, the basal plate, is present within the apical portion of the subacrosomal cone, showing a stopper-like shape (Fig. 2K).

Nucleus

The nucleus is elongated, electron-dense, and appears circular in transversal section (Fig. 2I). The

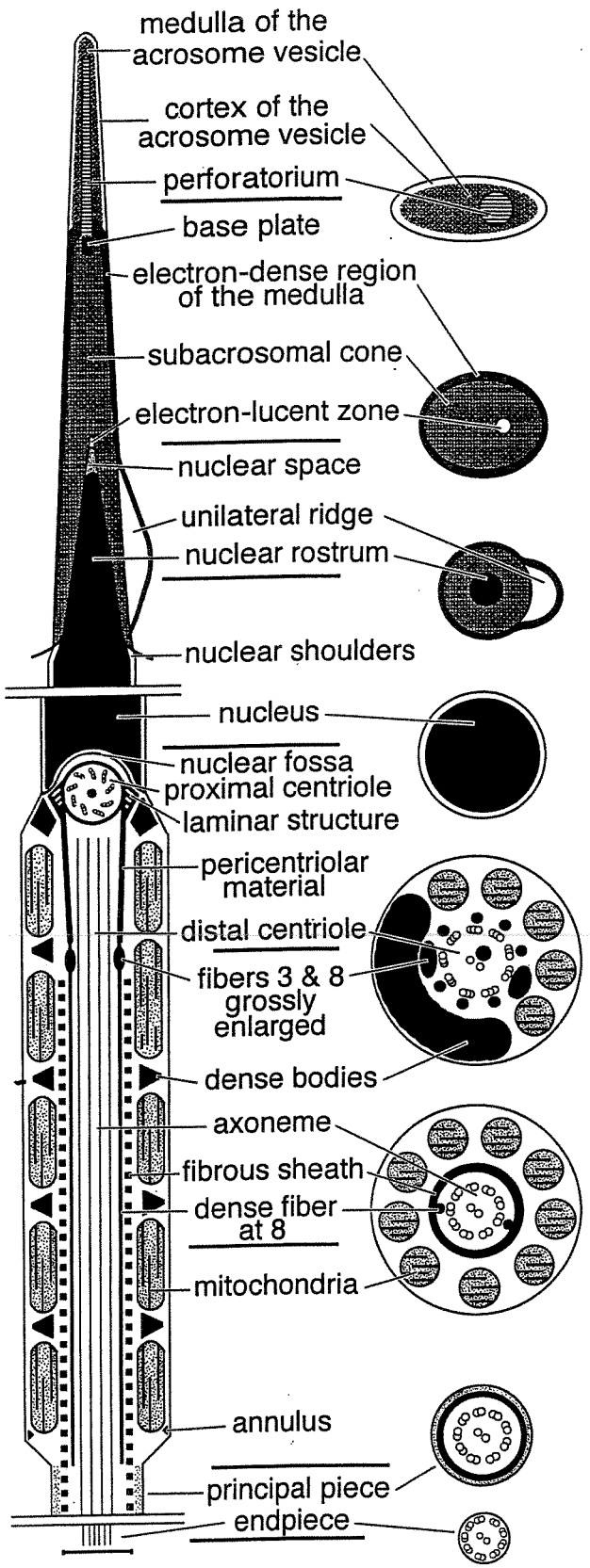

Fig. 1. *Ameiva ameiva*. Diagram of the spermatozoon, and corresponding transverse sections. Scale bar = 0.5 μm.

nuclear contents are strongly electron-dense, with an electron-lucent lacuna interspersed throughout it (Fig. 2I), and separated from the nuclear membrane by an overlying granular material at the anterior region, the nuclear space (Fig. 2L). At its anterior extremity, the nucleus forms a point deeply wedged in the acrosome, the nuclear rostrum, which is approximately 0.75 μm long (Fig. 2L). The nuclear shoulders form a well-defined region that marks the transition from the nuclear rostrum to the cylindrical portion of the nucleus, supporting the posterior end of the acrosome. They appear round and moderately developed (Fig. 2B). At its base, next to the nuclear fossa, the diameter of the nucleus is approximately 0.5 μm (Fig. 3J).

Neck Region

The neck region is the junction between the nucleus and the midpiece. It contains the proximal and distal centrioles, including the first ring of dense bodies. The proximal centriole is surrounded by dense pericentriolar material from the nuclear fossa, conforms in shape to it, and joins the peripheral fibers longitudinally (Fig. 3J). A striated density within or lateral to the pericentriolar material, called the stratified laminar structure, projects on both sides of the proximal centriole, near its anterior limit (Fig. 3J). A central, electron-dense structure lies at the interior of the proximal centriole (Fig. 3J). The distal centriole is in the long axis of the flagellum. It lies perpendicular to the proximal centriole, occupying a small fraction of the midpiece, and does not project into the fibrous sheath. The distal cent-

Fig. 2. Spermatozoa of *Ameiva ameiva*. **A:** Light micrograph of the spermatozoon showing whole spermatozoon with head, midpiece, and flagellum. **B–L:** Transmission electron micrographs of the head (acrosome and nucleus). **B:** Longitudinal section through the acrosome showing the acrosome vesicle with cortex and medulla, the subacrosomal cone, and perforatorium. Note the nuclear shoulders indicated by arrows. **C:** Longitudinal section through the acrosome. Note its flattened apical region. **D–H:** Successive transverse sections through the acrosome. Note that anteriorly, in **D** and **E**, the acrosome appears depressed, while posteriorly, in **F** and **H**, it is more circular. Note an electron-lucent space (*) between the acrosome vesicle and the subacrosomal cone in **E** and **F**. In **G**, the acrosome appears in oblique section showing the radial aspect of the subacrosomal material. **I:** Transverse section through the nucleus showing the lacuna. **J:** Detail of the acrosome vesicle showing the electron density differences in the cortex and medulla. **K:** Longitudinal section of the acrosome showing the stopper-like perforatorium base plate (arrow) embedded into the subacrosomal cone. **L:** Detail of the acrosome complex showing the unilateral ridge, formed by the electron-lucent space (*) between the acrosome vesicle and the subacrosomal cone. Note the epinuclear lucent zone and the nuclear space (arrow) filled with granular material at nucleus tip. a, acrosome vesicle; co, cortex of acrosome vesicle; et, epinuclear lucent zone; f, flagellum; h, head; l, nuclear lacuna; me, medulla of the acrosome vesicle; mp, midpiece; n, nucleus; p, perforatorium; sc, subacrosomal cone. **A**: scale bar = 10 μm. **B,C:** scale bar = 0.5 μm. **D–L:** scale bar = 0.2 μm.

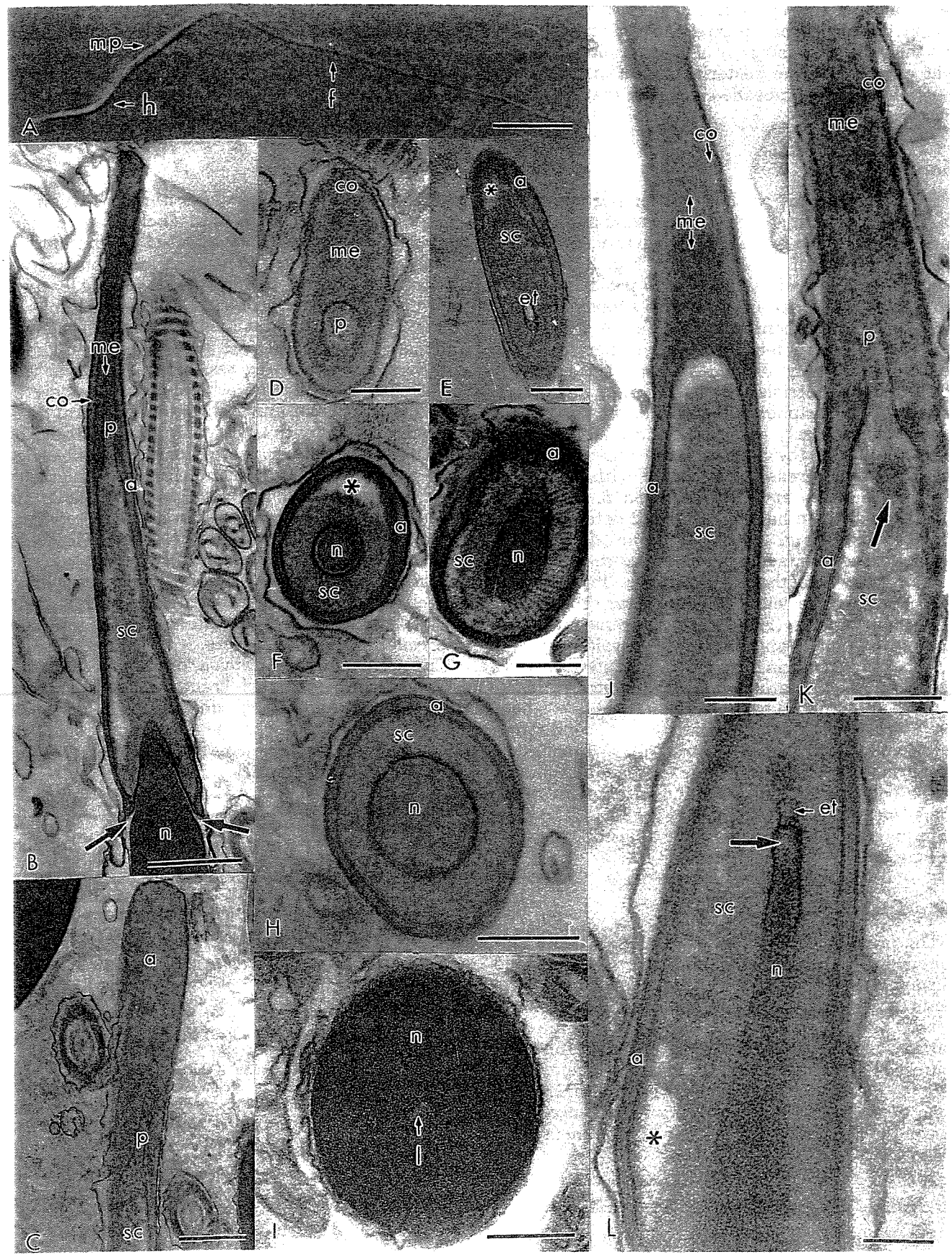
A
mp
h
f
B
me
co
p
a
sc
n
C
a
p
sc
D
co
me
p
E
a
sc
ef
F
a
n
sc
G
a
sc
n
H
a
sc
n
I
n
l
J
co
me
a
sc
K
co
me
p
a
sc
L
ef
sc
n
a
*

Figure 2

riole consists of nine triplets of microtubules, nine peripheral fibers that partially cover the triplets, and the two central singlets of the axoneme (Fig. 3C) that extend into the posterior region of the distal centriole and are embedded in dense material (Fig. 3A).

Midpiece

The midpiece lies at the anterior portion of the flagellum, consisting of the neck region and the axoneme surrounded by the fibrous sheath, mitochondria, and rings of dense bodies (Fig. 3A,K). The midpiece is relatively short and its posterior end is marked by a distinct annulus. The axoneme is posterior to the distal centriole and has a 9+2 microtubule pattern, surrounded by nine peripheral fibers of dense material (Fig. 3D,E). At the posterior portion of the distal centriole, near the beginning of the axoneme, the peripheral fibers adjacent to doublets 3 and 8 are grossly enlarged for a short distance (Fig. 3D). Along the axoneme, the nine peripheral fibers rapidly decrease in diameter, with the exception of the fibers at doublets 3 and 8, which are thicker than the others, double, and detached from their doublets (Fig. 3E). The fibrous sheath surrounds the axoneme and extends into the midpiece, reaching the end of the distal centriole (Fig. 3A). The mitochondria are elongate columnar structures, with linear cristae (Fig. 3A,K). In transversal section, mitochondria appear round or ovoid (Fig. 3C–E). The mitochondria surround the distal centriole and the fibrous sheath as hollow elongate cylinders, separated by irregularly spaced rings of dense bodies. The dense bodies are well-developed solid structures and appear more electron-dense than mitochondria (Fig. 3A,K). These intermitochondrial dense bodies form complete and incomplete rings, sometimes in a spiral fashion (Fig. 3A,D,E,K). The annulus appears like irregularly shaped structures in longitudinal section (Fig. 3A,B,K).

Principal Piece

The principal piece consists of the axoneme surrounded by the fibrous sheath, cytoplasm, and plasma membrane. In this region the axoneme presents a 9+2 microtubule pattern and peripheral dense fibers do not occur (Fig. 3F,G). In its anterior portion, immediately behind the annulus, the spermatozoon shows a slight decrease in diameter relative to the midpiece diameter (Fig. 3B) and a thin zone of finely granular cytoplasm is observed between the fibrous sheath and the plasma membrane (Fig. 3B,F).

Endpiece

The endpiece is the final part of the flagellum, posterior to the termination of the fibrous sheath and peripheral fibers. It consists of the axoneme and plasma membrane, with an undetermined length. The pattern of microtubules is maintained, although their diameter is very reduced (Fig. 3H) and, in the posterior portion of the endpiece, the pattern appears unorganized (Fig. 3I).

DISCUSSION

The spermatozoon of *Ameiva ameiva* exhibits an elongate acrosome vesicle that encloses a similarly shaped subacrosomal cone, located on the anterior region of the tapered nucleus, a synapomorphy of tetrapods (Jamieson, 1995a). The following features, regarded as synapomorphies of amniotes (Jamieson, 1995a), are also present in *A. ameiva*: an elongate nucleus; a distal centriole extending through the midpiece, penetrated by two central singlets from the axoneme; several mitochondria in cross section of the midpiece; an annulus; nine peripheral dense fibers associated with the nine doublets of the axoneme; and enlarged peripheral fibers adjacent to doublets 3 and 8, forming a double structure detached from their respective doublets. *Ameiva ameiva* also has a number of character-states considered synapomorphies of Squamata (Jamieson, 1995b): single and wholly prenuclear perforatorium; an absence of endonuclear canal; an epinuclear lucent zone; linear mitochondrial cristae; intermitochondrial dense bodies; a fibrous sheath extending into the midpiece; and round nuclear shoulders.

The teiids *Ameiva ameiva* and *Cnemidophorus sexlineatus* (Newton and Trauth, 1992) share with the gymnophthalmid *Micrablepharus maximiliani* (Teixeira et al., 1999b) the following features: a large nuclear rostrum (length ≥ 1.3 μm); the pres-

Fig. 3. **A–K:** Spermatozoa of *Ameiva ameiva*. Transmission electron micrographs of the tail (midpiece and principal piece). **A:** Longitudinal section of the midpiece showing the distal centriole and the axoneme. **B:** Detail of the transition region between the midpiece and the principal piece. **C:** Transverse section through the distal centriole showing the pair of central microtubules and the dense material within it. **D:** Transverse section through the posterior portion of the distal centriole and the beginning of the axoneme showing the grossly enlarged fibers 3 and 8 (arrows). Note that the dense bodies forms a complete ring around the fibrous sheath. **E:** Transverse section of the axoneme showing that the peripheral fibers at 3 and 8 (arrows) are thicker than the others and are detached from their doublets. **F:** Transverse section through the anterior region of the principal piece. **G:** Transverse section through the posterior end of the principal piece. **H–I:** Transverse section of the endpiece. **J:** Longitudinal section of the neck region showing the nuclear fossa, the pericentriolar material, and the centrioles. Note the bilateral laminar structure projecting from the pericentriolar material. **K:** Longitudinal section of the full length of the midpiece showing the mitochondria and dense bodies arrangement. a, annulus; ax, axoneme; db, dense bodies; dc, distal centriole; fs, fibrous sheath; ls, laminar structure; m, mitochondria; n, nucleus; nf, nuclear fossa; pc, proximal centriole; pf, peripheral fibers; pm, pericentriolar material. **A–J:** scale bar = 0.2 μm. **K:** scale bar = 0.5 μm.

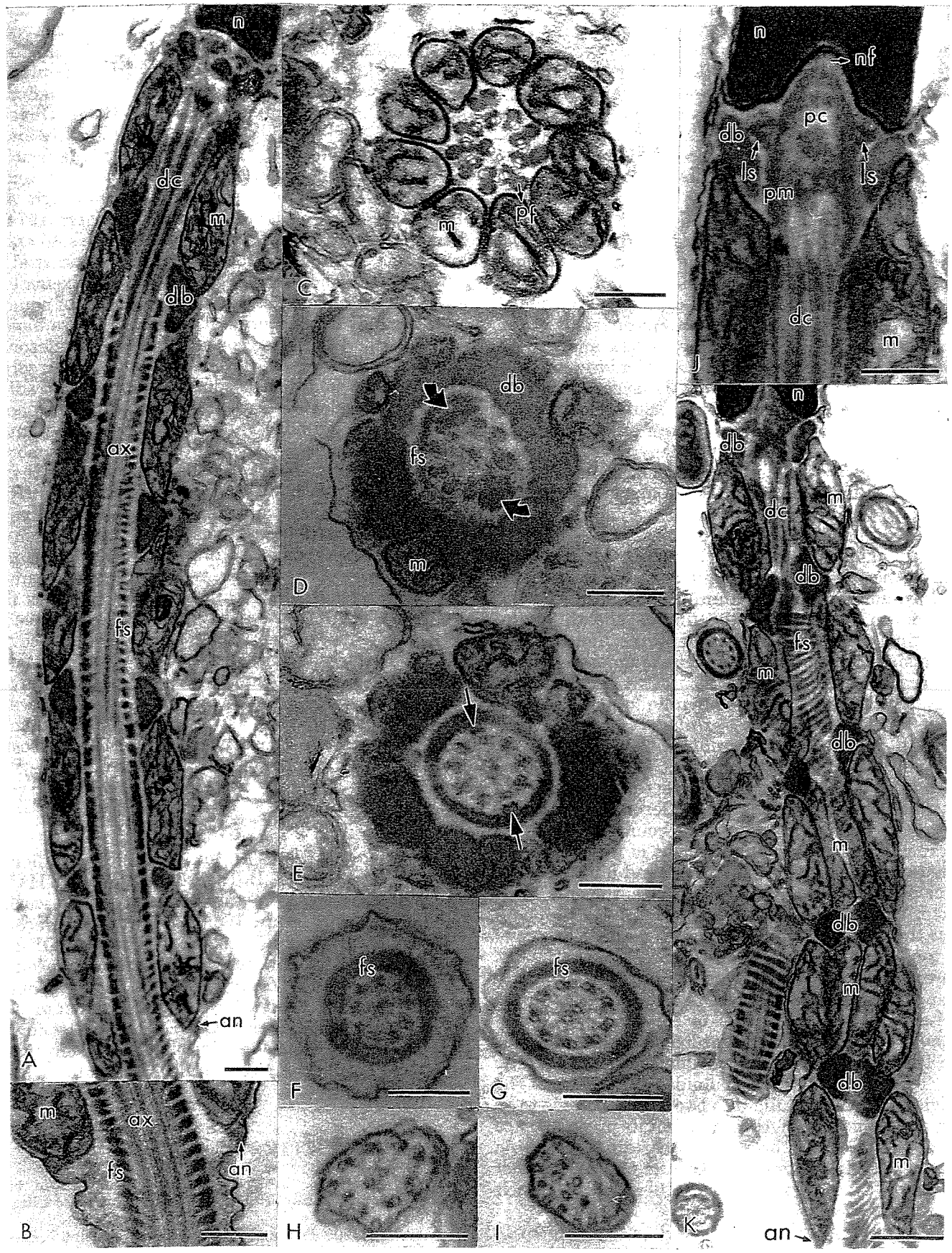
n
dc
m
db
ax
fs
an
A
m
ax
fs
an
B
C
m
pf
D
db
fs
m
E
fs
F
fs
G
H
I
n
nf
pc
db
ls
ls
pm
dc
m
J
n
db
m
dc
db
fs
m
db
m
db
m
db
m
K
an

Figure 3

ence of round nuclear shoulders at the base of the rostrum; an elongate nuclear shape; a diameter of the nuclear base less than 0.85 μm; a short midpiece; dense bodies well-developed, with solid aspect, and more electron-dense than mitochondria; and the presence of a slight decrease in the midpiece diameter after the annulus. These character-states, however, have also been documented in other squamate families (Jamieson, 1995b; Teixeira et al., 1999c).

Character-states shared between the teiids *Ameiva ameiva* and *Cnemidophorus sexlineatus* (Newton and Trauth, 1992), but not with the gymnophthalmid *Micrablepharus maximiliani* (Teixeira et al., 1999b), include: a depressed apical portion of the acrosome in transverse section; divisions of the acrosome vesicle into a narrow cortex and a wide medulla; an epinuclear lucent zone; a large nuclear rostrum (length ≥ 1.3 μm); round nuclear shoulders; an elongate nuclear shape, with basal diameter less than 0.85 μm; a laminar structure on both sides of the proximal centriole; a relatively short midpiece (length < 8.5 μm); elongate mitochondria, forming tiers of columnar structures separated from each other by intermitochondrial dense bodies; dense bodies well-developed, with solid aspect, and more electron-dense than mitochondria, arranged in rings; the presence of a slight decrease in the midpiece diameter after the annulus; and a thin zone of cytoplasm surrounding the fibrous sheath in the principal piece. None of these features, however, are exclusive to the two teiid genera (Jamieson, 1995b; Teixeira et al., 1999b,c).

Ameiva ameiva shows four unique features relative to *Cnemidophorus sexlineatus* (Newton and Trauth, 1992) and *Micrablepharus maximiliani* (Teixeira et al., 1999b): an electron-lucent, unilateral ridge at the acrosome surface; the division of the medulla into two regions with different electron densities; an epinuclear lucent zone bounded by a membrane; and the gross enlargement of the peripheral fibers associated with doublets 3 and 8 in the anterior portion of the axoneme. To date, the only character that distinguishes *Ameiva* from *Cnemidophorus* throughout their entire range is the presence of a tongue sheath in *Ameiva* (Presch, 1971). The differences in sperm ultrastructure outlined above add support to the validity of the two genera. Overall, we detected no unique traits of *Ameiva* and *Cnemidophorus* that could be regarded as synapomorphies of Teiidae. Neither have we identified unique traits of Teiioidea (Gymnophthalmidae + Teiidae). The division of the medulla into two regions seems to be an autapomorphy of *A. ameiva*, but its presence in *C. sexlineatus* cannot be safely ascertained based on the work of Newton and Trauth (1992). Further work on *Cnemidophorus* and other teiid genera is necessary to clarify this issue.

Our findings of high levels of polymorphism in sperm ultrastructure characters of two teiids support previous suggestions that intrafamilial variability may be higher than currently thought (Teixeira et al., 1999b,d). Polymorphic traits in the ultrastructure of spermatozoa exist in all families where more than one species have been studied, including Chamaeleonidae (Jamieson, 1995b; Oliver et al., 1996), Gekkonidae (Furieri, 1970; Phillips and Asa, 1993; Jamieson et al., 1996), Lacertidae (Furieri, 1970; Butler and Gabri, 1984; Courtens and Depeiges, 1985), Phrynosomatidae (Scheltinga et al., 2000), Polychrotidae (Clark, 1967; Furieri, 1974; Teixeira et al., 1999a), Scincidae (Jamieson and Scheltinga, 1994; Jamieson, 1995b; Jamieson et al., 1996), and Tropiduridae (Furieri, 1974; Teixeira et al., 1999d). Previous phylogenetic analyses of squamate families using sperm ultrastructure data have produced poorly resolved consensus trees (Jamieson, 1995b; Teixeira et al., 1999b,c) that were largely incongruent with those produced from more "traditional" morphological data (Estes et al., 1988; Lee, 1998; Caldwell, 1999). This result may be the outcome of the high levels of intrafamilial polymorphism in sperm ultrastructure data and the fact that families were used as terminal taxa. Apparently, splitting up higher taxa and using species as terminals can give more accurate estimates of phylogeny than other methods of coding polymorphic traits (Wiens, 1998a). Under these circumstances, sampling multiple genera within squamate families is essential if sperm ultrastructure data are to be used in phylogenetic analyses at the family level. Uncovering the intergeneric variability (polymorphism) in sperm ultrastructure characters may improve phylogenetic analyses of Squamata at the family level and aid in determining at which level of the taxonomical hierarchy these characters will be most profitably used in phylogenetic reconstruction.

ACKNOWLEDGMENTS

We thank A.K. Péres Jr. for assistance with field work. We also thank L.B. Tavares and Gustavo H.C. Vieira for assistance in the laboratory. This work was supported by grant 193.052/98 from Fundação de Apoio à Pesquisa do Distrito Federal-FAPDF to SNB and GRC, a fellowship from Programa Especial de Treinamento-PET/BIO to LGG, a doctorate fellowship from Coordenação de Aperfeiçoamento de Pessoal de Nível Superior-CAPES to RDT, and a fellowship from Conselho Nacional de Desenvolvimento Científico e Tecnológico-CNPq to GRC (302343/88-1).

LITERATURE CITED

Butler RD, Gabri MS. 1984. Structure and development of the sperm head in the lizard *Podarcis* (=*Lacerta*) *taurica*. J Ultrastr Res 88:261–274.

Caldwell MW. 1999. Squamate phylogeny and the relationships of snakes and mosasauroids. Zool J Linn Soc 125:115–147.

Clark AW. 1967. Some aspects of spermiogenesis in a lizard. Am J Anat 121:369–400.

Cole CJ, Dessauer HC. 1993. Unisexual and bisexual whiptail lizards of the *Cnemidophorus lemniscatus* complex (Squamata: Teiidae) of the Guiana region, South America, with descriptions of new species. Am Mus Novitates 3081:1–30.

Cole CJ, Dessauer HC, Townsend CR, Arnold MG. 1990. Unisexual lizards of the genus *Gymnophthalmus* (Reptilia: Teiidae) in the Neotropics: genetics, origin, and systematics. Am Mus Novitates 2994:1–29.

Cole CJ, Dessauer HC, Markezich AL. 1993. Missing link found: the second ancestor of *Gymnophthalmus underwoodi* (Squamata: Teiidae), a South American unisexual lizard of hybrid origin. Am Mus Novitates 3055:1–13.

Courtens JL, Depeiges A. 1985. Spermiogenesis of *Lacerta vivipara*. J Ultrastr Res 90:203–220.

Estes R, Pregill G. 1988. Phylogenetic relationships of the lizard families. Essays commemorating Charles L. Camp. Stanford, CA: Stanford University Press.

Estes R, de Queiroz K, Gauthier J. 1988. Phylogenetic relationships within Squamata. In: Estes R , Pregill G, editors. Phylogenetic relationships of the lizard families. Essays commemorating Charles L. Camp. Stanford, CA: Stanford University Press. p. 119–281.

Furieri P. 1970. Sperm morphology of some reptiles: Squamata and Chelonia. In: Baccetti B, editor. Comparative spermatology. Rome: Accademia Nazionale dei Lincei. p 115–131.

Furieri P. 1974. Spermi e spermatogenesi in alcuni iguanidi argentini. Riv Biol 67:233–279.

Hillis DM, Mable BK, Moritz C. 1996. Applications of molecular systematics: the state of the field and a look to the future. In: Hillis DM, Moritz C, Mable BK, editors. Molecular systematics. Sunderland, MA: Sinauer Associates. p 515–543.

Hsiao C, Chatterton NJ, Asay KH, Jensen KB. 1994. Phylogenetic relationships of 10 grass species: an assessment of phylogenetic utility of the internal transcribed spacer region in nuclear ribosomal DNA in monocots. Genome 37:112–120.

Jamieson BGM. 1995a. Evolution of tetrapod spermatozoa with particular reference to amniotes. In: Jamieson BGM, Ausio J, Justine J, editors. Advances in spermatozoal phylogeny and taxonomy. Paris: Muséum National d'Histoire Naturelle. p 343–358.

Jamieson BGM. 1995b. The ultrastructure of spermatozoa of the Squamata (Reptilia) with phylogenetic considerations. In: Jamieson BGM, Ausio J, Justine J, editors. Advances in spermatozoal phylogeny and taxonomy. Paris: Muséum National d'Histoire Naturelle. p 359–383.

Jamieson BGM, Scheltinga DM. 1994. The ultrastructure of spermatozoa of the Australian skinks, *Ctenotus taeniolatus, Carlia pectoralis* and *Tiliqua scincoides scincoides* (Scincidae, Reptilia). Mem Queensl Mus 37:181–193.

Jamieson BGM, Oliver SC, Scheltinga DM. 1996. The ultrastructure of spermatozoa of Squamata. I. Scincidae, Gekkonidae and Pygopodidae (Reptilia). Acta Zool (Stockh) 77:85–100.

Lee MSY. 1998. Convergent evolution and character correlation in burrowing reptiles: Towards a resolution of squamate relationships. Biol J Linn Soc 65:369–453.

Newton WD, Trauth SE. 1992. Ultrastructure of the spermatozoon of the lizard *Cnemidophorus sexlineatus* (Sauria: Teiidae). Herpetologica 48:330–343.

Nielsen C. 1998. Morphological approaches to phylogeny. Am Zool 38:942–952.

Oliver SC, Jamieson BGM, Scheltinga DM. 1996. The ultrastructure of spermatozoa of Squamata. II. Agamidae, Varanidae, Colubridae, Elapidae, and Boidae (Reptilia). Herpetologica 52: 216–241.

Phillips DM, Asa CS. 1993. Strategies for formation of the midpiece. In: Baccetti B, editor. Comparative spermatology 20 years after. New York: Raven Press. p 997–1000.

Presch WF Jr. 1971. Tongue structure of the teiid lizard genera *Ameiva* and *Cnemidophorus* with a reallocation of *Ameiva vanzoi*. J Herpetol 5:183–185.

Presch WF Jr. 1974. Evolutionary relationships and biogeography of the macroteiid lizards (Family Teiidae, Subfamily Teiinae). Bull So Calif Acad Sci 73:23–32.

Presch WF Jr. 1983. The lizard family Teiidae: is it a monophyletic group? Zool J Linn Soc 77:189–197.

Scheltinga DM, Jamieson BGM, Trauth SE, McAllister CT. 2000. Morphology of the spermatozoa of the iguanian lizards *Uta stansburiana* and *Urosaurus ornatus* (Squamata, Phrynosomatidae). J Submicr Cytol Pathol 32:261–271.

Simon C, Frati F, Beckenbach A, Crespi B, Liu H, Flook P. 1994. Evolution, weighting, and phylogenetic utility of mitochondrial gene sequences and a compilation of conserved polymerase chain reaction primers. Ann Entomol Soc Am 87:651–701.

Sites JW Jr, Murphy RW. 1991. Isozyme evidence for independently derived, duplicate G3PDH loci among squamate reptiles. Can J Zool 69:2381–2396.

Soto-Adames FN, Robertson HM, Berlocher SH. 1994. Phylogenetic utility of partial DNA sequences of G6pdh at different taxonomic levels in Hexapoda with emphasis on Diptera. Ann Entomol Soc Am 87:723–736.

Teixeira RD, Colli GR, Báo SN. 1999a. The ultrastructure of spermatozoa of the lizard *Polychrus acutirostris* (Squamata, Polychrotidae). J Submicr Cytol Pathol 31:387–395.

Teixeira RD, Colli GR, Báo SN. 1999b. The ultrastructure of the spermatozoa of the lizard *Micrablepharus maximiliani* (Squamata, Gymnophthalmidae), with considerations on the use of sperm ultrastructure characters in phylogenetic reconstruction. Acta Zool (Stockh) 80:47–59.

Teixeira RD, Colli GR, Báo SN. 1999c. The ultrastructure of the spermatozoa of the worm-lizard *Amphisbaena alba* (Squamata, Amphisbaenidae), and the phylogenetic relationships of amphisbaenians. Can J Zool 77:1254–1264.

Teixeira RD, Vieira GHC, Colli GR, Báo SN. 1999d. Ultrastructural study of spermatozoa of the neotropical lizards, *Tropidurus semitaeniatus* and *Tropidurus torquatus* (Squamata, Tropiduridae). Tissue Cell 31:308–317.

Wiens JJ. 1995. Polymorphic characters in phylogenetic systematics. Syst Biol 44:482–500.

Wiens JJ. 1998a. The accuracy of methods for coding and sampling higher-level taxa for phylogenetic analysis: a simulation study. Syst Biol 47:397–413.

Wiens JJ. 1998b. Testing phylogenetic methods with tree congruence: Phylogenetic analysis of polymorphic morphological characters in phrynosomatid lizards. Syst Biol 47:427–444.

Wiens JJ. 1999. Polymorphism in systematics and comparative biology. Annu Rev Ecol Syst 30:327–362.

Wiens JJ, Servedio MR. 1997. Accuracy of phylogenetic analysis including and excluding polymorphic characters. Syst Biol 46: 332–345.

2.1.2 – ARTIGO PUBLICADO 2

TAVARES-BASTOS, Leonora; **TEIXEIRA, Ruscaia Dias**; COLLI, Guarino Rinaldi; BÁO, Sônia Nair. Polymorphism in the sperm ultrastructure among four species of lizards in the genus *Tupinambis* (Squamata: Teiidae). Acta Zoologica, Stockholm, v. 83, p. 297-307, 2002.

Este artigo fez parte da dissertação de Mestrado de Leonora Tavares-Bastos, do Programa de Pós-graduação em Biologia Animal, do Instituto de Ciências Biológicas/UnB.

Acta Zoologica (Stockholm) 83: 297–307 (October 2002)

Polymorphism in the sperm ultrastructure among four species of lizards in the genus *Tupinambis* (Squamata: Teiidae)

L. Tavares-Bastos[1,2], R. D. Teixeira[2,3], G. R. Colli[4] and S. N. Báo[2]

[1]Pós-graduação em Biologia Animal, Universidade de Brasília, 70919–970, Brasília, DF, Brazil;
[2]Departamento de Biologia Celular, Universidade de Brasília, 70919–970, Brasília, DF, Brazil;
[3]Departamento de Biologia Celular, Universidade Estadual de Campinas, 13083–970 Campinas, SP, Brazil.
[4]Departamento de Zoologia, Universidade de Brasília, 70.919–970 Brasília, DF, Brazil.

Keywords:
lizard, polymorphism, spermatozoa, Teiidae, ultrastructure

Accepted for publication:
28 January 2001

Abstract

Tavares-Bastos, L., Teixeira, R. D., Colli, G. R. and Báo, S. N. 2002. Polymorphism in the sperm ultrastructure among four species of lizards in the genus *Tupinambis* (Squamata, Teiidae). — *Acta Zoologica* (Stockholm) 83: 297–307

We describe, for the first time, the ultrastructure of the spermatozoa of four species of the genus *Tupinambis* (Squamata, Teiidae). We identified seven polymorphic characters within this genus: the presence and shape of the perforatorial base plate, the presence of the epinuclear lucent zone, the presence of a unilateral ridge in the acrosome, the presence of a central density within the proximal centriole, the number of mitochondria and dense-bodies sets, and the shape of mitochondria. We analysed the evolution of the seven polymorphic characters by mapping them onto a current phylogeny of the species of *Tupinambis*, using the teiids *Ameiva ameiva* and *Cnemidophorus sexlineatus* as outgroups. Our results indicate that sperm ultrastucture characters, although of great value for phylogeny at higher taxonomic levels in reptiles and other groups, are poor predictors of phylogeny when considering the species of *Tupinambis* studied here. We failed to identify evidences that homoplasy in sperm ultrastructure among the species of *Tupinambis* is due to convergent adaptation, suggesting that the polymorphism may be selectively neutral in this group.

Sônia N. Báo, Departamento de Biologia Celular, Universidade de Brasília, 70.919–970, Brasília-DF, Brazil E-mail: snbao@unb.br

Introduction

Polymorphism has received considerable attention during the last 20 years (Farris 1981; Wiens 1995, 2000b; Murphy and Doyle 1998). These studies have fostered knowledge on the use of polymorphic characters for increasing the accuracy of phylogeny analyses, and they have also provided a variety of methods that have been developed to deal with polymorphic characters in phylogeny reconstructions. Nevertheless, the performance and the appropriateness of these different methods for polymorphism treatment have been extremely controversial and have been the subject of several debates (e.g. Swofford and Berlocher 1987; Crother 1990; Campbell and Frost 1993; Murphy and Doyle 1998; Wiens 1998). Recent studies have attempted to find the most efficient method to extract significant phylogenetic signal from the polymorphic characters in most data sets (e.g. Wiens and Servedio 1997; Wiens 1999). Detailed studies on the Squamata have revealed that the sperm ultrastructure provides an alternate source of characters and can profitably be used in phylogenetic analyses, indicating that it contains significant phylogenetic information (Jamieson 1995; Teixeira *et al.* 1999b,c).

The analysis of the degree of variability in sperm ultrastructure characters across taxonomic categories can reveal the most profitable taxonomic level at which phylogenetic analyses should be carried out (Teixeira *et al.* 1999d). So far, phylogenetic analyses of squamates based on ultrastructure characters have been conducted solely at the family level (Jamieson 1995; Jamieson *et al.* 1996; Oliver *et al.* 1996; Teixeira *et al.* 1999b,c). Nevertheless, polymorphism in sperm ultrastructure characters has been detected among genera in all families of Squamata with more than one genus studied: Boidae (Jamieson *et al.* 1996; Oliver *et al.* 1996),

Chamaeleonidae (Jamieson 1995; Oliver *et al.* 1996), Colubridae and Elapidae (Jamieson and Koehler 1994; Jamieson *et al.* 1996; Oliver *et al.* 1996), Gekkonidae (Furieri 1970; Jamieson *et al.* 1996), Lacertidae (Furieri 1970; Butler and Gabri 1984), Phrynosomatidae (Scheltinga *et al.* 2000), Polychrotidae (Furieri 1974; Teixeira *et al.* 1999a), Pygopodidae (Jamieson *et al.* 1996), Scincidae (Furieri 1970; Jamieson and Scheltinga 1993, 1994; Jamieson 1995; Jamieson *et al.* 1996), and Teiidae (Newton and Trauth 1992; Giugliano *et al.* 2002). In addition, polymorphism in sperm ultrastructure characters has also been detected among congeneric species of *Tropidurus* (Teixeira *et al.* 1999d) and *Ramphotyphlops* (Harding *et al.* 1995). Overall, sperm ultrastructure characters seem to be less conservative than previously thought (Jamieson *et al.* 1996), but additional studies are necessary to enhance our knowledge of the intrageneric stability of ultrastructure spermatozoa characters.

Lizards of the genus *Tupinambis* are the largest terrestrial lizards of the New World, and are restricted to South America, east of the Andes, and reaching the north of Patagonia (Presch 1973; Cei and Scolaro 1982; Peters and Orejas-Miranda 1986). The genus currently comprises six species (Fitzgerald *et al.* 1999). In this study we provide, for the first time, a detailed description of the ultrastructure of the spermatozoon of four species of *Tupinambis* (*T. duseni*, *T. merianae*, *T. quadrilineatus*, and *T. teguixin*) to investigate the degree of intrageneric variability in sperm ultrastructure characters. Further, we also delineate scenarios for the evolution of the sperm ultrastructure within the genus based on previously published phylogenies of *Tupinambis* lizards (Colli *et al.* 1998; Fitzgerald *et al.* 1999).

Material and Methods

We obtained mature spermatozoa from adult individuals of the following species: *Tupinambis duseni* (Coleção Herpetológica da Universidade de Brasília, CHUNB 20361), collected at Mineiros, Goiás, Brazil; *T. merianae* (CHUNB 14851), collected at Chapada dos Guimarães, Mato Grosso State, Brazil; *T. quadrilineatus* (CHUNB 08448), collected at Minaçu, Goiás State, Brazil; and *T. teguixin* (CHUNB 03695), collected at Santa Terezinha, Mato Grosso State, Brazil. We killed the specimens with Tiopental®, removed the epididymides by dissection, placed them in a Petri dish with phosphate buffered saline (PBS) pH 7.2, and cut them into small pieces. We fixed epididymal tissues in a solution containing 2.5% glutaraldehyde, 2% paraformaldehyde, and 3% sucrose in 0.1 M sodium cacodylate buffer pH 7.2 at 4 °C overnight. Subsequently, we washed the samples in 0.1 M sodium cacodylate buffer, pH 7.2, with 3% sucrose, and postfixed them for 1 h in 1% osmium tetroxide, 0.8% potassium ferricyanide, and 5 mM $CaCl_2$ in 0.1 M sodium cacodylate buffer, pH 7.2. We dehydrated the material in a series of ascending acetone (30–100%) and embedded tissues in Spurr's epoxy resin. We stained ultrathin sections with uranyl acetate and lead citrate, and made observations in a Jeol® 100 C transmission electron microscope. We made light microscopic observations of spermatozoa from glutaraldehyde-paraformaldehyde fixed smears under Normarski contrast using a Zeiss® Axiophot microscope.

To study the evolution of sperm ultrastructure characters among the species of *Tupinambis*, we optimized the transformation of polymorphic characters on a phylogeny of the genus based on allozymes (Colli *et al.* 1998) and partial sequences of cytochrome b and ND4 genes (Fitzgerald *et al.* 1999), using MacClade 4.0 (Maddison and Maddison 1992) and Fitch optimization (Kitching *et al.* 1998). When more than one most-parsimonious reconstruction (MPR) existed for a character, we examined all MPRs. We used the teiids *Ameiva ameiva* (Giugliano *et al.* 2002) and *Cnemidophorus sexlineatus* (Newton and Trauth 1992) as outgroups to ascertain the direction of evolutionary change in the characters.

Results

Ultrastructure of Spermatozoa

A generalized spermatozoon is represented diagrammatically in Figure 1. Spermatozoa of *Tupinambis duseni*, *T. merianae*, *T. quadrilineatus*, and *T. teguixin* are filiform, approximately 82.3 μm long, consisting of a head region containing the nucleus and acrosome complex, a midpiece, and a tail region (flagellum) subdivided into principal piece and endpiece (Fig. 2A). The head is approximately 23.5 μm in total length, as measured from light microscopy. The midpiece is approximately 3.3 μm in total length in *T. quadrilineatus* and *T. teguixin*, and 4.2 μm in *T. duseni* and *T. merianae*, as determined from transmission electron microscopy. The tail is approximately 55.5 μm, as measured from light microscopy.

Acrosome complex

The acrosome complex, which is located in the anteriormost region of the head, is comprised of an external and elongate acrosome vesicle, an internal cap, the subacrosomal cone, and the perforatorium (Fig. 2B–C). In longitudinal section, the acrosome complex is long and flattened (Fig. 2O) and, in cross section, it is depressed (Fig. 2G–J) becoming more circular at its base (Fig. 2K). In *Tupinambis teguixin*, the acrosome complex develops a unilateral electron-lucent ridge anteriorly (Fig. 2E). The acrosome vesicle is divided into a narrow cortex and a wide medulla at its anterior portion. The cortex consists of two electron-densities: an external, thin electron-dense layer which surrounds an electron-lucent layer (Fig. 2M). In transversal section (Fig. 2H) and in longitudinal section (Fig. 2N), the internal electron-lucent portion of the cortex exhibits a tubular organization. The medulla appears as a strong electron-dense structure, filling the interior of the acrosome vesicle (Fig. 2H,I,M). The perforatorium is a slender rod with a pointed tip, that extends

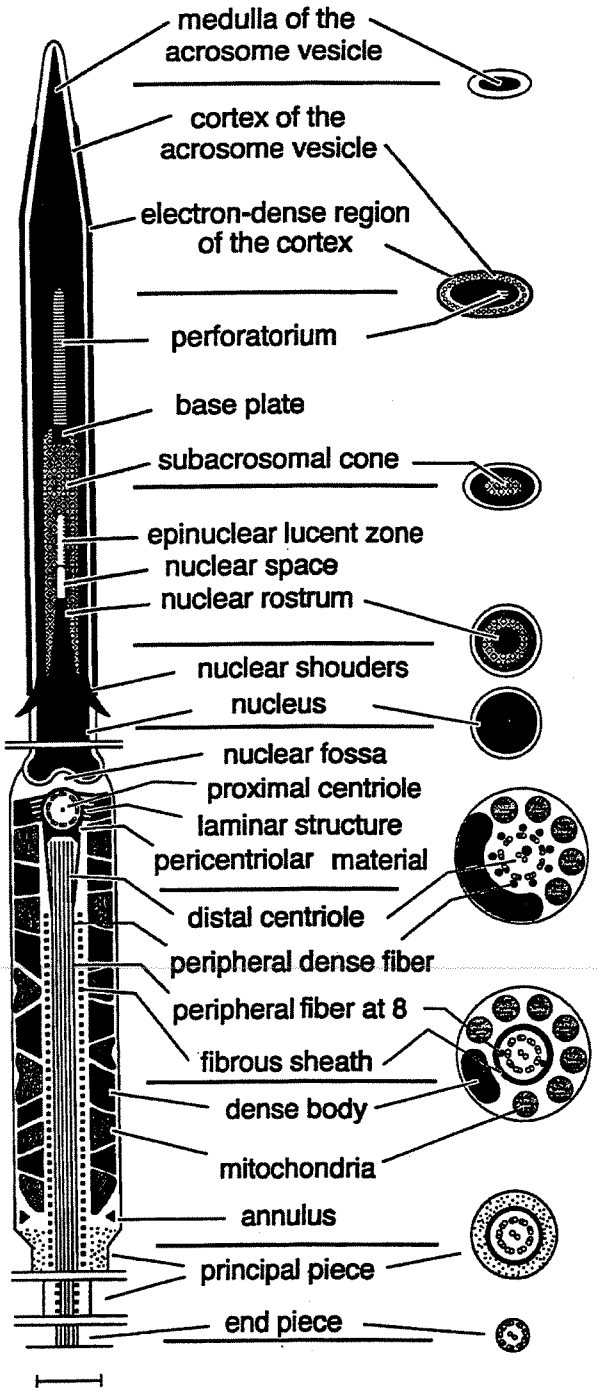

Fig. 1—Diagram of the spermatozoon of *Tupinambis quadrilineatus* in longitudinal section and corresponding transverse section. Scales of various components are only approximate. Scale bar 0.5 μm.

anteriorly from the subacrosomal cone into the acrosome vesicle. At the perforatorium's posterior end, the base plate is cylindrical in *T. duseni*, *T. merianae*, and *T. quadrilineatus* (Fig. 2B), and trapezoid in *T. teguixin* (Fig. 2C). In cross section, the subacrosomal cone exhibits a paracrystalline structure and has a radial arrangement around the nuclear tip (Fig. 2K). The epinuclear lucent zone, a narrow chamber within the anterior limit of the subacrosomal cone at the anterior end of the nucleus, is bounded by a membrane and is approximately 0.05 μm long in *T. merianae* (Fig. 2F), 0.8 μm in *T. duseni* and *T. quadrilineatus* (Fig. 2D), and absent in *T. teguixin* (Fig. 2E).

Nucleus

The nucleus is a curved cylinder, with the apical region tapered within the subacrosomal cone (Fig. 2B,D–F). In transverse section, the nucleus is circular (Fig. 2L). The chromatin is strongly electron-dense, with an electron-lucent lacuna interspersed through it. At its anterior extremity, it forms a point deeply wedged in the acrosome, the nuclear rostrum, approximately 0.6 μm long. The spermatozoa of the four species of *Tupinambis* have a nuclear space which appears filled with an electron-lucent substance and present a membrane of its own (Fig. 2D–F). The epinuclear lucent zone extends anteriorly, from the tip of the nuclear space (Fig. 2D,F), but is absent in *T. teguixin* (Fig. 2E). The transition from the tapered apical portion to the cylindrical region is abrupt and marked by small and round nuclear shouders (Fig. 2D–F). The base of the nucleus is marked by a concave depression, the nuclear fossa, that receives the centriolar apparatus (Fig. 3C). At its base, next to the nuclear fossa, the diameter of the nucleus is approximately 0.4 μm in the four species.

Midpiece

The midpiece consists of the neck region and the axoneme, surrounded by the fibrous sheath, mitochondria, and rings of dense bodies (Fig. 3A–B). The neck region contains the proximal and distal centrioles, the first ring of dense bodies, and mitochondria (Fig. 3C). The proximal centriole is short and partially surrounded by the pericentriolar material, that conforms in shape to the nuclear fossa and extends posteriorly between the two centrioles (Fig. 3C). A striated density lateral to the pericentriolar material, the stratified laminar structure, projects on both sides of the proximal centriole (Fig. 3C). A central, electron-dense structure is observed within the proximal centriole (Fig. 3C, inset), but this structure is absent in *T. merianae*. The distal centriole forms the basal body of the axoneme and consists of nine triplets of microtubules, nine peripheral fibres that partially cover the triplets, and two central singlets of the axoneme, which extend into the posterior region of the distal centriole and are embedded in a dense material (Fig. 3D).

The midpiece is approximately 3.3 μm long in *T. quadrilineatus* and *T. teguixin* (Fig. 3A), and 4.2 μm in *T. duseni* (Fig. 4) and *T. merianae* (Fig. 3B). The axial component of the midpiece is the axoneme, formed by a pair of central microtubules surrounded by nine doublets and nine

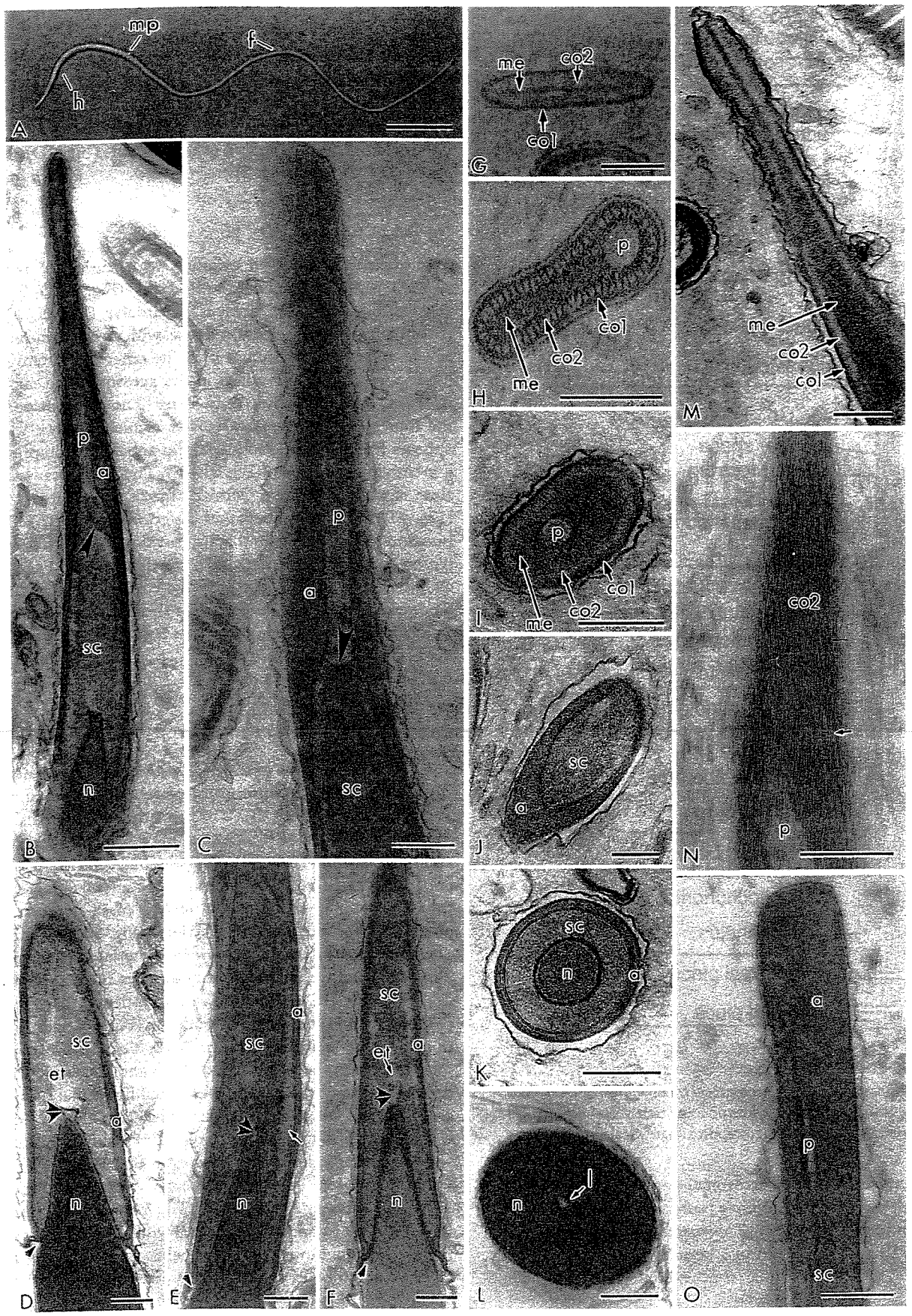

peripheral fibers. The peripheral fibers associated with doublets 3 and 8 are thicker than the others and are separated from their corresponding doublets (Fig. 3E). A fibrous sheath surrounds the axoneme, extending into the midpiece posterior to the distal centriole (Fig. 3A–B). In longitudinal section, mitochondria are columnar in *T. duseni* (Fig. 4), *T. merianae*, and *T. teguixin* (Fig. 3B), and trapezoid in *T. quadrilineatus* (Fig. 3A). In cross section, they appear as irregular structures with linear cristae (Fig. 3E). The mitochondria are separated by complete or incomplete rings of dense bodies (Fig. 3J), and usually six sets of mitochondria are seen around the axoneme intercalated with six sets of dense bodies in *T. quadrilineatus* and *T. teguixin* (Fig. 3A), seven sets in *T. duseni* (Fig. 4), and eight sets in *T. merianae* (Fig. 3B). Dense bodies are well-developed and appear as solid structures (Fig. 3A,B and Fig. 4). Posteriorly, the midpiece terminates at the annulus, which is closely attached to the inner surface of the plasma membrane, marking the beginning of the principal piece (Fig. 3A,B and Fig. 4).

Table 1 States of seven polymorphic characters of the ultrastructure of sperm among four species of *Tupinambis* and two other species of teiids, used as outgroups

	Characters						
Taxa	1	2	3	4	5	6	7
Ameiva ameiva	1	1	1	1	1	0	0
Cnemidophorus sexlineatus	0	0	1	0	0	0	0
Tupinambis duseni	1	1	1	0	1	2	0
Tupinambis merianae	1	1	1	0	0	3	0
Tupinambis quadrilineatus	1	1	1	0	1	1	1
Tupinambis teguixin	1	2	0	1	1	1	0

Character list and state names: 1, perforatorial base plate: (0) absent (1) present; 2, shape of perforatorial base plate: (0) absent (1) cylindric (2) trapezoid; 3, epinuclear lucent zone: (0) absent (1) present; 4, unilateral ridge in the acrosome: (0) absent (1) present; 5, central density within proximal centriole: (0) absent (1) present; 6, number of mitochondria and dense bodies sets: (0) 5 (1) 6 (2) 7 (3) 8; 7, shape of mitochondria: (0) columnar (1) trapezoid.

Principal piece

The principal piece forms the tail of the spermatozoon. It consists of the axoneme, with a 9 + 2 microtubules pattern, surrounded by the fibrous sheath and the plasma membrane. In the anterior portion of the principal piece, a wide zone of finely granular cytoplasm is observed between the fibrous sheath and the plasma membrane (Fig. 3F). The fibres adjacent to microtubule doublets 3 and 8 are absent from the anterior region of the principal piece. Posteriorly, the plasma membrane becomes closely attached to the fibrous sheath (Fig. 3G).

Endpiece

The endpiece forms the very slender tail of the spermatozoa, posterior to the termination of the fibrous sheath. It consists of the axoneme and plasma membrane and has an undetermined length. In the anterior portion of the endpiece the 9 + 2 pattern of microtubules is maintained, although its diameter becomes reduced (Fig. 3H). However, in the posterior portion of the endpiece, the 9 + 2 pattern becomes disarrayed and the doublets break apart into singlets (Fig. 3I).

Evolution of sperm ultrastructure characters

We coded the seven polymorphic characters identified among the four species of *Tupinambis* (Fig. 5) into discrete states (Table 1). Mapping the evolution of these characters in the most-corroborated phylogeny of *Tupinambis* lizards (Colli *et al.* 1998; Fitzgerald *et al.* 1999), using *Ameiva ameiva* and *Cnemidophorus sexlineatus* as outgroups, resulted in a treelength of 12, a consistency index (CI) of 0.83 and a retention index (RI) of 0.33. This indicates the presence of some homoplasy and low levels of synapomorphy among the characters. Indeed, no character transformation unequivocally supports the clade uniting the four species of *Tupinambis* or the clades uniting *T. duseni* + *T. merianae*, and *T. quadrilineatus* + *T. teguixin* (Fig. 6). Six of the polymorphic characters change unequivocally on the phylogeny, but all of them specify autapomorphies (Fig. 6). The evolution of character 6 (number of mitochondria and dense-bodies sets)

Fig. 2—Spermatozoa of *Tupinambis duseni*, *T. merianae*, *T. quadrilineatus*, and *T. teguixin*. —**A**. Light micrograph showing whole spermatozoon of *T. quadrilineatus*, with head (h), midpiece (mp) and flagellum (f). —**B–F**. Transmission electron micrographs of the head (acrosome complex and nucleus). B–C: Longitudinal sections of the acrosome complex of the spermatozooa of the *T. quadrilineatus* and *T. merianae*, respectively, showing base plate (arrowhead). D–F: Posterior region of the acrosome complex of the *T. quadrilineatus*, *T. teguixin* and *T. merianae*, respectively, showing the nuclear shoulders (arrowhead) and the nuclear space (double arrowhead). Note the electron-lucent unilateral ridge (arrow) in the *T. teguixin* sperm. —**G–K**. Successive transverse sections through the acrosome of *Tupinambis*. Note that anteriorly, in G–J, the acrosome appears very depressed, while posteriorly, in K, it is more circular. —**L**. Transverse section through the nucleus showing nuclear lacuna (l). —**M–O**. Longitudinal section through the anterior portion of the acrosome of the sperm of *T. quadrilineatus* (M and N) and *T. teguixin* (O). M: Note the electron-densities differences between the cortex and medulla. N: Note the tubular organization of the cortex (arrow). O: Flattened aspect of the acrosome. a = acrosome vesicle; co1 = external cortex of acrosome vesicle; co2 = internal cortex of acrosome vesicle; et = epinuclear lucent zone; me = medulla of the acrosome vesicle; n = nucleus; p = perforatorium; sc = subacrosomal cone. Scale bars: A = 10 μm, B, O = 0.5 μm, C–N = 0.2 μm.

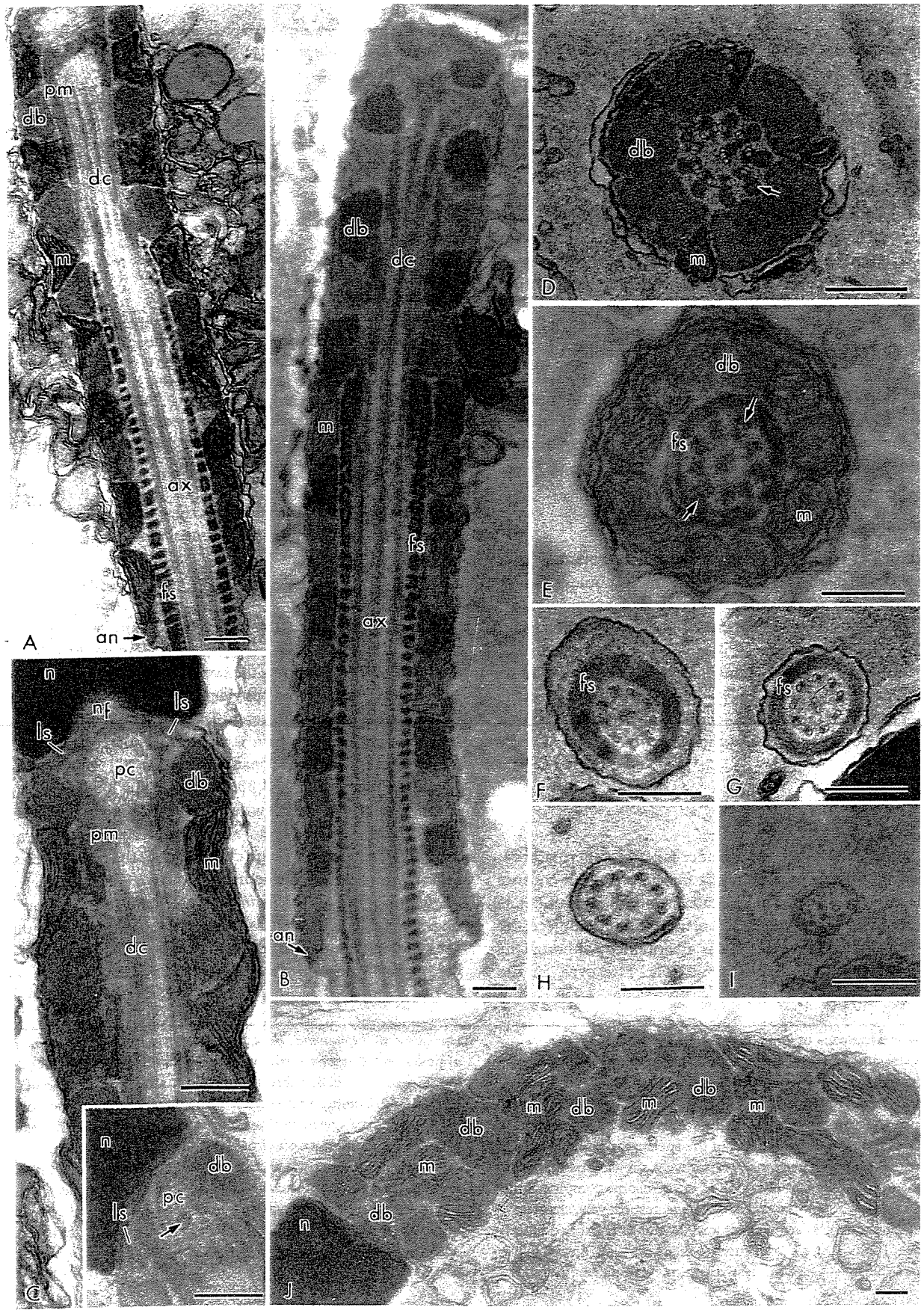

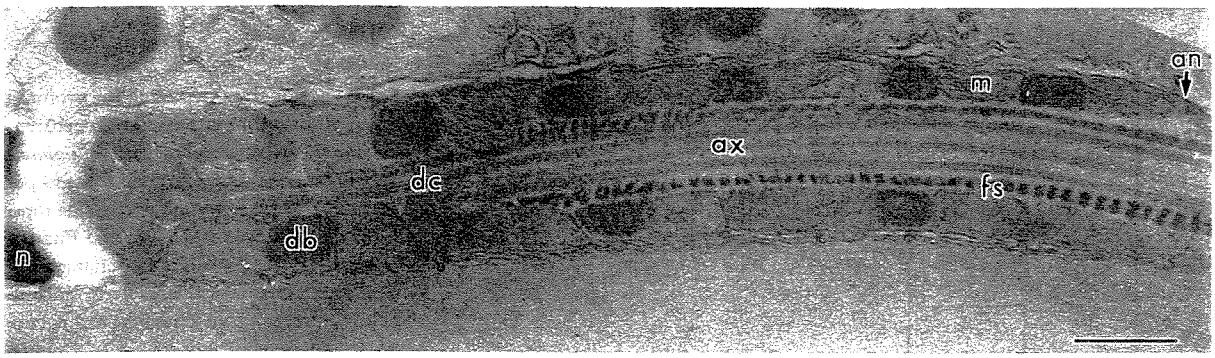

Fig. 4—Spermatozoa of *Tupinambis duseni*. Longitudinal section of midpiece showing the sets of mitochondria and dense bodies. an = annulus; ax = axoneme; db = dense body; dc = distal centriole; fs = fibrous sheath; m = mitochondria; n = nucleus. Scale bar 0.5 μm.

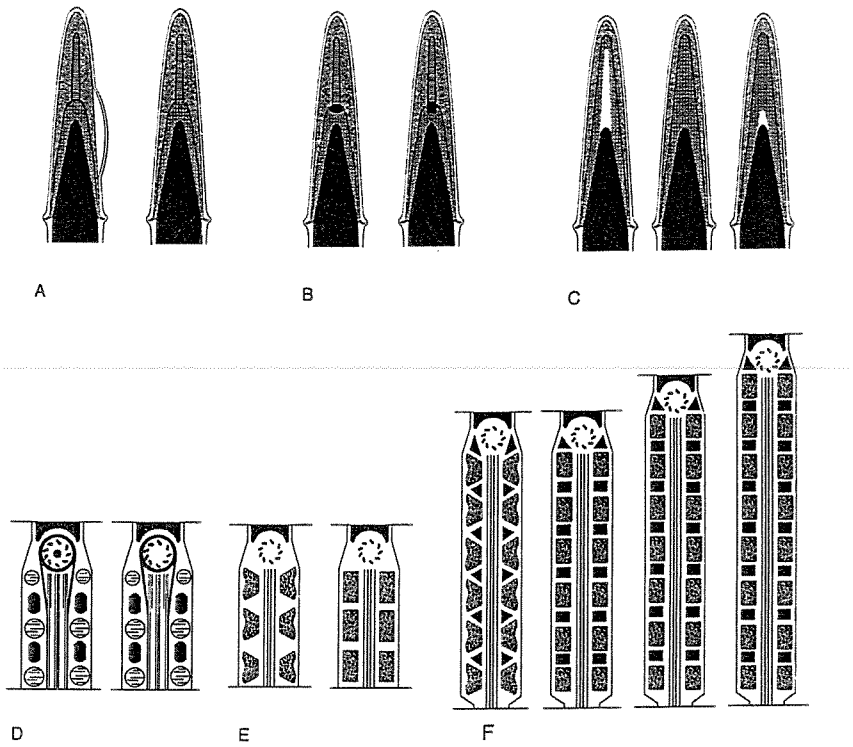

Fig. 5—Diagram of the spermatozoa of *Tupinambis* showing the polymorphic characters. —**A–C**. Longitudinal sections of the acrosome complex region. A: Presence of the unilateral ridge in *T. teguixin* and absence of this structure in *T. duseni*, *T. merianae*, and *T. quadrilineatus*. B: Base plate with a trapezoid shape in *T. teguixin* and with a cylindrical shape in *T. duseni*, *T. merianae*, and *T. quadrilineatus*. C: Three states of the electron lucent zone of the sperm. —**D**. Detail of the neck region showing the presence of the central dense body in *T. duseni*, *T. quadrilineatus*, and *T. teguixin*, and the absence of this structure in *T. merianae*. —**E**. Longitudinal section of the midpiece showing the mitochondrial shape. In *T. quadrilineatus* the mitochondria are trapezoid, in *T. duseni*, *T. merianae*, and *T. teguixin* they are columnar. —**F**. Longitudinal section of the midpiece showing the number of sets of the mitochondria and dense body consisting of six in *T. quadrilineatus* and *T. teguixin*, seven in *T. duseni*, and eight in *T. merianae*.

Fig. 3—Spermatozoa of *Tupinambis duseni*, *T. merianae*, *T. quadrilineatus*, and *T. teguixin*. —**A–J**. Transmission electron micrographs of the tail (midpiece, principal piece, and endpiece). A–B: Longitudinal section of the midpiece of *T. quadrilineatus* and *T. merianae*, respectively. C: Longitudinal section of the neck region showing the nuclear fossa, the pericentriolar material, the centrioles and stratified laminar structure. Inset: Detail of the neck region showing central dense body (arrow). D: Transverse section through the distal centriole showing the pair of central microtubules and peripheral fibers (arrow). E: Transverse section through the axoneme showing the nine peripheral fibres associated with doublets. Note that the peripheral fibres 3 and 8 (arrows) are double and detached. F–G: Transverse sections through the anterior and posterior region, respectively, of the principal piece. H–I: Transverse section of the end piece. J: Longitudinal section of the midpiece showing the mitochondria and dense body arrangement. an = annulus; ax = axoneme; db = dense body; dc = distal centriole; fs = fibrous sheath; ls = laminar structure; m = mitochondria; n = nucleus; nf = nuclear fossa; pc = proximal centriole; pm = pericentriolar material. Scale bars: A–I = 0.2 μm, J = 0.5 μm.

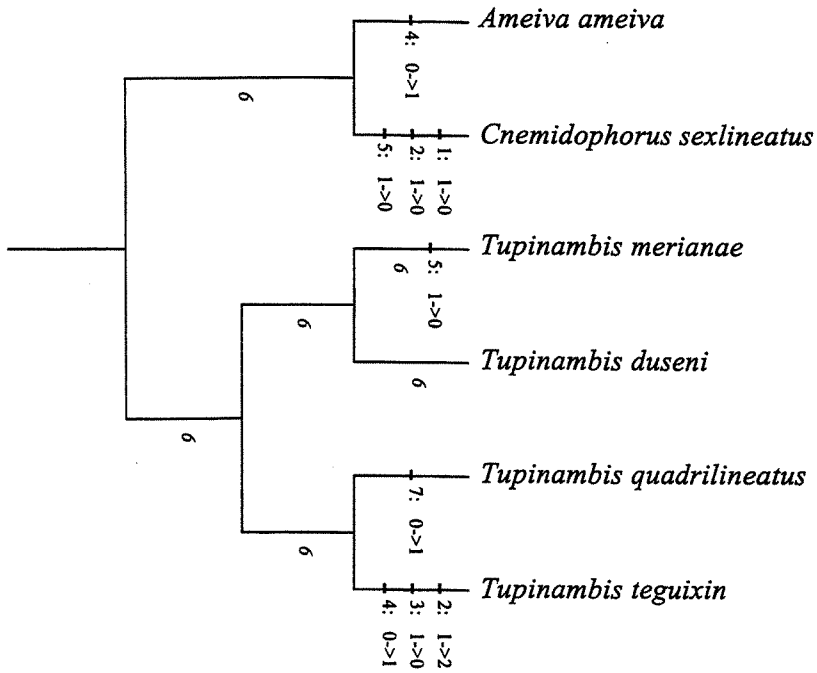

Fig. 6—Cladogram depicting the evolution of seven polymorphic sperm ultrastructure characters among four species of *Tupinambis*. The teiids *Ameiva ameiva* and *Cnemidophorus sexlineatus* are used as outgroups. The topology is based on Colli *et al.* (1998) and Fitzgerald *et al.* (1999). The evolution of character 6 cannot be unequivocally resolved, since there exist 13 most-parsimonious reconstructions. Note the lack of synapomorphies. Character and state names: 1, perforatorial base plate: (0) absent (1) present; 2, shape of perforatorial base plate: (0) absent (1) cylindric (2) trapezoid; 3, epinuclear lucent zone: (0) absent (1) present; 4, unilateral ridge in the acrosome: (0) absent (1) present; 5, central density within proximal centriole: (0) absent (1) present; 6, number of mitochondria and dense bodies sets: (0) 5 (1) 6 (2) 7 (3) 8; 7, shape of mitochondria: (0) columnar (1) trapezoid.

Table 2 Comparative polymorphic characters of *Ramphotyphlops*, *Tropidurus* and *Tupinambis*. All data from Harding *et al.* (1995), Teixeira *et al.* (1999d) and the present study

	Sperm ultrastructure characters and the region where they are observed		
Genera	Head (acrosome and nucleus)	Midpiece	Flagellum
Ramphotyphlops	Perforatorium length Acrosomal vacuity subdivision	Neck cylinder electron-density Mitochondria length and arrangement Dense bodies: presence and electron-density	
Tropidurus	Acrosome flattening Nuclear base bulging		Microtubules arrangement in endpiece
Tupinambis	Perforatorial base plate shape Epinuclear lucent zone Unilateral ridge in acrosome complex	Central dense body within proximal centriole Mitochondria shape Sets of mitochondria and dense bodies	

cannot be unequivocally resolved, as there exist 13 most-parsimonious reconstructions (MPR). Five MPRs support the monophyly of Teiidae: in three MPRs, state 1 (6 sets of mitochondria and dense bodies) is a synapomorphy of Teiidae and in the remaining two MPRs, either state 2 (7 sets) or 3 (8 sets) is a synapomorphy of Teiidae. Five MPRs support the monophyly of *Tupinambis*: in three MPRs, state 1 is a synapomorphy of *Tupinambis* and in the remaining two MPRs, either state 2 or 3 is a synapomorphy of *Tupinambis*. Six MPRs support the monophyly of *T. duseni* + *T. merianae*: in three MPRs, state 2 is a synapomorphy of the group, whereas in the other three MPRs state 3 is a synapomorphy of the group. Finally, in seven MPRs the clade *T. quadrilineatus* + *T. teguixin* is supported by the shared presence of state 1 of character 6.

Discussion

We identified seven polymorphic characters among the congeneric species *Tupinambis duseni*, *T. merianae*, *T. quadrilineatus*, and *T. teguixin*: the presence and shape of the perforatorial base plate, the presence of the epinuclear lucent zone, the presence of a unilateral ridge in the acrosome, the presence of a central density within the proximal centriole, the number of mitochondria and dense bodies sets, and the shape of mitochondria. All polymorphic characters in *Tupinambis* occur in the acrosome complex and midpiece regions (Table 2). Polymorphic traits in sperm ultrastructure characters among congeneric species have also been reported in worm snakes of the genus *Ramphotyphlops* (Harding *et al.* 1995) and *Tropidurus* lizards (Teixeira *et al.* 1999d). In both

genera, polymorphism occurs chiefly in the acrosome and midpiece (Table 2). Therefore, the available evidence indicates that the polymorphism in sperm ultrastructure characters among congeneric species of Squamata is mainly concentrated in the acrosome complex and midpiece regions.

At first glance, one might suggest that the greater variability in the acrosome and midpiece simply derives from the high concentration of characters in both regions: the more characters a given region contains, the more likely that it will contain polymorphic characters. According to this view, rates of evolutionary change are the same across all characters or, in other words, changes that have occurred during evolution were selectively neutral (Ridley 1993). This implies that most variability is a product of random processes, without any underlying adaptive causes related to the ecology of their bearers. Hence, the great intrageneric variability in sperm ultrastructure characters in the acrosome and midpiece regions may not be really surprising, being a necessary product of the evolutionary process.

Conversely, it is plausible that spermatozoa from different species have become adapted to various modes of fertilization, to the various types of eggs envelopes they have to penetrate, and to the various environments in which they operate (Anderson and Personne 1973). Since the acrosome is responsible for the sperm penetration into the ovum and the midpiece provides energy for sperm movement, the greater variability we observed in the two regions may be related to fertilization processes and physiological environment demands. The spermatozoa of animals with external fertilization, such as mussels, annelid worms, and sea urchins, in many cases lack the acrosome and have a midpiece containing only one or few mitochondria, whereas in groups with internal fertilization, the acrosome is present and the midpiece is more complex, containing several different structures and modifications (Baccetti 1986). A correlation seems to exist between the length of the sperm head and the mode of fertilization among external fertilizing anurans: in aquatic fertilizing species the sperm heads and acrosomes are significantly shorter than those of terrestrial fertilizing species (Van der Horst *et al.* 1995). Further, in hibernating bats, spermatozoa present a well-developed midpiece containing abundant and larger mitochondria, presumably as an adaptation for prolonged survival of spermatozoa in the female reproductive tract during the hibernation period (Mori 1995).

Nevertheless, lizards in the genus *Tupinambis* are very similar in terms of their reproductive ecology (Fitzgerald *et al.* 1993; Herrera and Robinson 2000) and, to the best of our knowledge, there are no compelling arguments to establish a firm association between the polymorphism in sperm ultrastructure characters and differences in the reproductive ecology of the species. Therefore, the polymorphism in sperm ultrastructure characters among species of *Tupinambis* appears to be selectively neutral, lacking an adaptive basis.

Mapping characters onto a proposed phylogeny permits the identification of similarity due to common inheritance vs. that due to repeated and independent evolutionary events (Brooks and McLennan 1991; Harvey and Pagel 1991). Good agreement between mapped characters and a proposed phylogeny is considered an indication that characters are constrained in their evolution or, in other words, that the distribution of characters across taxa is largely attributable to phylogenetic inertia (e.g. Schwenk 1993; Brown *et al.* 2000). Conversely, a poor fit between mapped characters and the phylogeny (i.e. homoplasy) indicates that convergent adaptation has a substantial influence (e.g. McCracken *et al.* 1999; Wiens 2000a). Our results indicate that sperm ultrastructure characters are poor predictors of phylogeny, when considering the species of *Tupinambis* studied. None of the seven polymorphic characters we identified uniquely characterizes any of the three ingroup clades in the phylogeny (*Tupinambis*, *T. duseni* + *T. merianae*, or *T. quadrilineatus* + *T. teguixin*). Variation in sperm ultrastructure within the genus *Tupinambis* therefore apparently is not a reflection of group membership. However, as indicated above, claims that homoplasy in sperm ultrastructure among species of *Tupinambis* is due to convergent adaptation are not supported by current knowledge on the reproductive biology of the species. Hence, the polymorphic sperm ultrastructure characters may be evolutionarily labile and selectively neutral in this group.

Acknowledgements

We thank Ayrton K. Péres Jr., Gustavo H. C. Vieira, and Frederico G. R. França for assistance during fieldwork. This study was supported by a master's fellowship from CAPES to LTB, and by research fellowships from CNPq to GRC (# 302343/88–1) and to SNB (# 520130/97–9).

References

Anderson, W. A. and Personne, P. 1973. The form and function of spermatozoa: a comparative view. In: *The Functional Anatomy of the Spermatozoon*. (ed. B. A. Afzelius), pp. 3–14. Pergamon Press, Oxford.

Baccetti, B. 1986. Evolucionary trends in sperm structure. – *Comparative Biochemistry and Physiology* 85: 29–36.

Brooks, D. R. and McLennan, D. A. 1991. *Phylogeny, Ecology, and Behavior, a Research Program in Comparative Biology*. The University of Chicago Press, Chicago.

Brown, B., Emberson, R. M. and Paterson, A. M. 2000. Morphological character evolution in hepialid moths (Lepidoptera: Hepialidae) from New Zealand. – *Biological Journal of the Linnean Society* 69: 383–397.

Butler, R. D. and Gabri, M. S. 1984. Structure and development of the sperm head in the lizard *Podarcis* (= *Lacerta*) *taurica*. – *Journal of Ultrastructure Research* 88: 261–274.

Campbell, J. A. and Frost, D. R. 1993. Anguid lizards of the genus *Abronia*: revisionary note, description of four new species, a

phylogenetic analysis, and key. – *Bulletin of the American Museum of Natural History* 216: 1–121.

Cei, J. M. and Scolaro, J. A. 1982. Geographic distribution: *Tupinambis rufescens*. – *Herpetological Review* 13: 26.

Colli, G. R., Péres, A. K. Jr and da Cunha, H. J. 1998. A new species of *Tupinambis* (Sauria, Teiidae) from central Brazil, with an analysis of morphological and genetic variation in the genus. – *Herpetologica* 54: 477–492.

Crother, B. I. 1990. Is 'some better than none' or do allele frequencies contain phylogenetically useful information? – *Cladistics* 6: 277–281.

Farris, J. S. 1981. Distance data in phylogenetic analysis. In: *Advances in Cladistics. Proceedings of the First Meeting of the Willi Hennig Society* (eds V. A. Funk, D. R. Brooks), pp. 3–23. New York Botanical Garden, New York.

Fitzgerald, L. A., Cook, J. A. and Aquino, A. L. 1999. Molecular phylogenetics and conservation of *Tupinambis* (Sauria: Teiidae). – *Copeia* 1999: 894–905.

Fitzgerald, L. A., Cruz, F. B. and Perotti, G. 1993. The reproductive cycle and the size at maturity of *Tupinambis rufescens* (Sauria: Teiidae) in the dry Chaco of Argentina. – *Journal of Herpetology* 27: 70–78.

Furieri, P. 1970. Sperm morphology of some reptiles: Squamata and Chelonia. In: *Comparative Spermatology*. (ed. B. Baccetti), pp. 115–131. Accademia Nazionale Dei Lincei, Rome, Italy.

Furieri, P. 1974. Spermi e spermatogenesi in alcuni iguanidi argentini. – *Rivista Di Biologia* 67: 233–279.

Giugliano, L. G., Teixeira, R. D., Colli, G. R. and Báo, S. N. (2002). The ultrastructure of spermatozoa of the lizard *Ameiva ameiva* (Squamata, Teiidae). – *Journal of Morphology* 252.

Harding, H. R., Aplin, K. P. and Mazur, M. 1995. Ultrastructure of spermatozoa of Australian blindsnakes, *Ramphotyphlops* spp. (Typhlopidae, Squamata): first observation on the mature spermatozoon of scolecophidian snakes. In: *Advances in Spermatozoal Phylogeny and Taxonomy* (eds B. G. M. Jamieson, J. Ausió, J. L. Justine), pp. 385–396. Muséum National d'Histoire Naturelle, Paris.

Harvey, P. H. and Pagel, M. D. 1991. *The Comparative Method in Evolutionary Biology*. Oxford University Press, New York.

Herrera, E. A. and Robinson, M. D. 2000. Reproductive and fat body cycles of the tegu lizards, *Tupinambis teguixin*, in the llanos of Venezuela. – *Journal of Herpetology* 34: 598–601.

Jamieson, B. G. M. 1995. The ultrastructure of spermatozoa of the Squamata (Reptilia) with phylogenetic considerations. In: *Advances in Spermatozoal Phylogeny and Taxonomy* (eds B. G. M. Jamieson, J. Ausio, J. Justine), pp. 359–383. Muséum National d'Histoire Naturelle, Paris, France.

Jamieson, B. G. M. and Koehler, L. 1994. The ultrastructure of the spermatozoon of the northern water snake, *Nerodia sipedon* (Colubridae, Serpentes), with phylogenetic considerations. – *Canadian Journal of Zoology* 72: 1648–1652.

Jamieson, B. G. M., Oliver, S. C. and Scheltinga, D. M. 1996. The ultrastructure of spermatozoa of Squamata. I. Scincidae, Gekkonidae and Pygopodidae (Reptilia). – *Acta Zoologica (Stockholm)* 77: 85–100.

Jamieson, B. G. M. and Scheltinga, D. M. 1993. The ultrastructure of spermatozoa of *Nangura spinosa* (Scincidae, Reptilia). – *Memoirs of the Queensland Museum* 34: 169–179.

Jamieson, B. G. M. and Scheltinga, D. M. 1994. The ultrastructure of spermatozoa of the Australian skinks, *Ctenotus taeniolatus*, *Carlia pectoralis* and *Tiliqua scincoides scincoides* (Scincidae, Reptilia). – *Memoirs of the Queensland Museum* 37: 181–193.

Kitching, I. J., Forey, P. L., Humphries, C. J. and Williams, D. M. 1998. *Cladistics. The Theory and Practice of Parsimony Analysis*. Oxford University Press, Oxford.

Maddison, W. P. and Maddison, D. R. 1992. *MacClade: Analysis of Phylogeny and Character Evolution, Version* 3.04. Sinauer Associates Inc, Sunderland, Massachusetts.

McCracken, K. G., Harshman, J., McClellan, D. A. and Afton, A. D. 1999. Data set incongruence and correlated character evolution: an example of functional convergence in the hind-limbs of stifftail diving ducks. – *Systematic Biology* 48: 683–714.

Mori, T. 1995. Comparative sperm structure in bats (Chiroptera): some taxonomic and adaptive implications. In: *Advances in Spermatozoal Phylogeny and Taxonomy* (eds B. G. M. Jamieson, J. Ausio, J.-L. Justine), pp. 421–429. Muséum national d'Histoire naturelle, Paris.

Murphy, R. W. and Doyle, K. D. 1998. Phylophenetics: frequencies and polymorphic characters in genealogical estimation. – *Systematic Biology* 47: 737–761.

Newton, W. D. and Trauth, S. E. 1992. Ultrastructure of the spermatozoon of the lizard *Cnemidophorus sexlineatus* (Sauria: Teiidae). – *Herpetologica* 48: 330–343.

Oliver, S. C., Jamieson, B. G. M. and Scheltinga, D. M. 1996. The ultrastructure of spermatozoa of Squamata. II. Agamidae, Varanidae, Colubridae, Elapidae, and Boidae (Reptilia). – *Herpetologica* 52: 216–241.

Peters, J. A. and Orejas-Miranda, B. 1986. *Catalogue of the Neotropical Squamata. Part II, Lizards and Amphisbaenians* (Revised edn). Smithsonian Institution Press, Washington, D.C.

Presch, W. F. Jr. 1973. A review of the tegus, lizard genus *Tupinambis* (Sauria: Teiidae) from South America. – *Copeia* 1973: 740–746.

Ridley, M. 1993. *Evolution*. Blackwell Scientific Publications, Boston.

Scheltinga, D. M., Jameison, B. G. M., Trauth, S. E. and McAllister, C. T. 2000. Morphology of the spermatozoa of the iguanian lizards *Uta stansburiana* and *Urosaurus ornatus* (Squamata, Phrynosomatidae). – *Journal of Submicroscopic Cytology and Pathology* 32: 261–271.

Schwenk, K. 1993. The evolution of chemoreception in squamate reptiles: a phylogenetic approach. – *Brain Behavior and Evolution* 41: 124–137.

Swofford, D. L. and Berlocher, S. H. 1987. Inferring evolutionary trees from gene frequency data under the principle of maximum parsimony. – *Systematic Zoology* 36: 293–325.

Teixeira, R. D., Colli, G. R. and Báo, S. N. 1999a. The ultrastructure of spermatozoa of the lizard *Polychrus acutirostris* (Squamata, Polychrotidae). – *Journal of Submicroscopic Cytology and Pathology* 31: 387–395.

Teixeira, R. D., Colli, G. R. and Báo, S. N. 1999b. The ultrastructure of the spermatozoa of the lizard *Micrablepharus maximiliani* (Squamata, Gymnophthalmidae), with considerations on the use of sperm ultrastructure characters in phylogenetic reconstruction. – *Acta Zoologica (Stockholm)* 80: 47–59.

Teixeira, R. D., Colli, G. R. and Báo, S. N. 1999c. The ultrastructure of the spermatozoa of the worm-lizard *Amphisbaena alba* (Squamata, Amphisbaenidae), and the phylogenetic relationships of amphisbaenians. – *Canadian Journal of Zoology* 77: 1254–1264.

Teixeira, R. D., Vieira, G. H. C., Colli, G. R. and Báo, S. N. 1999d. Ultrastructural study of spermatozoa of the neotropical lizards, *Tropidurus semitaeniatus* and *Tropidurus torquatus* (Squamata, Tropiduridae). – *Tissue and Cell* 31: 308–317.

Van der Horst, G., Wilson, B. and Channing, A. 1995. Amphibian sperm: phylogeny and fertilization environment. In: *Advances in Spermatozoal Phylogeny and Taxonomy* (eds B. G. M. Jamieson, J. Ausio, J.-L. Justine), pp. 333–342. Muséum national d'Histoire naturelle, Paris.

Wiens, J. J. 1995. Polymorphic characters in phylogenetic systematics. – *Systematic Biology* **44**: 482–500.

Wiens, J. J. 1998. Testing phylogenetic methods with tree congruence: Phylogenetic analysis of polymorphic morphological characters in phrynosomatid lizards. – *Systematic Biology* 47: 427–444.

Wiens, J. J. 1999. Polymorphism in systematics and comparative biology. *Annual Review of Ecology and Systematics* **30**: 327–362.

Wiens, J. J. 2000a. Decoupled evolution of display morphology and display behaviour in phrynosomatid lizards. – *Biological Journal of the Linnean Society* **70**: 597–612.

Wiens, J. J. 2000b. Reconstructing phylogenies from allozyme data: testing method performance with congruence. – *Biological Journal of the Linnean Society* **70**: 613–632.

Wiens, J. J. and Servedio, M. R. 1997. Accuracy of phylogenetic analysis including and excluding polymorphic characters. – *Systematic Biology* **46**: 332–345.

2.1.3 – ARTIGO PUBLICADO 3

TEIXEIRA, Ruscaia Dias; SCHELTINGA, David M; TRAUTH, S E; BÁO, Sônia Nair. A comparative ultrastructural study of spermatozoa of the teiid lizards, *Cnemidophorus gularis gularis*, *Cnemidophorus ocellifer* and *Kentropyx altamazonica* (Reptilia, Squamata, Teiidae). Tissue & Cell, EUA, v. 34, n. 3, p. 135-142, 2002.

Tissue & Cell, 2002 34 (3) 135–142

doi:10.1016/S0040-8166(02)00021-6, available online at http://www.idealibrary.com IDEAL®

Tissue&Cell

A comparative ultrastructural study of spermatozoa of the teiid lizards *Cnemidophorus gularis gularis*, *Cnemidophorus ocellifer*, and *Kentropyx altamazonica* (Reptilia, Squamata, Teiidae)

R. D. Teixeira,[1,2] D. M. Scheltinga,[3] S. E. Trauth,[4] G. R. Colli,[5] S. N. Báo[2]

Abstract. The ultrastructure of the spermatozoa of *Cnemidophorus gularis gularis*, *Cnemidophorus ocellifer*, and *Kentropyx altamazonica* is described for the first time. Mature spermatozoa of *Cnemidophorus* spp. and *K. altamazonica* differ in the occurrence of a perforatorial base plate, the enlargement of axonemal fibers 3 and 8, and shape of mitochondria. The comparisons of the ultrastructure sperm of *Cnemidophorus* spp. and *K. altamazonica* with *Ameiva ameiva* [J. Morphol. (2002) in press] suggest that *Ameiva* and *Cnemidophorus* are more similar to each other than either is to *Kentropyx*. Statistical analyses reveal that sperm of all three species studied are significantly different in the following dimensions: head, acrosome, distal centriole length, and nuclear shoulders width. There was no variable statistically different between the *Cnemidophorus* spp. only. The length of the tail, midpiece, entire sperm, and nuclear rostrum are significantly different between *K. altamazonica* and *Cnemidophorus* spp. Our results indicate that sperm ultrastructure presents intra and intergeneric variability.

Keywords: *Cnemidophorus*, *Kentropyx*, lizards, spermatozoa, Teiidae, ultrastructure

[1]Departamento de Biologia Celular, Universidade Estadual de Campinas, 13083-970 Campinas, SP, Brazil, [2]Departamento de Biologia Celular, Universidade de Brasília, 70919-970 Brasília, DF, Brazil, [3]Department of Zoology and Entomology, University of Queensland, Brisbane, Qld., 4072, Australia, [4]Department of Biological Sciences, Arkansas State University, PO Box 599, State University, AR 72467-0599, USA, [5]Departamento de Zoologia, Universidade de Brasília, 70919-970 Brasília, DF, Brazil

Received 27 December 2001
Revised 25 February 2002
Accepted 26 February 2002

Correspondence to: Professor Sônia Nair Báo, Departamento de Biologia Celular, Universidade de Brasília, 70919-970, Brasília, DF, Brazil; E-mails:ruscaia@hotmail.com, dscheltinga@zen.uq.edu.au, strauth@astate.edu, grcolli@unb.br, snbao@unb.br

Introduction

Although several studies have attempted to clarify the phylogenetic relationships of teiid genera (Vanzolini & Valencia, 1965; Presch, 1974; Rieppel, 1980), additional studies are necessary to develop a comprehensive phylogenetic hypothesis for the family. Several detailed studies have revealed that sperm character data sets contain significant phylogenetic information which can be used in phylogenetic analyses (Jamieson, 1995, 1999; Teixeira et al., 1999a,b). However, high levels of polymorphism in sperm characters of the teiids *Cnemidophorus sexlineatus* (Newton & Trauth, 1992) and

Ameiva ameiva (Giugliano et al., 2002), and within the teiid genus *Tupinambis* (Tavares-Bastos et al., 2002) have recently been revealed. Thus, intrafamilial variability might be higher than currently thought. Although variability in sperm characters may be a problem in phylogenetic reconstruction, their exclusion from analyses may lead to reduced accuracy (Wiens, 1995). Hence, additional studies on sperm ultrastructure of teiid genera are essential to clarify the level of variability within the family and to assist in the resolution of phylogenetic relationships of teiids.

The Texas spotted whiptail, *Cnemidophorus gularis gularis*, is a moderately sized lizard and is one of 22 or so bisexual members of the *C. sexlineatus* species group (Wright, 1993). It ranges from southern Oklahoma to northern Mexico and from eastern Texas to southeastern New Mexico and southwestern Texas. Seven subspecies have been recognized, but the actual number remains in dispute (Degenhardt et al., 1996). *Cnemidophorus ocellifer* has a wide distribution in South America, ranging from northeastern and central Brazil to northern Argentina (Vanzolini et al., 1980; Peters & Orejas-Miranda, 1986; Colli et al., 1998). Several studies have suggested that *C. ocellifer* is actually a complex of species (Rocha et al., 1997, 2000). *Kentropyx altamazonica* is a South American lizard which occurs in open areas of Amazonia, Brazil (Avila-Pires, 1995). The genus *Kentropyx* is a well-defined taxonomic group, being the only teiid genus to possess phyloid keeled scutes (Magnusson & Lima, 1984; Gallagher et al., 1986).

The mature spermatozoa of the teiids *C. sexlineatus* (Newton & Trauth, 1992), *A. ameiva* (Giugliano et al., 2002), and four species of *Tupinambis* (*T. duseni*, *T. merianae*, *T. quadrilineatus*, and *T. teguixin*) (Tavares-Bastos et al., 2002) have been previously examined. We here provide, for the first time, a detailed description of the mature spermatozoa of *C. gularis gularis*, *C. ocellifer*, and *K. altamazonica*. Further, we perform statistical analyses of sperm dimensions of the three species, to determine the presence of any significant difference and to ascertain the degree of intrafamilial and intergeneric variability.

Material and methods

Spermatozoal ultrastructure

Mature spermatozoa were obtained from adult specimens of *C. gularis gularis* (Arkansas State University Museum of Zoology, ASUMZ 19019, 18959) collected at Llano County and Somervell County, TX, USA, *C. ocellifer* (Coleção Herpetológica da Universidade de Brasília, CHUNB 16943, 16944) collected at Pirinópolis, Goiás State, Brazil, and *K. altamazonica* (CHUNB 5777, 5784) collected at Vilhena, Rondônia State, Brazil.

Two specimens of *C. gularis gularis* were killed by an injection of sodium pentabarbitol within 72 h of capture. Histotechnical procedures as discussed by Newton and Trauth (1992) were employed to prepare gonads and sperm ducts for transmission electron microscopy (TEM). Testes and

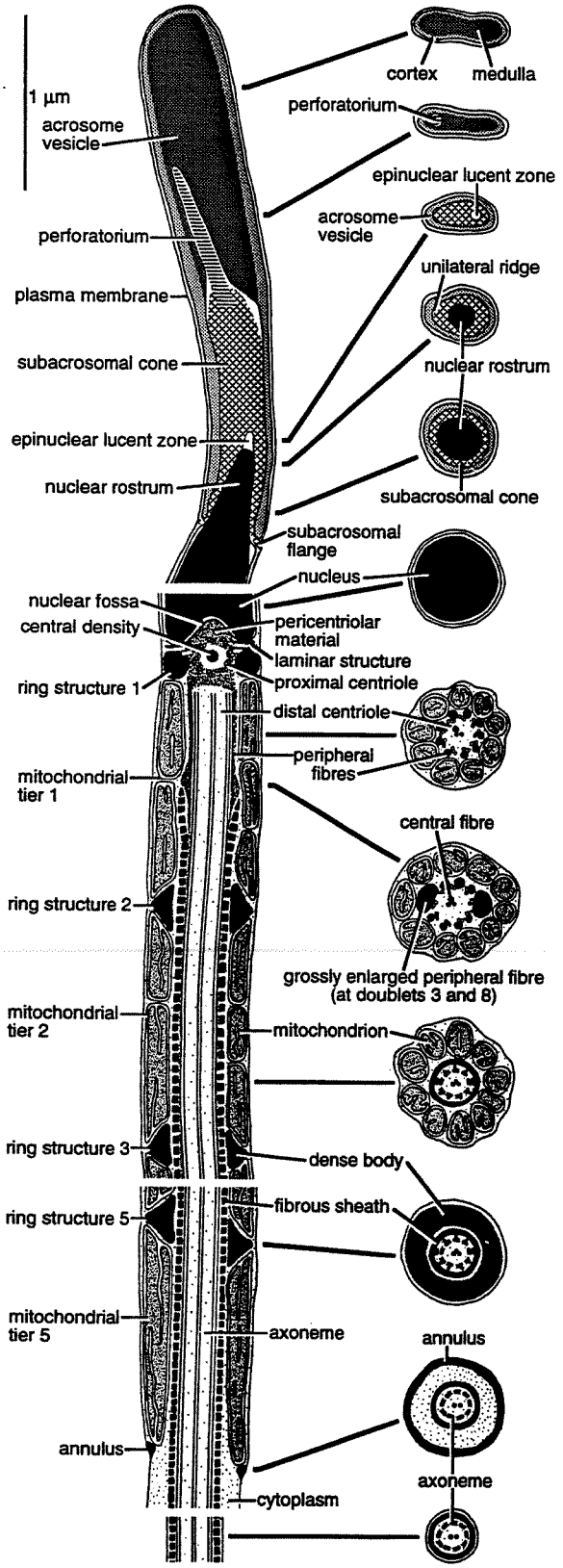

Fig. 1 *Kentropyx altamazonica*. Drawing of a spermatozoon, in longitudinal and corresponding transverse sections. Drawn from several TEM micrographs.

epididymides were placed into separate vials containing 2% glutaraldehyde in 0.2 M sodium cacodylate buffer (pH 7.2). Following fixation for 2 h in this solution, the material was rinsed in four changes of 0.1 M cacodylate buffer; postfixed in similarly buffered 1% osmium tetroxide; rinsed in buffer; dehydrated through an ascending series of ethanol/acetone mixtures; infiltrated overnight in a dilute acetone/epoxy resin mixture, and embedded in Mollenhauer's Epon–Araldite mixture number 2. The embedded tissues were then transported to Brisbane, Australia for sectioning and TEM.

Specimens of *C. ocellifer* and *K. altamazonica* were killed by an injection of Tiopental®. Epididymides were removed and placed in a Petri dish with phosphate-buffered saline (PBS), pH 7.2, and cut into small pieces. Epididymal tissues were then fixed in a solution containing 2.5% glutaraldehyde, 2% paraformaldehyde, and 3% sucrose in 0.1 M sodium cacodylate buffer, pH 7.2, at 4 °C overnight. Tissue samples were then rinsed in 0.1 M phosphate buffer, pH 7.2, postfixed for 80 min in similarly buffered 1% osmium tetroxide; rinsed in buffer; dehydrated through series of ascending acetone series (30–100%) and embedded in Spurr's epoxy resin. Ultrathin sections were stained for 30 s in Reynold's lead citrate, rinsed in distilled water, then in 6% aqueous uranyl acetate for 4 min, rinsed in distilled water, and stained for a further 2 min in lead citrate before final rinsing. Electron micrographs were taken on a Hitachi 300 transmission electron microscope at 75 kV.

Light microscopic observations and photographs of glutaraldehyde–paraformaldehyde fixed smears of *C. ocellifer* and *K. altamazonica* spermatozoa were made under Nomarski interference contrast using an Olympus BH2 microscope and an attached OM-2 camera. Measurements of *C. gularis gularis* spermatozoa were taken from scanning electron micrographs, tissues processed for scanning electron microscopy (SEM) as per Newton and Trauth (1992).

Statistical analyses

The following dimensions were measured from micrographs of each species: head length, tail length, entire sperm length, midpiece length, acrosome length, nucleus base width, nuclear rostrum length, distal centriole length, epinuclear lucent zone length and width, nuclear shoulder width, ratio principal piece diameter just posterior to annulus to midpiece diameter just anterior to annulus, and ratio principal piece diameter to fibrous sheath diameter just posterior to annulus. Since the assumption of normality was not met, original variables were ranked prior to analyses. To test the null hypothesis of no difference in sperm dimensions among the three species, a separate analysis of variance (ANOVA) was performed for each variable. This univariate approach was adopted because complete sets of measurements could not be obtained from individual cells. To avoid the inflation of Type I error, the Bonferroni procedure was adopted: the significance level of 5% was divided by the number of tests (13), resulting in a significance level of 0.3% (Zar, 1998). The Tukey test was used to test for pairwise differences among means. Statistical analyses were conducted with SAS v. 8.0 and Systat v. 9.0 for Windows. Throughout the text, means are given ±1 SD.

Results

Spermatozoal ultrastructure

The spermatozoa of *K. altamazonica* (Fig. 3), *C. gularis gularis*, and *C. ocellifer* (Fig. 2) are filiform, consisting of a head region containing acrosomal structures and the nucleus, a midpiece, and a tail region subdivided into principal piece and endpiece (Fig. 2Q & R). The spermatozoa of all three species are sufficiently similar to be described together with any differences noted. The spermatozoon of *K. altamazonica* is depicted diagrammatically in Figure 1. Dimensions of the sperm are provided in Table 1.

Table 1 Sperm dimensions in *Cnemidophorus gularis gularis*, *Cnemidophorus ocellifer*, and *Kentropyx altamazonica*

Characters	*Cnemidophorus gularis gularis*	*Cnemidophorus ocellifer*	*Kentropyx altamazonica*	*F*	*P*
HL	10.83 ± 0.29 ($n = 3$) a	13.30 ± 0.61 ($n = 14$) b	14.71 ± 0.45 ($n = 13$) c	53.56	<0.001*
TL	40.25 ± 0.35 ($n = 2$) a	40.13 ± 2.82 ($n = 7$) a	53.64 ± 2.81 ($n = 8$) b	22.40	<0.001*
ESL	54.50 ± 0.00 ($n = 2$) a	56.42 ± 2.09 ($n = 11$) a	75.58 ± 2.49 ($n = 10$) b	33.90	<0.001*
MPL	3.48 ± 0.27 ($n = 5$) a	3.35 ± 0.32 ($n = 9$) a	7.55 ± 0.35 ($n = 8$) b	24.00	<0.001*
AL	3.96 ± 0.11 ($n = 8$) a	3.08 ± 0.14 ($n = 6$) b	3.44 ± 0.22 ($n = 8$) c	15.05	0.0001*
NBW	0.68 ± 0.04 ($n = 5$) a	0.53 ± 0.03 ($n = 3$) a	0.64 ± 0.03 ($n = 3$) a	9.18	0.0085
NRL	0.77 ± 0.03 ($n = 5$) a	0.71 ± 0.05 ($n = 10$) a	0.62 ± 0.05 ($n = 10$) b	20.21	<0.0001*
DCL	0.92 ± 0.11 ($n = 6$) a	0.72 ± 0.07 ($n = 7$) b	0.65 ± 0.03 ($n = 7$) c	24.40	<0.0001*
ETL	3.96 ± 0.11 ($n = 5$) a	3.08 ± 0.14 ($n = 6$) a	3.44 ± 0.22 ($n = 7$) a	3.89	0.04
ETW	0.05 ± 0.01 ($n = 4$) a	0.04 ± 0.00 ($n = 5$) a	0.04 ± 0.01 ($n = 7$) a	0.68	0.52
NSW	0.5 ± 0.02 ($n = 5$) a	0.37 ± 0.02 ($n = 4$) b	0.42 ± 0.03 ($n = 5$) c	35.44	<0.0001*
RD	1.00 ± 0.00 ($n = 3$) a	0.96 ± 0.04 ($n = 3$) a	0.95 ± 0.01 ($n = 2$) a	2.79	0.15
RC	1.78 ± 0.24 ($n = 3$) a	1.89 ± 0.22 ($n = 3$) a	1.96 ± 0.06 ($n = 2$) a	0.44	0.66

Values in micrometers and represented by means ±1 SD. *F* values are for ANOVA. Asterisk (*) indicates means of sperm characters are significantly different at the 0.3% level, using the Bonferroni method. Different letters represent significant differences at the 5% level using the Tukey multiple comparisons test. HL: head length, TL: tail length, ESL: entire sperm length, MPL: midpiece length, AL: acrosome length, NBW: nucleus base width, NRL: nuclear rostrum length, DCL: distal centriole length, ETL: epinuclear lucent zone length, ETW: epinuclear lucent zone width, NSW: nuclear shoulders width, RD: ratio diameter of the principal piece diameter to midpiece diameter, and RC: ratio cytoplasm between fibrous sheath to principal diameter.

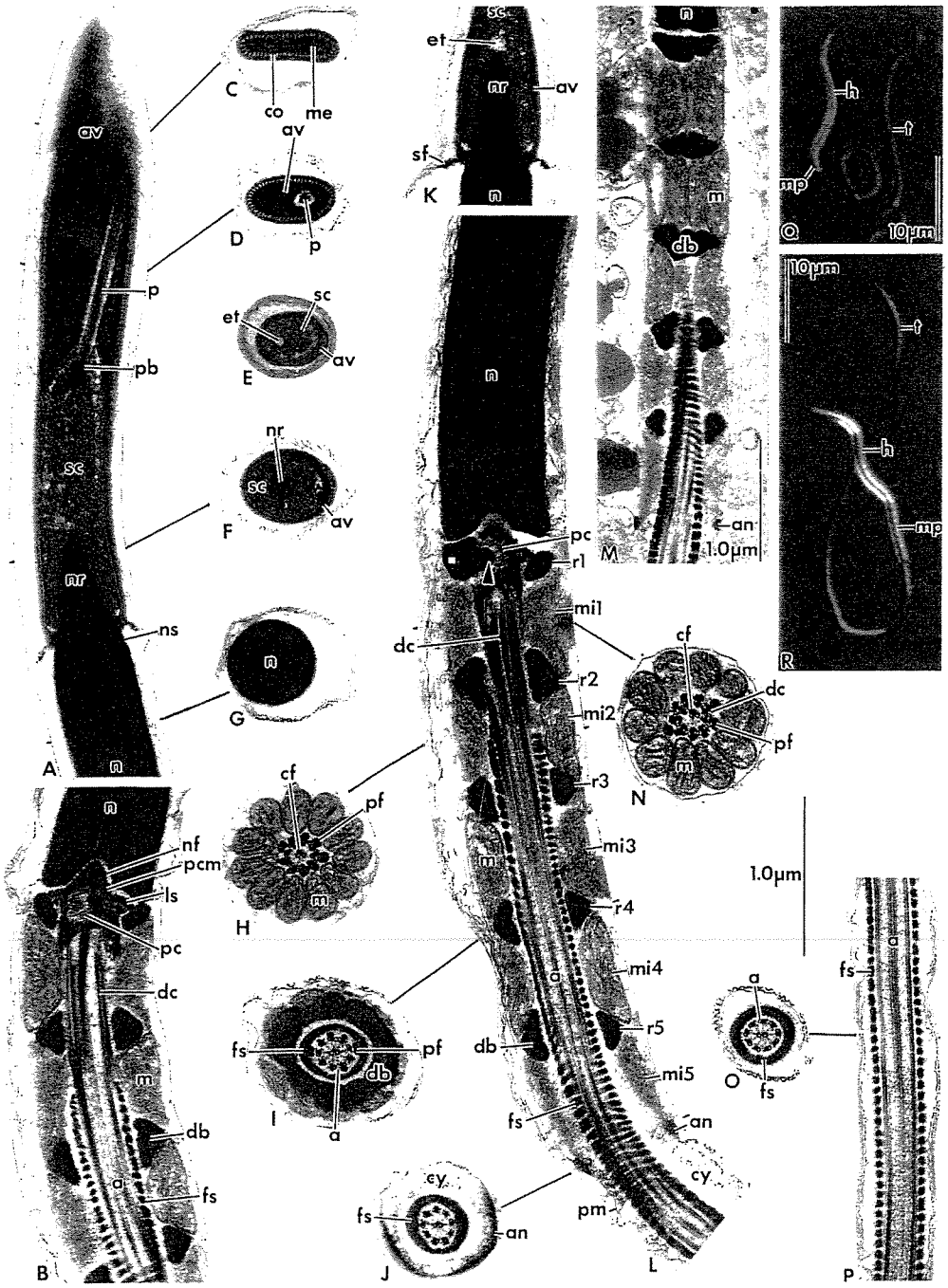

Fig. 2 Spermatozoa of *Cnemidophorus gularis gularis* (A–D, F–L, & N–P) and *Cnemidophorus ocellifer* (E, M). (A–P) Transmission electron micrographs. (A) Longitudinal section (LS) through the acrosome complex showing the acrosome vesicle with cortex and medulla, the subacrosomal cone, and perforatorium. Note the stopper-like perforatorium base plate. (B) LS of the anterior portion of the midpiece showing the neck region with the nuclear fossa, pericentriolar material, centrioles, and the stratified laminar structure. (C–J) A series of transverse sections (TSs) through the spermatozoon as indicated. Note that anteriorly, (C & D), the acrosome appears depressed, while posteriorly, (E & F), it is unilaterally ridged, (G) through the nucleus, (H) through posterior portion of the distal centriole, (I) through the complete dense body ring structure of the midpiece showing the peripheral fibers 3 and 8 thicker than the others, double and detached from their doublets, (J) through the annulus level. (K) LS of the nucleus rostrum. Note the epinuclear lucent zone at the nucleus tip. (L) LS of the full length of the midpiece showing five ring structures and mitochondrial tiers. Arrow indicates extension of dense body into center of the proximal centriole. (M) Oblique LS of the midpiece showing the mitochondrial and dense body arrangement. (N) TS through anterior portion of the distal centriole. (O) TS through the principal piece. (P) LS through the principal piece. (Q & R) Light micrographs showing whole spermatozoon of (Q) *C. ocellifer* and (R) *Kentropyx altamazonica*. (A–P) Same scale as indicated. Abbreviations, a: axoneme; an: annulus; av: acrosome vesicle; cf: central fiber; co: cortex; cy: cytoplasm; db: dense bodies; dc: distal centriole; et: epinuclear lucent zone; fs: fibrous sheath; h: head; ls: stratified laminar structure; m: mitochondrion; me: medulla; mi: mitochondrial tier; mp: midpiece; n: nucleus; nf: nuclear fossa; nr: nuclear rostrum; ns: nuclear shoulder; p: perforatorium; pb: perforatorial base plate; pc: proximal centriole; pcm: pericentriolar material; pf: peripheral fiber; pm:plasma membrane; rs: dense body ring structure; sc: subacrosomal cone; sf: flange of the subacrosomal material; t: tail.

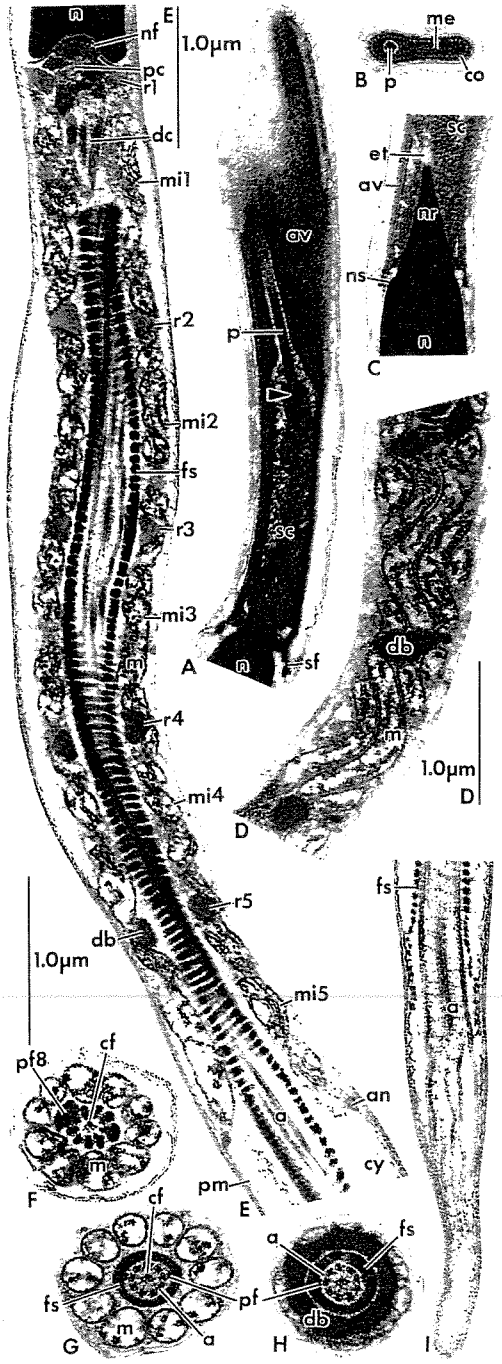

Fig. 3 Spermatozoa of *Kentropyx altamazonica*. (A–I) Transmission electron micrographs. (A) Longitudinal section (LS) through the acrosome showing the acrosome vesicle surrounding the subacrosomal cone and perforatorium. Arrow indicates a densification of the subacrosomal cone, may be a perforatorial base plate. (B) Transverse section (TS) through the anterior depressed portion of the acrosome. (C) LS through the nucleus rostrum. Note the epinuclear lucent zone at the nucleus tip. (D) Oblique LS of the midpiece, showing the mitochondrial and dense body arrangement. (E) LS through the entire length of the midpiece showing five dense body ring structures and mitochondrial tiers. (F) TS through posterior portion of the distal centriole showing that peripheral fibers 3 and 8 are grossly enlarged. (G) TS through the midpiece showing peripheral fibers 3 and 8 thicker than the others and detached from their doublets. (H) TS through a complete dense body ring structure of the midpiece. (I) LS through the posterior portion of the principal piece and the endpiece. (A–C) and (F–I) Same scale as indicated. (D & E) Scale as indicated. Abbreviations.

a: axoneme; an: annulus; av: acrosome vesicle; cf: central fiber; co: cortex; cy: cytoplasm; db: dense body; dc: distal centriole; et: epinuclear lucent zone; fs: fibrous sheath; m: mitochondrion; me: medulla; mi: mitochondrial tier; n: nucleus; nf: nuclear fossa; nr: nuclear rostrum; ns: nuclear shoulder; p: perforatorium; pc: proximal centriole; pf: peripheral fiber; pf8: peripheral fiber at doublet 8; pm: plasma membrane; rs: dense body ring structure; sc: subacrosomal cone; sf: flange of subacrosomal material.

Acrosome complex

The acrosome complex is long and flattened apically and consists of two caps: an external cap, the acrosome vesicle, and an internal cap, the subacrosomal cone (Figs 2A & 3A). In cross-section, the acrosome vesicle is depressed apically (Figs 2C & 3B), becoming circular at its base (Fig. 2D–F). Within approximately the basal one third of the acrosome, the acrosome surface presents a lateral ridge, formed by a longitudinal protuberance of the acrosome vesicle (Fig. 2E). The acrosome vesicle caps the subacrosomal cone and is uniformly divided into a narrow cortex and a wide medulla at its anterior portion (Figs 2C, D, & 3B). In transverse (Figs 2C, D, & 3B) and longitudinal sections (Figs 2A & 3A), the cortex exhibits a tubular organization. The medulla appears as a moderately electron-dense structure, filling the interior of the acrosome vesicle. The subacrosomal cone surrounds the tapered anterior end of the nucleus and exhibits a paracrystalline structure (Fig. 2E & F). The single perforatorium extends from the anterior region of the subacrosomal cone into the acrosome vesicle and ends with a rounded tip (Figs 2A & 3A). Apically, the perforatorium is not axial and in cross-section can be observed to occur outside the central one third of the flattened acrosome (Figs 2D & 3B). The two species of *Cnemidophorus* posses a stopper-like perforatorial base plate, embedded in the apex of the subacrosomal cone (Fig. 2A). In *K. altamazonica*, there is a slight densification between the base of the perforatorium and the anterior extremity of the subacrosomal cone. However, we do not consider this feature to be a perforatorial base plate. Within the anterior limit of the subacrosomal cone, anterior to the condensed chromatin of the nuclear rostrum, an epinuclear electron lucent zone is present (Figs 2K & 3C).

Nucleus

The nucleus is elongated and composed of highly condensed, electron-dense chromatin. In transverse section, the nucleus is circular throughout (Fig. 2F & G). At its anterior extremity, the nucleus forms a point within the acrosome complex, the nuclear rostrum. The transition from the nuclear rostrum to the cylindrical portion of the nucleus is abrupt and marked by rounded nuclear shoulders (Figs 2A, K, & 3C). Basally the nucleus terminates with a shallow concave depression, the nuclear fossa, which houses the anterior half of the proximal centriole and dense pericentriolar material (Figs 2B, L, & 3E).

Neck region

The neck region lies at the junction between nucleus and midpiece. It contains the proximal and distal centrioles, the

first ring of dense bodies, and mitochondria (Figs 2B, L, & 3E). The proximal centriole is composed of nine short triplets and lies at approximately 80° to the long axis of the spermatozoon (Figs 2B, L, & 3E). A short, solid cylinder of electron-dense material extends from the first dense body ring structure into the center of the proximal centriole, for approximately half its length (Fig. 2L). The distal centriole constitutes the basal body of the axoneme. It is perpendicular to the proximal centriole, occupying a small fraction of the midpiece, and does not project into the fibrous sheath (Fig. 2B & L). Dense pericentriolar material surrounds the proximal centriole and extends into the nuclear fossa. Posteriorly, it contacts the anterior portion of the distal centriole and provides a base for the nine peripheral dense fibers (Fig. 2B & L). A poorly developed striated density, termed the stratified laminar structure, is continuous with the pericentriolar material and projects laterally from both sides of the anterior limit of the proximal centriole (Fig. 2B).

Midpiece

The midpiece lies at the anterior portion of the flagellum. It includes the neck region and consists of the axoneme surrounded by mitochondria, rings of dense bodies, and the fibrous sheath (Figs 2B, H, I, L–N, & 3D–H). The midpiece begins with the first ring of dense bodies and ends posteriorly at a small annulus (Figs 2L, M, & 3E). The dense bodies occur as complete regular ring structures with a solid homogenous composition (Figs 2B, I, L, M, & 3D, E, H). In transverse section, these ring structures appear juxtaposed to the fibrous sheath (Figs 2I & 3H). The dense bodies are separated longitudinally by one tier of columnar mitochondria. In *K. altamazonica*, the average distance between the ring structures is 1.29 μm, while in the two species of *Cnemidophorus* the distance is 0.44–0.45 μm. The ring structure and mitochondria arrangement pattern can be represented by the expression rs1/mi1, rs2/mi2, rs3/mi3, rs4/mi4, rs5/mi5, (Figs 2L & 3E). In both species of *Cnemidophorus*, the mitochondria, when viewed in oblique section (Fig. 2M), extend anterioposteriorly along the midpiece in a strictly columnar appearance, while in longitudinal section they appear trapezoidal (Fig. 2B & L). In *K. altamazonica*, the columnar mitochondria have a regular, slightly curved appearance in oblique section (Fig. 3D). These mitochondria are not considered to be short sinuous tubes because they do not curve at an angle of greater than 45° and back upon themselves. In *K. altamazonica*, the ends of the mitochondria have a rounded shape as observed in longitudinal section (Fig. 3E).

The axial component of the midpiece is the axoneme, which is composed of a pair of central microtubules (singlets) surrounded by nine doublets of microtubules. The singlets of the axoneme extend anteriorly throughout the length of the distal centriole (Figs 2H, N, & 3F). Associated with the two singlets is a central fiber which is anteriorly located closer to triplet 9; posteriorly it decreases in size and is positioned centrally between the singlets of the axoneme (Figs 2H, I, N, & 3F–H). The central fiber is vestigial at the level of the annulus (Fig. 2J).

A peripheral dense fiber is associated with each of the nine triplets of the distal centriole (Figs 2H, N, & 3F). For a short distance, at the level of the distal centriole/axoneme junction, the peripheral fibers adjacent to doublets 3 and 8 appear grossly enlarged in *K. altamazonica* (Fig. 3F), whereas in *Cnemidophorus* the peripheral fibers associated with the distal centriole are all of a similar size. In all species, the nine peripheral fibers rapidly decrease in diameter posteriorly along the axoneme, with the exception of the fibers at doublets 3 and 8, which are thicker and form double fiber structures which are separated from their corresponding doublets and become closely associated with the fibrous sheath. At the level of the annulus, all nine dense fibers are vestigial or absent (Fig. 2J).

The fibrous sheath encloses the axoneme and extends into the midpiece, reaching the base of the distal centriole (Figs 2L & 3E). In both species of *Cnemidophorus*, the fibrous sheath extends anteriorly into the midpiece to the level of mitochondrial tier 2 (mi2) (Fig. 2B & L), occupying 68–69% of the total midpiece length. In *K. altamazonica*, the fibrous sheath extends to the level of the first mitochondrial tier (mi1) (Fig. 3E), occupying 87% of the total midpiece length.

The annulus (Figs 2J, L, M, & 3E) is a small dense ring with an irregular triangular shape in longitudinal section. It is closely attached to the inner surface of the plasma membrane and marks the end of the midpiece.

Principal piece

The principal piece is the longest part of the spermatozoon and occurs behind the midpiece. It consists of the axoneme surrounded by fibrous sheath, cytoplasm, and plasma membrane. In this region, all dense fibers, dense bodies, and mitochondria are absent (Fig. 2O & P). In the anterior portion of the principal piece, immediately after the annulus, the diameter of the spermatozoon does not decrease relative to the annulus diameter and the plasma membrane is widely separated from the fibrous sheath by a thick region of granular cytoplasm (Figs 2L & 3E; Table 1). Posteriorly, the plasma membrane becomes closely attached to the fibrous sheath (Fig. 2P).

Endpiece

A short length of axoneme extends beyond the posterior limit of the fibrous sheath as the endpiece (Fig. 3I). Posteriorly within the endpiece, the arrangement of microtubules becomes disrupted (Fig. 3I).

Comparisons of spermatozoal dimensions

All three species differed significantly in the dimensions of head, acrosome, distal centriole lengths, and nuclear shoulder width (Table 1). Lengths of the tail, entire sperm, midpiece, and nuclear rostrum were significantly different between *K. altamazonica* and *C. gularis gularis*, and between *K. altamazonica* and *C. ocellifer*, but not between the two species of *Cnemidophorus*. There was no statistical difference between any of the three species in nuclear base width, epinuclear lucent zone width or length, ratio of the diameter of the

anterior principal piece to midpiece diameter, or the amount of cytoplasm within the anterior region of the principal piece (ratio of diameter of fibrous sheath to principal piece diameter) (Table 1).

Discussion

The spermatozoa *C. gularis gularis*, *C. ocellifer*, and *K. altamazonica* exhibit the following squamate synapomorphies: a single wholly prenuclear perforatorium, endonuclear canal absent, paracrystalline subacrosomal material, mitochondrial cristae linear, intermitochondrial dense bodies present, and fibrous sheath extending into midpiece (Jamieson & Healy, 1992).

The three species of teiids studied share several characteristics in sperm ultrastructure: apical portion of acrosome depressed; acrosome vesicle divided into medulla and cortex; cortex with tubular organization; anterior portion of perforatorium positioned outside central one third of the flattened acrosome; epinuclear lucent zone short and thin; nuclear rostrum short; nucleus narrow basally; stratified laminar structure bilateral, poorly developed; central dense body within proximal centriole; distal centriole moderately long; midpiece short; mitochondria columnar; dense bodies solid, in regular and complete rings, juxtaposed to the fibrous sheath; ring structures of dense bodies separated by mitochondrial tiers; and thick zone of cytoplasm between plasma membrane and fibrous sheath in the anterior portion of principal piece.

Based on morphological data sets, Vanzolini and Valencia (1965) and Presch (1970) have suggested the presence of two groups within the family. One group is comprised of the genera *Callopistes*, *Crocodilurus*, *Tupinambis*, and *Dracaena* (subfamily Tupinambinae) and the other is comprised of *Cnemidophorus*, *Ameiva*, *Teius*, *Kentropyx*, and *Dicrodon* (subfamily Teiinae). This division is corroborated by one spermatozoal trait, the number of dense body ring structures, and mitochondrial tiers in the midpiece. In *Cnemidophorus*, *A. ameiva* (Giugliano et al., 2002), and *K. altamazonica*, the midpiece has five sets of mitochondria intercalated with five sets of dense bodies, while in *Tupinambis*, Tavares-Bastos et al. (2002) observed six sets in *T. quadrilineatus* and *T. teguixin*, seven sets in *T. duseni*, and eight sets in *T. merianae*. However, despite members of Teiinae sharing more morphological characters with each other than with members of Tupinambinae (Presch, 1970), *Cnemidophorus* and *A. ameiva* share more sperm characters with *Tupinambis* than with *K. altamazonica*. The mitochondria of *K. altamazonica* are round ended while those of *Cnemidophorus*, *A. ameiva* (Giugliano et al., 2002), and *Tupinambis* (Tavares-Bastos et al., 2002) appear trapezoidal in longitudinal section. In *K. altamazonica*, the fibrous sheath occupies 87% of the entire midpiece, the highest proportion among all teiids studied. In *A. ameiva* (Giugliano et al., 2002), the fibrous sheath occupies 75% of midpiece, in *Cnemidophorus* 68–69%, and in *Tupinambis* (Tavares-Bastos et al., 2002) it occupies 61–63%. The average distance between ring structures of the midpiece is 1.29 μm in *K. altamazonica*, 0.75 μm in *A. ameiva* (Giugliano et al., 2002), 0.45 μm in *Cnemidophorus*, and 0.27 μm in *Tupinambis* spp. (Tavares-Bastos et al., 2002), being two, three, and five times longer in *K. altamazonica* than in the other teiid genera, respectively. The mitochondria in *K. altamazonica* are longer and slightly curved, while in all other teiids studied, the mitochondria are straight and strictly columnar. These differences suggest that, among all these species examined, *K. altamazonica* sperm may be the most derived. Comparisons of the sperm of *Cnemidophorus* spp. and *K. altamazonica* with that of previously examined teiids ultrastructure sperm indicate that the tubular organization observed in the cortex of the acrosomal vesicle is also present in *A. ameiva* (Giugliano et al., 2002) and *Tupinambis* spp. (Tavares-Bastos et al., 2002). This feature seems to be an autapomorphy of the teiid lizards, however, more research on the other teiid genera sperm structure is needed to ascertain this character.

Cnemidophorus is regarded as the sister taxon of *Ameiva* (Vanzolini & Valencia, 1965). The only morphological character that distinguishes *Cnemidophorus* from *Ameiva* is the presence of a tongue sheath in *Ameiva* (Presch, 1971). From sperm ultrastructure data, there are three characters that differ between the two genera: the absence of grossly enlarged fibers 3 and 8 at the distal centriole/axoneme junction in *Cnemidophorus* (present in *A. ameiva*), a slightly decreasing principal piece diameter immediately after annulus in *A. ameiva* (no decrease in *Cnemidophorus*); and the beginning of the fibrous sheath at mi2 in *Cnemidophorus* and at mi1 in *A. ameiva* (Giugliano et al., 2002).

The two Teiinae species previously studied, *C. sexlineatus* (Newton & Trauth, 1992) and *A. ameiva* (Giugliano et al., 2002), show the same sperm characters as those species described here. According to Presch (1970), *Kentropyx* is closer to *Ameiva* and *Cnemidophorus* than to other Teiinae genera (*Teius* and *Dicrodon*). The unique character that distinguishes *Kentropyx* from *Ameiva* and *Cnemidophorus* is the shape of the parietal–frontal roof (Presch, 1974). Spermatozoal ultrastructure distinguishes *K. altamazonica* from *A. ameiva* (Giugliano et al., 2002) and *Cnemidophorus* in two features: the absence of a real perforatorial base plate and the presence of mitochondria with rounded ends instead of a trapezoidal shape in longitudinal section in the former. The sperm of *K. altamazonica* and *A. ameiva* (Giugliano et al., 2002) are similar to each other and differ from those of *Cnemidophorus* in having peripheral fibers 3 and 8 grossly enlarged at the level of the distal centriole/axoneme junction and the fibrous sheath beginning at the level of mi1. In contrast to *A. ameiva* (Giugliano et al., 2002), the principal piece of *K. altamazonica* sperm does not decrease in diameter immediately after the annulus. These results thus reveal that among the three genera of Teiinae studied, *Ameiva* shares two unique features with *Cnemidophorus* and *Kentropyx*, respectively, while *Kentropyx* and *Cnemidophorus* share only one unique feature, suggesting that *Ameiva* and *Cnemidophorus* may be more similar to each other than either is to *Kentropyx* [*Kentropyx* + (*Ameiva* + *Cnemidophorus*)].

This study has revealed that *Cnemidophorus* and *Kentropyx* sperm differ in three ultrastructural characters: presence of base plate, gross enlargement of peripheral fibers, and in the shape of the mitochondria. Furthermore, statistical analyses of the dimensions of 13 sperm characters found that four were significantly different between *Cnemidophorus* and *Kentropyx*, distinguishing these two genera. These results suggest high levels of intrafamily polymorphism in sperm ultrastructure within Teiidae. Conversely, the intrageneric variability appears to be relatively low, with sperm morphology of the congeneric *C. gularis gularis* and *C. ocellifer* being practically identical. They differ only in the dimensions of four sperm characters, i.e. head, acrosome, distal centriole lengths, and nuclear shoulder width. Additional work describing spermatozoal ultrastructure and statistical analyses of sperm dimensions of the teiid genera *Callopistes*, *Crocodilurus*, *Dicrodon*, *Dracaena*, and *Teius* are warranted to determine the real degree of variability in sperm ultrastructure between teiid genera and may cast light on the phylogenetic relationships of teiids.

ACKNOWLEDGEMENTS

We thank Adrian A. Garda, Daniel Diniz, and Renato G. Faria for assistance during fieldwork, and Daniel O. Mesquita and Gustavo H.C. Vieira for assistance with statistical analyses. Barrie G.M. Jamieson provided insightful comments on an earlier version of the manuscript. This work was supported by the School of Life Sciences and Department of Zoology and Entomology at the University of Queensland, CAPES, and CNPq.

REFERENCES

Avila-Pires, T.C.S. 1995. Lizards of Brazilian Amazonia. Nationaal Natuurhistorisch Museum, Alblasserdam, pp 514–516.

Colli, G.R., Péres Jr., A.K. and da Cunha, H.J. 1998. A new species of *Tupinambis* (Sauria, Teiidae) from central Brazil, with an analysis of morphological and genetic variation in the genus. Herpetologica, 54, 477–492.

Degenhardt, W.G., Painter, C.W. and Price, A.H. 1996. Amphibians and Reptiles of New Mexico. University New Mexico Press, Albuquerque, p 431.

Gallagher Jr., D.S., Dixon, J.R. and Schmidly, D.J. 1986. Geographic variation in the *Kentropyx calcarata* species group (Sauria: Teiidae): a possible example of morphological character displacement. J. Herpetol., 20, 179–189.

Giugliano, L.G., Teixeira, R.D., Colli, G.R. and Báo, S.N. 2002. The ultrastructure of spermatozoa of the lizard *Ameiva ameiva* (Squamata, Teiidae). J. Morphol., 252, in press.

Jamieson, B.G.M. 1995. The ultrastructure of spermatozoa of the Squamata (Reptilia) with phylogenetic considerations. In: Jamieson, B.G.M., Ausio, J. and Justine J. (eds) Advances in Spermatozoal Phylogeny and Taxonomy. Muséum National d'Histoire Naturelle Paris, France, pp 359–383.

Jamieson, B.G.M. 1999. Spermatozoal phylogeny of the vertebrata. In: Gagnon, C. (ed) The Male Gamete: From Basic Science to Clinical Applications. Cache River Press, Vienna, Illinois, pp 303–331.

Jamieson, B.G.M. and Healy, J.M. 1992. The phylogenetic position of the tuatara *Sphenodon* (Sphenodontidae, Amniota), as indicated by cladistic analysis of the ultrastructure of spermatozoa. Phil. Trans. R. Soc. Lond. Biol. B: Biol. Sci., 335, 207–219.

Magnusson, W.E. and Lima, A.P. 1984. Perennial communal nesting by *Kentropyx calcaratus*. J. Herpetol., 18, 73–75.

Newton, W.D. and Trauth, S.E. 1992. Ultrastructure of the spermatozoon of the lizard *Cnemidophorus sexlineatus* (Sauria: Teiidae). Herpetologica, 48, 330–343.

Peters, J.A. and Orejas-Miranda, B. 1986. Catalogue of the Neotropical Squamata. Part II, Lizards and Amphisbaenians. Smithsonian Institution Press, Washington, D.C., p 293.

Presch Jr., W.R. 1970. The evolution of macroteiid lizards: an osteological interpretation. Ph.D. Thesis, University of Southern California, Los Angeles, CA.

Presch Jr., W.R. 1971. Tongue structure of the teiid lizard genera *Ameiva* and *Cnemidophorus* with a realocation of *Ameiva vanzoi*. J. Herpetol., 5, 183–185.

Presch Jr., W.F. 1974. Evolutionary relationships and biogeography of the macroteiid lizards (Family Teiidae, Subfamily Teiinae). Bull. Soc. Calif. Acad. Sci., 73, 23–32.

Rieppel, O. 1980. The trigeminal jaw adductor musculature of *Tupinambis*, with comments on the phylogenetic relationships of the Teiidae (Reptilia, Lacertilia). Zool. J. Linn. Soc., 69, 1–29.

Rocha, C.F.D., Araujo, A.F.B., Vrcibradic, D. and Costa, E.M.M. 2000. New *Cnemidophorus* (Squamata Teiidae) from coastal Rio de Janeiro state, southeastern Brazil. Copeia, 2000, 501–509.

Rocha, C.F.D., Bergallo, H.G. and Peccinini-Seale, D. 1997. Evidence of an unisexual population of the Brazilian whiptail lizard genus *Cnemidophorus* (Teiidae), with description of a new species. Herpetologica, 53, 374–382.

Tavares-Bastos, L., Teixeira, R.D., Colli, G.R. and Báo, S.N. 2002. Polymorphism in the sperm ultrastructure among four species of lizards in the genus *Tupinambis* (Squamata: Teiidae). Acta Zool. (Stockholm), 83, in press.

Teixeira, R.D., Colli, G.R. and Báo, S.N. 1999a. The ultrastructure of the spermatozoa of the lizard *Micrablepharus maximiliani* (Squamata, Gymnophthalmidae), with considerations on the use of sperm ultrastructure characters in phylogenetic reconstruction. Acta Zool. (Stockholm), 80, 47–59.

Teixeira, R.D., Colli, G.R. and Báo, S.N. 1999b. The ultrastructure of the spermatozoa of the worm-lizard *Amphisbaena alba* (Squamata, Amphisbaenidae), and the phylogenetic relationships of amphisbaenians. Can. J. Zool., 77, 1254–1264.

Vanzolini, P.E. and Valencia, J. 1965. The genus *Dracaena*, with a brief consideration of macroteiid relationships (Sauria, Teiidae). Arq. Zool., 13, 7–46.

Vanzolini, P.E., Ramos-Costa, A.M.M. and Vitt, L.J. 1980. Répteis das Caatingas. Academia Brasileira de Ciências, Rio de Janeiro, Brasil, p 161.

Wiens, J.J. 1995. Polymorphic characters in phylogenetic systematics. Syst. Biol., 44, 482–500.

Wright, J.W. 1993. Evolution of the lizards of the genus *Cnemidophorus*. In: Wright, J.W. and Vitt, L.J. (eds) Biology of Whiptail Lizards (Genus *Cnemidophorus*). The Oklahoma Museum of Natural History, Norman, OK, pp 27–81.

Zar, J.H. 1998. Biostatistical Analysis. Prentice-Hall, Inc., Englewood Cliffs, NJ, p 663.

2.1.4 – ARTIGO 4

TEIXEIRA, Ruscaia Dias; SCHELTINGA, David Michel; MESQUITA, Daniel Oliveira; WIEDERHECKER, Helga C; COLLI, Guarino Rinaldi; BÁO, Sônia Nair. Comparative study of sperm ultrastructure of five species of teiid lizards (Teiidae, Squamata), and *Cercosaura ocelata* (Gymnophthalmidae, Squamata).

Comparative study of sperm ultrastructure of five species of teiid lizards (Teiidae, Squamata), and *Cercosaura ocelata* (Gymnophthalmidae, Squamata)

R. D. Teixeira [1,2], D. M. Scheltinga [3], D. O. Mesquita [4], H. C. Wiederhecker [4], G. R. Colli [4] & S. N. Báo [1]*

[1]Departamento de Biologia Celular, Universidade de Brasília

70919-970 Brasília, DF, BRASIL, E-mail: snbao@unb.br

[2]Departamento de Biologia Celular, Universidade Estadual de Campinas

13083-970 Campinas, SP, BRASIL, E-mail: ruscaiadt@terra.com.br

[3]Department of Zoology and Entomology, University of Queensland

Brisbane, Qld, 4072, AUSTRALIA, E-mail: dscheltinga@zen.uq.edu.au

[4]Departamento de Zoologia, Universidade de Brasília

70919-970 Brasília, DF, BRASIL, E-mail: grcolli@unb.br

Running headline: Sperm ultrastructure of teiid lizards

Corresponding author: Sônia N. Báo, Departamento de Biologia Celular, Universidade de Brasília, 70919-970 Brasília, DF, Brasil, fax: 55 61 347 6533, e-mail: snbao@unb.br

Key words: ultrastructure, spermatozoa, *Callopistes*, *Crocodilurus*, *Dicrodon*, *Dracaena*, *Teius*, *Cercosaura*, Squamata, Teiidae.

ABSTRACT Sperm ultrastructure of the teiid lizards, *Callopistes flavipunctatus*, *Crocodilurus amazonicus*, *Dicrodon guttulatum*, *Dracaena guianensis* and *Teius ocelatus*, and the gymnophthalmid lizard *Cercosaura ocelata* is described for the first time. Comparisons of sperm ultrastructure of these species with those of the previously examined teiid species *Tupinambis teguixin* and *Ameiva ameiva* revealed that sperm ultrastructural data distinguished the two components of Teiioidea (Gymnophthalmidae and Teiidae), and the two subfamilies of Teiidae family (Teiinae and Tupinambinae), and appeared similar between *Cnemidophorus* and *Aspidoscelis*, and *Crocodilurus* and *Dracaena*. Statistical tests of sperm dimensions showed high number of dimensions significantly different between *Callopistes flavipunctatus* and each species of subfamily Teiinae, only two dimensions significantly different between *Cnemidophorus* and *Aspidoscelis*, and no significant difference between *Crocodilurus* and *Dracaena*. Our results indicate that teiid sperm ultrastructure displays inter-generic variability, which produces a profitable data set useful in analyzing relationships among families. Nevertheless, previous study indicates high levels of intrageneric variability within teiid genera. Splitting up higher taxa and using species as terminal can give more accurate estimates of Teiidae phylogeny than other methods of coding polymorphic traits.

The lizard family Teiidae is composed by 10 genera, which are grouped in two monophyletic subfamilies, Teiinae and Tupinambinae (Presch, 1974). The Teiinae subfamily comprises the genera *Ameiva*, *Cnemidophorus*, *Aspidoscelis*, *Dicrodon*, *Kentropyx* and *Teius*. The Tupinambinae subfamily comprises the genera *Callopistes*, *Dracaena*, *Crocodilurus* and *Tupinambis*. The genus *Aspidoscelis* is a new genus proposed by Reeder et al. (2002), based on molecular, allozymes and morphological data, comprising the *Cnemidophorus* species from North America (*deppii*, *sexlineatus*, and *tigris* groups). Despite several studies based on morphological data (Vanzolini and Valencia, 1965; Gorman, 1970; Presch, 1974; Rieppel, 1980; Veronese and Krause, 1997; Moro and Abdala, 2000) have attempted to clarify the relationships among the teiid genera, the phylogeny of the family is still incompletely solved.

Sperm ultrastructure of reptiles has been used as an alternate source of characters for phylogenetic analyses, which contain significant phylogenetic information and are especially useful when other character sets are not enlightening (Jamieson, 1995b, a; Oliver et al., 1996; Teixeira et al., 1999a, b). The analysis of the degree of variability in sperm ultrastructure characters across taxonomic categories can reveal the most profitable taxonomic level at which phylogenetic analyses should be carried out (Giugliano et al., 2002). Previous studies described the sperm ultrastructure of the teiids *Cnemidophorus sexlineatus* (Newton and Trauth, 1992), *Ameiva ameiva* (Giugliano et al., 2002), *Tupinambis duseni*, *T. Merianae*, *T. quadrilineatus*, and *T. teguixin* (Tavares-Bastos et al., 2002), and *Cnemidophorus gularis gularis*, *C. ocellifer* and *Kentropyx altamazonica* (Teixeira et al., 2002). These studies have revealed high levels of variability among teiid genera. Nevertheless, it is still necessary to analyze the level of sperm variability among all

10 teiid genera, in order to clarify if sperm ultrastructural data can profitably be used for phylogenetic analyses of teiids.

We here describe in detail the sperm ultrastructure of the teiid lizards *Callopistes flavipunctatus*, *Crocodilurus amazonicus*, *Dicrodon guttulatum*, *Dracaena guianensis* and *Teius oculatus*, and the gymnophthalmid lizard *Cercosaura ocellata*. We also make comparisons among these species and with those of the previously examined Tupinambinae species *Tupinambis teguixin* (Tavares-Bastos et al., 2002) and Teiinae species *Ameiva ameiva* (Giugliano et al., 2002). Finally, we perform statistical analyses of sperm dimensions of the sperm dimensions of all teiid genera. The aims of this study are to: 1) determine the presence of any significant difference in sperm ultrastructure among all teiid genera and between teiid and the gymnophthalmid *Cercosaura ocellata*, 2) ascertain the degree of inter-generic variability, in order to determine the phylogenetic utility of sperm ultrastructure at the generic level.

MATERIALS AND METHODS

Spermatozoal Ultrastructure

Mature spermatozoa were obtained from adult specimens of *Dicrodon guttulatum* (Museo del Historia Natural San Marco, MHNSM uncatologued) and *Callopistes flavipunctatus* (MHNSM uncatologued) collected at Chiclayo, Peru; *Crocodilurus amazonicus* (Coleção Herpetológica da Universidade de Brasília, CHUNB 15192) and *Dracaena guianensis* (CHUNB 15197, 15198, 15199) collected at Amapá, Amapá state, Brazil; *Teius oculatus* (Coleção Herpetológica da Universidade de Brasília, CHUNB 21861, 21862) collected at Porto Alegre, Rio Grande do Sul state, Brazil, and *Cercosaura*

ocellata (CHUNB 18272) collected at Pimenta Bueno, Rondônia, Brazil.

The lizards were killed by an injection of Tiopental®. Epididymides were removed and placed in a Petri dish with phosphate buffered saline (PBS), pH 7.2, and cut into small pieces. Epididymal tissues were then fixed in a solution containing 2% glutaraldehyde, 2% paraformaldehyde, and 3% sucrose in 0.1 M sodium cacodylate buffer, pH 7.2, at 4°C overnight. Tissue samples were then rinsed in 0.1 M sodium cacodylate buffer, pH 7.2; postfixed for 80 min in similarly buffered 1% osmium tetroxide; rinsed in buffer; dehydrated through series of ascending acetone series (30%-100%) and embedded in Spurr's epoxy resin. Ultrathin sections were stained for 30s in Reynold's lead citrate, rinsed in distilled water, then in 3% aqueous uranyl acetate for 4 mins, rinsed in distilled water, and stained for a further 2 mins in lead citrate before final rinsing. Electron micrographs were taken on a JEOL 100C transmission electron microscope at 80kV.

Light microscopic observations and photographs of glutaraldehyde-paraformaldehyde fixed smears *Callopistes flavipunctatus*, *Crocodilurus amazonicus*, *Dicrodon guttulatum*, *Dracaena guianensis*, *Teius oculatus*, and *Cercosaura ocellata* spermatozoa were made under Nomarski interference contrast using a Zeiss Axiophot microscope.

Statistical Analyses

The following dimensions were measured from micrographs obtained from each species of the present study, *Tupinambis teguixin* (Tavares-Bastos et al., 2002), and *Ameiva ameiva* (Giugliano et al., 2002): head length (HL), tail length (TL), entire sperm length (ESL), midpiece length (MPL), acrosome length (AL), nucleus base width (NBW), nuclear rostrum length (NRL), distal centriole length (DCL), epinuclear lucent zone length (ETL)

and width (ETW), nuclear shoulder width (NSW), ratio anterior principal piece diameter to midpiece diameter (RD), and ratio anterior principal piece diameter to fibrous sheath diameter (RC) As the assumption of normality was not met, original variables were ranked prior to analyses. To test the null hypothesis of no difference in sperm dimensions among the five species, a separate analysis of variance (ANOVA) was performed for each variable. This univariate approach was adopted because complete sets of measurements could not be obtained from individual sperm cells. To avoid the inflation of Type I error, the Bonferroni procedure was adopted: the significance level of 5% was divided by the number of tests (13), resulting in a significance level of 0.3% (Zar, 1998). The Tukey test was used to test for pairwise differences among means. Statistical analyses were conducted with SAS v. 8.0 and Systat v. 9.0 for Windows. Throughout the text, means are given ± 1 standard deviation.

RESULTS

Spermatozoa *Callopistes flavipunctatus*, *Crocodilurus amazonicus*, *Dicrodon guttulatum*, *Dracaena guianensis*, *Teius oculatus*, and *Cercosaura ocellata* are filiform, consisting of a head region containing acrosomal structures and the nucleus, a midpiece, and a tail region subdivided into principal piece and endpiece (Figs. 2K, L, M, 8P, Q, R). The spermatozoa of all six species are sufficiently similar to be described together with any differences noted. The spermatozoon of *Dicrodon guttulatum* and *Teius oculatus* are diagrammatically represented in Figure 1. Variable features among the six species studied are provided in Table 1.

Acrosome Complex

Apically, the acrosome complex appears sharply attenuated in one plane (Figs. 2A, 6A, 7B, 8A) and flattened and spatulate in the other plane (Figs. 2I, 7A). It is circular at its base, and becomes increasingly depressed in transverse section near the anterior tip (Figs. 2B-G, 6C-G, 7C-G, 8C-G). The acrosome consists of two caps: an external cap, the acrosome vesicle, and an internal cap, the subacrosomal cone (Figs. 2A, I-J, 6A-B, E-G, 7A-B, E-F, I, 8A, E-G). The acrosome vesicle forms a protuberance, appearing as a lateral ridge in the acrosome surface (Figs. 2E-F, 6E-F, 7E-F, 8F). The acrosome vesicle caps the subacrosomal cone, and anteriorly can be divided into a narrow outer cortex surrounding a wide, central medulla (Figs. 2A-D, J, 6A, C-D, 7A, C-D, 8A, C-D). In transverse sections of all teiids (Figs. 2C-D, 6C-D, 7D,), the cortex exhibits a tubular organization within its anterior portion. In teiids and in *Cercosaura*, the medulla appears as a moderately electron-dense structure, filling the interior of the acrosome vesicle.

A slender rod, the perforatorium, extends from the anterior region of the subacrosomal cone into the medulla portion of the acrosome vesicle (Figs. 2I, 7A, I, 8A). The perforatorium has a rounded apical tip and when viewed in transverse section is seen to occur outside the central one third of the flattened acrosome (Figs. 2C-D, 6D, 7D, 8D). Posteriorly, only in teiid species, the perforatorium presents a stopper-like base plate, between the base of the perforatorium and the anterior extremity of the subacrosomal cone, embedded in its material (Figs. 2J). Only, *Teius oculatus* and *Dicrodon guttulatum*, present the perforatorial base plate not embedded in subacrosomal material (Figs. 6B, 7A). In the gymnophthalmid *Cercosaura ocellata*, the perforatorium is not present. This species sperm present a densification within the apex of the subacrosomal material (Fig. 8A).

The underlying subacrosomal cone surrounds the tapered anterior end of the nucleus and exhibits a paracrystalline structure (Figs. 2F, 6G, 7G, 8F). Within the anterior region of the subacrosomal cone, immediately anterior to the nuclear tip, an epinuclear electron-lucent zone is present (Figs. 2A, E, 6B, E, 7B, E, 8A, E).

Nucleus

The elongated nucleus consists of a highly condensed, electron-dense chromatin. In transverse section, the nucleus is circular throughout (Figs. 2H, 6H, 7H, 8H). The nucleus tapers anteriorly to form a slender cone within the acrosome complex, the nuclear rostrum. The nuclear rostrum is distinguished from the main part of the cylindrical nucleus by abrupt and marked rounded nuclear shoulders (Figs. 2A, 6A, 7I, 8A). Basally the nucleus ends with a shallow concave depression, the nuclear fossa, which houses the anterior half of the proximal centriole and dense pericentriolar material (Figs. 3A, I-J, 4A, 5A, 6I, 7K, 8B).

Neck Region

The neck region occurs at the junction between nucleus and midpiece. It includes the proximal and distal centrioles, the first ring of dense bodies and mitochondria (Figs. 3A, I-J, 4 A, 5A, 6I, 7K, 8B). The proximal centriole is composed of nine short triplets and lies anterior to the distal centriole (Figs. 3I, 4A, 5A, 6I, 7K, 8B). In *Callopistes flavipunctatus*, *Dicrodon guttulatum* and *Teius ocelatus*, an electron-dense body is present within the center of the proximal centriole (Figs. 3J, 6I, 7K, 8B). This electron-dense material is similar in density and composition to that of the dense bodies of the midpiece. The distal centriole consists of nine triplets of microtubules and constitutes the basal body of the axoneme. Nine peripheral fibers that partially cover each of the triplets are present. The

distal centriole lies in the long axis of the spermatozoon, occupying a small fraction of the midpiece, and does not project into the fibrous sheath (Figs. 3A, I-J, 4A, 5A, 6I, 7K, 8B). A compact dense material, the pericentriolar material, surrounds the proximal centriole and projects bilaterally from both sides of the anterior limit of the proximal centriole as a laminar structure (Figs. 3A, I-J, 4A, 5A, 6I, 7K, 8B). This material extends posteriorly around the distal centriole, providing a base for the nine peripheral dense fibers (Figs. 3C, 4B, 5B, 6K, 7L, 8I).

Midpiece

The midpiece lies at the anterior portion of the flagellum, and includes the neck region at its anterior end. The midpiece begins with the first ring of dense bodies and ends posteriorly at a small annulus (Figs. 3A-B, I-J, 4A, H, 5A, 6I, 7K, 8B). It consists of the axoneme surrounded by the fibrous sheath, mitochondrial tiers, and rings of dense bodies (ring structures) (Figs. 3A, I-J, 4A, 5A, 6I, 7K, 8B).

The axoneme is the axial component of the midpiece and is composed of a pair of central microtubules (singlets) surrounded by nine doublets of microtubules, which are surrounded by nine peripheral dense fibers (Figs. 3D-E, 4C-D, 5C-D, 6L-N, 7M-O, 8J, L). The singlets of the axoneme extend anteriorly throughout the length of the distal centriole (Figs. 3C, 4B, 5B, 6K, 7L, 8I). Associated with the two singlets is a central fiber which is anteriorly located closer to triplet 9; posteriorly it decreases its size and is positioned centrally between the singlets of the axoneme (Figs. 3C-E, 4 B-D, 5B-D, 6K-N, 7L-O, 8I-L). At the transition of the distal centriole to axoneme, the peripheral fibers adjacent to the doublets 3 and 8 are grossly enlarged, for a short distance (Figs. 4C, 5C, 6L, 7M, 8J), except in *Callopistes flavipunctatus* (Fig. 3C-D). In all species, the peripheral fibers rapidly

decrease in diameter posteriorly, with the exception of fibers at doublets 3 and 8, which are thicker and form a double structure which is separated from their corresponding doublet and become closely associated with the fibrous sheath (Figs. 3E, 4D, 5D, 6M-N, 7N-O, 8L). Posteriorly to the annulus, all nine peripheral fibers are vestigial or absent (Figs. 3F-G, 4E-H, 5E, 6O-P, 7P, 8M-N).

In all teiid species described, the dense bodies appear juxtaposed to the fibrous sheath in transverse section (Figs. 3D-E, 4C-D, 5C, 6M, 7O), while in the gymnophthalmid species, they are separated from the fibrous sheath by mitochondria (Figs. 8J). In the teiids species, the dense bodies form complete and incomplete rings, termed ring structures (Figs. 3B, 4H, 6J, 7J). In the gymnophthalmid *Cercosaura ocellata*, the dense bodies do not form ring structures, appearing as isolate dense structures (Fig. 8K). In the teiids species *Teius ocelatus* and *Dicrodon guttulatum*, inside the ring structures, the dense bodies appear as fused structures, that sometimes present a spiral fashion (Figs. 6J, 7J), whereas, in *Crocodilurus amazonicus, Callopistes flavipunctatus* and *Dracaena guianensis*, the dense bodies are not fused within ring structures (Figs. 3B, 4H). Longitudinally, columnar mitochondrial tiers separate the ring structures in the teiids and the isolated dense rings in the gymnophthalmid species.

In *Crocodilurus amazonicus* and *Cercosaura ocelata* the average distance between the ring structures is 0.30 μm, in *Callopistes flavipunctatus* and *Dicrodon gutullatum* the average distance is 0.40 μm, *Dracaena guianensis* is 0.45 μm, and in *Teius oculatus* is 0.55 μm. Three sets of mitochondrial tiers are seen around the axoneme intercalated with three sets of ring structures in *C. flavipunctatus* (Fig. 3A-B, I-J), five sets in *D. gutullatum* (Fig. 7K) and *T. oculatus* (Fig. 6I) whereas, in *C. amazonicus* and *D. guianensis*, six sets of mitochondria and six sets of ring structures are observed (Figs. 4A, 5A). In *C. amazonicus*,

seven sets of mitochondria and ring structures are also observed in the midpiece (Fig. 4H). The ring structure and mitochondria arrangement pattern can be represented by the abbreviated expression rs3/mi3 (previously expressed as rs1/mi1, rs2/mi2, rs3/mi3) in *C. flavipunctatus* (Fig. 3B, I), rs5/mi5 in *Cercosaura ocelata*, *Dicrodon gutullatum* and *Teius oculatus* (previously, rs1/mi1, rs2/mi2, rs3/mi3 rs4/mi4, rs5/mi5) (Figs. 6I, 7K, 8B) and rs6/mi6 (previously, rs1/mi1, rs2/mi2, rs3/mi3 rs4/mi4, rs5/mi5, rs6/mi6) in *C. amazonicus* and *D. guianensis* (Figs. 4A, 5A). In the gymnophthalmid *C. ocellata* and in the teiids *C. flavipunctatus* and *D. guttulatum*, the mitochondria, when viewed in oblique section (Figs. 3B, 7J), extend anteriorly along the midpiece in a strictly columnar appearance, while in longitudinal section they appear trapezoidal (Figs. 3A, I-J, 7K). In *C. amazonicus* and *D. guianensis*, the mitochondria have a strictly columnar appearance when viewed in longitudinal section (Fig. 4A), and in longitudinal section, the ends of the mitochondria have a symmetrical round shape (Figs. 4H). In *T. oculatus*, the columnar mitochondria have a regular, slightly curved appearance in oblique section (Fig. 6J), but are not considered to be sinuous tubes because they do not curve at an angle of grater than 45° and back upon themselves. In *Teius oculatus*, the ends of the mitochondria have a symmetrical round shape as observed in longitudinal section (Fig. 6I).

The fibrous sheath encloses the axoneme and extends into the midpiece, reaching the base of the distal centriole (Figs. 3A, I-J, 4A, 5A, 6I, 7K, 8B). In the teiids *Crocodilurus amazonicus* and *Dracaena guianensis*, and in the gymnophthalmid *Cercosaura ocellata*, the fibrous sheath extends anteriorly into the midpiece to the level of mitochondrial tier 3 (mi3) (Figs. 4A, 5A, 8B), occupying 63%, 72% and 73% of the total midpiece length, respectively. In the teiids *Callopistes flavipunctatus*, *Dicrodon guttulatum*a and *Teius oculatus*, the fibrous sheath extends to the level of the second

mitochondrial tier (mi2) (Figs. 3A, I-J, 6I, 7K), occupying 68%, 85% and 86% of the total midpiece length, respectively.

Posteriorly, the midpiece terminates at the annulus, which is closely attached to the inner surface of the plasma membrane. The annulus (Figs. 3A-B, I-J, 4A, H, 5A, 6I, 7K, 8B, K) is a small dense ring with an irregular shape when viewed in longitudinal section.

Principal Piece

The principal piece is the longest part of the spermatozoon and occurs posterior to the midpiece. It consists of the axoneme surrounded by fibrous sheath, cytoplasm and plasma membrane. In this region, the peripheral dense fibers, dense bodies, and mitochondria are absent (Figs. 3F, 4E-F, 5E, 6O-P, 7P, 8M-N). Within the anterior portion of the principal piece, immediately after the annulus, the diameter of the spermatozoon does not decrease relative to the annulus with the plasma membrane being widely separated from the fibrous sheath by a thick region of granular cytoplasm (Figs. 3A, F, 4A, E, 5A, 6I, O, 7K, P, 8B, M). Posteriorly, the amount of cytoplasm decreases and the plasma membrane becomes closely associated with the fibrous sheath (Figs. 3G, 4F-G, 5E, 6P, 8N).

Endpiece

A short length of axoneme extends beyond the posterior limit of the fibrous sheath as the endpiece (Figs. 5F, 8O). The 9+2 pattern of the axonemal microtubules is initially maintained, although their diameter is reduced. Posteriorly, the arrangement of microtubules becomes increasingly disrupted (Fig. 3H, 6Q-R, 7R).

Comparisons of Spermatozoal Dimensions

The analyses of variance showed that all teiid species and the gymnophthalmid *Cercosaura ocellata* differed significantly in major analyzed dimensions of acrosome, distal centriole, epinuclear lucent zone, nuclear rostrum, midpiece, tail, and entire sperm lengths, nuclear base width, and amount of cytoplasm in the anterior portion of the principal piece, and degree of diameter reduction between the end of midpiece and the beginning of principal piece (Figs. 9, 10, 11). There was no statistical difference between any species in epinuclear lucent zone width. Results of the Tukey multiple comparisons test are represented in figures 9, 10 and 11.

DISCUSSION

In all teiid genera, *Ameiva* (Giugliano et al., 2002), *Cnemidophorus*, *Aspidoscelis*, *Kentropyx* (Teixeira et al., 2002), *Tupinambis* (Tavares-Bastos et al., 2002), *Dracaena*, *Crocodilurus*, *Callopistes*, *Teius*, *Dicrodon*, and in the gymnophthalmid *Cercosaura* (present study), the sperm ultrastructure presents a plesiomoprhic condition of the tetrapods (Jamieson, 1995b), the acrosome complex forming a tripartite pattern (acrosome vesicle, subacrosomal cone and the constricted nucleat tip). The following features, regarded a plesiomorphic in amniotes (Jamieson, 1995a), are also seen in teiids and in *Cercosaura* (Gymnophthalmidae): nucleus elongate; distal centriole extending trough midpiece; penetrated by two central singlets from the axoneme; several mitochondria in cross section of midpiece; annulus present; nine peripheral fibers associated with the nine doublets of the axoneme; peripheral fibers adjacent to doublets 3 and 8 enlarged, forming a double

structure detached from their respective doublets. The ten teiid genera and *Cercosaura* (Gymnophthalmidae) have a number of character-states considered synapomorphies of Squamata (Jamieson, 1995b): perforatorium single, wholly prenuclear; endonuclear canal absent; epinuclear lucent zone present; mitochondrial cristae linear; intermitochondrial dense bodies present; fibrous sheath extending into midpiece; and nuclear shoulders presence at the transition from the nuclear rostrum to the cylindrical portion of the nucleus.

In the acrosome complex, several differences are observed among teiid genera and between teiids and *Cercosaura* (Gymnophthalmidae) (Table 1). The unilateral ridge present in the acrosome surface is seen in all teiid genera, whereas in *Cercosaura*, this feature is not observed in longitudinal sections. All teiid sperm show a tubular organization in the cortex of the acrosome vesicle, whereas in Cercosaura this feature is not observed. The perforatorial base plate is seen in all teiids studied, except in *Kentropyx* (Teixeira et al., 2002) and in *Cercosaura* (Gymnophthalmidae). According to Teixeira et al (2002), *Kentropyx* presents a slight densification in the apex of the subacrosomal cone, but did not consider a perforatorium base plate. This densification is also seen in *Cercosaura*. Among the genera that present the base plate, only *Tupinambis* (Tavares-Bastos et al., 2002) show a base plate knob-like shaped, whereas the others present a stopper-like shaped base plate. With exception of *Dicrodon* and *Teius*, the base plate is embedded in the apex of the subacrosomal material. Nevertheless, a suite of common features is seen among teiids and between teiids and *Cercosaura* (Gymnophthalmidae): acrosome depressed and flattened at its anterior portion, posteriorly becoming circular; presence of medulla and cortex in the acrosome vesicle, tubular organization of the anterior portion of cortex of acrosome vesicle, perforatorial base plate observed outside the central one third of the flattened acrosome, and presence of the epinuclear lucent zone.

In the neck region (Table 1), the laminar structure is well developed in teiids, being projected by the pericentriolar material from both side of the proximal centriole, whereas in *Cercosaura* (present study), it appears poor developed and projected in only one side of the proximal centriole. The short, solid cylinder of electron-dense material extending from the first dense body ring structure into the center of the proximal centriole can be observed in all teiids, with exception of *Crocodilurus* and *Dracaena*, and *Cercosaura* (Gymnophthalmidae).

In the midpiece (Table 1), the dense bodies are separated by mitochondrial tiers, presenting the arrangement pattern dense bodies/mitochondrial tiers/dense bodies is a common feature of Teiidae and Gymnophthalmidae. Nevertheless, major variability among teiid genera and between Teiidae and Gymnophthalmidae is seen in the midpiece. Only in *Ameiva* (Giugliano et al., 2002), *Kentropyx* (Teixeira et al., 2002), *Dicrodon*, *Teius*, *Callopistes*, *Crocodilurus*, *Dracaena* and *Cercosaura* (present study), the peripheral fibers appear grossly enlarged for a short distance, at the level of the distal centriole/axoneme junction. In all Teiinae subfamily genera and in *Cercosaura* (Gymnophthalmidae), the dense body and mitochondrial tiers forms five sets, whereas in the Tupinambinae genera, this arrangement presents three, five or six sets of dense bodies and mitochondrial tiers. *Kentropyx*, is the only genera studied which presents slightly curved mitochondria, instead of a strictly columnar mitochondria. At longitudinal section, the mitochondria appear with trapezoidal shapes in *Ameiva* (Giugliano et al., 2002), *Aspidoscelis*, *Cnemidophorus* (Teixeira et al., 2002), *Dicrodon*, *Teius*, *Callopistes* (present study), *Tupinambis* (Tavares-Bastos et al., 2002) and *Cercosaura* (present study), whereas in the others, the mitochondria appears with rounded ends. In all teiids, the dense bodies form ring structures around the fibrous sheath, and are directly juxtaposed to the fibrous sheath, while in

Cercosaura (Gymnophthalmidae), the dense bodies neither form ring structures nor are juxtaposed to fibrous sheath. In all Teiinae genera, the dense bodies are fused into the ring structures, whereas the Tupinambinae genera the dense bodies are not fused. Finally, the fibrous sheath begins at the first mitochondrial tier level in *Kentropyx* (Teixeira et al., 2002), at the second mitochondrial tier level in the others Teiinae genera and in the Tuinambinae genera *Callopistes*, and at the third mitochondrial tier level in the others Tupinambinae genera and in *Cercosaura* (Gymnophthalmiae) (present study).

In the principal piece (Table 1), absence of all nine dense fibers and the presence of cytoplasm between the fibrous sheath and the plasma membrane immediately posterior to the annulus are common features observed in Teiidae and Gymnophthalmidae families. No variability is found at this region.

In the endpiece (Table 1), the disrupted arrangement of microtubules at its posterior portion is observed in Teiidae and Gymnophthalmidae families. No variability is found at this region.

Finally, the comparisons among teiid sperm ultrastructure features (Table 1) has revealed that sperm ultrastructural data add support to the validity of the two families of Teiioidea (Gymnophthalmidae + Teiidae), and the two teiid subfamilies (Teiinae and Tupinambinae). Based on data from osteology (Presch, 1983), locomotion and feeding (MacLean, 1974), adductor musculature (Rieppel, 1980), and chromosome morphology (Gorman, 1970), Gymnophthalmidae is regarded as sister-taxon of Teiidae family. In addition, based on external morphological data (Vanzolini and Valencia, 1965), chromosomal data (Gorman, 1970), osteological data (Presch, 1970; Veronese and Krause, 1997), and myology (Rieppel, 1980), Teiidae family is split into two subfamiles, Teiinae and Tupinambinae. Our results detected a suite of character states present in the mature

sperm ultrastructure of all teiid genera, distinguishing teiids from the gymnophthalmid *Cercosaura ocellata*: presence of a unilateral ridge in the acrosome surface; a well-developed laminar structure bilaterally projected from the pericentriolar material to the first ring structure; dense bodies forming ring structures around the axoneme; and dense bodies juxtaposed to the fibrous sheath. Within Teiidae family, we have identified unique two traits distinguishing Teiinae subfamily from Tupinambinae subfamily: presence of 5 sets of mitochondrial tiers and ring structures; and dense bodies fused in the ring structures.

The statistical analysis of the dimensions of the 13 sperm morphometric characters found highest numbers of significant differences between *Callopistes* and all Teiinae species, well distinguishing *Callopistes* from Teiinae genera. *Crocodilurus* and *Dracaena* sperm are similar in all ultrastructural characters and according to statistical analysis of the dimensions of 13 sperm characters, there are no significant difference, having these genera identical sperm. Despite *Cnemidophorus* and *Aspidoscelis* sperm are similar in all ultrastructural characters, statistical analyses found two significant differences, acrosome and distal centriole lengths, distinguished these two genera. These results support Reeder's hypothesis (2002) that *leminiscatus* group (*Cnemidophorus ocellifer*) and *Cnemidophorus* groups from North America (*Aspidoscelis gularis gularis*) belong to two different genera. According to sperm ultrastructure features, *Dicrodon* and *Teius* are identical, however, statistically their dimension have six significant differences.

These results suggest high levels of inter-generic variability in sperm ultrastructure within Teiidae, showing that sperm ultrastructural data set can be profitably used in phylogenetic reconstruction of generic level, but less informative if used at family level. These findings support Giugliano et al. (2002) study of variability within Teiidae family, and previous suggestions that intrafamilial variability may be higher than currently though

(Teixeira et al., 1999a, b). However, Tavares-Bastos et al. (2002) found variability in sperm ultrastructure features among four species of *Tupinambis*, showing that even at generic level, sperm ultrastructural data varies within teiid species. Teixeira et al. (1999a, b) argue that variability in sperm ultrastructure within squamates families may be producing unsatisfactory results in terms of resolving the phylogenetic position of amphisbaenians and incongruent phylogeny with that derived from traditional morphological data. Despite, the ideal characters are those that vary between the terminal units of an analysis but do not vary within them (Thiele, 1993), it is common to find many characters that vary within species or aggregates of species (e.g., genera, families) (Poe and Wiens, 2000). Systematists may use a variety of methods for dealing with this variation, including (1) breaking up the terminal taxon into smaller, invariant units, (2) excluding variable characters, and (3) using different methods for inclusion and coding of variable characters (Wiens, 1995). Simulations and some empirical data (Wiens, 2000) suggest strongly that breaking up higher taxa and using species as terminal will give more accurate results than will using methods of coding polymorphic traits, coding higher taxa as terminals, or excluding characters that vary within them. Splitting up higher taxa and using species as terminal can give more accurate estimates of phylogeny than other methods of coding polymorphic traits (Wiens, 1998). So far, under high levels of variability in sperm ultrastructure within teiid genera, sampling multiple species within teiid genera is essential to be used in phylogenetic analyses at the genera level.

LITERATURE CITED

Giugliano LG, Teixeira RD, Colli GR, Báo SN. 2002. Ultrastructure of spermatozoa of the lizard *Ameiva ameiva*, with considerations on polymorphism within the family Teiidae (Squamata). J Morphol 253:264-271.

Gorman GC. 1970. Chromosomes and the systematics of the family Teiidae. Copeia 1970:230-245.

Jamieson BGM. 1995a. Evolution of tetrapod spermatozoa with particular reference to amniotes. In: Jamieson BGM, Ausio J, Justine J, editors. Advances in Spermatozoal Phylogeny and Taxonomy. Paris, France: Muséum National d'Histoire Naturelle. p. 343-358.

Jamieson BGM. 1995b. The ultrastructure of spermatozoa of the Squamata (Reptilia) with phylogenetic considerations. In: Jamieson BGM, Ausio J, Justine J, editors. Advances in Spermatozoal Phylogeny and Taxonomy. Paris, France: Muséum National d'Histoire Naturelle. p. 359-383.

MacLean WP. 1974. Feeding and locomotor mechanisms of teiid lizards: functional morphology and evolution. Pap Avul Zool, S Paulo 27:179-213.

Moro S, Abdala V. 2000. Cladistic analysis of Teiidae (Squamata) based on myological characters. Rus J Herpetol 7:87-102.

Newton WD, Trauth SE. 1992. Ultrastructure of the spermatozoon of the lizard *Cnemidophorus sexlineatus* (Sauria: Teiidae). Herpetologica 48:330-343.

Oliver SC, Jamieson BGM, Scheltinga DM. 1996. The ultrastructure of spermatozoa of Squamata. II. Agamidae, Varanidae, Colubridae, Elapidae, and Boidae (Reptilia). Herpetologica 52:216-241.

Poe S, Wiens JJ. 2000. Character selection and the methodology of morphological phylogenetics. In: Wiens JJ, editor. Phylogenetic analysis of morphological data. Washigton D. C.: Smithsonian Institution Press. p. 20-36.

Presch WF, Jr. 1970. The evolution of macroteiid lizards: an osteological interpretation. Ph.D., University of Southern California, Los Angeles, CA.

Presch WF, Jr. 1974. Evolutionary relationships and biogeography of the macroteiid lizards (Family Teiidae, Subfamily Teiinae). Bull So Calif Acad Sci 73:23-32.

Presch WF, Jr. 1983. The lizard family Teiidae: is it a monophyletic group? Zool J Linn Soc 77:189-197.

Reeder TW, Cole CJ, Dessauer HC. 2002. Phylogenetic relationships of whiptail lizards of the genus *Cnemidophorus* (Squamata: Teiidae): a test of monophyly, reevaluation of karyotypic evolution, and review of hybrid origins. American Museum Novitates 3365:1-61.

Rieppel O. 1980. The trigeminal jaw adductor musculature of *Tupinambis*, with comments on the phylogenetic relationships of the Teiidae (Reptilia, Lacertilia). Zool J Linn Soc 69:1-29.

Tavares-Bastos L, Teixeira RD, Colli GR, Báo SN. 2002. Polymorphism in the sperm ultrastructure among four species of lizards in the genus *Tupinambis* (Squamata: Teiidae). Acta Zool (Stockholm) 83:297-307.

Teixeira RD, Colli GR, Báo SN. 1999a. The ultrastructure of the spermatozoa of the lizard *Micrablepharus maximiliani* (Squamata, Gymnophthalmidae), with considerations on the use of sperm ultrastructure characters in phylogenetic reconstruction. Acta Zool (Stockholm) 80:47-59.

Teixeira RD, Colli GR, Báo SN. 1999b. The ultrastructure of the spermatozoa of the worm-lizard *Amphisbaena alba* (Squamata, Amphisbaenidae), and the phylogenetic relationships of amphisbaenians. Can J Zool 77:1254-1264.

Teixeira RD, Scheltinga DM, Trauth SE, Colli GR, Báo SN. 2002. A comparative ultrastructural study of spermatozoa of the teiid lizards, *Cnemidophorus gularis gularis*, *Cnemidophorus ocellifer*, and *Kentropyx altamazonica (Reptilia, Squamata, Teiidae)*. Tissue & Cell 34:135-142.

Thiele K. 1993. The holy grail of the perfect character: the cladistic treatment of morphometric data. Cladistics 9:275-304.

Vanzolini PE, Valencia J. 1965. The genus *Dracaena*, with a brief consideration of macroteiid relationships (Sauria, Teiidae). Arq Zool, S Paulo 13:7-46.

Veronese LB, Krause L. 1997. Esqueleto pré-sacral e sacral dos lagartos teiídeos (Squamata, Teiidae). Revta bras Zool 14:15-34.

Wiens JJ. 1995. Polymorphic characters in phylogenetic systematics. Syst Biol 44:482-500.

Wiens JJ. 1998. Testing phylogenetic methods with tree congruence: Phylogenetic analysis of polymorphic morphological characters in phrynosomatid lizards. Syst Biol 47:427-444.

Wiens JJ. 2000. Coding morphological variation within species and higher taxa for phylogenetic analysis. In: Wiens JJ, editor. Phylogenetic analysis of morphological data. Washington D. C.: Smithsonian Institution Press. p. 115-145.

Zar JH. 1998. Biostatistical Analysis (4th ed.). Englewood Cliffs, New Jersey: Prentice-Hall, Inc. 663 p.

TABLE 1. Comparative variable features of the ultrastructure of sperm among teiid genera and Cercosaura (Gymnophthalmidae)

Species	UR	AV	BP	BP	BP in SC material	SL	SL	CD in PC
Ameiva	Present	Tubular	Present	Stopper-like	Embedded	Well developed	Bilateral	Present
Aspidoscelis	Present	Tubular	Present	Stopper-like	Embedded	Well developed	Bilateral	Present
Cnemidophorus	Present	Tubular	Present	Stopper-like	Embedded	Well developed	Bilateral	Present
Kentropyx	Present	Tubular	Absent	——	Embedded	Well developed	Bilateral	Present
Dicrodon	Present	Tubular	Present	Stopper-like	Not embedded	Well developed	Bilateral	Present
Teius	Present	Tubular	Present	Stopper-like	Not embedded	Well developed	Bilateral	Present
Callopistes	Present	Tubular	Present	Stopper-like	Embedded	Well developed	Bilateral	Present
Crocodilurus	Present	Tubular	Present	Stopper-like	Embedded	Well developed	Bilateral	Absent
Dracaena	Present	Tubular	Present	Stopper-like	Embedded	Well developed	Bilateral	Absent
Tupinambis	Present	Tubular	Present	Knob-like	Embedded	Well developed	Bilateral	Present
Cercosaura	Absent	No tubular	Absent	——	Embedded	Poor developed	Unilateral	Absent

Note: UR, unilateral ridge; AV, acrosome vesicle; BP, base plate; SC, subacrosomal cone; SL, laminar structure; CD, central density; PC, proximal centriole.

Species	Fibers 3 & 8	Number of Sets	Mi in OS	Mi in LS	RS	Dense bodies in the RS	Mi between DB & FS	Beginning of FS
Ameiva	Gross	5 sets	Columnar	Trapezoidal	Form RS	Fused	Absent	Mi2
Aspidoscelis	Not gross	5 sets	Columnar	Trapezoidal	Form RS	Fused	Absent	Mi2
Cnemidophorus	Not gross	5 sets	Columnar	Trapezoidal	Form RS	Fused	Absent	Mi2
Kentropyx	Gross	5 sets	Slightly curved	Round ended	Form RS	Fused	Absent	Mi1
Dicrodon	Gross	5 sets	Columnar	Trapezoidal	Form RS	Fused	Absent	Mi2
Teius	Gross	5 sets	Columnar	Trapezoidal	Form RS	Fused	Absent	Mi2
Callopistes	Gross	3 sets	Columnar	Trapezoidal	Form RS	Not fused	Absent	Mi2
Crocodilurus	Gross	6 sets	Columnar	Round ended	Form RS	Not fused	Absent	Mi3
Dracaena	Gross	6 sets	Columnar	Round ended	Form RS	Not fused	Absent	Mi3
Tupinambis	Not gross	6 sets	Columnar	Trapezoidal	Form RS	Not fused	Absent	Mi3
Cercosaura	Gross	5 sets	Columnar	Trapezoidal	Not form RS	———	Present	Mi3

Note: Mi, mitochondria; OS, oblique section; LS, longitudinal section; RS, ring structure; DB, dense bodies; FS, fibrous sheath

FIGURE LEGENDS

Fig. 1. *Dicrodon guttulatum* and *Teius oculatus*. Diagram of the spermatozoon, and corresponding transverse sections. Scale bar 0.5 μm.

Fig. 2. Spermatozoa of *Callopistes flavipunctatus*, *Crocodilurus amazonicus*, and *Dracaena guianensis*. **A-J:** Transmission electron micrographs through sperm head (acrosome complex and nucleus). In **A, B, I** and **J**, *Callopistes flavipunctatus*, in **C, D, F-I**, *Crocodilurus amazonicus*, and in **E** *Dracaena guianensis*. **A:** Longitudinal section (LS) through the acrosome complex showing the acrosome vesicle with cortex and medulla, the subacrosomal cone, and the nuclear rostrum. Note the epinuclear lucent zone at the nucleus tip. **B-G:** A series of transverse sections (TSs) through the sperm head as indicated. Note that anteriorly, in **B - D**, the acrosome appears depressed, while posteriorly, in **E** and **F** it is unilaterally ridged, in **G**, the acrosome more circular. **H:** transversal section through the nucleus. **I:** LS of the acrosome complex, showing the flattened apical region. Note the perforatorium and the electron space between subacrosomal cone and the acrosome vesicle (*). **J:** LS of the acrosome complex showing the stopper-like base plate, embedded in the subacrosomal material. **K-M:** Light micrographs showing whole spermatozoon of *Callopistes flavipunctatus*, in **K,** *Crocodilurus amazonicus* in **L**, and *Dracaena guianensis* in **M**. **B-H:** to same scale as indicated. av, acrosome vesicle; bp, perforatorial base plate; co, cortex; et, epinuclear lucent zone; h, head; me, medulla; mp, midpiece; n, nucleus; nr, nuclear rostrum; ns, nuclear shoulder; p, perforatorium; pm, plasma membrane; sc, subacrosomal cone; t: tail; ur, unilateral ridge.

Fig. 3. Spermatozoa of *Callopistes flavipunctatus*. **A-J:** Transmission electron micrographs of the tail (midpiece, principal piece and endpiece). **A:** Longitudinal section (LS) through the midpiece showing the distal centriole, axoneme, fibrous sheath, mitochondria dense bodies and annulus. **B:** LS through the midpiece showing the mitochondrial and dense body arrangement. **C – H:** A series of transverse sections (TSs) through the sperm tail as indicated. Note that anteriorly, in **C**, distal centriole showing the pair of central microtubules and the dense material within it, in **D,** the beginning of the axoneme showing the grossly enlarged fibers 3 and 8, in **E,** the axoneme showing that the peripheral fibers at 3 and 8 are thicker than the others and are detached from their doublets, in **F,** the anterior region of the principal piece, in **G,** the posterior end of the principal piece, **H**, the endpiece with disarranged microtubules pattern. **I:** LS of the midpiece showing bilateral laminar structure. **J:** LS of the midpiece showing central density within the proximal centriole. **A-J:** to same scale as indicated. an, annulus; ax, axoneme; cf, central fiber; cy, cytoplasm; db, dense bodies; dc, distal centriole; fs, fibrous sheath; ls, laminar structure; mi, mitochondrial tier; n, nucleus; nf, nuclear fossa; pc, proximal centriole; pf, peripheral fibers; pm, plasma membrane; pcm, pericentriolar material; rs, dense body ring structure.

Fig. 4. Spermatozoa of *Crocodilurus amazonicus*. **A-H:** Transmission electron micrographs of the tail (midpiece and principal piece). **A:** Longitudinal section (LS) through the midpiece showing neck region, the distal centriole, axoneme, fibrous sheath, mitochondria dense bodies, and annulus. **B – G:** A series of transverse sections (TSs) through the sperm tail as indicated. Note that anteriorly, in **B**, distal centriole showing the pair of central microtubules and the dense material within it, in **C,** the beginning of the axoneme showing the grossly enlarged fibers 3 and 8, in **D,** the axoneme showing that the peripheral fibers at

3 and 8 are thicker than the others and are detached from their doublets, in **E,** the anterior region of the principal piece, in **F** and **G,** the posterior end of the principal piece. **H:** LS through the midpiece showing the mitochondrial and dense body arrangement. Note the dense bodies not fused within the ring structure. **B-G:** to same scale as indicated. an, annulus; ax, axoneme; cf, central fiber; cy, cytoplasm; db, dense bodies; dc, distal centriole; fs, fibrous sheath; ls, laminar structure; mi, mitochondrial tier; n, nucleus; nf, nuclear fossa; pc, proximal centriole; pf, peripheral fibers; pm, plasma membrane; pcm, pericentriolar material; rs, dense body ring structure.

Fig. 5. Spermatozoa of *Dracaena guianensis*. **A-F:** Transmission electron micrographs of the tail (midpiece, principal piece and endpiece). **A:** Longitudinal section (LS) of the entire midpiece length, showing neck region, the distal centriole, axoneme, fibrous sheath, mitochondria dense bodies, and annulus. **B – E:** A series of transverse sections (TSs) through the sperm tail as indicated. Note that anteriorly, in **B**, distal centriole showing the pair of central microtubules and the dense material within it, in **C,** the beginning of the axoneme showing the grossly enlarged fibers 3 and 8, in **D,** the axoneme showing that the peripheral fibers at 3 and 8 are thicker than the others and are detached from their doublets, in **E,** the anterior region of the principal piece, in **F,** endpiece. **A-F:** to same scale as indicated. an, annulus; ax, axoneme; cf, central fiber; cy, cytoplasm; db, dense bodies; dc, distal centriole; fs, fibrous sheath; ls, laminar structure; mi, mitochondrial tier; n, nucleus; nf, nuclear fossa; pc, proximal centriole; pf, peripheral fibers; pm, plasma membrane; pcm, pericentriolar material; rs, dense body ring structure.

Fig. 6. Spermatozoa of *Teius oculatus*. **A-R:** Transmission electron micrographs. **A:** Longitudinal section (LS) through the acrosome complex showing the acrosome vesicle with cortex and medulla, the subacrosomal cone, the nuclear rostrum, and the electron lucent zone. **B:** LS of the acrosome complex showing its flattened appearance at anterior portion and the stopper-like base plate not embedded in the subacrosomal cone. **C-G:** A series of transverse sections (TSs) through the spermatozoon as indicated. Note that anteriorly, in **C - D**, the acrosome appears depressed, while posteriorly, in **E- F**, it is unilaterally ridged and the electron lucent region between the acrosome vesicle and the subacrosomal cone, in **G**, it appear more circular at its base. **H:** TS through the nucleus. **I:** LS of the full length of the midpiece showing the neck region with the nuclear fossa, pericentriolar material, centrioles, the stratified laminar structure, and five ring structures and five mitochondrial tiers. Arrow indicates extension of dense body into center of the proximal centriole. **J:** Oblique section of the midpiece showing the mitochondrial and dense body arrangement. **K-Q:** A series of transverse sections (TSs) through the spermatozoon as indicated. Note that anteriorly, in **K**, through posterior portion of the distal centriole, in **L**, through the dense body ring structure of the midpiece showing the grossly enlarged peripheral fibers 3 and 8, in **M**, through the complete ring structure, in **N**, through the axoneme showing peripheral fibers 3 and 8 thicker than the others, double and detached from their doublets, in **O** and **P** through anterior and posterior portion of the principal piece, respectively, and in **Q**, through the endpiece showing the disarranged microtubules pattern. **R:** LS of the transition region between principal piece and the endpiece. **C-H** and **K-Q:** to same scale as indicated. a: axoneme; an: annulus; av: acrosome vesicle; cf: central fiber; co: cortex; cy: cytoplasm; db: dense bodies; dc: distal centriole; et: epinuclear lucent zone; fs: fibrous sheath; ls: stratified laminar structure; m: mitochondrion; me: medulla; mi:

mitochondrial tier; n: nucleus; nf: nuclear fossa; nr: nuclear rostrum; p: perforatorium; pb: perforatorial base plate; pc: proximal centriole; pcm: pericentriolar material; pf: peripheral fiber; pm: plasma membrane; rs: dense body ring structure; sc: subacrosomal cone.

Fig. 7. Spermatozoa of *Dicrodon guttulatum*. **A-R:** Transmission electron micrographs. **A:** Longitudinal section (LS) through the acrosome complex showing the acrosome vesicle with cortex and medulla, the subacrosomal cone, the stopper-like perforatorial base plate not embedded in the subacrosomal cone. **B:** LS of the acrosome complex showing the epinuclear lucent zone. **C-G:** A series of transverse sections (TSs) through the spermatozoon as indicated. Note that anteriorly, in **C - D**, the acrosome appears depressed, while posteriorly, in **E- F**, it is unilaterally ridged and the electron lucent region between the acrosome vesicle and the subacrosomal cone, and in **G,** it appear more circular at its base. **H:** TS through the nucleus. **I:** LS of the acrosome complex showing the nuclear rostrum, the unilateral ridge. **J:** Oblique section of the midpiece showing the mitochondrial and dense body arrangement. **K:** LS of the full length of the midpiece showing the neck region with the nuclear fossa, pericentriolar material, centrioles, the stratified laminar structure, and five ring structures and five mitochondrial tiers. Arrow indicates the dense body into center of the proximal centriole. **L-R:** A series of transverse sections (TSs) through the spermatozoon as indicated. Note that anteriorly, in **L,** through posterior portion of the distal centriole, in **M,** through axoneme showing the grossly enlarged peripheral fibers 3 and 8, in **N**, through the axoneme showing peripheral fibers 3 and 8 thicker than the others, double and detached from their doublets, in **O,** through the incomplete ring structure, in **P** and **Q,** through anterior and posterior portion of the principal piece, respectively, and in **R**, through the endpiece showing the disarranged microtubules pattern.

C-H and **L-R:** to same scale as indicated. a: axoneme; an: annulus; av: acrosome vesicle; cf: central fiber; co: cortex; cy: cytoplasm; db: dense bodies; dc: distal centriole; et: epinuclear lucent zone; fs: fibrous sheath; ls: stratified laminar structure; m: mitochondrion; me: medulla; mi: mitochondrial tier; n: nucleus; nf: nuclear fossa; nr: nuclear rostrum; ns: nuclear shoulder; p: perforatorium; pb: perforatorial base plate; pc: proximal centriole; pcm: pericentriolar material; pf: peripheral fiber; pm:plasma membrane; rs: dense body ring structure; sc: subacrosomal cone.

Fig. 8. Spermatozoa of *Cercosaura ocellata*. **A-O:** Transmission electron micrographs. **A:** Longitudinal section (LS) through the acrosome complex showing the acrosome vesicle the subacrosomal cone, the densification within the apex of the subacrosomal material (arrow). **B:** LS of the full length of the midpiece showing the neck region with the nuclear fossa, pericentriolar material, centrioles, and the stratified laminar structure. Arrow indicates the dense body into center of the proximal centriole. **C-J** and **L-M:** A series of transverse sections (TSs) through the spermatozoon as indicated. Note that anteriorly, in **C - D**, the acrosome appears depressed, while posteriorly, in **E- G**, it becomes circular at its base, in **H,** through the nucleus, in **I,** through posterior portion of the distal centriole, in **J**, through axoneme showing the grossly enlarged peripheral fibers 3 and 8, in **L**, through the axoneme showing peripheral fibers 3 and 8 thicker than the others, double and detached from their doublets, in **M** and **N,** through anterior and posterior portion of the principal piece, respectively, and in **O**, through the endpiece showing the disarranged microtubules pattern. **K:** Oblique section of the midpiece showing the five ring structures and five mitochondrial tiers. **P-R:** Light micrographs showing whole spermatozoon of *Cercosaura ocellata*, in **P,** *Dicrodon guttulatum* in **Q**, and *Teius oculatus*, in **R**. **C-J** and **L-O:** to same scale as

indicated. a: axoneme; an: annulus; av: acrosome vesicle; cf: central fiber; co: cortex; cy: cytoplasm; db: dense bodies; dc: distal centriole; et: epinuclear lucent zone; fs: fibrous sheath; h: head; ls: stratified laminar structure; m: mitochondrion; me: medulla; mi: mitochondrial tier; mp: midpiece; n: nucleus; nf: nuclear fossa; nr: nuclear rostrum; ns: nuclear shoulder; p: perforatorium; pb: perforatorial base plate; pc: proximal centriole; pcm: pericentriolar material; pf: peripheral fiber; pm:plasma membrane; rs: dense body ring structure; sc: subacrosomal cone.

Fig. 9. Sperm dimensions in teiid genera lizards, and *Cercosaura* (Gymnophthalmidae). Values are in micrometers and represented by means ± 1SD. Different letters represent significant differences at the 5% level using the Tukey test multiple comparisons test. *n* is represented by numbers above each value. TL: tail length, ESL: entire sperm length, MPL: midpiece length, HL: head length, AL: acrosome length.

Fig. 10. Sperm dimensions in teiid genera lizards, and *Cercosaura* (Gymnophthalmidae). Values are in micrometers and represented by means ± 1SD. Different letters represent significant differences at the 5% level using the Tukey test multiple comparisons test. *n* is represented by numbers above each value. NBW: nuclear base width, NRL: nuclear rostrum length, DCL: distal centriole length, ETL: epinuclear lucent zone.

Fig. 11. Sperm dimensions in teiid genera lizards, and *Cercosaura* (Gymnophthalmidae). Values are in micrometers and represented by means ± 1SD. Different letters represent significant differences at the 5% level using the Tukey test multiple comparisons test. *n* is represented by numbers above each value. ETW: epinuclear lucent width, NSW: nuclear

shoulders width, PPcy: amount of cytoplasm between fibrous sheath and plasma membrane at the anterior region of the principal piece, PPdi: degree of reduction of the diameter between the posterior portion of the midpiece and the anterior portion of the principal piece.

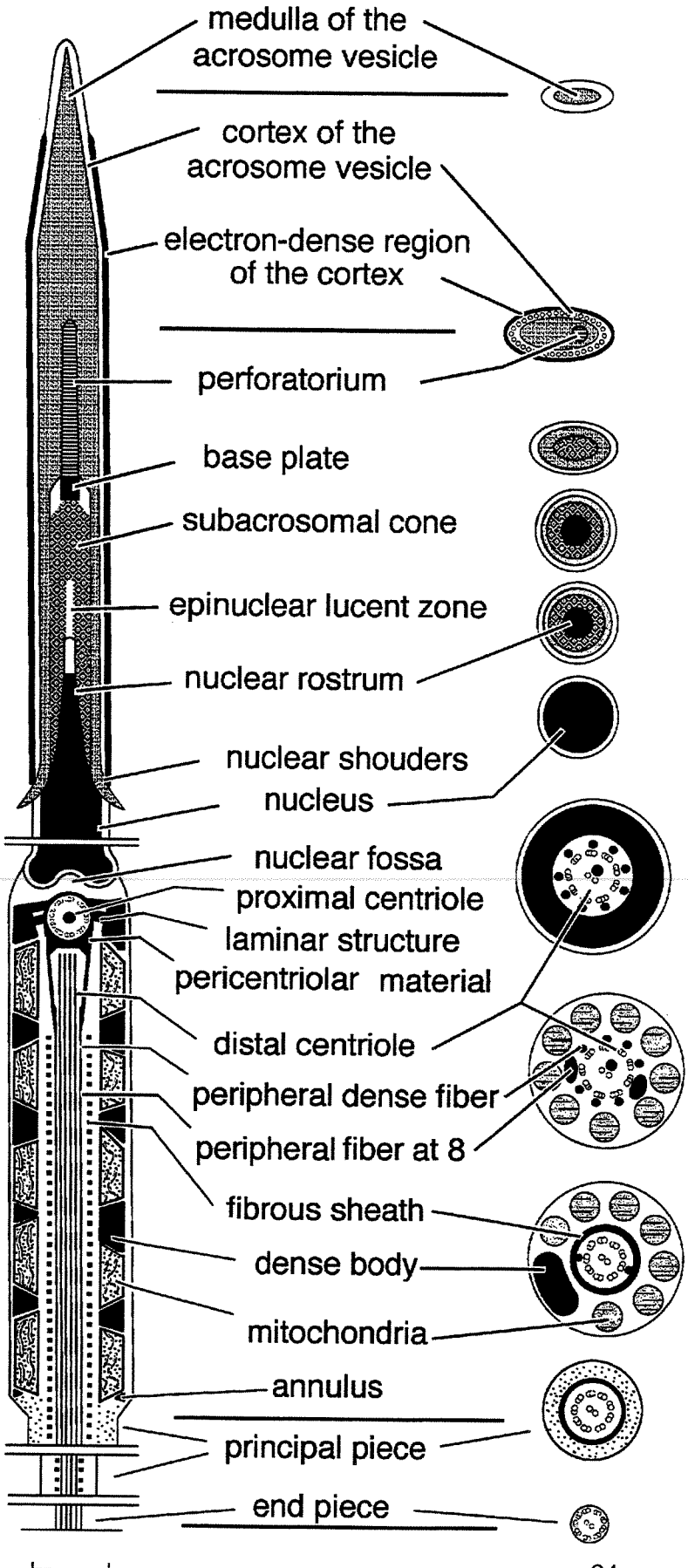
medulla of the acrosome vesicle
cortex of the acrosome vesicle
electron-dense region of the cortex
perforatorium
base plate
subacrosomal cone
epinuclear lucent zone
nuclear rostrum
nuclear shouders
nucleus
nuclear fossa
proximal centriole
laminar structure
pericentriolar material
distal centriole
peripheral dense fiber
peripheral fiber at 8
fibrous sheath
dense body
mitochondria
annulus
principal piece
end piece

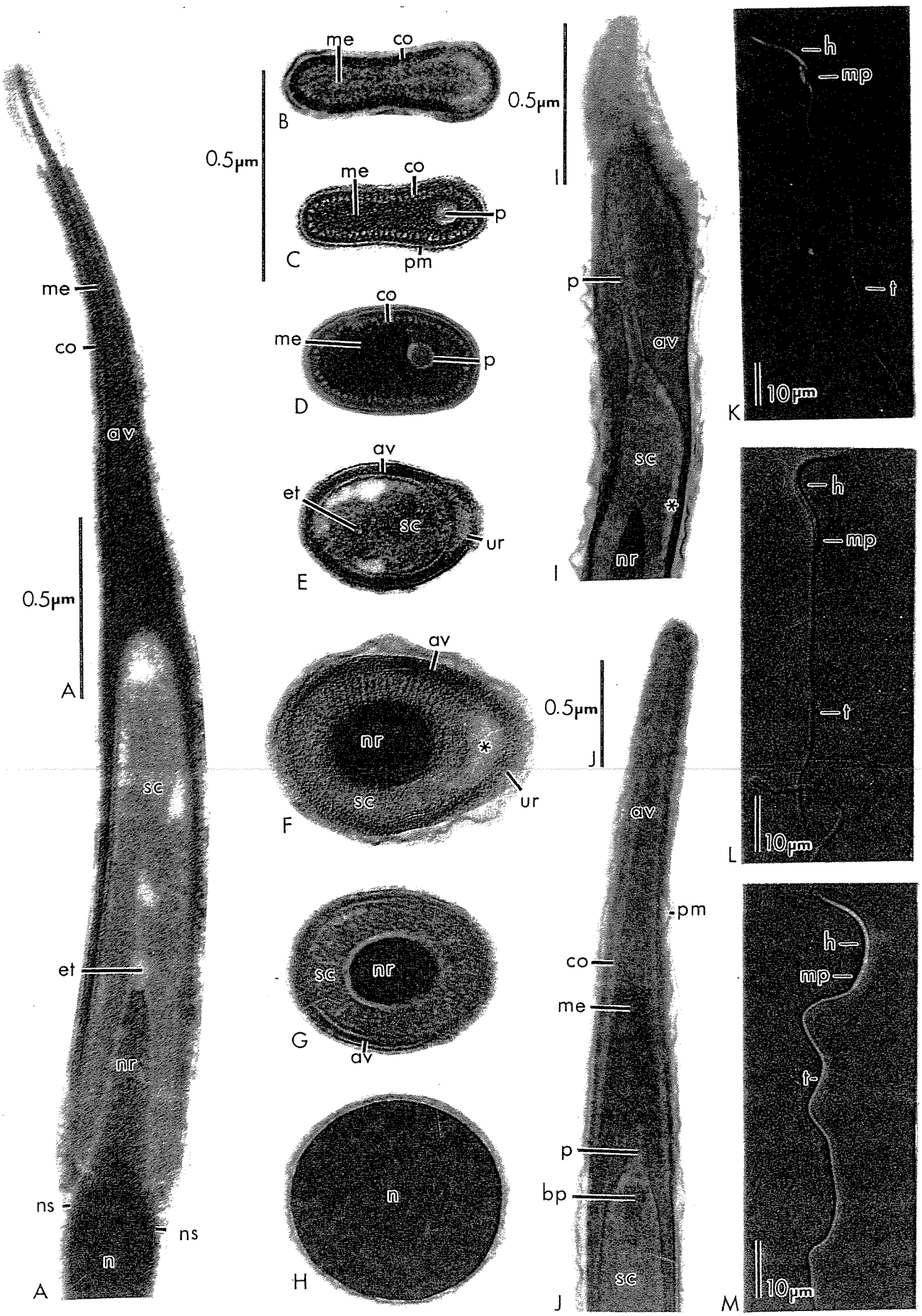
me
co
av
0.5µm
A
sc
et
nr
ns
ns
n
A
me
co
B
0.5µm
p
pm
C
co
me
p
D
av
et
sc
ur
E
av
nr
sc
ur
F
sc
nr
av
G
n
H
0.5µm
I
p
av
sc
nr
I
h
mp
t
10µm
K
h
mp
t
10µm
L
0.5µm
J
av
pm
co
me
p
bp
sc
J
h
mp
t
10µm
M

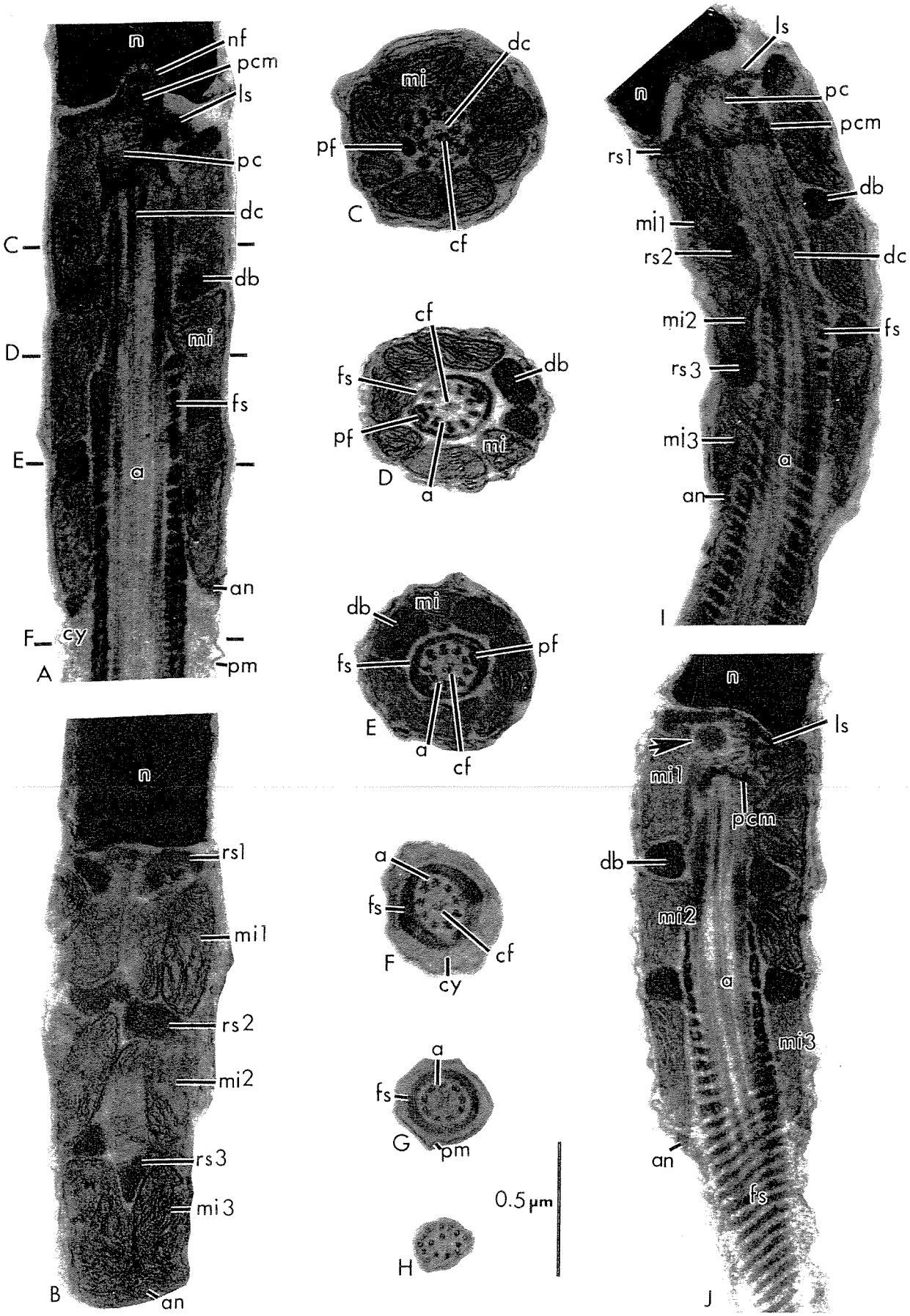
n
nf
pcm
ls
pc
dc
C
db
mi
D
fs
E
a
an
F
cy
A
pm
dc
mi
pf
C
cf
cf
fs
db
pf
mi
D
a
db
mi
fs
pf
E
a
cf
a
fs
cf
F
cy
a
fs
G
pm
H
0.5 µm
ls
n
pc
pcm
rs1
db
mi1
rs2
dc
mi2
fs
rs3
mi3
a
an
I
n
rs1
mi1
rs2
mi2
rs3
mi3
an
B
n
ls
mi1
pcm
db
mi2
a
mi3
an
fs
J

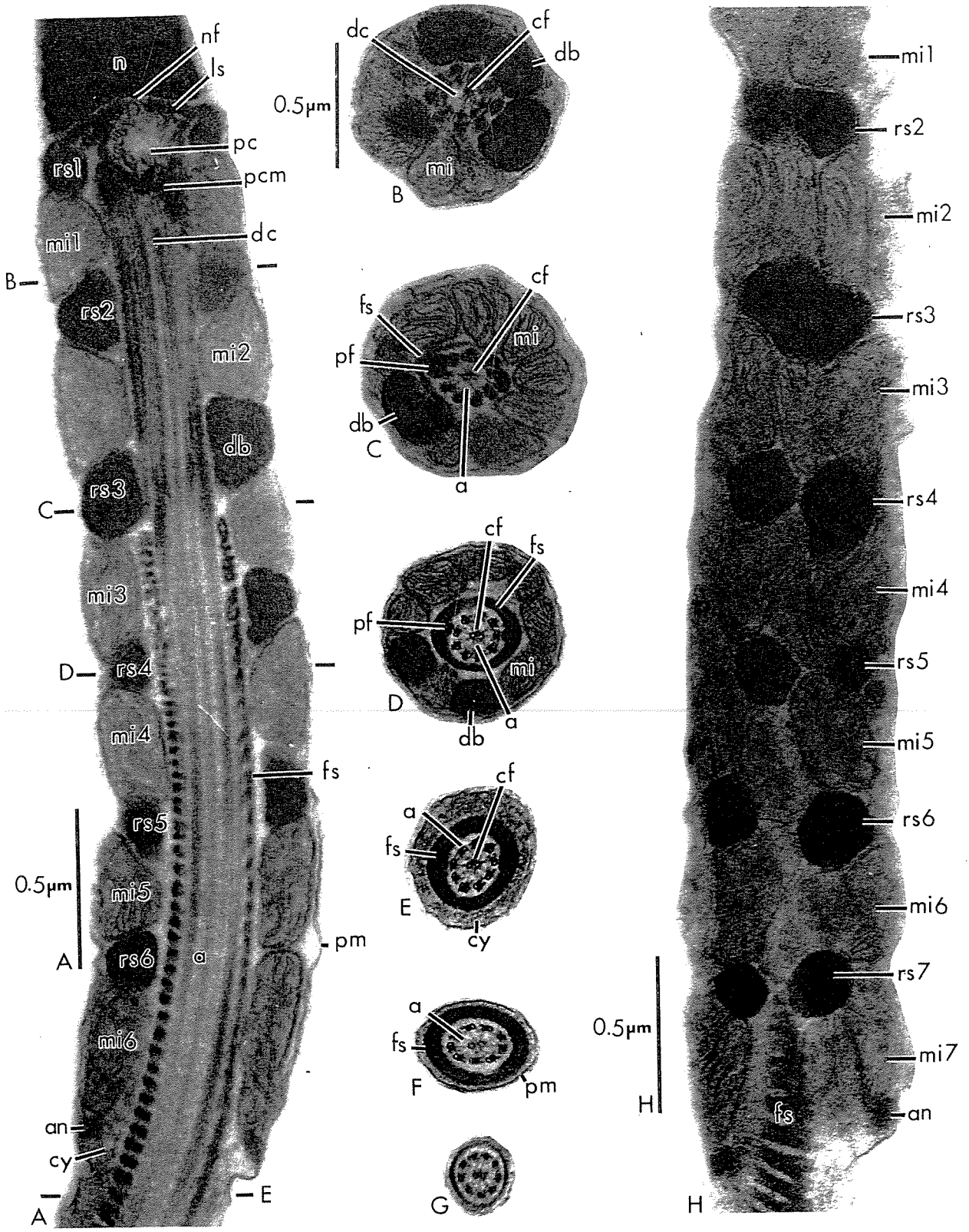
n
nf
ls
pc
pcm
rs1
mi1
dc
B
rs2
mi2
db
C
rs3
mi3
D
rs4
mi4
fs
rs5
0.5µm
mi5
A
rs6
a
pm
mi6
an
cy
A
E
dc
cf
db
0.5µm
mi
B
cf
fs
pf
mi
db
C
a
cf
fs
pf
mi
D
a
db
cf
a
fs
E
cy
a
fs
F
pm
G
mi1
rs2
mi2
rs3
mi3
rs4
mi4
rs5
mi5
rs6
mi6
rs7
0.5µm
mi7
H
fs
an
H

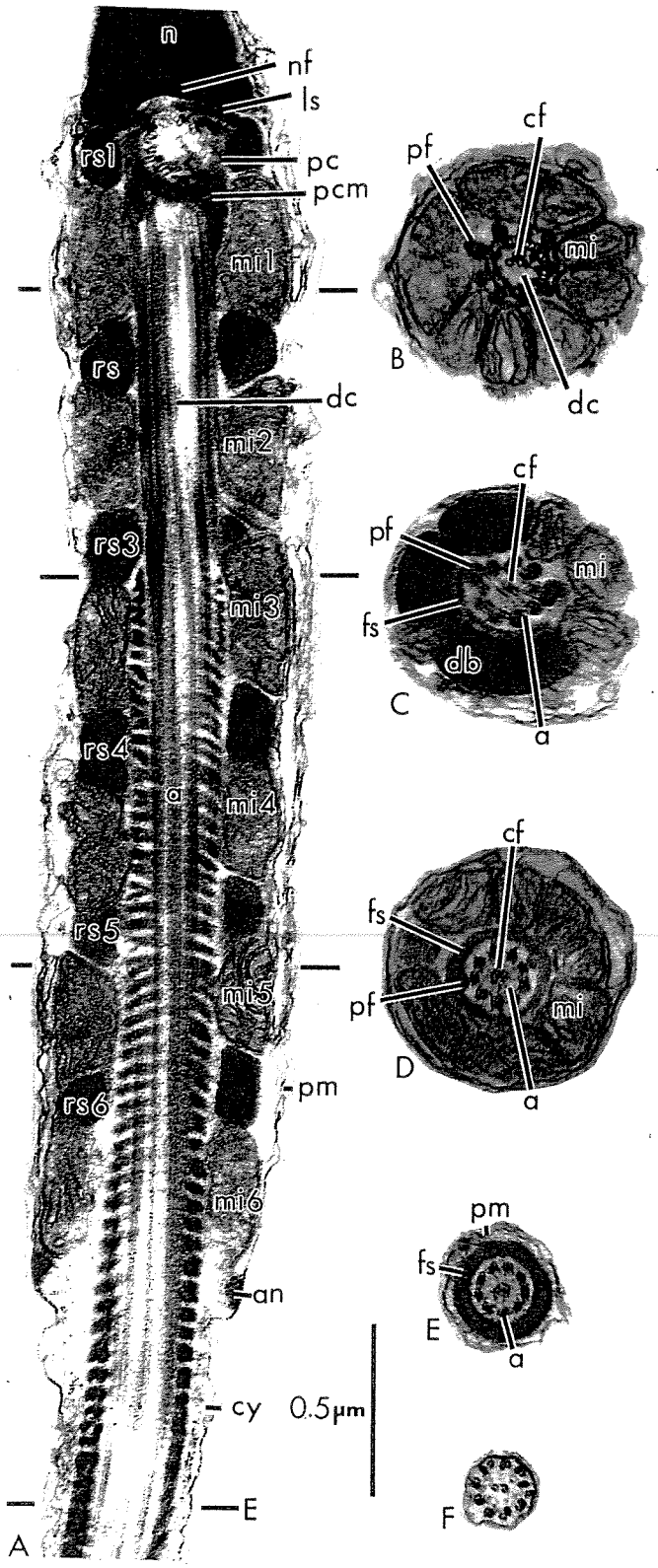
n
nf
ls
rs1
pc
pcm
mi1
rs
dc
mi2
rs3
mi3
rs4
a
mi4
rs5
mi5
pm
rs6
mi6
an
cy
E
A
0.5µm
cf
pf
mi
B
dc
cf
pf
mi
fs
db
C
a
cf
fs
pf
mi
D
a
pm
fs
E
a
F

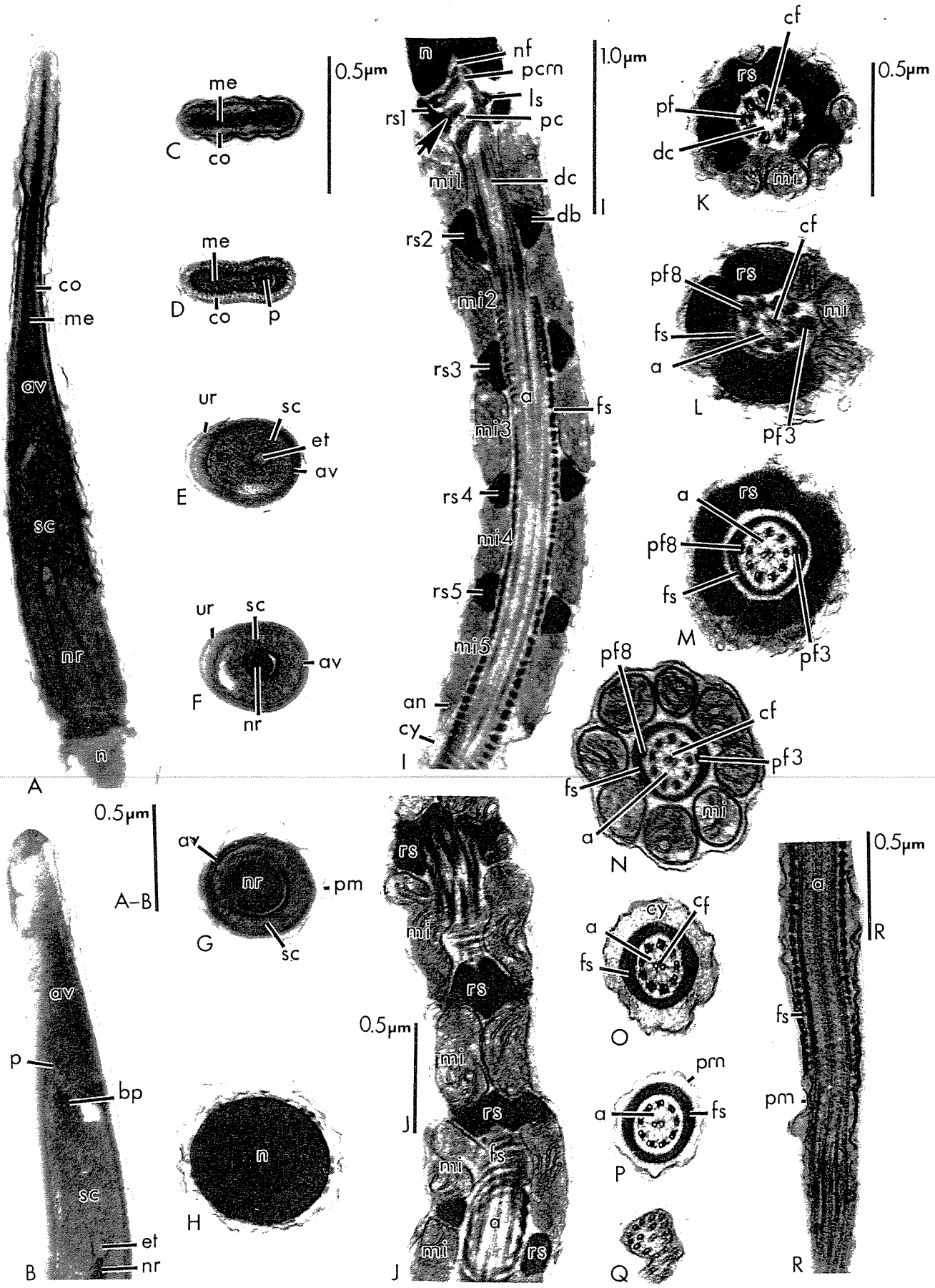
A
co
me
av
sc
nr
n
B
et
nr
bp
p
C
me
co
D
me
co
p
E
ur
sc
et
av
F
ur
sc
av
nr
G
av
nr
pm
sc
H
n
I
n
nf
pcm
ls
rs1
pc
mi1
dc
db
rs2
mi2
rs3
a
fs
mi3
rs4
mi4
rs5
mi5
an
cy
J
rs
mi
rs
mi
rs
fs
mi
a
mi
rs
K
cf
rs
pf
dc
mi
L
cf
pf8
rs
mi
fs
a
pf3
M
a
rs
pf8
fs
pf3
N
pf8
cf
pf3
fs
a
mi
O
cy
cf
a
fs
P
pm
a
fs
Q
R
a
fs
pm
0.5µm
A–B
1.0µm
0.5µm
0.5µm
0.5µm
R

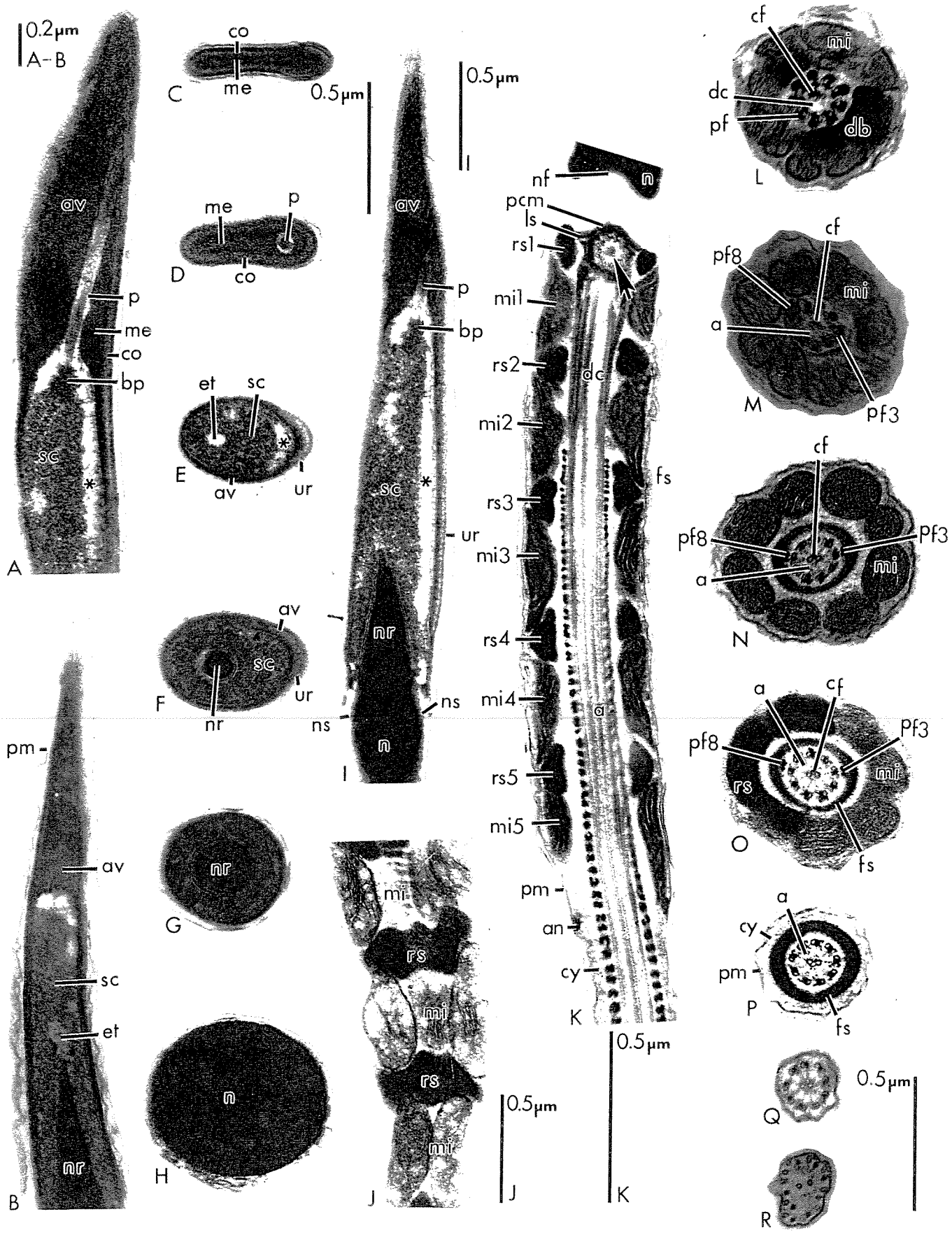
0.2µm
A–B
av
p
me
co
bp
sc
A
co
me
C
0.5µm
me
p
co
D
et
sc
av
ur
E
av
sc
ur
nr
F
pm
av
sc
et
nr
B
nr
G
n
H
0.5µm
av
p
bp
sc
ur
nr
ns
n
I
mi
rs
mi
rs
mi
J
0.5µm
J
nf
n
pcm
ls
rs1
mi1
rs2
dc
mi2
fs
rs3
mi3
rs4
mi4
a
rs5
mi5
pm
an
cy
K
0.5µm
K
cf
mi
dc
pf
db
L
cf
pf8
mi
a
M
pf3
cf
pf8
Pf3
mi
a
N
a
cf
pf8
Pf3
rs
mi
O
fs
a
cy
pm
P
fs
Q
0.5µm
R

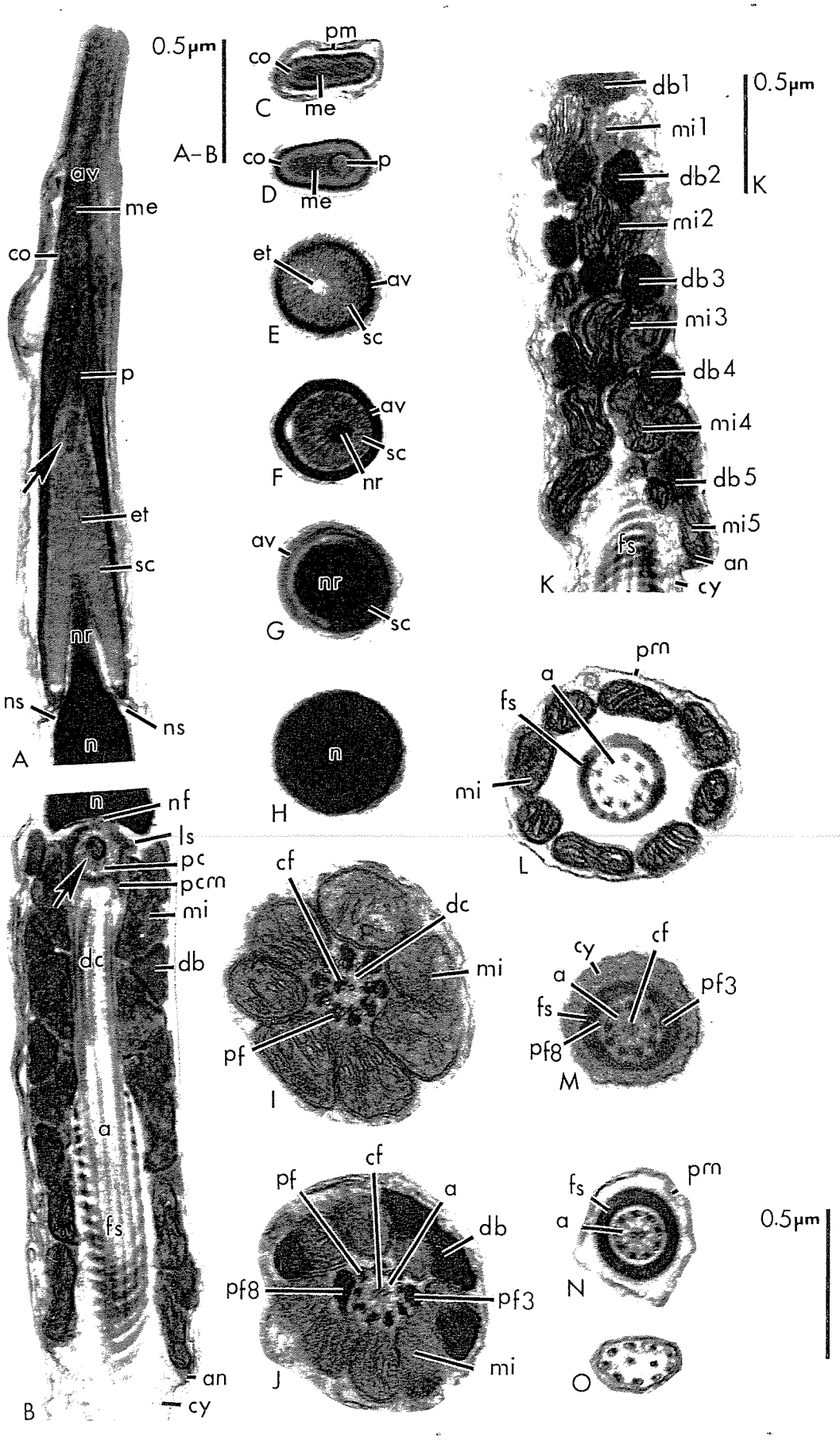
0.5µm
A–B
av
me
co
p
et
sc
nr
ns
n
A
pm
co
me
C
co
p
me
D
et
av
sc
E
av
sc
nr
F
av
nr
sc
G
n
H
db1
mi1
db2
mi2
db3
mi3
db4
mi4
db5
mi5
fs
an
cy
K
0.5µm
pm
a
fs
mi
L
n
nf
ls
pc
pcm
mi
dc
db
a
fs
an
cy
B
cf
dc
mi
pf
I
cy
cf
a
pf3
fs
pf8
M
pf
cf
a
db
pf8
pf3
mi
J
fs
pm
a
N
O
0.5µm
h
mp
f
P
10µm
h
mp
f
Q
10µm
h
mp
f
R
10µm

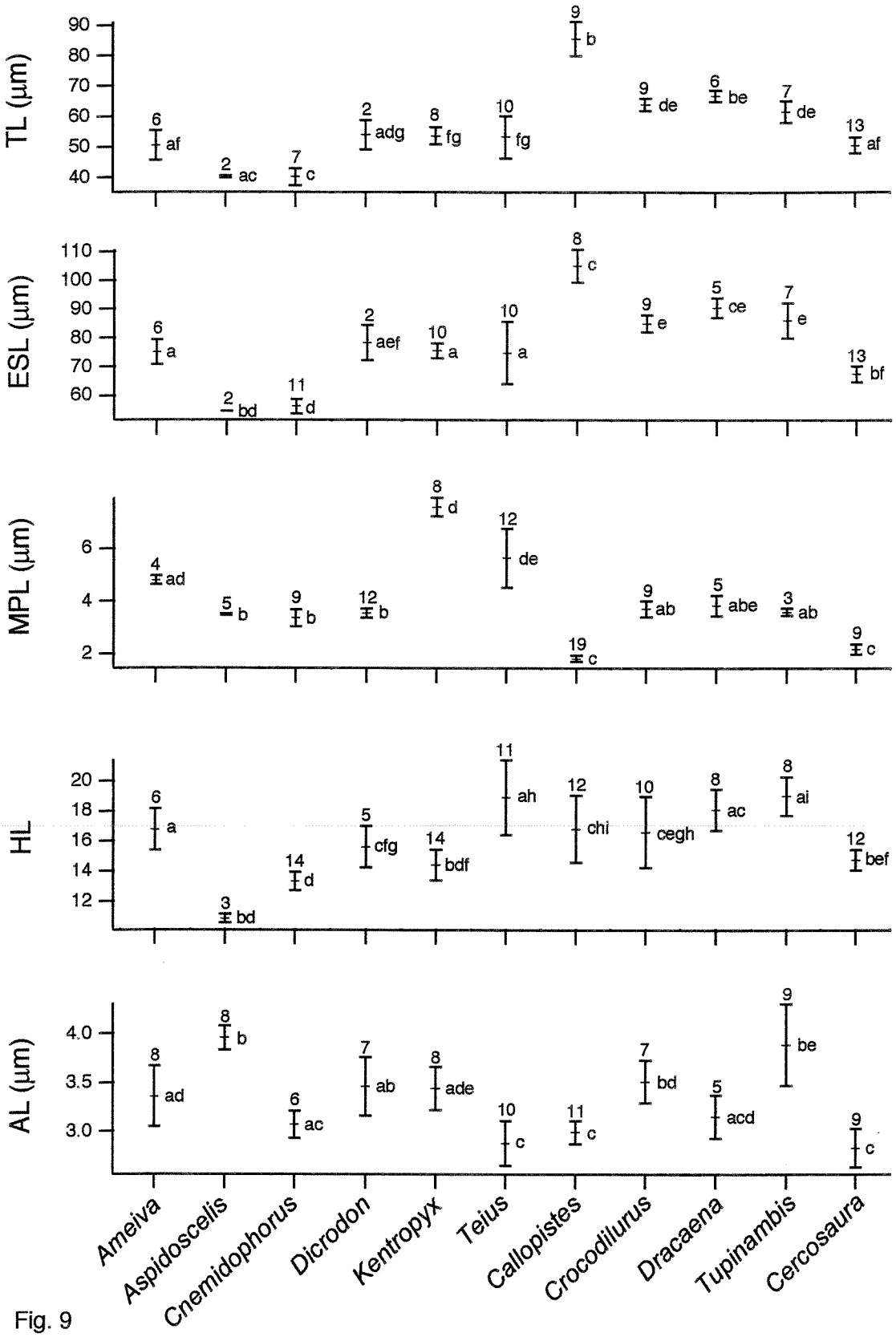
TL (µm)
ESL (µm)
MPL (µm)
HL
AL (µm)
Ameiva
Aspidoscelis
Cnemidophorus
Dicrodon
Kentropyx
Teius
Callopistes
Crocodilurus
Dracaena
Tupinambis
Cercosaura

Fig. 9

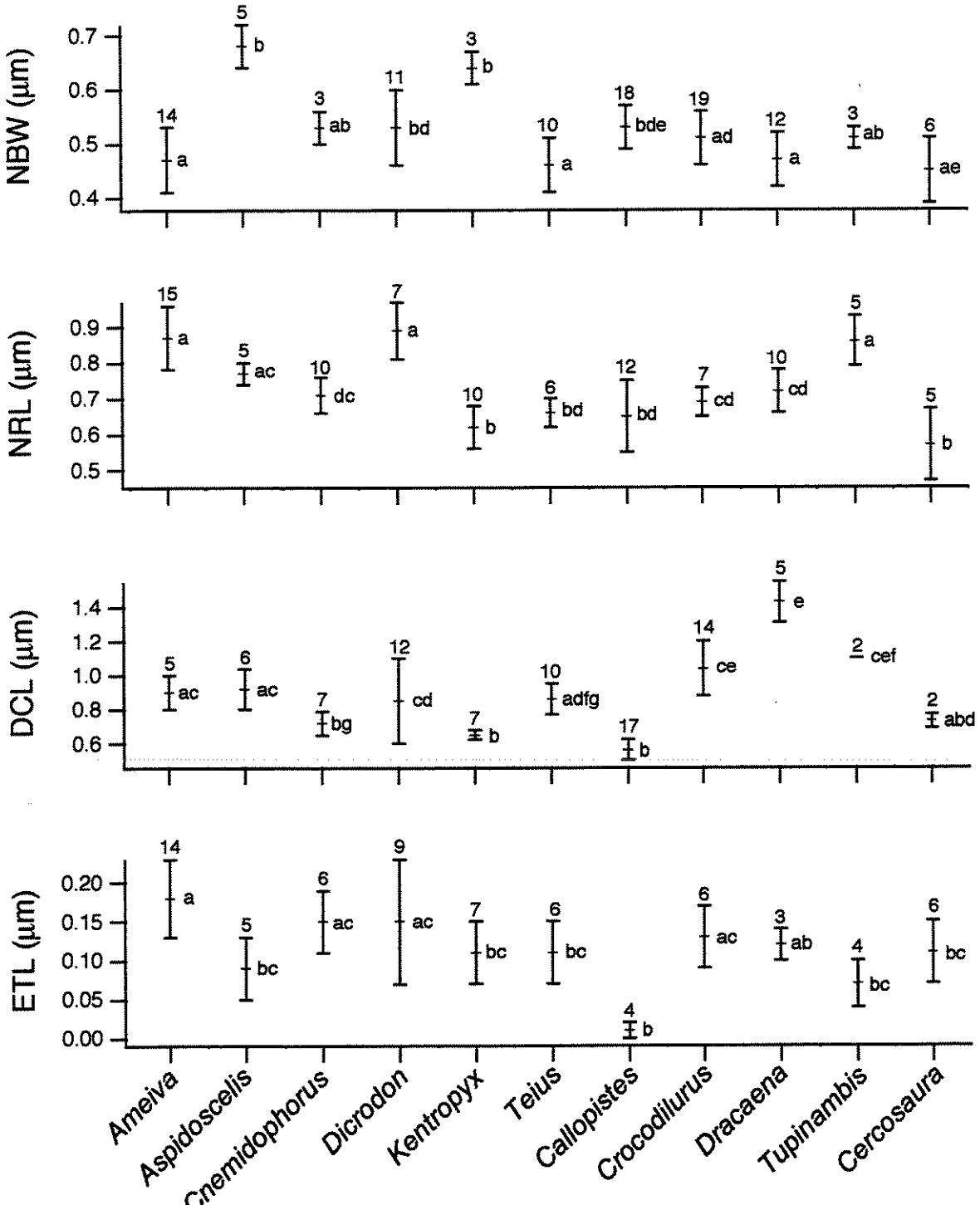
NBW (µm)
0.7
0.6
0.5
0.4
14 a
5 b
3 ab
11 bd
3 b
10 a
18 bde
19 ad
12 a
3 ab
6 ae
NRL (µm)
0.9
0.8
0.7
0.6
0.5
15 a
5 ac
10 dc
7 a
10 b
6 bd
12 bd
7 cd
10 cd
5 a
5 b
DCL (µm)
1.4
1.2
1.0
0.8
0.6
5 ac
6 ac
7 bg
12 cd
7 b
10 adfg
17 b
14 ce
5 e
2 cef
2 abd
ETL (µm)
0.20
0.15
0.10
0.05
0.00
14 a
5 bc
6 ac
9 ac
7 bc
6 bc
4 b
6 ac
3 ab
4 bc
6 bc
Ameiva
Aspidoscelis
Cnemidophorus
Dicrodon
Kentropyx
Teius
Callopistes
Crocodilurus
Dracaena
Tupinambis
Cercosaura

Fig. 10

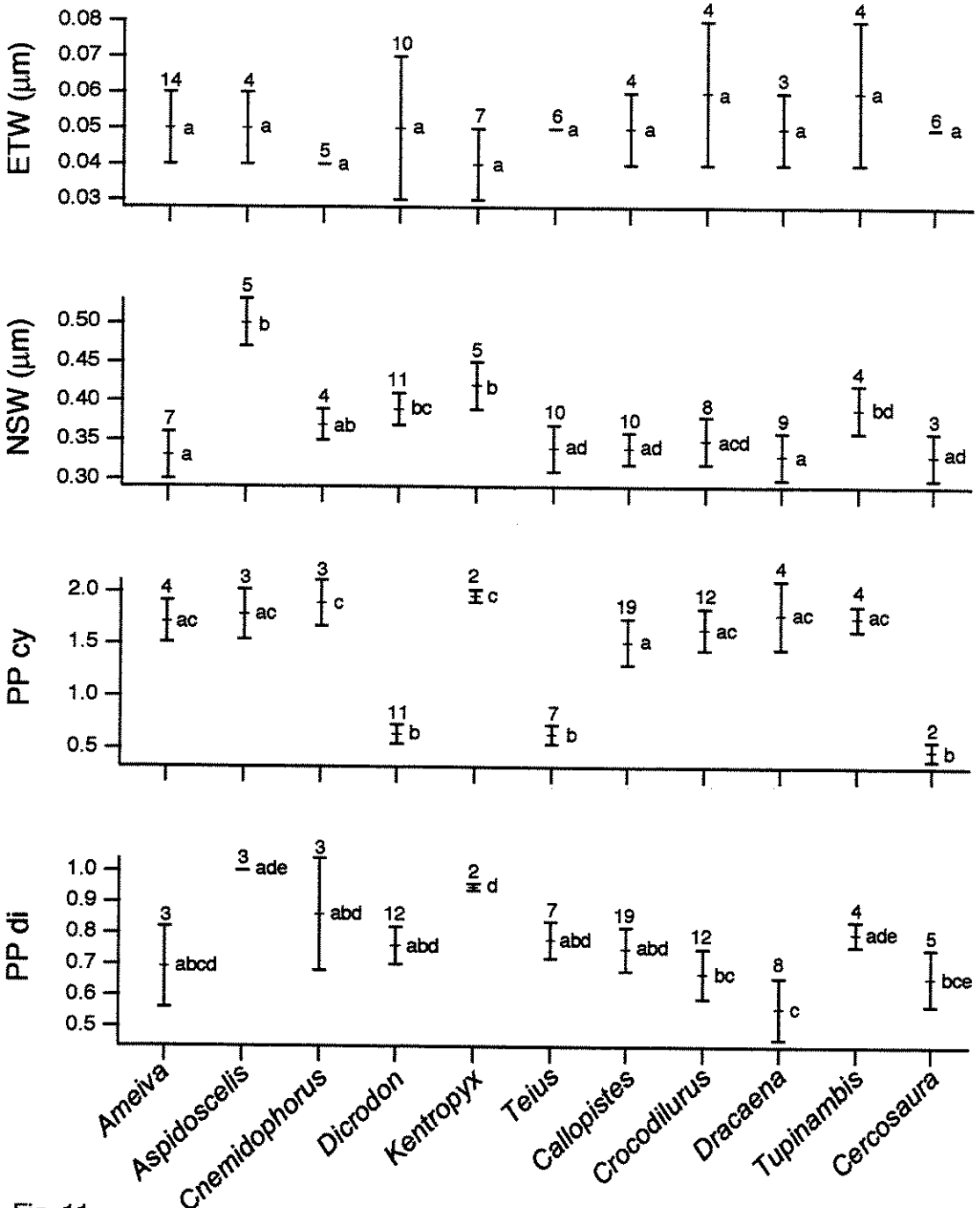
ETW (µm)
0.08
0.07
0.06
0.05
0.04
0.03
14 a
4 a
5 a
10 a
7 a
6 a
4 a
4 a
3 a
4 a
6 a
NSW (µm)
0.50
0.45
0.40
0.35
0.30
7 a
5 b
4 ab
11 bc
5 b
10 ad
10 ad
8 acd
9 a
4 bd
3 ad
PP cy
2.0
1.5
1.0
0.5
4 ac
3 ac
3 c
11 b
2 c
7 b
19 a
12 ac
4 ac
4 ac
2 b
PP di
1.0
0.9
0.8
0.7
0.6
0.5
3 abcd
3 ade
3 abd
12 abd
2 d
7 abd
19 abd
12 bc
8 c
4 ade
5 bce
Ameiva
Aspidoscelis
Cnemidophorus
Dicrodon
Kentropyx
Teius
Callopistes
Crocodilurus
Dracaena
Tupinambis
Cercosaura

Fig. 11

2.2 – CAPÍTULO II

ANÁLISES FILOGENÉTICAS DA FAMÍLIA TEIIDAE, E A UTILIDADE FILOGENÉTICA DA ULTRA-ESTRUTURA DE ESPERMATOZÓIDE.

2.2.1 – ARTIGO 5

TEIXEIRA, Ruscaia Dias, WIENS, John; VIEIRA, Gustavo Henrique Calazans; PERES JR., Ayrton Klier; COLLI, Guarino Rinaldi; BÁO, Sônia Nair. Phylogenetic relationships among teiid genera (Teiidae; Squamata; Reptilia), and the phylogenetic utility of sperm ultrastructure.

PHYLOGENETIC RELATIONSHIPS AMONG TEIID GENERA (TEIIDAE; SQUAMATA; REPTILIA), AND THE PHYLOGENETIC UTILITY OF SPERM ULTRASTRUCTURE

RUSCAIA D. TEIXEIRA [1,2], JOHN J. WIENS [3], GUSTAVO H. C. VIEIRA [4], AYRTON K. PÉRES JR. [4], GUARINO R. COLLI [5], AND SÔNIA N. BÁO [2]

[1]*Departamento de Biologia Celular, Universidade Estadual de Campinas, 13083-970, Campinas, SP, Brasil*

[2]*Departamento de Biologia Celular, Universidade de Brasília, 70919-970, Brasília, DF, Brasil*

[3]*Section of Amphibians and Reptiles, Carnegie Museum of Natural History, Pittsburgh, Pennsylvania 15213-4080, U.S.A*

[4]*Pos-graduação em Biologia Animal, Instituto de Biologia, Universidade de Brasília, 70919-970, Brasília, DF, Brasil*

[5]*Departamento de Zoologia, Universidade de Brasília, 70919-970, Brasília, DF, Brasil*

[5]Author to whom Correspondence should be addressed (grcolli@unb.br).

ABSTRACT: Phylogenetic analysis of teiid genera based on sperm ultrastructural data show major congruent areas with the tree based on traditional morphological data. On the other hand, the topology based on sperm ultrastructure tree resulted in weaker and more not supported clades than the traditional morphological tree. Two reasons might be producing low bootstrap values on the sperm ultrastructure tree; (1) high levels of homoplasy, and/or (2) low number of characters in the data set. Comparisons between the consistence indices of trees derived from the two data sets show that sperm ultrastructure characters are not more homoplastic than to traditional morphological characters. A resampling bootstrap analysis of the morphological data indicated that low bootstrap values of the sperm ultrastructure tree clades might be caused by the lower number of characters. Therefore, we considered a combined analysis the best approach, due to the high number of characters employed. The phylogeny based on the combined data splits the Teiidae in two subfamilies (Tupinambinae and Teiinae), corroborating previous phylogenetic hypotheses. The subfamily Teiinae consists of *Ameiva*, *Teius*, *Dicrodon*, *Kentropyx*, *Cnemidophorus*, *Aspidoscelis* and *Callopistes*. Tupinambinae consists of *Tupinambis*, *Crocodilurus*, and *Dracaena*. Within Teiinae, *Ameiva* is the sister-group of *Teius*, whereas the sister-group *Cnemidophorus* – *Aspidoscelis* is more closely related to *Kentropyx*. Within Tupinambinae, *Crocodilurus* and *Dracaena* are sister-groups. Future works are warranted to expand the sperm ultrastructural data set and cast light on the usefulness of these characters in phylogenetic reconstruction at the generic level.

ADDITIONAL KEYWORDS: Sperm ultrastructure – Traditional morphology – lizards – Teiidae – Tupinambinae – Teiinae – Phylogeny – Squamata – Reptilia

Recently, the ultrastructure of spermatozoa of Squamata has been used as a new source of characters in phylogenetic analysis (Jamieson, 1995, 1999; Teixeira et al., 1999a, b). On one hand, sperm ultrastructural data contain significant phylogenetic information (Teixeira et al., 1999a). On the other, phylogenetic analyses of Squamata based on sperm ultrastructural data have produced unresolved consensus trees that were largely incongruent with trees based on traditional morphological data (Jamieson, 1995; Teixeira et al., 1999a, b). This result is likely due to (1) high levels of intrafamilial variability in sperm ultrastructure and (2) the fact that families were used as terminal taxa (Teixeira et al., 1999a, b). According to Giugliano et al. (2002), the use of sperm ultrastructural data can be profitably useful to investigate phylogenetic relationships at the interfamilial level, using species as terminal taxa and sampling multiple genera within families. As sperm ultrastructural data have been used to investigate Squamate relationships solely at the family level (Jamieson, 1995; Jamieson et al., 1996; Oliver et al., 1996; Teixeira et al., 1999a, b), it is still unclear at which level of the taxonomical hierarchy they can be most profitably used in phylogenetic analysis.

The lizard family Teiidae is restricted to the New World, ranging from the northern United States to central Argentina and Chile (Cei and Scolaro, 1982; Wright, 1993). The group is known since the Late Cretaceous in North America and Central Asia (Carrol, 1988; Gao and Fox, 1996), and comprises 10 genera (Reeder et al., 2002) with a total of 117 species. All genera are restricted to South America, with the exception of *Cnemidophorus*, *Aspidoscelis* and *Ameiva* that also occur in North and Central America.

Boulenger (1885) split the family Teiidae into four groups. Group I is characterized by having the anterior nasal plates not separated by fronto-nasal scales, limbs well developed, and all members are medium to large bodied. The Groups II, III and IV have anterior nasal plates separated by one or two fronto-nasal scales, and contain the smaller genera, many of which show partial or complete reduction of the limbs. Ruibal (1952) divided the family in two groups: Group I, including the large-bodied genera *Ameiva*, *Callopistes*, *Cnemidophorus*, *Crocodilurus*, *Dicrodon*, *Dracaena*, *Kentropyx*, *Teius*, and *Tupinambis*, commonly called macroteiids, and Group II, including the remaining genera (microteiids). Presch (1983) confirmed the monophyly of these two groups, based on data from osteology, hemipenis, brain morphology (Northcutt, 1978), adductor musculature (Rieppel, 1980), and chromosome morphology (Gorman et al., 1980), placing the microteiids in the family Gymnophthalmidae and the macroteiids in the family Teiidae. However, Presch's arrangement was not widely accepted (Harris, 1985; Myers and Donnelly, 2001).

Reeder et al. (2002) found *Cnemidophorus* is not monophyletic, being *lemniscatus* group taxa more closely related to *Ameiva* and *Kentropyx* than to the strongly supported North American clade of *Cnemidophorus* (*deppii*, *sexlineatus*, and *tigris* groups). Reeder et al. (2002) also found the paraphyly of *lemniscatus* group, whereas the monophyly of the *deppii*, *sexlineatus*, and *tigris* groups of the North American *Cnemidophorus* clade was strongly supported. Hence, Reeder et al. (2002) suggest to apply the name *Aspidoscelis* to accommodate the taxa of the North American clade of *Cnemidophorus*, and the name *Cnemidophorus* to the *lemniscatus* group.

Several studies have attempted to clarify the relationship among the teiid genera, based on external morphology (Vanzolini and Valencia, 1965), chromosomes (Gorman, 1970), osteology (Boulenger, 1885; Presch, 1970; Veronese and Krause, 1997), and myology (Rieppel, 1980; Moro and Abdala, 2000). In all these studies, with the exception of Moro and Abdala (2000), the family is formed by two monophyletic groups: the subfamily Teiinae, comprising *Ameiva*, *Cnemidophorus*, *Dicrodon*, *Kentropyx*, and *Teius*, and the subfamily Tupinambinae, comprising *Callopistes*, *Crocodilurus*, *Dracaena*, and *Tupinambis*. Vanzolini and Valencia (1965) and Presch (1974) discussed the relationships among generic, and concluded that *Ameiva* is closely related to *Cnemidophorus* and that *Tupinambis* is closely related to *Dracaena*. However, Presch (1974) considered *Crocodilurus* the sister-group of the pair *Tupinambis* + *Dracaena*, whereas Vanzolini and Valencia (1965) considered *Crocodilurus* closer to *Callopistes*. Moro and Abdala (2000) conducted a phylogenetic analysis of cranial musculature and concluded that Teiidae is monophyletic if *Pantodactylus* is included, and found no support for the subfamilies Teiinae and Tupinambinae. Further, their results are not coincident with those obtained by Vanzolini and Valencia (1965) and Presch (1974). Despite these accounts tried to solve teiid phylogeny, the relationships among genera are not completely solved.

Herein, we conduct combined and partitioned phylogenetic analyses of teiid lizards, based on sperm ultrastructural data and traditional morphological data including new characters from hemipenes, scales, and tongue. We attempt to evaluate the level of incongruence between trees derived from the two data sets and the usefulness of sperm

ultrastructure characters in phylogenetic reconstruction at the generic level. Further, we propose a new taxonomic arrangement of teiid genera.

MATERIAL AND METHODS

Traditional Morphological Data

We used data from osteology, external morphology, cranial myology, external and internal morphology of the tongue, and hemipenial morphology. We used osteological data from Presch (1970) and Veronese and Krause (1997) and characters of external morphology from Vanzolini and Valencia (1965). We obtained data on cranial myology from Moro and Abdala (2000). We also obtained additional scales characters from alcohol-preserved museum specimens, which are listed in Appendix I.

We scored tongue characters in this study from alcohol-preserved museum specimens (see Appendix I). We examined the arrangement of muscles and connective tissues within the tongue by sectioning and histological staining. Each tongue was removed by dissection, cut in three parts (anterior, medium and posterior portions), and fixed for 48h in a Bouin solution. We dehydrated the material in a series of ascending ethanol series (30%-100%), washed tissues in a series of ascending xilol series (30%-100%), and embedded them in Paraplast resin. We stained the sections with hematoxylin-eosin, and made observations with a Zeiss® Germany Stem SV 11 microscope. Terminology for tongue morphology followed Presch (1971), Harris (1985), and Schwenk (1988).

We obtained data on hemipenial morphology based on either the left or right organ, removed from live specimens (listed in Appendix I) by manually everting the

structure with 10% formaldehyde. We submerged the everted organ in 10% formaldehyde overnight and filled it with 2.5% (small specimens) or 3% (large specimens) solution of agarose (Manzani and Abe, 1988). Terminology for hemipenial morphology followed Klaver and Bohme (1986), Ziegler and Bohme (1997), and Savage (1997).

We scored a total of 138 variable morphological characters, consisting of: 28 from osteology (27 qualitative and 1 meristic), 35 from scales and other external morphology (19 qualitative and 16 meristic), 14 from external tongue morphology (13 qualitative and 1 meristic), five from internal tongue morphology (all qualitative), 19 from hemipenis (18 qualitative and 1 meristic), and 37 from cranial myology (all qualitative). The data matrix is given in Table 1, and means of quantitative characters are given in Table 2.

Sperm Ultrastructural Data

We obtained data from the literature for the following species: *Ameiva ameiva* (Giugliano et al., 2002), *Cnemidophorus ocellifer*, *C. gularis gularis* and *Kentropyx altamazonica* (Teixeira et al., 2002), *Tupinambis teguixin* (Tavares-Bastos et al., 2002), and *Callopistes flavipunctatus*, *Cercosaura ocellata*, *Crocodilurus amazonicus*, *Dicrodon guttulatum*, *Dracaena guianensis*, and *Teius oculatus* (Teixeira's personal comments).

The spermatozoa of teiid lizards consist of a head region containing of the nucleus and the acrosome complex, a midpiece, and a tail region (flagellum) subdivided into principal piece and endpiece (Giugliano et al., 2002; Tavares-Bastos et al., 2002; Teixeira

et al., 2002). A generalized spermatozoon of the family is represented diagrammatically in Figure 1.

Based on the ultrastructural features of spermatozoa, a total of 25 variable characters could be scored, consisting of 14 qualitative and fixed characters, and 11 morphometric characters. The data matrix is presented in the Table 1, proportions of the quantitative characters are given in Table 3, and sperm dimensions are given in Table 4.

Characters Descriptions

Character states are designated as "0" or '1" for the purposes of description only, and not to indicate polarity.

Traditional Morphological Qualitative Characters

OSTEOLOGY

1. *Postorbital and postfrontal.*— (0) separated, (1) fused (Presch, 1970).
2. *Quadrate process of the pterygoid.*— (0) not expanded, (1) expanded (Presch, 1970).
3. *Pterygoid flange.*— (0) low, (1) high (Presch, 1970).
4. *Dorsal process of the squamosal.*— (0) present, (1) absent (Presch, 1970).
5. *Expanded quadrate.*— (0) no, (1) yes (Presch, 1970).
6. *Teeth on the pterygoid.*— (0) absent, (1) present (Presch, 1970).
7. *Teeth on the premaxillary.*— (0) conical, (1) bi-, triconodont (Presch, 1970).
8. *Clavicle shape.*— (0) expanded, (1) simple rod-shaped (Presch, 1970).
9. *Clavicle hook.*— (0) absent, (1) present (Presch, 1970).

10. *Interclavicle median process.*— (0) short, (1) long (Presch, 1970).

11. *Scapular foramen.*— (0) absent, (1) present (Presch, 1970).

12. *Number of post-xiphisternal ribs.*— (0) 12, (1) 11 (Presch, 1970).

13. *Number of presacral vertebrae.*— (0) 25, (1) 26 (Presch, 1970).

14. *Neural arch, first autotomic caudal vertebrae.*— (0) low, (1) high (Presch, 1970).

15. *Second ceratobranchial.*— (0) present, (1) absent (Presch, 1970).

16. *Anterior teeth on the maxillary bone.*— (0) iso-, bi- or triconodont, (1) molariform and expanded (Presch, 1970).

17. *Supra-angular window.*— (0) present, (1) absent (Presch, 1970).

18. *Contribution of the ectopterygoid to the inferior orbital foramen.*— (0) high, (1) low (Presch, 1970).

19. *Shape of the frontal-parietal roof.*— (0) concave, (1) convex (Presch, 1970).

20. *Retroarticular process orientation, lower jaw.*— (0) ventral; (1) ventro-medial (Presch, 1970).

21. *Condition of the fifth digit of the hind limb.*— (0) normal, (1) reduced (Presch, 1970).

22. *Number of xiphisternal ribs.*— (0) 2, (1) 3 (Presch, 1970).

23. *First cervical vertebra with rib.*— (0) fourth cervical vertebrae, (1) third cervical vertebrae (Veronese & Krause, 1997).

24. *Last vertebra with rib.*— (0) 25, (1) 24 (Veronese & Krause, 1997).

25. *Hypapophysis in the third cervical vertebra.*— (0) absent, (1) present (Veronese & Krause, 1997).

26. *Neural spine of the third cervical vertebra.*— (0) elongated, (1) reduced (Veronese & Krause, 1997).

27. *Number of vertebrae in dorsal region.*— (0) 16, (1) 17 (Veronese & Krause, 1997).

SCALES AND OTHER EXTERNAL MORPHOLOGY

28. *Postnasal scale* .— (0) absent; (1) present (Vanzolini & Valencia, 1965).

29. *Ventral scales* .— (0) imbricate; (1) juxtaposed (Vanzolini & Valencia, 1965).

30. *Carpal tubercles* .— (0) absent; (1) present (Vanzolini & Valencia, 1965):

31. *Ventral scales, shape* .— (0) rectangular; (1) phylloid (Vanzolini & Valencia, 1965).

32. *Ventral scales, keeled* .— (0) absent; (1) present (Vanzolini & Valencia, 1965).

33. *Dorsal scales, shape* .— (0) polygonal; (1) granular; (2) phylloid (Vanzolini & Valencia, 1965).

34. *Dorsal scales, tubercles* .— (0) absent; (1) present (Vanzolini & Valencia, 1965).

35. *Dorsal scales, keeled.*— (0) present; (1) absent (Vanzolini & Valencia, 1965).

36. *Number of Loreals scales.*— (0) one; (1) two.

37. *Neck scales are larger than dorsals.*— (0) no; (1) yes.

38. *Supraciliaries in contact with supraoculars.*— (0) yes; (1) no.

39. *Mentals in contact with infralabials.*— (0) yes; (1) no.

40. *Temporals are smaller than dorsals.*— (0) yes; (1) no.

41. *Gular fold.*— (0) no; (1) yes.

42. *Transversal stripe in the tail.*— (0) no; (1) yes.

43. *Intertympanic sulci.*— (0) absent; (1) present.

44. *Intermandibular sulci.*— (0) absent; (1) present.

45. *Laterally compressed tail.*— (0) absent; (1) present.

46. *Dorsal tail cristae.*— (0) absent; (1) present.

EXTERNAL MORPHOLOGY OF THE TONGUE

47. *Proportion between the anterior tongue and the posterior tongue.*— (0) one fourth; (1) one third; (2) half.

48. *Ventral medium sulci.*— (0) deep; (1) shallow.

49. *Lateral projection of the tongue.*— (0) invaginated; (1) not invaginated.

50. *Shape of the tongue.*— (0) phylloid; (1) linear.

51. *Case in the tongue base.*— (0) absent; (1) present.

52. *Scales in the tongue bifurcation.*— (0) present; (1) absent.

53. *Anterior tongue sulci.*— (0) shallow; (1) deep, originated in the tongue base; (2) deep, originated in the middle of the tongue.

54. *Tongue base reaches the larynx.*— (0) yes; (1) no

55. *Infralingual plicae.*— (0) well visible; (1) feeble.

56. *Posterior infralingual plicae related to the anterior plicae.*— (0) no change in size; (1) decrease gradually from the anterior plicae; (2) abruptly smaller, but more numerous; (3) abruptly smaller, but less numerous.

57. *Posterior plicae distribution.*— (0) alternate from side to side; (1) not alternate.

58. *Tongue sheath.*— (0) absent; (1) present.

59. *Infralingual plicae shape.*— (0) swollen; (1) thin; (2) degenerated.

INTERNAL MORPHOLOGY OF THE TONGUE

60. *Tongue shape in transverse section (anterior region)* .— (0) concave; (1) convex.

61. *Tongue shape in transverse section (media region)* .— (0) concave; (1) convex.

62. *Tongue shape in transverse section (posterior region)* .— (0) concave; (1) convex.

63. *Genioglossus muscle lateral of the tongue (anterior region)* .— (0) well developed; (1) not developed.

64. *Distance between the two bundles of hyoglossus muscle (anterior region)* .— (0) short; (1) long.

HEMIPENIS

65. *Shape of the hemipenis.*— (0) subcylindrical; (1) clavate.

66. *Rotulae, two smooth ornaments in the apex of the hemipenis.*— (0) well developed; (1) developed; (2) not developed.

67. *Pendunculus, two projections in the apex of the hemipenis.*— (0) developed; (1) well developed; (2) not developed.

68. *Auricula, two bulged ornament in the apex of the hemipenis.*— (0) well developed; (1) developed.

69. *Lobes.*— (0) slightly bilobed; (1) bilobed.

70. *Laminae in the sulcal surface.*— (0) present; (1) absent. Fixed (ci = 0.333).

71. *Laminae in the pedicel.*— (0) absent; (1) present.

72. *Depth of the lateral laminae.*— (0) swollen and deep; (1) skinny and deep; (2) shallow; (3) smooth.

73. *Depth of the asulcal lamelae in the lateral protuberances.*— (0) deep; (1) shallow.

74. *Continuity of the laminae surrounding the hemepenis.*— (0) continue; (1) not continue.

75. *Dark pigmentation of the laminae.*— (0) absent; (1) present.

76. *Dark pigmentation in the sulcus spermaticus.*— (0) absent; (1) present.

77. *Dark pigmentation in the sulcus spermaticus in the sulcal lips.*— (0) absent; (1) present.

78. *Dark pigmentation in the sulcal surface.*— (0) absent; (1) present.

79. *Dark pigmentation in the ornaments.*— (0) absent; (1) present.

80. *Type of ornament with dark pigmentation.*— (0) rotulae and pedunculus; (1) pedunculus.

81. *Shape of the asulcal sign in the apex of the hemipenis.*— (0) linear; (1) fuse-shape; (2) bulge; (3) lance tip shape.

82. *Type of pigmentation in the asulcal sign in the apex of the hemipenis.*— (0) pale; (1) dark.

CRANIAL MYOLOGY

83. *Adductor aponeurosis size.*— (0) scarcely noticeable; (1) narrow; (2) wide (Moro & Abdala, 2000).

84. *Levator anguli oris shape.*— (0) wide triangular; (1) narrow triangular; (2) narrow rectangular (Moro & Abdala, 2000).

85. *Levator anguli oris origin.*— (0) includes postorbital and julgal; (1) does not include postorbital and julgal (Moro & Abdala, 2000).

86. *Levator anguli oris origin not including postorbital.*— (0) includes quadrate; (1) does not include quadrate (Moro & Abdala, 2000)

87. *Levator anguli oris origin not including postorbital but including quadrate.*— (0) includes julgal, squamosal, and quadrate; (1) includes squamosal and quadrate; (2) includes just quadrate. (Moro & Abdala, 2000).

88. *Adductor mandibuale externus superficialis origin not including postorbital.*— (0) extends on jugal, squamosal, and quadrate; (1) extends on squamosal and quadrate. (Moro & Abdala, 2000).

89. *Adductor mandibulae externus superficialis insertion.*— (0) does not include coronoid; (1) includes coronoid (Moro & Abdala, 2000).

90. *Extension of the adductor mandibulae externus medialis origin not including parietal* — (0) over prootic; (1) over prootic and squamosal (Moro & Abdala, 2000).

91. *Extension of the adductor mandibulae externus medialis origin including parietal.*— (0) over parietal and prootic; (1) over parietal, prootic, and quadrate; (2) over parietal, prootic, quadrate, squamosal, and postorbital; (3) over parietal and squamosal (Moro & Abdala, 2000).

92. *Extension of the adductor mandibulae externus medialis insertion.*— (0) over thejust bodenaponeurosis; (1) over both coronoid and bodenaponeurosis (Moro & Abdala, 2000).

93. *Adductor mandibulae externus profundus insertion.*— (0) including mandibular fossa; (1) bodenaponeurosis (Moro & Abdala, 2000).

94. *Extension of the pseudotemporalis superficialis origin not including postorbital.*— (0) over parietal; (1) over parietal and prootic crista alaris; (2) parietal, crista alaris, and squamosal (Moro & Abdala, 2000).

95. *Extension of the pseudotemporalis superficialis insertion.*— (0) over bodenaponeurosis; (1) over both coronoid and bodenaponeurosis (Moro & Abdala, 2000).

96. *Pterygomandibularis shape.*— (0) bulky; (1) flattened (Moro & Abdala, 2000).

97. *Sexual dimorphism in the pterygomandibularis.*— (0) absent; (1) present (Moro & Abdala, 2000).

98. *Levator pterygoid length.*— (0) long; (1) short (Moro & Abdala, 2000).

99. *Protractor pterygoid origin.*— (0) basisphenoid; (1) basisphenoid and prootic; (2) prootic (Moro & Abdala, 2000).

100. *Intermandibularis anterior profundus aponeurosis.*— (0) absent; (1) present (Moro & Abdala, 2000).

101. *Intermandibularis anterior profundus shape.*— (0) irregular; (1) rectangular (Moro & Abdala, 2000).

102. *Depressor mandibulae superficialis.*— (0) undivided; (1) divided (Moro & Abdala, 2000).

103. *Cervicomandibularis shape.*— (0) narrow and covers partially the pterygomandibularis; (1) wide and covers partially the pterygomandibularis; (2) wide and covers completely the pterygomandibularis (Moro & Abdala, 2000).

104. *Hyoglossus origin.*— (0) ceratobranchial I and basihyal; (1) ceratobranchial I; (2) ceratobranchial I and epibranchial I (Moro & Abdala, 2000).

105. *Genioglossus contact.*— (0) with contact only at the origin end; (1) with contact along all the mid-ventral line (Moro & Abdala, 2000).

106. *Mandibulohyoideus I shape.*— (0) triangular; (1) trapezoidal; (2) rectangular (Moro & Abdala, 2000).

107. *Mandibulohyoideus I insertion.*— (0) ceratobranchial I and basihyal; (1) ceratobranchial I; (2) ceratobranchial I and epibranchial I; (3) ceratobranchial I, basihyal, epibranchial I, and entoglossal process (Moro & Abdala, 2000).

108. *Mandibulohyoideus II.*— (0) absent; (1) present (Moro & Abdala, 2000)

109. *Division of the mandibulohyoideus II.*— (0) divided; (1) undivided (Moro & Abdala, 2000).

110. *Mandibulohyoideus II insertion.*— (0) basihyal and entoglossal process; (1) basihyal (Moro & Abdala, 2000).

111. *Mandibulohyoideus III.*— (0) absent; (1) present (Moro & Abdala, 2000).

112. *Branchiohyoideus origin.*— (0) ceratobranchial I; (1) ceratobranchial I and epibranchial I (Moro & Abdala, 2000).

113. *Geniohipohyoideus.*— (0) absent; (1) present (Moro & Abdala, 2000).

114. *Omohyoideus origin.*— (0) Clavicular bar; (1) Clavicular bar and interclavicle; (2) Clavicular bar and sternum; (3) clavicular bar, sternum, and interclavicle; (4) clavicular bar, interclavicle, and suprascapular (Moro & Abdala, 2000).

115. *Omohyoideus insertion not including basihyal.*— (0) ceratobranchial I, ceratobranchial II and basihyal; (1) ceratobranchial I and basihyal (Moro & Abdala, 2000).

116. *Omohyoideus insertion including basihyal.*— (0) ceratobranchial I, ceratobranchial II and basihyal; (1) ceratobranchial I and basihyal (Moro & Abdala, 2000).

117. *Sternohyoideus aoneurosis.*— (0) pigmented; (1) no pigmented (Moro & Abdala, 2000).

118. *Sternohyoideus insertion.*— (0) ceratobranchial I and basihyal; (1) ceratobranchial I; (2) ceratobranchial I, epibranchial I, and basihyal (Moro & Abdala, 2000).

119. *Sternohyoideus.*— (0) absent; (1) present (Moro & Abdala, 2000).

Traditional Morphological Quantitative Characters

120. *Number of caudal vertebrae* (Presch, 1970).

121. *Number of femoral pores.*

122. *Number of supralabial scales.* Scales bordering the upper edge of the mouth (except at the tip of the snout where the rostral occurs) terminating when scales begin to be divided in smaller ones and become numerous small scales near the angle of the jaw.

123. *Number of infralabial scales*. Scales bordering the lower edge of the mouth, except at the anterior median tip, terminating when scales begin to be divided in smaller ones and become numerous small scales near the angle of the jaw.

124. *Number of supratemporal scales rows*. Scales notably enlarged in the upper portion of the temporal area.

125. *Number of lamellae of the fourth finger (foreleg)*. Ventral keeled scales of the fourth finger of the foreleg.

126. *Number of lamellae of the fourth toe (hind limb)*. Ventral keeled scales of the fourth finger of the foreleg.

127. *Number of dorsal scales.* Scales on the back, counted from the posterior head scale (interparietal), in a straight line at the middorsal line as far back as a line about even with the posterior margins of the thights, when the hind legs are held at the right angles to the body.

128. *Number of scales around the mid-body.*

129. *Number of ventral scale rows*. Scales on the sides of the body, counted from the gular fold, or from a line even with the anterior margins of the forelegs, to the anterior edge of the anus.

130. *Number of scales in a single ventral row.*

131. *Number of cloacal pores.*

132. *Number of prefemoral scales*. Anterior scales of the upper hind leg.

133. *Number of prefemoral scale rows*. Rows of anterior scales of the upper hind leg.

134. *Number of infratibial scale rows*. Rows of ventral scales of the lower hind leg.

135. *Number of preanals scales*. Scales immediately preceding the anus. The preanal area is well outlined as a V-shaped area in front of the anus, bordered on either side by small postfemoral scales, and terminating anteriorly at the mediuan ends of the femoral pore series.

136. *Number of scales in the 15th scale row around the tail.*

137. *Number of infralingual plicae.*

138. *Number of hemipenial lateral laminae.*

Sperm ultrastructural qualitative characters

139. Acrosome complex, unilateral ridge on acrosome surface (Fig. 2): (0) absent; (1) present.

140. Perforatorium, base plate (Fig. 3): (0) absent; (1) present.

141. Perforatorium, base plate shape (Fig. 3): (0) knoblike; (1) stopper-like.

142. Neck region, stratified laminar structure (Fig. 4A): (0) poorly developed; (1) well developed.

143. Neck region, stratified laminar structure projection (Fig. 4B): (0) unilateral; (1) bilateral.

144. Neck region, electron dense structure inside the proximal centriole (Fig. 4C): (0) absent; (1) present.

145. Midpiece, fibers 3 and 8 (Fig. 5): (0) grossly enlarged; (1) not grossly enlarged.

146. Midpiece, number of sets of mitochondria and ring structures (Fig. 6): (0) 3 sets; (1) 4 sets; (2) 5 sets; (3) 6 sets.

147. Midpiece, mitochondria in oblique section (Fig. 7): (0) columnar; (1) slightly curved.

148. Midpiece, mitochondria shape in longitudinal section (Fig. 8): (0) trapezoidal; (1) rounded ends.

149. Midpiece, dense bodies forming ring structures (Fig. 9): (0) do not form ring structures; (1) form ring structures.

150. Midpiece, appearance of dense bodies in the ring structures in oblique section (Fig. 10): (0) fused, forming compacted ring structures; (1) not fused, forming not compacted ring structures.

151. Midpiece, intermitochondrial dense bodies in transverse section (Fig. 11): (0) separated from the fibrous sheath by mitochondria; (1) juxtaposed to fibrous sheath.

152. Midpiece, beginning of the fibrous sheath in the midpiece (Fig. 12): (0) level of the mitochondria tier 3; (1) level of the mitochondria tier 2 (mi2); (2) level of the mitochondria tier 1 (mi1).

Sperm ultrastructural Quantitative characters

153. Ratio of head length to total sperm length (Fig. 13A). Head length is the distance between the acrosome complex tip and the nucleus posterior base. Total sperm length is the distance between the head anterior extremity and the posterior extremity of the endpiece.

154. Ratio of the acrosome length to head length (Fig. 13B). Acrosome length is the distance between the acrosome complex tip and the nucleus shoulders, which is an

abrupt and marked transition region from the nuclear rostrum to the cylindrical portion of the nucleus.

155. Ratio of midpiece length to flagellum length (Fig. 13C). The midpiece is the region between the nucleus posterior base (posterior end of the head) and the annulus. Flagellum length is the distance from the posterior end of the head to the posterior extremity of the endpiece.

156. Ratio of distal centriole length to midpiece length (Fig. 14A). The distal centriole begins at the posterior portion of the proximal centriole, and its anterior portion is covered with the periocentriolar material. The posterior end of the distal centriole is the beginning of the axoneme, where the fibrous sheath begins.

157. Ratio of mitochondrial tier length to midpiece length (Fig. 14B). The mitochondria tier length is measured from the posterior end of a ring structure to the anterior portion of the next ring structure below.

158. Ratio of the ring structure tier length to midpiece length (Fig. 15A). The ring structure tier length is the distance between the mitochondrial tiers.

159. Ratio of ring structure tier length to mitochondrial tier length (Fig. 15B).

160. Ratio of nuclear rostrum length to acrosome length (Fig. 16A). The nuclear rostrum length is the distance between the nuclear rostrum tip and the nucleus shoulders.

161. Ratio of the electron lucent zone length to the electron lucent zone width (Fig. 16B). The electron lucent zone length is the distance between the anterior portion of the condensed chromatin of the nucleus rostrum and the end of the electron lucent narrow chamber within the subacrosomal cone.

162. Ratio of the diameter of the anterior region of the principal piece to the diameter of the annulus region (Fig. 17A). This character quantifies the degree of decreasing from the annulus diameter to the beginning of the principal piece diameter.

163. Ratio of the fibrous sheath width to the principal piece width (Fig. 17B). This character quantifies the amount of cytoplasm between the plasma membrane and the fibrous sheath in the anterior portion of the principal piece.

Coding Variation

The meristic (i.e., number of caudal vertebrae, scales, infralingual plicae, hemipenial lateral lamellae) and morphometric data (ultrastructural sperm data) were treated as continuous quantitative variables, and coded using step matrix gap-weighting (Wiens, 2001), a modification of the gap-weighting method of Thiele (1993).

Step matrices are used to assign relative costs of character-state changes during phylogenetic analysis (Maddison and Maddison, 1992). In the step matrix gap-weighting method, the mean trait value (X) of each taxon is converted to a score (Xs) between 0 and 999 by the following formula:

$$X_s = \frac{(X - \min)}{(\max - \min)} \times 1{,}000$$

Where "min" is the minimum (lowest) species mean of the trait across all species and "max" is the maximum. The number 999 is the maximum cost a character-state change can receive using the software MacClade. In the step matrix, the cost of a transformation between states is the difference in their scores.

Fixed, multistate characters were ordered based on morphological intermediacy (Wilkinson, 1992). Whenever two or more species of a single genus had more than one state for a given qualitative character, we coded the variable taxon as having two states.

As the maximum cost of a transformation in each of the meristic and morphometric characters was 999 in MacClade, and the cost of a transformation in a quantitative character should be equivalent to the weight of a qualitative character (Wiens, 2001), we weighted qualitative characters by 999.

Phylogenetic Analysis

We used the ten genera of Teiidae as terminals in the analysis. Hence, we collapsed congeneric species into genera, when different data sets were not available for the same species. Species used in analyses are listed in Appendix I.

We performed phylogenetic analyses using PAUP version. 4.0.b s for Macintosh (Swofford, 1991). We sought shortest trees using an exhaustive search. Support for individual clades was evaluated using non-parametric bootstrapping (Felsenstein, 1985), using 10,000 pseudoreplicates per analysis with 10 random addition sequences per pseudoreplicate. We used a bootstrap value of 70% as cut-off for considering results strongly supported (Hillis & Bull, 1993).

The monophyly of Teiidae was proposed by Presch (1983), and corroborated by Estes (1988), Lee (1998), Caldwell (1999), and Moro and Abdala (2000). These studies considered Gymnophthalmidae as the sister-taxon of this family. Hence, the phylogeny of Teiidae was rooted by inclusion of the gymnophthalmid *Cercosaura ocellata* (*Cercosaura*) as outgroup. Although *Pantodactylus*, *Prionodactylus* are now consisdered

junior synonyms of *Cercosaura* by Doan (2003), we do not includes data from these two genera in our analysis as further study of the gymnophthalmid subfamily Cercosaurinae is clearly warranted.

Combining Data Sets

To handle the possibility of different data sets having different phylogenetic histories, we employed the congruence approach described by Wiens (1998b). First, we performed separate analyses of the traditional morphological and sperm ultrastructural data sets, evaluating the support for individual clades in each. Next, we combined both data sets, using resulting tree(s) as the best estimate(s) of phylogeny, but considering questionable those parts of the tree(s) in strongly supported conflict between the separately analyzed data sets.

RESULTS

Phylogenetic Analysis

Traditional morphological analysis.— We scored a total of 138 variable morphological characters of which 100 were parsimony-informative. Parsimony analysis of the traditional morphological data resulted in a single shortest tree of length 252906 (Fig. 18A). The shortest tree has a consistency index of 0.558 (excluding uninformative characters), and a retention index of 0.532, a rescaled consistency index of 0.334 (excluding step-matrix characters). The family is split into two monophyletic groups. One consists of *Tupinambis*, *Crocodilurus* and *Dracaena*. The other group consists of

Callopistes, *Ameiva*, *Teius*, *Dicrodon*, *Kentropyx*, *Cnemidophorus*, and *Aspidoscelis*. Within the first group, *Dracaeana* and *Crocodilurus* are closer related, and makes up the sister taxon of *Tupinambis*. In the second major group, *Callopistes* appears as sister group of the clade represented by *Ameiva*, *Teius*, *Dicrodon*, *Kentropyx*, *Cnemidophorus*, and *Aspidoscelis* genera. *Ameiva* and *Teius* appear closer related, *Dicrodon* appears closely related to *Kentropyx*, and to the pair *Cnemidophorus – Aspidoscelis*.

In Bootstrap 50% majority-rule tree (Fig. 18B), three clades emerge from a basal polytomy. One of these clades contains just a single genus, *Callopistes*. The second clade, composed by *Tupinambis*, *Crocodilurus* and *Dracaena*, is weakly supported by 66% bootstrap values. Within this clade, the pair *Crocodilurus-Dracaena* appears with 54% supporting. The third clade contains *Ameiva*, *Aspidoscelis*, *Cnemidophorus*, *Kentropyx*, *Dicrodon* and *Teius*, and appears strongly supported by the bootstrap value, with 97% supporting.

In the following paragraphs we describe some of the synapomorphies supporting the clades in the tree based on traditional morphological characters (Fig. 18A). We mention only the synapomorphies that are unambiguously placed at the stem in question (independent of optimization routine).

According to the traditional morphological data, Teiidae family (stem A) has no unambiguous synapomorphies defining the clade. The first major group, consisting of *Tupinambis*, *Crocodilurus* and *Dracaena* (Tupinambinae) (stem B), is well supported by the following synapomorphies: bi-triconodont teeth on the premaxillary bone (7.1), long interclavicle median process (10.1), absence of second ceratobranchial (15.1), retroarticular process of lower jaw ventromedially oriented (20.1), and increase in the

mean numbers of lamellae of the fourth hind limb (126), cloacal pores (131) and hemipenial lateral laminae (138). The clade *Crocodilurus* + *Dracaena* (stem C) is supported by: presence of a laterally compressed tail (45.1), presence of dorsal tail cristae (46.1), muscle mandibulohyoideus I with a triangular shape (106.0), a reduction in the mean number of caudal vertebrae (120), and increase in the mean numbers of infralabial scales (123) and lamellae of fourth foreleg (125).

Monophyly of the clade including *Ameiva*, *Teius*, *Dicrodon*, *Kentropyx*, *Cnemidophorus*, *Aspidoscelis* and *Callopistes* (stem D) is well supported by 8 synapomorphies that include: presence of teeth on the pterygoid (6.1), carpal tubercles (30.1), no contact between supraciliaries and supraoculars (38.1), posterior infralingual plicae abruptly smaller, and more numerous than the anterior plicae of the tongue (56.2), anterior region of the tongue convex in transverse section (60.1), pedunculus ornament not developed in the apex of the hemipenis (67.2), and an increase in the mean numbers of dorsal scale (127) and scales around midbody (128).

The clade consisting of *Ameiva*, *Teius*, *Dicrodon*, *Kentropyx*, *Cnemidophorus* and *Aspidoscelis* (Teiinae) (stem E) is well supported by 17 synapomorphies including: fused postorbital and postfrontal bones (1.1), expanded quadrate process in pterygoid (2.1), presence of squamosal process (4.0), presence of clavicular hook (9.1), presence of scapular foramen (11.1), 12 post-xiphisternal ribs (12.0), 26 pre-sacral vertebrae (13.1), high neural arch in the first autotomic caudal vertebrae (14.1), the last 25 vertebrae with rib (24.0), 17 dorsal vertebrae (27.1), posterior infralingual plicae abruptly smaller, and less numerous than anterior plicae (56.3), shallow lateral laminae in the lateral protuberance of the hemipenis (72.2), an increase in the number of femoral pores (121),

an reduction in the mean number of supralabial scales (122), an increase in the mean number of supratemporal scales rows (124), and reduction in the mean numbers of lamellae of foreleg (125) and prefemoral scales (132).

The clade *Ameiva* + *Teius* (stem F) is supported by the following synapomorphies: narrow triangular shape of the levator anguli oris (84.1), protactor pterygoid originating from the basisphenoid and prootic (99.1), rectangular intermandibularis anterior profundus (101.1), an increase in the mean number of femoral pores (121), a reduction in the mean number of lamellae of foreleg (125), an increase in the mean number of dorsal scales (127), and reduction in the mean number of prefemoral scales (132), prefemoral scales rows (133) and infratibial scales (134).

The clade consisting of *Dicrodon*, *Kentropyx*, *Aspidoscelis* and *Cnemidophorus* (stem G) is supported by levator anguli oris with origin not including postorbital but including quadrate and squamosal (87.1), adductor mandibulae externus profundus insertion including bodenaponeurosis (93.1), absence of sexual dimorphism in the pterygomandibularis (97.0), mandibulohyoideus I insertion in the ceratobranchial I and epibranchial I (107.2), absence of mandibulohyoideus III (111.0), and a reduction in the mean number of scales in the 15th scales row of the tail (136).

The clade containing *Kentropyx*, *Aspidoscelis* and *Cnemidophorus* (stem H) is supported by low contribution of the ectopterygoid to the inferior orbital foramen (18.1), ventro-medial orientation of the retroarticular process in the lower jaw (20.1), presence of laminae n the hemipenial pedicel (71.1), presence of geniohipohyoideus muscle (113.1), and increase in the supralabial scales row (122) and hemipenial lateral laminae (138).

The clade consisting of the pair *Cnemidophorus – Aspidoscelis* (stem I) is supported by no contact of mental with infralabial scales (39.1), an increase in the mean number of supralabial scales (122), a reduction in the mean number of lamellae of the fourth foreleg (125), an increase in the mean number of dorsal scales (127), and reduction in the mean number of scales in a ventral scale row (130) and prefemoral scales (132).

Sperm ultrastructural analysis.— Based on the ultrastructural features of spermatozoa, a total of 25 variable characters could be scored, of which 18 were parsimony-informative. The analyses based on sperm ultra-structural data yielded a single shortest tree of length 41401 (Fig. 19A). The shortest tree has a consistency index of 0.603 (excluding uninformative characters), a retention index of 0.556, and a rescaled consistency index of 0.373 (excluding step matrix characters). The tree split the family into the same two major monophyletic groups of the tree based on traditional morphological data set. One consists of *Tupinambis*, *Crocodilurus* and *Dracaena*. The other group consists of *Callopistes*, *Ameiva*, *Teius*, *Dicrodon*, *Kentropyx*, *Cnemidophorus*, and *Aspidoscelis*. Within the first group, *Dracaena* and *Crocodilurus* are closer related, and makes up the sister taxon of *Tupinambis*. In the second major group, *Callopistes* appears as sister group of the clade represented by *Ameiva*, *Teius*, *Dicrodon*, *Kentropyx*, *Cnemidophorus*, and *Aspidoscelis* genera. This last group is split into two subgroups. In the first subgroup *Dicrodon* appears closely related to the pair sister *Ameiva – Kentropyx*, and in the other subgroup *Teius* appears closer related to the pair sister *Cnemidophorus – Aspidoscelis*.

The Bootstrap 50% majority-rule tree (Fig. 19B) indicates four clades emerging from a basal polytomy. Two of these clades contain just a single genus: *Callopistes* and

Tupinambis. The third clade appear well supported by bootstrap value with 87% supporting and comprises *Crocodilurus* and *Dracaena.* The fourth clade appears weakly supported with bootstrap value of 58% and comprises *Ameiva*, *Aspidoscelis*, *Cnemidophorus*, *Kentropyx*, Dicrodon, and *Teius* in a basal politomy.

In the following paragraphs, we describe some of the characters that support the groups within Teiidae (Fig. 19A). As in the tree based on traditional morphological data, characters are mentioned only if they are unambiguously placed on a brand independent of optimization routine.

Teiid lizards (stem A) have no common unambiguous character to support their clade. One major monophyletic group consisting of *Tupinambis*, *Crocodilurus* and *Dracaena* (stem B) is supported by three synapomorphies: six sets of mitochondria and ring structures in the midpiece (146.3), a reduction in the ratio of the mitochondria tier length to midpiece length (157), and an increase in the ratio of the fibrous sheath width to the principal piece width (163). The close relationship between *Crocodilurus* and *Dracaena* (stem C) is supported by the mitochondria having rounded ends in longitudinal section (148.1), and increase of the ratio of the ring structure tier length to midpiece length (158) and ratio of the ring structure tier length to mitochondrial tier length (159).

The other major monophyletic group consisting of *Ameiva*, *Dicrodon*, *Teius*, *Cnemidophorus*, *Kentropyx*, and *Callopistes* (stem D) is supported by only one synapomorphy: beginning of the fibrous sheath in the midpiece at the level of the second mitochondria tier (152.1). The clade comprising of *Dicrodon*, *Ameiva*, *Kentropyx*, *Teius*, *Aspidoscelis*, and *Cnemidophorus* (stem E) is supported by five synapomorphies: fused dense bodies forming compacted ring structures (150.0), an increase of the ratio of

midpiece length to flagellum length (155), a reduction of the ratio of distal centriole length to midpiece length (156), increase in the ratios of nuclear rostrum length to acrosome length (160) and the diameter of the anterior region of the principal piece to the diameter of the annulus region (162). The clade consisting of *Dicrodon*, *Ameiva* and *Kentropyx* (stem F) is supported by an increase in the ratio of the electron lucent zone length to the electron lucent zone width (161). The pair *Ameiva* and *Kentropyx* (stem G) is supported by six synapomorphies: an increase of the ratio of midpiece length to flagellum length (155), a reduction of the ratio of distal centriole to midpiece length (156), an increase of ratio of the mitochondria tier length to midpiece length (157), reduction of the ratios of ring structure tier length to midpiece length (158) and the ring structure tier length to mitochondria tier length (159), and an increase of the fibrous sheath width to the principal piece width (163). The clade consisting of *Teius*, *Aspidoscelis* and *Cnemidophorus* (stem H) is supported by fibers 3 & 8 not grossly enlarged (145.1), and increase of the ratios of head length to total sperm length (153.2) and the diamenter of the anterior region of the principal piece to the diameter of the annulus region (162). The sister group *Cnemidophorus – Aspidoscelis* is supported by four synapomorphies: increase of the ratios of acrosome length to head length (154), midpiece length to flagellum length (155), diameter of the anterior region of the principal piece to the diameter of the annulus region (162), and the fibrous sheath width to the principal piece width (163).

Congruence between sperm ultrastructural and traditional morphological trees.—Several major clades found in the sperm ultrastructural data tree are also found in the tree based

on morphological data. These congruences include: (1) the two major monophyletic groups of Teiidae family (2) *Callopistes* as sister group of *Ameiva*, *Cnemidophorus*, *Aspidoscelis*, *Dicrodon*, *Kentropyx*, and *Teius*, (3) the clade *Crocodilurus* + *Dracaena*, and (4) the clade *Cnemidophorus* – *Aspidoscelis*. Major prints of incongruence occur among relationships of *Ameiva*, the pair *Cnemidophorus* – *Aspidoscelis*, *Dicrodon*, *Kentropyx*, and *Teius*. The genus *Ameiva* is sister group of *Teius* in the traditional morphological tree, whereas in sperm ultrastructural tree, the genus *Ameiva* is closely related to *Kentropyx*. The genus *Dicrodon* appears as sister group of *Kentropyx* and the pair *Aspidoscelis* – *Cnemidophorus* in the traditional morphological tree, whereas in sperm ultrastructural tree, it appears as sister group of the pair *Ameiva* – *Kentropyx*. Finally, the pair *Cnemidophorus* – *Aspidoscelis* is closer related to *Kentropyx* in the traditional morphological tree, whereas in the tree based in the sperm ultrastructural data the pair is closer to *Teius*.

Combined analysis.—The combined data set includes 118 phylogenetically informative characters. Parsimony analysis of the combined data provides a single shortest tree of length 295054 (Fig. 20A). The shortest tree has a consistency index of 0.563 (excluding uninformative characters), a retention index of 0.532, and a rescaled consistency index of 0.336. The combined data supports two major monophyletic groups within Teiidae family as occur in the trees based in separated data sets (Figs. 18A, 19A). The first comprises *Callopistes*, *Ameiva*, *Teius*, *Dicrodon*, *Kentropyx*, *Cnemidophorus* and

Aspidoscelis. The other major group consists of *Tupinambis*, *Crocodilurus* and *Dracaena*.

In the combined data bootstrap 50% majority-rule consensus tree (Fig. 20B), all major clades are supported by bootstrap values. The bootstrapping suggests that in one of the major monophyletic group, the pair *Dracaena* and *Crocodilurus* is supported by 76% of bootstrap value, and makes up the sister taxon of *Tupinambis,* with 78% of bootstrapping support. The other major monophyletic group appears weakly supported by 61% of bootstrap value. The clade consisting by *Ameiva*, *Dicrodon*, *Teius*, *Kentropyx*, *Aspidoscelis* and *Cnemidophorus* is strongly supported by 97% of bootstrap value. Three clades emerge from a basal politomy. Three clades contain single genera: *Ameiva*, *Dicrodon* and *Teius* are not supported by the boostrapping. The fourth clade the pair *Cnemidophorus* and *Aspidoscelis*, with 53% of bootstrap supporting makes up sister group of *Kentropyx*, with 61% of supporting.

In the following paragraphs we describe both sperm ultrastructure and traditional morphological synapomorphies supporting the clades in the tree based on the combined characters (Fig. 20A). We mention only the synapomorphies that are unambiguously placed at the stem in question (independent of optimization routine). As the traditional morphological synapomorphies are identical in both traditional morphological tree and combined data tree, we describe only the sperm ultrastructural synapomorphies.

According to the combined data, Teiidae family (stem A) is supported by no unambiguous characters. One major monophyletic group (*Tupinambis*, *Crocodilurus* and *Dracaena)* (stem B) of the family Teiidae is supported by seven traditional morphological synapomorphies and three sperm ultrastructural synapomorphies, which

consist of six sets of mitochondria and ring structures in the midpiece (146.3), a reduction in the ratio of the mitochondria tier length to midpiece length (157), and an increase in the ratio of the fibrous sheath width to the principal piece width (163).

The clade *Crocodilurus* + *Dracaena* (stem C) is supported by six traditional morphological synapomorphies and by the following sperm ultrastructural features: the mitochondria having rounded ends in longitudinal section (148.1), a reduction of the ratio of the head length to total sperm length (153), increase of the ratios of the ring structure tier length to midpiece length (158) and ratio of the ring structure tier length to mitochondrial tier length (159).

Monophyly of the other major group of Teiidae family (stem D) is supported eigth traditional morphological synapomorphies and only one sperm ultrastructural feature, the beginning of the fibrous sheath at the level of the second mitochondria tier (152.1).

The clade consisting of *Ameiva*, *Aspidoscelis*, *Cnemidophorus*, *Kentropyx*, *Dicrodon* and *Teius* (stem E) is well supported by 17 traditional morphological synapomorphies and four sperm ultrastructural features: fused dense bodies forming compacted ring structures (150.0), an increase of the ratio of midpiece length to flagellum length (155), a reduction of the ratio of distal centriole length to midpiece length (156), and an increase of the ratio of nuclear rostrum length to acrosome length (160).

The clade *Ameiva* and *Teius* (stem F) is supported by nine traditional morphological synapomorphies and four sperm ultrastructural features: an increase of the ratio of the head length to total sperm length (153), reduction of the ratios of acrosome

length to head length (154), the ring structure tier length to midpiece length (158) and the ring structure tier length to mitochondrial tier length (159).

The clade consisting of *Dicrodon, Kentropyx, Cnemidophorus* and *Aspidoscelis* (stem G) is supported by six traditional morphological features and three sperm ultrastructural synapomorphies: increase of the ratios of acrosome length to head length (154), the ring structure tier length to mitochondrial tier length (159) and diameter of the anterior region of the principal piece to the diameter of the annulus region (162).

The clade consisting of *Kentropyx, Cnemidophorus* and *Aspidoscelis* (stem H) is supported by six traditional morphological synapomorphies and four sperm ultrastructural features: an increase the ratios of acrosome length to head length (154), increase of the ratios of midpiece length to flagellum length (155), diameter of the anterior region of the principal piece to the diameter of the annulus region (162) and amount of cytoplasm between the plasma membrane and the fibrous sheath in the anterior portion of principal piece (163).

The clade of *Cnemidophorus* + *Aspidoscelis* (stem I) is supported by five traditional morphological synapomorphies and three sperm ultrastructural features: fibers 3 & 8 not grossly enlarged (145.1), increase of the ratios of the head length to total sperm length (153), and diameter of the anterior region of the principal piece to the diameter of the annulus region (162).

DISCUSSION

Sperm Ultrastructure Versus Traditional Morphological Phylogeny

Both trees (1) split the family into the two major subfamilies (Teiinae and Tupinambinae) as the phylogeetic and phenetic studies based on external morphology (Vanzolini and Valencia, 1965), chromosomes (Gorman, 1970), osteology (Boulenger, 1885; Presch, 1970; Veronese and Krause, 1997), and myology (Rieppel, 1980), (2) place *Callopistes* inside Teiinae, and (3) consider *Crocodilurus* and *Dracaena* closely related.

Nevertheless, among Teiinae genera (excluding *Callopistes*), the data sets produce some incongruences in the relationships among Teiinae, and in the degree support. Traditional morphological data tree indicates (1) *Ameiva* and *Teius* closer related, and (2) *Dicrodon* sister group of *Kentropyx* and the pair *Aspidoscelis – Cnemidophorus*. Sperm ultrastructural data tree indicates (1) *Ameiva* and *Kentropyx* closed related, (2) *Dicrodon* sister group of *Ameiva* and *Kentropyx*, and (3) *Teius* sister group of the pair *Aspidoscelis – Cnemidophorus*. In addition, the results indicate that sperm ultrastructural data produce weaker and not supported clades than traditional morphological data according to bootstrap 50% majority-rule consensus trees. Sperm ultrastructural data does not produce bootstrapping support to *Callopistes* within Teiinae subfamily neither to *Tupinambis* within Tupinambinae subfamily. Traditional morphological data does not produce bootstrapping support only to *Callopistes* within Teiinae subfamily. Further, Teiinae subfamily with exception of *Callopistes*, appears strongly supported by 97% of bootstrapping values in traditional morphological data tree, whereas sperm ultrastructural data abruptly reduced this value to 58% bootstrapping

support. Also, sperm ultrastructural data does not give bootstrapping support to Teiinae subfamily including *Callopistes* neither among any Teiinae, however the same results were produced by traditional morphological data.

Despite, sperm ultrastructural data produce weak bootstrap supporting values to Teiinae clade, the pair *Crocodilurus – Dracaena*, within Tupinambinae subfamily, is well supported with 87% of bootstrapping, whereas the traditional morphological data produced the pair with only 54% of bootstrapping support.

It is clear that ultrastructural data alone is not sufficient to support the major clades (Tupinambinae and Teiinae including *Callopistes*). The degree of support for the Teiinae clade (excluding *Callopistes*) in the tree derived from the traditional morphological data set surpass to a large extent that clade in the tree derived from the sperm ultrastructural data. This outcome in bootstrap support derived by sperm ultrastructural data seemingly derives from two possible reasons: (1) the high levels of homoplasy, which can be a result of problems in the codification, sperm ultrastructure plasticity or convergent evolution, and (2) the few available number of characters possibly detected among the teiid genera sperm ultrastructure as suggested by Teixeira et al. (1999b).

High levels of homoplasy in sperm ultrastructure characters might be reducing the boostrap values of the topology clade based on this new data set. Our results indicate that the levels of homoplasy in both tree topologies are not so different from each other as expected (see consistence indice in Appendice II). Among the 25 sperm ultrastructural characters five of them including: the ratio between head length to the total length, acrosome length to head length, quantity of citoplasm between plasma membrane and

fibrous sheath, fibers 3 and 8 grossly enlarged, and mitochondria with trapezoid shape or with rounded ends shape are very homoplastic, where homoplasy occur in more than 50% of the situations. In eight characters including: the ratio between mitochondria to midpiece, nuclear rostrum to acrosome length, epinuclear lucent zone to epinuclear lucent zone length, diameter of annulus region to diameter of principal piece region, presence and shape of base plate, density within the distal centriole, and mitochondria curved or columnar shape are homoplastic in 50% of situations. Only the characters of dense bodies fused or not and the beginning of the fibrous sheath in the midpiece are 100% informative and no homoplastic. In the traditional morphological characters only 16 characters are 100% informative and no homoplasic. So far, 88% of traditional morphological characters and 92% of sperm ultrastructural characters are homoplastic. In this way, the level of homoplasy in both data sets are almost similar, suggesting that the low values of bootstrap values of sperm ultrastructure tree clades and the unresolved phylogeny based on sperm ultrastructural data are not caused by the high levels of homoplasic characters.

The possibility of the low number of characters might be affecting bootstrap values in sperm ultrastructural tree leaded us to test the effect of the undersampling in the traditional morphological phylogeny. We randomly resample the traditional morphological data in the bootstrapping support method, using the same number of characters employed in sperm ultrastructural data. According to our results, the reduction of the number of character produce unresolved phylogeny and tree topology clades weakly supported by bootstrap values (Fig. 21). The undersampling of traditional morphological data produced a tree topology that shows poorly resolved relationships

among genera within Teiinae subfamily, similarly to the tree topology derived by sperm ultrastrucutural data, but the degree support of Teiinae clade (excluding *Callopistes*) was drastically reduced from 97% to 65% of support values.

Sperm ultrastructure studies of *Tupinambis* species (Tavares-Bastos et al., 2002) show high levels of variability within this genera, and indicate that sperm ultrastructure characters, although of great value for phylogeny at higher taxonomic levels in reptiles (Teixeira et al., 1999a), are poor predictors of phylogeny when considering the species of *Tupinambis*. Nevertheless, our results suggest that sperm ultrastructural characters may be a good indicator of phylogeny, at generic level, due to two reasons: (1) the inter generic variability in sperm ultrastructural characters is higher than currently though (Giugliano, 2002; Teixeira, 1999 a, c), indicating that sperm ultrastructural characters show variability among terminal taxons which is profitable in phylogenetic analyses at generic level (Thiele, 1993); and (2) despite the high levels of intrageneric variability (Giugliano et al., 2002), sperm ultrastructural data phylogeny show major areas in congruence with the traditional morphological phylogeny, having only few incongruent areas weakly supportted with the traditional topology. Hence, few numbers of sperm ultrastructure characters seemingly be the major reason of the problems found in sperm ultrastructure phylogeny. So far, considerable effort is still necessary to increase the number of characters, using more electron microscopy methodology as immunocytochemistry or cytochemistry. These developments will surely provide significant contributions to the useful of sperm ultrastructure in phylogenetic reconstructions at generic level.

Combined phylogeny

According to Teixeira et al (1999a), tree topology estimates derived from sperm ultrastructural data might have some incongruent clades with those derived from traditional morphological characters, because of heterogeneous rates of evolution. However, the tree congruence evaluation indicates that the few incongruent areas are weakly supported, and the trees based on different data sets are congruent, having major similar areas. So, sperm ultrastructural data and traditional morphological data can be regarded as dependents and compatibles data sets, according to Wiens suggestions (Wiens, 1998a).

The possibility that data sets may have different phylogenetic histories has been considered a strong argument against combining such data sets in phylogenetic analysis (Bull et al., 1993; de Queiroz et al., 1995). Nonetheless, the mismatch regions between topologies derived from different data sets are weakly supported conflicts and might not be a matter of different phylogenetic histories as argued by Wiens (1998a). Hence, the different data sets combined, increased the number of characters and improved the accuracy of our analysis, having the combine tree, the best estimate of Teiidae genera relationships.

Further, the combined data support a phylogeny that is nearly identical to that based on the traditional morphological data. The unique difference occurs on the degree of support. The bootstrap supporting of the clades of the combined data tree are higher than the identical clades obtained from the traditional morphological data. The clade consisting of *Tupinambis*, *Crocodilurus* and *Dracaena* is 78% supported by bootstrap values in the bootstrap 50% majority-rule consensus tree based in the combined data,

whereas the same clade obtained by only the traditional morphological data appears weakly supported with 66% of the bootstrap values. The clade *Crocodilurus* + *Dracaena* is 76% well supported in the bootstrap 50% majority-rule consensus tree based in the combined data, whereas the clade appears weakly supported with 54% of the bootstrap values in the bootstrap 50% majority-rule consensus tree based only in the traditional morphological data. The clade consisting of *Callopistes* + the other Teiinae genera is weakly supported by bootstrap values (67%) in the combined data bootstrap tree, but in the bootstrap tree derived by only the traditional morphological data, *Callopistes* and the other Teiinae genera is not represented in a supported clade by bootstrap values. Within the Teiinae (excluding *Callopistes*), the bootstrap 50% majority-rule consensus tree based in combined data sets indicates 61% of bootstrap supporting to the clade *Kentropyx*, *Aspidoscelis*, *Cnemidophorus* and 53% of bootstrap supporting to the pair *Aspidoscelis* + *Cnemidophorus*. In the bootstrap 50% majority-rule consensus tree based only in the traditional morphological data, there is not bootstrapping support to the clade consisting by the Teiinae (excluding *Callopistes*). The results indicate that the combined analysis give better estimates than the estimate from the two data sets separately analyze (Wiens, 1998a).

Sperm ultrastructural data produce a phylogeny of Teiidae family with some incongruences among the relationships of Teiinae subfamily with the traditional morphological data phylogeny. Nevertheless, the sperm ultrastructural data combined with the traditional morphological data produced the same phylogeny obtained by the traditional morphological data, with higher degrees of support. The phylogeny derived from the combined data sets indicate that sperm ultrastructural data are good

phylogenetic indicators when used as an additional morphological source of characters to the traditional morphological data.

The analyses derived from the combined data contribute for phylogenetic reconstruction of Teiidae family and better refletct the evolutionary history of the family. The existance of the two subfamiles, Teiinae and Tupinambiane, and the closer relationship between *Dracaena* and *Crocodilurus* are clearly resolved and strongly supported by the combined analysis. However, further studies are necessary to completely solve Teiinae relationships, mainly among *Ameiva*, *Dicrodon* and *Teius*, and increase the degree support of the *Callopistes* inclusion into Teiinae subfamily and among all other Teiinae genera. Additional studies includiding more species of each genera can clarify the relationships within each teiid subfamily.

Taxonomic Comparisons with Previous Studies

The division of the family Teiidae into the two subfamilies, Teiinae and Tupinambinae, formely proposed by Presch (1974) was generally corroborated by our phylogeny based on sperm ultrastructural data + traditional morphological data (including new characters of hemipenis, tongue and scales). Vanzolini and Valencia (1965), Gorman (1970), Rieppel (1980), and Veronese and Valencia (1997) also recognized the same groups within the family.

Our analysis places *Callopistes* with Teiinae rather than Tupinambinae as suggested by those previous hypotheses. In our analysis, *Callopistes* shares nine synapomorphies with other Teiinae: presence of teeth on the pterygoid, carpal tubercles, no contact between supraciliaries and supraoculars scales, posterior infralingual plicae

abruptly smaller, and more numerous than the anterior plicae of the tongue, anterior region of the tongue convex in transverse section, pedunculus ornament not developed in the apex of the hemipenis, and an increase in the mean numbers of dorsal scale, and scales around midbody related to *Tupinambis*, *Crocodilurus* and *Dracaena*, and one sperm ultrastructural feature, the beginning of the fibrous sheath at the level of the second mitochondria tier. The clade consisting of *Callopistes* as sister group of the other Teiinae genera is not supported by bootstrapping values. As either sperm ultrastructural and traditional morphological data were scored from only *Callopistes flavipunctatus* to the genus *Callopistes*, it may be a strong possible cause of the replacement of this genus in Teiinae instead of Tupinambinae. Hence, we recommended additional analysis with other *Callopistes* species to the formerly placement of *Callopistes* in the Teiinae rather than Tupinambinae.

Our combined data tree indicates that within Teiinae subfamily: (1) *Ameiva* closely related to *Teius*, (2) *Cnemidophorus* closely related to *Aspidoscelis*, (3) *Kentropyx* sister group of the pair *Cnemidophorus – Aspidoscelis* (4) *Dicrodon* sister group of *Kentropyx*, *Cnemidophorus*, and *Aspidoscelis*, and (4) *Callopistes* sister taxon of the other Teiinae genera. Within Tupinambinae, the combined data phylogeny suggests a close relationship between *Dracaena – Crocodilurus*. Analyses based on mitochondrial DNA, morphology, and allozymes support *Ameiva*, *Cnemidophorus*, and *Kentropyx* as a monophyletic group, the cnemidophirines which are related to the most basal lineages of Teiinae, *Teius* and *Dicrodon* (Reeder et al., 2002). Based on external morphology, Vanzolini and Valencia (1965) postulated a strong affinity between the pairs *Ameiva – Cnemidophorus*, *Teius – Dicrodon* within Teiinae, being *Kentropyx* the most

differentiated genus inside Teiinae, and *Dracaena – Tupinambis* closely related within Tupinambinae. Based on osteological data, Presch (1970) considered *Cnemidophorus* a synonym of *Ameiva*, and suggested *Ameiva/Cnemidophorus* closely related to *Kentropyx*. The position of *Crocodilurus* is other difference between the two previous hypotheses. Vanzolini and Valencia (1965) considered *Crocodilurus* closer related to *Callopistes* than to the pair *Tupinambis – Dracaena* as suggested by Presch (1974). In Moro and Abdala analysis (2000) based on cranial myology, *Ameiva* appears more related to *Teius* than to *Cnemidophorus*, supporting our hypothesis, *Callopistes* appears more related to *Crocodilurus*, being congruent with Rieppel's suggestions (1980). Despite our results have high levels of incongruence with those of previous hypotheses, we have two reasons to consider our phylogeny the best estimate of Teiidae family: (1) the previous studies based on different data sets have revealed incongruent areas with each other, and the relationships among teiid genera were not completely solved, finally, (2) our phylogeny is based on those data sets used in the previous hypotheses, combined with additional traditional morphological data (meristic, tongue and hemipenis) and sperm ultrastructural data, surely improving the estimates of teiid relationships.

Acknowledgments.—We thank the following individuals and institutions for loan of specimens: Museo del Historia Natural de San Marco (Lima, Peru), Herman Nunez (Museo del Historia Natural do Chile), Omar Pesantes, Marcos di Bernardo (Pontifícia Universidade Católica do Rio Grande do Sul), Sonia Cechin (Universidade Federal de Santa Maria), Jardim Botânico de Porto Alegre. We thank Marcia Renata Mortari, Silvia Moro, and Diana Simões for providing external morphological, myological and internal tongue morphology data, respectively. We thank Leonora Tavares-Bastos and Liliam Giugliano for providing sperm ultrastructure data of *Tupinambis* and *Ameiva*, respectively. We thank Hussam Zaher (Universidade de São Paulo) for providing literature from hemipenial data and Marco Antônio dos Santos Silva (Núcleo de Ilustração Científica, IB, Universidade de Brasília) for hemipenial characters illustrations. We thank Daniel O. Mesquita, Fernanda Werneck, and Adrian A. Garda for assistance during scoring data work. We thank Daniel Diniz, Renato G. Faria and Mariana Zatz for assistance during fieldwork. Patrick Stephens (University of Pittsburgh), John Rawlins (Section of Entomology, Carnegie Museum of Natural History, Pittsburgh) and Vitor Becker provided insightful on the manuscript. This work was supported by CAPES and CNPq.

LITERATURE CITED

BOULENGER, G. A. 1885. Catalogue of the Lizards in the British Museum (Natural History). British Museum of Natural History, London.

BULL, J. J., J. P. HUELSENBECK, C. W. CUNNINGHAM, D. L. SWOFFORD, and P. J. WADDELL. 1993. Partitioning and combining data in phylogenetic analysis. Systematic Biology 42:384-397.

CALDWELL, M. W. 1999. Squamate phylogeny and the relationships of snakes and mosasauroids. Zoological Journal of the Linnean Society 125:115-147.

CARROL, R. L. 1988. Vertebrate Paleontology and Evolution. W. H. Freeman and Company, New York.

CEI, J. M., and J. A. SCOLARO. 1982. Geographic distribution: *Tupinambis rufescens*. Herpetological Review 13:26.

DE QUEIROZ, A., M. J. DONOGHUE, and J. KIM. 1995. Separate versus combined analysis of phylogenetic evidence. Annual Review of Ecology and Systematics 26:657-681.

DOAN, T. M. 2003. A new phylogenetic classification for the gymnophthalmid genera *Cercosaura*, *Pantodactylus* and *Prionodactylus* (Reptilia: Squamata). Zoological Journal of the Linnean Society 137:101-115.

ESTES, R., K. DE QUEIROZ, and J. GAUTHIER. 1988. Phylogenetic relationships within Squamata. Pp. 119-281. *In* R. Estes and G. Pregill (Eds.), Phylogenetic Relationships of the Lizard Families. Essays Commemorating Charles L. Camp. Stanford University Press, Stanford, California.

FELSENSTEIN, J. 1985. Confidence limits on phylogenies: an approach using the bootstrap. Evolution 39:783-791.

GAO, K., and R. C. FOX. 1996. Taxonomy and evolution of Late Cretaceous lizards (Reptilia: Squamata) from western Canada. Bulletin of the Carnegie Museum of Natural History 33:1-107.

GIUGLIANO, L. G., R. D. TEIXEIRA, G. R. COLLI, and S. N. BÁO. 2002. Ultrastructure of spermatozoa of the lizard *Ameiva ameiva*, with considerations on polymorphism within the family Teiidae (Squamata). Journal of Morphology 253:264-271.

GORMAN, G. C. 1970. Chromosomes and the systematics of the family Teiidae. Copeia 1970:230-245.

GORMAN, G. C., D. G. BUTH, M. SOULÉ, and S. Y. YANG. 1980. The relationships of the *Anolis cristatellus* species group: electrophoretic analysis. Journal of Herpetology 14:269-278.

HARRIS, D. M. 1985. Infralingual plicae: support for Boulenger's Teiidae (Sauria). Copeia 1985:560-565.

HILLIS, D. M., and J. J. BULL. 1993. An empirical test of bootstrapping as a method for assessing confidence in phylogenetic analysis. Systematic Biology 42: 182-192.

JAMIESON, B. G. M. 1995. The ultrastructure of spermatozoa of the Squamata (Reptilia) with phylogenetic considerations. Pp. 359-383. *In* B. G. M. Jamieson, J. Ausio, and J. Justine (Eds.), Advances in Spermatozoal Phylogeny and Taxonomy. Muséum National d'Histoire Naturelle, Paris, France.

-----. 1999. Spermatozoal phylogeny of the vertebrata. Pp. 303-331. *In* C. Gagnon (Ed.), The Male Gamete: From Basic Science to Clinical Applications. Cache River Press, Vienna, Illinois.

JAMIESON, B. G. M., S. C. OLIVER, and D. M. SCHELTINGA. 1996. The ultrastructure of spermatozoa of Squamata. I. Scincidae, Gekkonidae and Pygopodidae (Reptilia). Acta Zoologica (Stockholm) 77:85-100.

KLAVER, C., and W. BOHME. 1986. Phylogeny and classification of the Chamaeleonidae (SAuria) with special reference to hemipenis morphology. Bonner Zoologische Monographien 22:1-64.

LEE, M. S. Y. 1998. Convergent evolution and character correlation in burrowing reptiles: Towards a resolution of squamate relationships. Biological Journal of the Linnean Society 65:369-453.

LEVITON, A., R. H. GIBBS, E. HEAL, and C. E. DAWSON. 1985. Standards in herpetology and ichthyology: Part I. Standard symbolic codes for institutional resource collections in herpetology and ichthyology. Copeia:802-832.

MADDISON, W. P., and D. R. MADDISON. 1992. MacClade: Analysis of Phylogeny and Character Evolution, Version 3.04. Sinauer Associates, Inc., Sunderland, Massachusetts.

MANZANI, P. R., and A. S. ABE. 1988. Sobre dois novos métodos de preparo do hemipênis de serpentes. Memorial do Instituto Butantan 50:15-20.

MORO, S., and V. ABDALA. 2000. Cladistic analysis of Teiidae (Squamata) based on myological characters. Russian Journal of Herpetology 7:87-102.

MYERS, C. W., and M. A. DONNELLY. 2001. Herpetofauna of the Yutaje-Corocoro massif, Venezuela: Second report from The Robert G. Goelet American Museum-terramar expedition to the northwestern tepuis. Bulletin of the American Museum of Natural History:1-85.

NORTHCUTT, R. G. 1978. Forebrain and midbrain organization in lizards and its phylogenetic significance. Pp. 11-64. *In* N. Greenberg and P. D. MacLean (Eds.), Behaviour and neurology of lizards. National Institutes of Mental Health, Rockville, Maryland.

OLIVER, S. C., B. G. M. JAMIESON, and D. M. SCHELTINGA. 1996. The ultrastructure of spermatozoa of Squamata. II. Agamidae, Varanidae, Colubridae, Elapidae, and Boidae (Reptilia). Herpetologica 52:216-241.

PRESCH, W. F., JR. 1970. The evolution of macroteiid lizards: an osteological interpretation. Ph.D., University of Southern California, Los Angeles, CA.

-----. 1971. Tongue structure of the teiid lizard genera *Ameiva* and *Cnemidophorus* with a realocation of *Ameiva vanzoi*. Journal of Herpetology 5:183-185.

-----. 1974. Evolutionary relationships and biogeography of the macroteiid lizards (Family Teiidae, Subfamily Teiinae). Bulletin of the Southern California Academy of Sciences 73:23-32.

-----. 1980. Evolutionary history of the South American microteiid lizards (Teiidae: Gymnophthalmidae). Copeia 1980: 35-56.

-----. 1983. The lizard family Teiidae: is it a monophyletic group? Zoological Journal of the Linnean Society 77:189-197.

REEDER, T. W., C. J. COLE, and H. C. DESSAUER. 2002. Phylogenetic relationships of whiptail lizards of the genus *Cnemidophorus* (Squamata: Teiidae): a test of monophyly, reevaluation of karyotypic evolution, and review of hybrid origins. American Museum Novitates 3365:1-61.

RIEPPEL, O. 1980. The trigeminal jaw adductor musculature of *Tupinambis*, with comments on the phylogenetic relationships of the Teiidae (Reptilia, Lacertilia). Zoological Journal of the Linnean Society 69:1-29.

RUIBAL, R. 1952. Revisionary studies of some South American Teiidae. Bulletin of the Museum of Comparative Zoology 106:477-529.

SAVAGE, J. M. 1997. On terminology for the description of the hemipenes description of the hemipenes of Squamata reptiles. KHerpetological Journal 7:23-25.

SCHWENK, K. 1988. Comparative morphology of the lepidosaur tongue and its relevance to squamate phylogeny. Pp. 569-598. *In* R. Estes and G. Pregill (Eds.), Phylogenetic Relationships of the Lizard Families. Essays Commemorating Charles L. Camp. Stanford University Press, Stanford, California.

SWOFFORD, D. L. 1991. PAUP: Phylogenetic Analysis Using Parsimony, Version 3.0s. Illinois Natural History Survey, Champaign, Illinois.

TAVARES-BASTOS, L., R. D. TEIXEIRA, G. R. COLLI, and S. N. BÁO. 2002. Polymorphism in the sperm ultrastructure among four species of lizards in the genus *Tupinambis* (Squamata: Teiidae). Acta Zoologica (Stockholm) 83:297-307.

TEIXEIRA, R. D., G. R. COLLI, and S. N. BÁO. 1999a. The ultrastructure of the spermatozoa of the lizard *Micrablepharus maximiliani* (Squamata,

Gymnophthalmidae), with considerations on the use of sperm ultrastructure characters in phylogenetic reconstruction. Acta Zoologica (Stockholm) 80:47-59.

-----. 1999b. The ultrastructure of the spermatozoa of the worm-lizard *Amphisbaena alba* (Squamata, Amphisbaenidae), and the phylogenetic relationships of amphisbaenians. Canadian Journal of Zoology 77:1254-1264.

TEIXEIRA, R. D., G. H. C. VIEIRA, G. R. COLLI, and S. N. BÁO. 1999c. Ultrastructural study of spermatozoa of the neotropical lizards, *Tropidurus semitaeniatus* and *Tropidurus torquatus* (Squamata, Tropiduridae). Tissue & Cell 31: 308-317.

TEIXEIRA, R. D., D. M. SCHELTINGA, S. E. TRAUTH, G. R. COLLI, and S. N. BÁO. 2002. A comparative ultrastructural study of spermatozoa of the teiid lizards, *Cnemidophorus gularis gularis*, *Cnemidophorus ocellifer*, and *Kentropyx altamazonica (Reptilia, Squamata, Teiidae)*. Tissue & Cell 34:135-142.

THIELE, K. 1993. The holy grail of the perfect character: the cladistic treatment of morphometric data. Cladistics 9:275-304.

VANZOLINI, P. E., and J. VALENCIA. 1965. The genus *Dracaena*, with a brief consideration of macroteiid relationships (Sauria, Teiidae). Arquivos de Zoologia, São Paulo 13:7-46.

VERONESE, L. B., and L. KRAUSE. 1997. Esqueleto pré-sacral e sacral dos lagartos teiídeos (Squamata, Teiidae). Revista Brasileira de Zoologia 14:15-34.

WIENS, J. J. 1998a. Combining data sets with different phylogenetic histories. Systematic Biology 47:568-581.

-----. 1998b. Testing phylogenetic methods with tree congruence: Phylogenetic analysis of polymorphic morphological characters in phrynosomatid lizards. Systematic Biology 47:427-444.

-----. 2001. Character analysis in morphological phylogenetics: problems and solutions. Systematic Biology 50:689-699.

WILKINSON, M. 1992. Ordered versus unordered characters. Cladistics 8:375-385.

WRIGHT, J. W. 1993. Evolution of the lizards of the genus *Cnemidophorus*. Pp. 27-81. *In* J. W. Wright and L. J. Vitt (Eds.), Biology of Whiptail Lizards (Genus *Cnemidophorus*). The Oklahoma Museum of Natural History, Norman, Oklahoma, U.S.A.

ZIEGLER, T., and W. BOHME. 1997. Genitalstrukturen und paarungsbiologie bei squamaten Reptilien, speziell den Platynota, mit bemerkungen zur systematik. Mertensiella 8:1-210.

APPENDIX I

Museum abbreviations are listed in Leviton et al. (1985). Other abbreviations used are: CHUNB (Coleçâo Herpetológica da Universidade de Brasília), GRColli (Guarino R. Colli field series), CRE (Costa Rican Expedition), USCA (University of Southern California), USNM (United States National Museum), MMZ (University of Michigan, Museum of Zoology), JRM (Private collection of John Raymond Meyer), RE (Private collection of Richard Etheridge), JMS (private collection of Jay M. Savage), WP (private collection of William Presch), LKZOO (private collection of Ligia Krause), ZUFSM (Museu de Zoologia da Universidade Federal de Santa Maria), PT (Private collection that Silvia Moro and Virginia Abdala obtained myological data).

Specimens Scored for Sperm Ultrastructural Characters

Ameiva ameiva: CHUNB 02120.

Aspidoscelis gularis gularis: ASUMZ 18959, 19019.

Callopistes flavipunctatus ($n = 1$): MHNJP uncatologued.

Cnemidophorus ocellifer: CHUNB 16943-44.

Crocodilurus lacertinus: CHUNB 15192.

Dicrodon guttulatum ($n = 2$): MHNJP uncatologued.

Dracaena guianensis: CHUNB 15197-99.

Kentropyx altamazonica: CHUNB 5777, 5784.

Teius oculatus: CHUNB 21861-62.

Tupinambis teguixin: CHUNB 03695.

Cercosaura ocellata: CHUNB 18272.

Specimens Scored for Osteological Characters

Abbreviation for specimens examined as dry skeletons is SK, as cleared and stained skeletons is CS, in radiographs of preserved specimens in alcohol or formalin is RD.

Data from Presch (1970)

Ameiva ameiva: LACM 44455-58 (RD); RE 435 (SK); WP 295-97 (SK). *Ameiva bifrontata*: JMS 1596, 1598 (SK); WP 291-94, 301-03 (SK). *Ameiva chrysolaema*: RE 1739, 1756 (SK); WP 275 (SK). *Ameiva festiva*: USCA 182-83, 266, 428, 458, 610-11 (RD); CRE 65, 138, 265, 714, 7154, 7159, 8045 (RD); LACM 44968-69 (RD), 44472 (RD); WP 198 (SK), 373 (SK). *Ameiva leptophrys*: CRE 7101E, 71010, 71016, 71076 (RD). *Ameiva lineolata:* RE 1481-82 (SK). *Ameiva quadrilineata*: RE 1315 (SK); WP 335, 342, 345 (SK); USCA 119, 142, 428 (RD). *Ameiva undulata*: USCA 427 (RD); CRE 3097, 6290, 6360, 6440, 6491 (RD). *Ameiva taeniura*: RE 1456-57 (SK).

Aspidoscelis costatus: 733-34, 756, 789, 791, 803, 1249 (SK). *Aspidoscelis deppi*: CRE 839-c, 2593, 8019a-c, 2856, 8214 (RD); WP 267, 286, 363 (SK). *Aspideoscelis guttatus*: WP 149, 179 (SK). *Aspidoscelis hyperythra*: RE 473-74 (SK). *Aspidoscelis inornatus*: WP 422 (SK). *Aspidoscelis maximus*: RE 531 (SK). *Aspidoscelis sexlineatus*: RE 247, 249 (SK). *Aspidoscelis tigris*: RE 587, 1389, 1436, 1618 (SK); JMS 01b, 10, 18, 64-65, 1100, 1402 (SK); WP 140 (SK).

Callopistes flavipunctatus: AMNH 28515 (RD), 28516 (RD) (SK); LACM (n = 1) uncatologued; MCZ 18981, 18770 (SK); USNM 38559 (RD). *Callopistes maculaus*: AMNH 36288-89, 65457-58 (RD); MCZ 2751 (SK); MMZ 118093, 119084 (RD); RE 1297 (SK); USNM 5517, 17537, 5844 (RD).

Cnemidophorus bridegi: LACM85008 (RD). *Cnemidophorus ceralbensis*: JMS 297, 475 (SK). *Cnemidophorus communis*: RE 35 (SK). *Cnemidophorus dickersonae*: WP 266 (SK). *Cnemidophorus exanguis*: RE 1188, 1239 (SK); WP 414 (SK). *Cnemidophorus labialis*: RE 1881 (SK). *Cnemidophorus lemniscatus*: CRE 1891, 1782, 1789, 1799, 1285, 1279, 2280, 2513 (RD); RE 522-23, 531, 1399 (SK); UMS 306, 522-23, 631 (SK); WP 299, 304, 308-09, 321-322, 334, 336, 358, 360, 409, 441, 1399 (SK). *Cnemidophorus montaguae*: JRM 2040, 2044-45 (RD); JMS 1548 (SK). *Cnemidophorus ocellifer*: LACM 44443, 44485 (RD). *Cnemidophorus sacki*: RE 736 (SK). *Cnemidophorus septemvittatus*: RE 949, 983, 1215, 1217, 1241 (SK).

Crocodilurus amazonicus: AMNH 46290 (RD) (SK); MCZ 2780 (SK); USNM 89371, 159226 (RD).

Dicrodon guttulatum: AMNH 21871 (SK), 28506-11 (RD); MCZ 59033, 60307, 61133 (RD), 83132-33 (SK); MMZ 234 (SK). *Dicrodon heterolepis*: AMNH 20741 (RD); MCZ 12329 (SK). *Dicrodon holmbergi*: AMNH 28585-87 (RD).

Dracaena guianensis: AMNH 46008, 77647 (SK); MMZ s-2286, s-2369 (SK); RE 656 (SK); UMS 336 (SK); USNM 71729, 136611 (RD). *Dracaena paraguayensis*: AMNH 5250 (RD); LACM uncatologued (1) (RD). *Dracaena sp.*: AMNH 32121, 73065 (SK).

Kentropyx calcaratus: LACM 31466-68 (RD); RE 1009, 1086 (SK); USC 184-85, 202, 322-24, 353, 390, 429, 430-32, 608-09, 669, 671, 744, 757 (RD); WP 218 (SK). *Ketropyx intermedius*: RE 992, 1016 (SK). *Kentropyx pelviceps*: USC 204, 240, 242-43, 255, 457, 685 (RD); WP 367 (SK). *Kentropyx striatus*: LACM 31466 (RD); MMZ 83623, 85237-38 (RD). *Kentropyx viridistriga:* MMZ 63825, 110028 (RD). *Kentropyx williamsoni*: MMZ 56823 (RD).

Teius teyou: AMNH 65216 (RD), 65217 (RD) (SK) 65218-20 (RD); LACM 37677-80 (RD); MCZ 43351a-c (SK); WP 350 (SK).

Tupinambis nigropunctata: AMNH 628-29, 1640-41, 1650, 18190, 25039, 37404, 37446, 57330-32, 60861, 61752, 65520-21, 73088, 91781, 97338-40, 97355-57, 101779, 101793 (RD); LACM 7961, 44462 (RD); MMZ 46119-21, 56801, 57434, 82846, 83633 (RD); RE 428 (SK); WP 154, 185 (SK); USNM 60678-80, 83948, 149133 (RD). *Tupinambis rufescens*: AMNH 71294, 76184, 79912-13, 81569-70 (RD); MMZ 109851-54 (RD); USNM 73506-08 (RD). *Tupinambis teguixin*: AMNH 23042, 37544, 62158, 62160, 62167-69, 62174-75, 65225-28, 75320, 87938, 94688, 91505-06, 101800 (RD); LACM 31501-02 (RD); USCA 258, 779 (RD); MMZ 68901-02, 110029, 110084-87 (RD); USNM 22735, 47952, 58618, 98601, 162213 (RD); WP 262, 277 (SK). *Tupinambis sp.:*RE 1521 (SK); WP 173 (SK).

Cercosaura ocellata ($n = 4$): uncatologued by Presch (1980) (SK) (CS) (RD).

Data from Veronese & Krause (1997)

Ameiva ameiva: MZUSP 55806 (SK). *Ameiva auben* ($n = 2$): uncatologued (RD). *Ameiva chrysolaema*: UMMZ 122819-20 (RD). *Ameiva edracantha* ($n = 2$): UMMZ

059026 (RD). *Ameiva fuscata*: UMMZ 046761, 067644 (RD). *Ameiva griswaldi* ($n = 3$): UMMZ 076098 (RD). *Ameiva septemlineata*: UMMZ 193249 (RD).

Aspidoscelis burti: UMMZ 069972, 072626 (RD).

Callopistes maculates maculates: MZUSP 08039 (SK); UFRGS 0084 (CS). *Callopistes maculates*: UMMZ 018094, 118093 (RD).

Cnemidophorus lacertoides: OUVC 008753 (RD); UFRGS 00998, 02227 (SK). *Cnemidophorus laredonensi:* UMMZ 131059-60 (RD). *Cnemidophorus lemniscatus* group: MPEG 03779 (SK); MZUSP 55800 (SK). *Cnemidophorus ocellifer*: MZUSP 55802 (CS); UFRGS 00045 (SK).

Crocodilurus lacertinus: MZUSP 52513 (SK); USNM 2006893 (RD).

Dicrodon guttulatum: MZUSP 12972 (SK); UMMZ 059033, 060307, 201532 (RD). *Dicrodon heterolepis*: UMMZ 306950 (RD).

Dracaena guianensis: UFRGS 00083 (SK). *Dracaena paraguayensis*: UFRGS 00128 (SK).

Kentropyx calcarata: MPEG 05634 (SK). *Kentropyx striata*: MPEG 06472 (SK). *Kentropyx borckiana*: UMMZ 163021, 163025 (RD). *Kentropyx pelviceps*: UMMZ 201569 (RD).

Teius oculatus: OUVC 008757-58 (RD); UFRGS 00038-39 (CS), 00040 (SK), 00096 (CS). *Teius teyou*: UFRGS 00215 (SK), ($n = 3$) no catalogued (RD).

Tupinambis merianae: LKZOO 001 (SK).

Specimens Scored for External Morphology Characters

Data from this present study (meristic - scales)

Ameiva ameiva: CHUNB 00868-77, 00920-50, 01553-58, 01603-06.

Aspidoscelis gularis gularis: CM 43149, 43152, 43154-55, 43157, 43159, 43161-66.

Callopistes flavipunctatus: BMNH 1924.8.28.1, 1926.3.24.34-37; MHNSN 00341-42, 00404, 00708, 01333-34, 07071-72.

Cnemidophorus ocellifer: CHUNB 00130, 01736, 01900-07, 01920-39, 03148-400, 05540, 05563-98, 07550-60, 07574-77, 07601-12, 07617-18, 07920-28, 07933-40, 07959, 08140-59, 08311-18, 08324-36, 08411-17, 08421-24, 09608. 09613, 09616, 09620, 09691-92, 09694, 10086, 10101, 10952-57, 11058-59, 11072, 11081-82, 11084-85. 11150-52, 11567, 11569, 12462-74, 12630, 12634, 12639, 12649, 12655, 12659, 12881, 12883-93, 12953-54, 12961-3011, 13117-18, 13125-27, 13524, 13526-32, 13615, 14043-63, 14351-93, 14860-881, 19197-201, 20065-70, 24220, 24261, 24805-06, 24866.

Crocodilurus amaznicus: BMNH 65.5.4.4, 1901.1.22.1, 1926.4.30.4, 1927.6.1.1-2, 1965.1316, 1970.496-97, RR 1961.1856; CHUNB 01318-24, 06663-64, 15192-96, FML 06772, 08793, MNRJ 0085, 4965; MUZUSP 11987-88, 13979, 14428, 26516, 26517-19, 28243, 28839-45, 28849, 31672, 35339-40, 37269, 39362-63, 41825-30, 41877-86, 47556-59, 57871, 57909, 60496, 60819, 73275-79.

Dicrodon heterolepis callicelis: MHNSM 13750-805, 16524-26.

Dracaena guianensis: BMNH 56.3.25.2, 67.6.13.82, 1925.11.3.1-2, 1970.4.99; CHUNB 01325-26, 15197-200; MNRJ 3534-35, MUZUSP 7285-86, 55589.

Kentropyx altamazonica: CHUNB 18163-217.

Teius oculatus: MCN 0816-17, 0819-20, 0822, 0824, 0826-28, 0830, 0832, 0835, 0836-38, 0841-45, 0849, 0850-53, 0857, 0862, 0969, 1140, 1170-71, 1246, 1416-19,

1430-31, 1524, 1597, 1996, 2076, 2112, 2491-93, 2569, 2710, 2791, 2814-15, 2817-18, 2879, 2910, 3014, 3243, 3282, 3456, 3455, 3458, 3474-75, 3541-42, 3582-83, 3584-88, 3635, 3654, 4065, 4487, 4639-41, 4677, 5854, 5870, 5910-12, 6065, 6155, 6582, 7043, 7810, 8640, 8954-55, 8968, 9413, 9832, ; MCP 288-90, 352-58, 1052, 1231, 1257, 1553, 2368, 2661, 2850, 3054, 3060, 3085, 3092, 3093, 3094, 3095-101, 3313, 3510, 3511-12, 3546, 3733, 4216, 4494, 4559, 4560, 4561, 4617, 4657, 4664, 4871, 5037, 5038, 5039, 5040, 5361, 6928, 6929, 6930, 6931, 7840, 7864, 7880, 7964-66, 8760, 8761, 8973, 10022, 11398, 11595, 11603, 11667, 11689, 11690, 11863, 11892, 11893, 11894, 11895, 11896, 11897, 12078, 12083, 12508-14; ZUFSM 000401, 000501, 000901, 001101, 003401, 007201, 007401, 008301, 008901, 009101, 009201, 009401, 009501, 009601, 009701, 009801, 009901, 010001, 01011, 01021, 0112, 0120, 0122, 0138.

Tupinambis teguixin: BMNH 111.2.A, 111.2.C, 111.2.D, 111.2.F, 111.2.G, 1901.11.20.1, 1912.11.1.31, 1922.7.27.1, 1922.7.27.2, 1926.4.30.3, 1931.10.18.86, 1934.11.1.83-84, 1946.4.3.39-41, 1976.383, 1994.234-35, 3.2.6, 49.9.22.12-13, 52.9.8.39-44, 53.4.6.2, 56.5.14.2-3, 81.5.13.5-6, 96.6.29.1; CHUNB 00121, 00476-78, 00485, 01327-31, 10751-90, 14012-25, 14842-50, 15201-09, 16185-90, 16694; MNRJ R1745, R2606-08; MUZUSP 2511, 3733, 3738, 4875, 4879, 4882, 4889, 4890, 6371-72, 6374-75, 7249, 8279, 8298, 9848, 11866, 11974, 13011, 13862, 16312, 17309-12, 21255-58, 21475, 25561, 25998, 27461, 31666, 31671, 31890, 32053, 36073, 37549, 41676, 45245, 46615, 47029, 47203, 47204, 47438-39, 51536, 53132, 53814, 55600, 55601, 55710, 56698, 58101, 60499, 66319, 66891, 70263, 70302, 72845-46, 73306-08, 73482, 73707, 73847-48, 79210, 79260, 79641, 81741, 81744, 81773, 82862, 83016, 83017, 83095; NRM 120-23, 1466-73, 5052, RBB 5642, 39147.

Cercosaura ocellata: CHUNB 07794, 07941, 07943, 07960, 07981, 07982, 07983, 08073-94, 08100-36, 13722, 18218-309, 18312, 18314, 18316-18, 18649.

Data from Vanzolini and Valencia (1965)

Ameiva ameiva: numerous specimens from all the range. *Ameiva auberi*: specimen from Cube ($n = 1$). *Ameiva bifrontata bifrontata* and *Ameiva bifrontata divisa*: several specimens from Venezuela, Colombia, Peru and Brazil. *Ameiva dorsalis*: specimens from Jamaica ($n = 3$). *Ameiva edracantha*: several specimens from Ecuador and Peru. *Ameiva festiva*: specimen from Nicaragua ($n = 1$). *Ameiva septemlineata*: several specimens from Ecuador. *Ameiva lacertoides*: several specimens from Uruguay and Brazil. All *Ameiva* specimens are deposited in MUZUSP.

Aspidoscelis sexlineatus: several specimens from the southern United States. All *Aspidoscelis* specimens are deposited in MUZUSP.

Callopistes maculatus and *Callopistes flavipunctatus*: several chilean examples. All specimens are deposited in MUZUSP.

Cnemidophrus murinus: specimen from Surinam ($n = 1$). *Cnemidophorus lemniscatus lemniscatus*: many specimens from all the range. *Cnemidophous lemniscatus nigricolor*: specimen from Los Roques ($n = 1$). *Cnemidophorus ocellifer*: many specimens from all the range. All specimens are deposited in MUZUSP.

Crocodilurus lacertinus: specimens from Pará ($n = 3$). All specimens are deposited in MUZUSP.

Dicrodon heterolepis: specimen from Peru ($n = 1$). *Dicrodon guttulatum*: paratype of Dicrodon barbouri ($n = 1$). Both specimens are deposited in MUZUSP.

Dracaena guianenis: MZUSP 506, 689, MSNV ($n = 2$) no catalogued; AMNH ($n = 1$) no catalogued; MNHN. *Dracaena paraguayensis*: MZUSP 7285-86.

Kentropyx: many specimens from all the range but Argentina.

Teius teyou: many specimens of both races, *teyou* and *cyanogaster*, from Uruguay, Brazil and Bolivia. Specimens are deposited in MUZUSP.

Tupinambis nigropunctatus and *Tupinambis teguixin*: many brazilian examples from all range. Specimens are deposited in MUZUSP.

Specimens Scored Morphology of the Tongue Characters

Data from this present study

Ameiva ameiva: CHUNB 25570.

Callopistes flavipunctatus ($n = 1$): MHNJP uncatologued.

Cnemidophorus ocellifer: GRColli 034222-23.

Crocodilurus lacertinus: CHUNB 15192.

Dicrodon guttulatum ($n = 2$): MHNJP uncatologued.

Dracaena guianensis: CHUNB 15197-99.

Kentropyx altamazonica: CHUNB 09819-23.

Teius oculatus: CHUNB 21861-62.

Tupinambis teguixin: CHUNB 10752, 10774-75, 14017, 14020.

Cercosaura ocellata: CHUNB 18272.

Specimens Scored for Hemipenial Characters

Data from this present study

Ameiva ameiva: CHUNB 25570.

Callopistes flavipunctatus ($n = 1$): MHNJP uncatologued.

Cnemidophorus ocellifer: GRColli 034222-23.

Crocodilurus lacertinus: CHUNB 15192.

Dicrodon guttulatum ($n = 2$): MHNJP uncatologued.

Dracaena guianensis: CHUNB 15197-99.

Kentropyx altamazonica: CHUNB 09819-23.

Teius oculatus: CHUNB 21861-62.

Tupinambis teguixin: CHUNB 10752, 10774-75, 14017, 14020.

Cercosaura ocellata: CHUNB 18272.

Specimens Scored for Cranial Myology Characters

Data from Moro and Abdala (2000)

Ameiva ameiva:FML 03637 ($n = 2$).

Callopistes maculates: MZUSO 58107

Cnemidophorus ocellifer: FML 03389 ($n = 2$), 03396 ($n = 4$), 03409 ($n = 4$).

Crocodilurus lacertinus: MZUSO 12622, 16307.

Dicrodon guttulatum: FML 02017.

Dracaena paraguayensis: MZUSP52369.

Kentropyx lagartija: FML 01186.

Teius oculatus: FML 03625, 03629 ($n = 2$), 03630 ($n = 2$), 03632, 03633.

Tupinambis rufescens: PT 0084-85, 0597, 0889; FML 06413, 06423, 06425, 07428, 07429, 07431, 07432, 07433, 07434.

APPENDIX II

Characters are categorized as either qualitative, meristic or morphometric. Autapomorphies and ordering of multistate, qualitative characters are also noted. The consistency index (ci) of each character is given.

1. Postorbital and postfrontal: Fixed (ci = 0.500).
2. Quadrate process of the pterygoid: Fixed (ci = 1.000).
3. Pterygoid flange: Fixed (ci = 1.000).
4. Dorsal process of the squamosal: Fixed (ci = 1.000).
5. Expanded quadrate: Fixed (ci = 1.000).
6. Teeth on the pterygoid: Fixed (ci = 0.500).
7. Teeth on the premaxillary: Fixed (ci = 1.000).
8. Clavicle shape: Fixed (ci = 0.500).
9. Clavicle hook: Fixed (ci = 1.000).
10. Interclavicle median process: Fixed (ci = 1.000).
11. Scapular foramen: Fixed (ci = 1.000).
12. Number of post-xiphisternal ribs: Fixed (ci = 1.000).
13. Number of presacral vertebrae: Fixed (ci = 1.000).
14. Neural arch, first autotomic caudal vertebrae: Fixed (ci = 1.000).
15. Second ceratobranchial: Fixed (ci = 1.000).
16. Anterior teeth on the maxillary bone: Fixed (ci = 0.500).
17. Supra-angular window: Uninformative, autapomorphy of *Dracaena*.

18. Contribution of the ectopterygoid to the inferior orbital foramen: Fixed (ci = 0.500).

19. Shape of the frontal-parietal roof: Uninformative, autapomorphy of *Kentropyx*.

20. Retroarticular process orientation, lower jaw: Fixed (ci = 0.333).

21. Condition of the fifth digit of the hind limb: Uninformative, autapomorphy of *Teius*.

22. Number of xiphisternal ribs: Sinapomorfia de Teiidae.

23. First cervical vertebra with rib: Polymorphic (ci = 1.000).

24. Last vertebra with rib: Polymorphic (ci = 0.500).

25. Hypapophysis in the third cervical vertebra: Fixed (ci = 0.667).

26. Neural spine of the third cervical vertebra: Fixed (ci = 0.500).

27. Number of vertebrae in dorsal region: Fixed (ci = 1.000).

28. Postnasal scale: Uninformative, autapomorphy of *Dracaena*.

29. Ventral scales: Fixed (ci = 0.333).

30. Carpal tubercles: Fixed (ci = 1.000).

31. Ventral scales, shape: Uninformative, autapomorphy of *Kentropyx*.

32. Ventral scales, keeled: Fixed (ci = 0.500).

33. Dorsal scales, shape: Polymorphic and ordered (ci = 0.750).

34. Dorsal scales, tubercles: Uninformative, autapomorphy of *Dracaena*.

35. Dorsal scales, keeled: Polymorphic (ci = 0.800).

36. Loreals: Fixed (ci = 0.500).

37. Neck scales are larger than dorsals: Fixed (ci = 1.000).

38. Supraciliaries in contact with supraoculars: Fixed (ci = 1.000).

39. Mentals in contact with infralabials: Fixed (ci = 0.500).

40. Temporals are smaller than dorsals: Fixed (ci = 0.500).

41. Gular fold: Fixed (ci = 0.333).

42. Transversal stripe in the tail: Fixed (ci = 0.667).

43. Intertympanic sulci: Fixed (ci = 0.667).

44. intermandibular sulci: Fixed (ci = 0.500).

45. Laterally compressed tail: Fixed (ci = 1.000).

46. Dorsal tail cristae: Fixed (ci = 1.000).

47. Proportion anterior tongue / posterior tongue: Fixed and ordered (ci = 1.000).

48. Ventral medium sulci: Uninformative, autapomorphy of *Dracaena*.

49. Lateral projection of the tongue: Fixed (ci = 0.500).

50. Shape of the tongue: Uninformative, autapomorphy of *Ameiva*.

51. Case in the tongue base: Uninformative, autapomorphy of *Ameiva*.

52. Scales in the tongue bifurcation: Uninformative, autapomorphy of *Dracaena*.

53. Anterior tongue sulci: Fixed (ci = 1.000).

54. Tongue base reaches the larynx: Uninformative, autapomorphy of *Kentropyx*.

55. Infralingual plicae: Uninformative, autapomorphy of *Dracaena*.

56. Posterior infralingual plicae related to the anterior plicae: Fixed and ordered (ci = 0.750).

57. Posterior plicae distribution: Fixed (ci = 0.500).

58. Tongue sheath: Uninformative, autapomorphy of *Ameiva*.

59. Infralingual plicae shape: Polymorphic and ordered (ci = 0.833).

60. Tongue shape in transverse section (anterior region): Fixed (ci = 0.333).

61. Tongue shape in transverse section (media region): Fixed (ci = 0.500).

62. Tongue shape in transverse section (posterior region): Fixed (ci = 0.500).

63. Genioglossus muscle lateral of the tongue (anterior region): Fixed (ci = 0.500).

64. Distance between the two bundles of hyoglossus muscle (anterior region): Fixed (ci = 0.500).

65. Shape of the hemipenis: Fixed (ci = 0.333).

66. Rotulae in the apex of the hemipenis: Fixed (ci = 0.667).

67. Pedunculus in the apex of the hemipenis: Fixed (ci = 0.286).

68. Auricula in the apex of the hemipenis: Fixed and ordered (ci = 0.500).

69. Lobes: Fixed (ci = 0.333).

70. Laminae in the sulcal surface: Fixed (ci = 0.333).

71. Laminae in the pedicel: Fixed (ci = 0.500).

72. Depth of the lateral laminae: Fixed and ordered (ci = 0.500).

73. Depth of the asulcal lamelae in the lateral protuberances: Fixed (ci = 0.333).

74. Continuity of the laminae surrounding the hemepenis: Uninformative, autapomorphy of *Callopistes*.

75. Dark pigmentation of the laminae: Fixed (ci = 0.500).

76. Dark pigmentation in the sulcus spermaticus: Fixed (ci = 0.250).

77. Dark pigmentation in the sulcus spermaticus in the sulcal lips: Fixed (ci = 0.333).

78. Dark pigmentation in the sulcal surface: Fixed (ci = 0.250).

79. Dark pigmentation in the ornaments: Polymorphic (ci = 0.600).

80. Type of ornament with dark pigmentation: Fixed (ci = 0.500).

81. Shape of the asucal sign in the apex of the hemipenis: Fixed (ci = 0.500).

82. Type of pigmentation in the asulcal sign in the apex of the hemipenis: Uninformative, autapomorphy of *Teius*.

83. Adductor aponeurosis size: Polymorphic and ordered (ci = 1.000).

84. Levator anguli oris shape: Polymorphic and ordered (ci = 1.000).

85. Levator anguli oris origin: Uninformative, autapomorphy of *Tupinambis*.

86. Levator anguli oris origin not including postorbital: Uninformative, autapomorphy of *Callopistes*.

87. Levator anguli oris origin not including postorbital but including quadrate: Fixed (ci = 0.667).

88. Adductor mandibule externus superficialis origin not including postorbital: Polymorphic (ci = 0.667).

89. Adductor mandibule externus superficialis insertion: Uninformative, autapomorphy of *Dracaena*.

90. Extension of the adductor mandibule externus medialis origin not including parietal: Uninformative, autapomorphy of *Crocodilurus*.

91. Extension of the adductor mandibule externus medialis origin including parietal: Polymorphic and ordered (ci = 0.667).

92. Extension of the adductor mandibulae externus medialis insertion: Polymorphic (ci = 1.000).

93. Adductor mandibulae externus profundus insertion: Fixed (ci = 0.500).

94. Extension of the pseudotemporalis superficialis origin not including postorbital: Fixed (ci = 1.000).

95. Extension of the pseudotemporalis superficialis insertion: Polymorphic (ci = 1.000).

96. Pterygomandibularis shape: Uninformative, autapomorphy of *Dicrodon*.

97. Sexual dimorphism in the pterygomandibularis: Fixed (ci = 1.000).

98. Levator pterygoid length: Uninformative, autapomorphy of *Callopistes*.

99. Protractor pterygoid origin: Polymorphic (ci = 0.750).

100. Intermandibularis anterior profundus aponeurosis: Polymorphic (ci = 0.667).

101. Intermandibularis anterior profundus shape: Fixed (ci = 1.000).

102. Depressor mandibulae superficialis: Polymorphic and uninformative, autapomorphy of *Tupinambis*.

103. Cervicomandibularis shape: Fixed and ordered (ci = 0.667).

104. Hyoglossus origin: Polymorphic and ordered (ci = 0.500).

105. Genioglossus contact: Uninformative, autapomorphy of *Ameiva*.

106. Mandibulohyoideus I shape: Polymorphic (ci = 1.000).

107. Mandibulohyoideus I insertion: Polymorphic (ci = 0.833).

108. Mandibulohyoideus II: Fixed (ci = 0.333).

109. Division of the mandibulohyoideus II: Polymorphic (ci = 1.000).

110. Mandibulohyoideus II insertion: Uninformative, autapomorphy of Dracaena

111. Mandibulohyoideus III: Polymorphic (ci = 0.667).

112. Branchiohyoideus origin: Uninformative, autapomorphy of *Callopistes*.

113. Geniohipohyoideus: Polymorphic (ci = 1.000).

114. Omohyoideus origin: Fixed (ci = 0.500).

115. Omohyoideus insertion not including basihyal: Uninformative, autapomorphy of *Teius*.

116. Omohyoideus insertion including basihyal: Uninformative, autapomorphy of *Callopistes*.

117. Sternohyoideus aoneurosis: Fixed (ci = 0.333).

118. Sternohyoideus insertion: Polymorphic (ci = 0.600).

119. Sternothyroideus: Polymorphic (ci = 1.000).

120. Number of caudal vertebrae (Presch, 1970): Meristic (ci = 0.413).

121. Number of femoral pores: Meristic (ci = 0.664).

122. Number of supralabial scales: Meristic (ci = 0.713).

123. Number of infralabial scales: Meristic (ci = 0.686).

124. Number of supratemporal scales rows: Meristic (ci = 0.611).

125. Number of lamellae of the fourth finger (foreleg): Meristic (ci = 0.592).

126. Number of lamellae of the fourth toe (hind limb): Meristic (ci = 0.602).

127. Number of dorsal scales: Meristic (ci = 0.642).

128. Number of scales around the mid-body: Meristic (ci = 0.649).

129. Number of ventral scale rows: Meristic (ci = 0.822).

130. Number of scales in a single ventral row: Meristic (ci = 0.800).

131. Number of cloacal pores: Meristic (ci = 0.539).

132. Number of prefemoral scales: Meristic (ci = 0.751).

133. Number of prefemoral scale rows: Meristic (ci = 0.723).

134. Number of infratibial scale rows: Meristic (ci = 0.707).

135. Number of preanals scales: Meristic (ci = 0.867).

136. Number of scales in the 15^{th} scale row around the tail: Meristic (ci = 0.845).

137. Number of infralingual plicae: Meristic (ci = 0.632).

138. Number of hemipenial lateral laminae: Meristic (ci = 0.564).

139. Unilateral ridge on acrosome surface: Sinapomorfia de Teiidae.

140. Perforatorial base plate: Fixed (ci = 0.500).

141. Perforatorial base plate shape: Fixed (ci = 0.500).

142. Stratified laminar structure: sinapomorfia de Teiidae.

143. Stratified laminar structure projection: Sinapomorfia de Teiidae.

144. Electron dense structure inside the proximal centriole: Fixed (ci = 0.500).

145. Fibers 3 and 8: Fixed (ci = 0.250).

146. Number of sets of mitochondria and ring structures: Fixed and ordered (ci = 0.750).

147. Mitochondria in oblique section: Fixed (ci = 0.500).

148. Mitochondria shape in longitudinal section: Fixed (ci = 0.333).

149. Dense bodies in oblique section: Fixed (ci = 1.000).

150. Ring structures appearance in oblique section: Sinapomorfia de Teiidae

151. Dense bodies in transverse section: Sinapomorfia de Teiidae

152. Beginning of the fibrous sheath in the midpiece: Fixed and ordered (ci = 1.000).

153. Ratio of head length to total sperm length: Morphometric (ci = 0.476).

154. Ratio of the acrosome length to head length: Morphometric (ci = 0.348).

155. Ratio of midpiece length to flagellum length: Morphometric (ci = 0.714).

156. Ratio of distal centriole length to midpiece length: Morphometric (ci = 0.725).

157. Ratio of mitochondrial tier length to midpiece length: Morphometric (ci = 0.518).

158. Ratio of the ring structure tier length to midpiece length: Morphometric (ci = 0.667).

159. Ratio of ring structure tier length to mitochondrial tier length: Morphometric (ci = 0.675).

160. Ratio of nuclear rostrum length to acrosome length: Morphometric (ci = 0.533).

161. Ratio of the electron lucent zone length to the electron lucent zone width: Morphometric (ci = 0.567).

162. Ratio of the diameter of the anterior region of the principal piece to the diameter of the annulus region: Morphometric (ci = 0.556).

163. Ratio of the fibrous sheath width to the principal piece width: Morphometric (ci= 0.359).

TABLE 1: Matrix of the characters and their characters-states referred to each teiid genera and *Cercosaura* genus, used in the phylogenetic analyses.

Genera	10 · 20 · 30 · 40 ·
Ameiva	1 1 1 0 1 1 0 0 1 0 1 0 1 1 0 0 0 1 0 1 0 1 0 01 0 0 1 0 1 1 0 0 1 0 1 0 0 1 1 1 1 0
Aspidoscelis	1 1 1 0 1 1 0 0 1 0 1 0 1 1 0 0 0 1 0 1 0 1 0 0 0 1 1 0 1 1 0 0 1 0 1 1 0 1 1 1 1 0
Cnemidophorus	1 1 1 0 1 1 0 0 1 0 1 0 1 1 0 0 0 1 0 1 0 1 0 0 0 1 1 0 1 1 0 0 1 0 1 0 1 1 1 1 1 0
Kentropyx	1 1 1 0 1 1 0 0 1 0 1 0 1 1 0 0 0 1 1 1 0 1 0 0 0 1 1 0 0 1 1 1 12 0 0 0 0 1 0 0 1 0
Dicrodon	1 1 1 0 1 0 0 0 1 0 1 0 1 1 0 1 0 0 0 0 0 1 01 0 0 1 1 0 1 1 0 0 1 0 01 1 0 1 0 1 0 0
Teius	1 1 1 0 1 1 0 0 1 0 1 0 1 1 0 1 0 0 0 0 1 1 0 0 1 0 1 0 1 1 0 0 1 0 1 1 0 1 0 1 1 0
Callopistes	0 0 1 1 1 1 0 1 0 0 0 1 0 0 0 0 0 0 0 0 0 1 0 1 1 1 0 0 1 1 0 0 1 0 1 ? 0 1 1 1 0 1
Tupinambis	0 0 0 1 0 0 1 1 0 1 0 1 0 0 1 0 0 0 0 1 0 1 0 1 1 0 0 0 1 0 0 0 0 0 1 0 0 0 0 1 1 1
Crocodilurus	0 0 0 1 1 0 1 1 0 1 0 1 0 0 1 0 0 0 0 1 0 1 0 1 1 0 0 0 0 0 0 0 01 0 01 0 0 0 0 1 1 0
Dracaena	1 0 0 1 0 0 1 1 0 1 0 1 0 0 1 0 1 0 0 1 0 1 1 1 01 0 0 1 1 0 0 1 1 1 01 1 01 01 01 1 1 01
Cercosaura	0 ? ? ? ? 0 0 0 ? 0 0 ? 0 ? 0 0 ? 0 ? 0 0 0 ? ? ? ? ? 0 0 0 0 0 0 0 0 0 0 0 0 0 0 0

Genera	50 · 60 · 70 · 80 ·
Ameiva	0 0 0 0 2 0 1 1 1 0 1 0 0 3 1 1 1 1 1 1 0 0 0 1 2 0 0 1 0 2 1 0 0 0 0 0 01 1 0 0 ? 1 1 ? ? 1
Aspidoscelis	? ? 0 0 ?
Cnemidophorus	0 0 0 0 1 0 0 0 0 0 1 0 0 3 1 0 01 1 1 1 0 0 0 1 2 2 1 1 1 2 0 0 0 0 0 0 0 ? 1 0 0 0 1 0 1 01
Kentropyx	0 0 0 0 1 0 0 0 0 0 1 1 0 3 1 0 1 1 1 1 0 0 1 2 0 0 1 0 1 1 0 0 0 1 1 1 0 ? ? ? 0 0 1 0 1 0
Dicrodon	0 0 0 0 ? ? ? ? ? ? ? ? ? 0 3 1 0 01 0 1 1 0 1 1 1 1 0 1 1 0 3 1 0 0 0 0 0 01 1 2 0 0 0 1 0 1 1
Teius	0 0 0 0 ? ? ? ? ? ? ? ? ? 0 3 1 0 01 1 1 1 1 1 0 1 2 0 1 1 1 2 1 0 0 1 1 1 1 1 1 1 ? 1 1 0 0 0
Callopistes	1 0 0 0 ? ? ? ? ? ? ? ? ? 0 2 0 0 0 1 1 1 0 0 1 2 0 0 0 0 0 0 0 1 1 1 0 0 1 0 0 0 2 0 1 1 ? ?
Tupinambis	1 1 0 0 1 1 1 0 0 0 1 0 0 1 1 0 1 0 0 1 0 0 0 0 2 2 1 1 0 2 0 0 0 0 0 1 1 0 2 0 2 01 0 ? ? ?
Crocodilurus	0 0 1 1 1 1 0 0 0 0 1 0 0 1 1 0 1 0 1 0 1 0 0 0 2 2 0 1 0 1 0 0 1 1 1 1 1 1 3 0 02 0 1 0 0 ?
Dracaena	01 1 1 1 1 1 0 0 0 1 2 0 1 0 1 0 2 1 1 1 0 0 0 0 1 2 0 1 0 1 1 0 0 0 0 0 0 ? 3 0 ? 0 1 0 2 0
Cercosaura	0 0 0 0 0 0 0 0 0 0 0 0 0 0 0 0 ? 0 0 0 0 0 0 0 0 0 0 1 0 0 0 0 0 0 0 0 0 0 0 ? 0 ? ? ? ? ? ? ?

Genera	90										100										110										120			
Ameiva	1	?	0	0	0	1	0	0	1	1	1	0	0	0	1	1	0	1	1	1	0	1	1	?	0	1	0	1	1	0	0	0	0	0
Aspidoscelis	?	?	?	?	?	?	?	?	?	?	?	?	?	?	?	?	?	?	?	?	?	?	?	?	?	?	?	?	?	?	?	1	1	1
Cnemidophorus	1	?	01	01	1	1	01	0	0	1	01	1	1	0	1	12	1	12	02	1	01	1	0	1	1	0	1	12	02	1	01	2	2	2
Kentropyx	1	?	1	0	1	1	0	0	0	1	0	1	1	0	1	1	1	1	2	0	0	?	0	1	1	0	1	1	2	1	0	3	3	3
Dicrodon	1	?	0	1	1	1	1	1	0	1	0	0	1	0	0	2	1	1	2	1	?	1	0	1	0	?	1	1	2	?	?	4	4	4
Teius	1	?	1	0	0	0	0	0	1	1	1	0	0	0	2	2	1	1	1	1	0	1	?	?	0	2	1	1	1	0	0	5	5	5
Callopistes	1	0	?	0	0	1	0	0	?	0	0	1	1	0	1	1	1	2	3	0	?	?	1	0	0	1	1	2	3	2	?	6	6	6
Tupinambis	1	?	0	01	1	1	0	0	1	1	0	01	1	01	1	2	1	1	1	1	0	1	01	1	01	0	1	1	1	01	0	7	7	7
Crocodilurus	1	1	?	0	0	1	0	0	?	?	0	1	1	0	0	1	1	0	0	0	?	?	1	1	0	0	1	0	0	0	?	8	8	8
Dracaena	0	0	?	0	0	2	0	0	?	1	2	1	1	0	1	1	1	0	1	1	1	0	0	1	0	3	1	0	1	2	1	9	9	9
Cercosaura	?	?	?	?	?	?	?	?	?	?	?	?	?	?	?	?	?	?	?	?	?	?	?	?	?	?	?	?	?	?	?	?	A	A

Genera	130																140															150												160										
Ameiva	0	0	0	0	0	0	0	0	0	0	0	0	0	0	0	0	1	1	1	1	1	1	0	2	0	0	1	1	1	1	0	0	0	0	0	0	0	0	0	0	0	0	0	0	0	0	0	0	0	0	0
Aspidoscelis	1	1	1	1	1	1	1	1	1	1	1	1	1	1	1	?	1	1	1	1	1	1	1	2	0	0	1	C	1	1	1	1	1	1	1	1	1	1	1	1	1	1	1	1	1	1	1	1	1	1	1
Cnemidophorus	2	2	2	2	2	2	2	2	2	2	2	2	2	2	2	2	1	1	1	1	1	1	1	2	0	0	1	1	1	1	2	2	2	2	2	2	2	2	2	2	2	2	2	2	2	2	2	2	2	2	2
Kentropyx	3	3	3	3	3	3	3	3	3	3	3	3	3	3	3	3	1	0	?	1	1	1	0	2	1	1	1	1	1	2	3	3	3	3	3	3	3	3	3	3	3	3	3	3	3	3	3	3	3	3	3
Dicrodon	4	4	4	4	4	4	4	4	4	4	4	4	4	4	4	?	4	1	1	0	1	1	1	0	2	0	0	1	1	1	1	4	4	4	4	4	4	4	4	4	4	4	4	4	4	4	4	4	4	4	4
Teius	5	5	5	5	5	5	5	5	5	5	5	5	5	5	5	?	5	1	1	1	1	1	1	1	2	1	1	1	1	1	1	5	5	5	5	5	5	5	5	5	5	5	5	5	5	5	5	5	5	5	5
Callopistes	6	6	6	6	6	6	6	6	6	6	6	6	6	6	6	?	6	1	1	1	1	1	1	0	0	0	0	0	1	1	1	6	6	6	6	6	6	6	6	6	6	6	6	6	6	6	6	6	6	6	6
Tupinambis	7	7	7	7	7	7	7	7	7	7	7	7	7	7	7	7	7	1	1	0	1	1	1	1	3	0	0	0	1	1	0	7	7	7	7	7	7	7	7	7	7	7	7	7	7	7	7	7	7	7	7
Crocodilurus	8	8	8	8	8	8	8	8	8	8	8	8	8	8	8	8	8	1	1	1	1	1	0	0	3	0	1	0	1	1	0	8	8	8	8	8	8	8	8	8	8	8	8	8	8	8	8	8	8	8	8
Dracaena	9	9	9	9	9	9	9	9	9	9	9	9	9	9	9	9	9	1	1	1	1	1	0	1	2	0	1	0	1	1	0	9	9	9	9	9	9	9	9	9	9	9	9	9	9	9	9	9	9	9	9
Cercosaura	A	A	A	A	A	A	A	A	A	A	A	A	A	A	A	A	A	0	0	?	0	0	0	0	2	0	0	0	C	0	0	A	A	A	A	A	A	A	A	A	A	A	A	A	A	A	A	A	A	A	A	A	A

TABLE 2: Matrix of mean genera values for quantitative traditional morphological characters.

Genera	120	121	122	123	124	125
Ameiva	64.00	37.34 ± 0.97 (n = 41)	12.25 ± 0.63 (n = 40)	11.71 ± 0.93 (n = 41)	2.00 ± 0.00 (n = 41)	14.22 ± 1.67 (n = 41)
Aspidoscelis	64.00	35.30 ± 2.06 (n = 12)	12.92± 1.78 (n = 12)	12.33 ± 2.84 (n = 12)	2.00 ± 0.00 (n = 12)	14.04 ± 1.24 (n = 12)
Cnemidophorus	64.00	17.47 ± 2.04 (n = 478)	13.11 ± 1.09 (n = 435)	10.63 ± 0.96 (n = 453)	1.00 ± 0.00 (n = 497)	14.80 ± 1.16 (n = 493)
Kentropyx	62.00	33.17 ± 2.84 (n = 47)	12.65 ± 1.06 (n = 55)	13.02 ± 1.28 (n = 55)	2.85 ± 0.36 (n = 55)	17.71 ± 1.13 (n = 55)
Dicrodon	62.00	31.95 ± 3.36 (n = 59)	10.30 ± 0.65 (n = 59)	10.10 ± 0.71 (n = 59)	1.07 ± 0.25 (n = 59)	16.34 ± 1.09 (n = 59)
Teius	57.00	35.64 ± 3.64 (n = 192)	12.34 ± 1.20 (n = 190)	11.48 ± 1.43 (n = 191)	1.54 ± 0.50 (n = 192)	12.93 ± 1.40 (n = 194)
Callopistes	73.00	0.00 ± 0.00 (n = 13)	21.14 ± 2.68 (n = 11)	19.28 ± 1.76 (n = 11)	0.50 ± 0.23 (n = 13)	23.12 ± 1.54 (n = 13)
Tupinambis	72.00	14.28 ± 2.58 (n = 220)	14.66 ± 1.41 (n = 223)	11.80 ± 1.57 (n = 222)	1.00 ± 0.07 (n = 212)	16.42 ± 1.09 (n = 223)
Crocodilurus	54.00	13.13 ± 2.50 (n = 78)	13.65 ± 1.74 (n = 74)	12.00 ± 0.55 (n = 74)	1.00 ± 0.00 (n = 64)	19.40 ± 1.75 (n = 78)
Dracaena	56.00	4.43 ± 1.95 (n = 14)	16.87 ± 1.71 (n = 16)	20.43 ± 2.40 (n = 16)	1.33 ± 0.49 (n = 12)	24.00 ± 2.13 (n = 16)
Cercosaura	---	3.23 ± 2.53 (n = 158)	13.80 ± 0.67 (n = 159)	11.69 ± 0.76 (n = 159)	1.00 ± 0.00 (n = 159)	17.04 ± 1.47 (n = 158)

Genera	126	127	128	129	130	131
Ameiva	29.50 ± 2.24 (n = 40)	260.76 ± 16.35 (n = 41)	138.10 ± 6.42 (n = 41)	29.95 ± 1.24 (n = 41)	12.63 ± 4.06 (n = 41)	0.00 ± 0.00 (n = 41)
Aspidoscelis	30.42 ± 3.42 (n = 12)	204.00 ± 10.53 (n = 12)	89.67 ± 3.89 (n = 12)	33.17 ± 1.53 (n = 12)	8.17 ± 0.39 (n = 12)	0.00 ± 0.00 (n = 12)
Cnemidophorus	25.40 ± 2.21 (n = 495)	233.53 ± 14.67 (n = 448)	107.53 ± 6.80 (n = 426)	28.49 ± 1.35 (n = 453)	7.99 ± 0.18 (n = 472)	0.00 ± 0.00 (n = 497)
Kentropyx	27.10 ± 1.33 (n = 55)	146.24 ± 8.54 (n = 55)	122.5 ± 9.70 (n = 54)	32.74 ± 1.22 (n = 54)	16.04 ± 0.68 (n = 53)	0.00 ± 0.00 (n = 55)
Dicrodon	31.57 ± 1.63 (n = 56)	144.33 ± 13.37 (n = 58)	71.58 ± 15.82 (n = 59)	33.10 ± 1.29 (n = 58)	9.49 ± 0.86 (n = 59)	0.00 ± 0.00 (n = 59)
Teius	27.58 ± 2.64 (n = 191)	228.74 ± 15.57 (n = 189)	110.58 ± 9.08 (n = 193)	34.60 ± 2.71 (n = 194)	9.18 ± 0.88 (n = 194)	0.00 ± 0.00 (n = 194)
Callopistes	33.50 ± 1.89 (n = 13)	186.28 ± 17.72 (n = 12)	175.12 ± 9.10 (n = 13)	62.25 ± 1.72 (n = 13)	52.12 ± 7.00 (n = 13)	0.00 ± 0.00 (n = 13)
Tupinambis	34.19 ± 1.90 (n = 224)	112.94 ± 5.13 (n = 225)	107.00 ± 7.00 (n = 226)	34.4 ± 1.33 (n = 225)	24.10 ± 2.20 (n = 227)	8.02 ± 1.30 (n = 222)
Crocodilurus	29.68 ± 1.94 (n = 78)	119.88 ± 8,94 (n = 76)	86.34 ± 5.89 (n = 78)	34.92 ± 1.05 (n = 78)	20.04 ± 1.37 (n = 78)	6.99 ± 1.12 (n = 77)
Dracaena	35.44 ± 3.14 (n = 16)	101.14 ± 10.79 (n = 14)	105.62 ± 9.70 (n = 16)	33.81 ± 1.47 (n = 16)	38.06 ± 4.14 (n = 16)	6.56 ± 1.36 (n = 16)
Cercosaura	21.26 ± 1.42 (n = 159)	28.67 ± 1.13 (n = 158)	24.71 ± 2.88 (n = 152)	19.56 ± 1.30 (n = 149)	6.00 ± 0.00 (n = 152)	0.00 ± 0.00 (n = 159)

Genera	132	133	134	135	136	137	138
Ameiva	6.90 ± 0.77 (*n* = 41)	11.41 ± 1.16 (*n* = 41)	7.24 ± 0.54 (*n* = 41)	3.05 ± 0.50 (*n* = 41)	38.61 ± 2.43 (*n* = 41)	1.00	29.00
Aspidoscelis	6.25 ± 0.45 (*n* = 12)	12.92 ± 1.50 (*n* = 12)	9.08 ± 1.00 (*n* = 12)	4.00 ± 0.00 (*n* = 12)	23.00 ± 2.09 (*n* = 12)	3.00	---
Cnemidophorus	5.07 ± 0.96 (*n* = 485)	8.81 ± 0.64 (*n* = 484)	7.80 ± 0.67 (*n* = 486)	3.09 ± 0.31 (*n* = 483)	21.90 ± 0.46 (*n* = 495)	1.00	24.00
Kentropyx	10.53 ± 1.35 (*n* = 55)	14.89 ± 1.47 (*n* = 55)	11.63 ± 1.02 (*n* = 55)	4.00 ± 0.00 (*n* = 55)	18.96 ± 1.90 (*n* = 55)	1.00	30.00
Dicrodon	8.20 ± 0.80 (*n* = 59)	12.35 ± 0.91 (*n* = 59)	9.07 ± 0.89 (*n* = 59)	3.46 ± 0.50 (*n* = 58)	22.27 ± 1.41 (*n* = 59)	---	15.00
Teius	5.60 ± 0.67 (*n* = 194)	10.39 ± 1.42 (*n* = 194)	7.34 ± 1.31 (*n* = 194)	4.13 ± 0.49 (*n* = 194)	32.15 ± 2.73 (*n* = 194)	---	8.00
Callopistes	26.62 ± 4.29 (*n* = 13)	27.25 ± 3.13 (*n* = 13)	18.75 ± 2.22 (*n* = 13)	15.13 ± 2.25 (*n* = 13)	121.25 ± 7.58 (*n* = 13)	---	19.00
Tupinambis	19.95 ± 1.81 (*n* = 224)	18.32 ± 1.41 (*n* = 224)	9.40 ± 1.16 (*n* = 226)	4.52 ± 0.62 (*n* = 225)	81.25 ± 5.30 (*n* = 224)	13.00	76.50
Crocodilurus	14.86 ± 1.22 (*n* = 78)	14.19 ± 1.58 (*n* = 78)	8.16 ± 0.78 (*n* = 78)	3.58 ± 0.50 (*n* = 78)	51.39 ± 3.70 (*n* = 76)	4.00	61.5
Dracaena	17.40 ± 2.23 (*n* = 15)	14.00 ± 1.51 (*n* = 15)	8.00 ± 1.07 (*n* = 15)	4.19 ± 0.98 (*n* = 16)	52.60 ± 7.73 (*n* = 15)	3.00	42.00
Cercosaura	2.35 ± 0.48 (*n* = 158)	6.96 ± 1.00 (*n* = 157)	5.11 ± 0.68 (*n* = 158)	2.16 0.40 (*n* = 158)	13.83 0.89 (*n* = 143)	10.00	11.00

Note: Data of character 120 are from Presch (1970)., character 137 from Harris (1989) . Data of character 138 are from one specimen for each genus.

TABLE 3 – Matrix of ratio of the genera means values for quantitative sperm characters.

Genera	153	154	155	156	157	158	159	160	161	162	163
Ameiva	0.26	0.17	0.09	0.19	0.19	0.01	0.05	0.24	3.80	0.69	1.71
Aspidoscelis	0.27	0.37	0.09	0.26	0.13	0.07	0.55	0.19	1.80	1.00	1.78
Cnemidophorus	0.23	0.23	0.08	0.21	0.13	0.07	0.55	0.23	3.75	0.96	1.89
Kentropyx	0.19	0.23	0.12	0.08	0.17	0.03	0.15	0.18	2.75	0.95	1.96
Dicrodon	0.20	0.22	0.06	0.24	0.11	0.08	0.75	0.26	3.00	0.76	0.63
Teius	0.25	0.15	0.06	0.24	0.15	0.04	0.27	0.23	2.20	0.77	0.63
Callopistes	0.16	0.18	0.02	0.32	0.22	0.11	0.50	0.22	0.20	0.75	1.52
Tupinambis	0.22	0.20	0.05	0.31	0.11	0.05	0.50	0.22	1.20	0.80	1.75
Crocodilurus	0.19	0.21	0.05	0.28	0.08	0.08	1.00	0.20	2.20	0.67	1.64
Dracaena	0.20	0.17	0.05	0.37	0.12	0.08	0.67	0.23	2.40	0.56	1.78
Cercosaura	0.22	0.19	0.04	0.33	0.14	0.07	0.50	0.20	2.20	0.66	0.48

TABLE 4 –Sperm dimensions in genera.

Characters	*Ameiva*	*Aspidoscelis*	*Cnemidophorus*	*Dicrodon*	*Kentropyx*	*Teius*
HL	16.78 ± 1.38 (6)	10.83 ± 0.29 (3)	13.30 ± 0.61 (14)	15.60 ± 1.38 (5)	14.40 ± 0.61 (14)	18.91 ± 2.50 (11)
TL	50.45 ± 4.93 (6)	40.25 ± 0.35 (2)	40.13 ± 2.82 (7)	54.01 ± 4.72 (2)	53.64 ± 2.81 (8)	53.20 ± 6.96 (10)
ESL	75.11 ± 4.27 (6)	54.50 ± 0.00 (2)	56.24 ± 2.55 (11)	78.34 ± 6.13 (2)	75.58 ± 2.50 (10)	74.74 ± 10.73 (10)
MPL	4.79 ± 0.16 (4)	3.48 ± 0.03 (5)	3.35 ± 0.32 (9)	3.52 ± 0.17 (12)	7.55 ± 0.35 (8)	5.62 ± 1.12 (12)
AL	3.36 ± 0.71 (8)	3.96 ± 0.12 (8)	3.07 ± 0.14 (6)	3.46 ± 0.30 (7)	3.44 ± 0.22 (8)	2.88 ± 0.23 (10)
NBW	0.47 ± 0.06 (14)	0.68 ± 0.04 (5)	0.53 ± 0.03 (3)	0.53 ± 0.07 (11)	0.64 ± 0.03 (3)	0.46 ± 0.05 (10)
NRL	0.87 ± 0.9 (15)	0.77 ± 0.03 (5)	0.71 ± 0.05 (10)	0.89 ± 0.08 (7)	0.62 ± 0.06 (10)	0.66 ± 0.04 (6)
DCL	0.90 ± 0.10 (5)	0.92 ± 0.12 (6)	0.72 ± 0.07 (7)	0.85 ± 0.25 (12)	0.65 ± 0.03 (7)	0.86 ± 0.09 (10)
ETL	0.18 ± 0.05 (14)	0.09 ± 0.04 (5)	0.15 ± 0.04 (6)	0.15 ± 0.08 (9)	0.11 ± 0.04 (7)	0.11 ± 0.04 (6)
ETW	0.05 ± 0.01 (14)	0.05 ± 0.01 (4)	0.04 ± 0.00 (5)	0.05 ± 0.02 (10)	0.04 ± 0.01 (7)	0.05 ± 0.00 (6)
NSW	0.33 ± 0.03 (7)	0.50 ± 0.03 (5)	0.37 ± 0.02 (4)	0.39 ± 0.02 (11)	0.42 ± 0.03 (5)	0.34 ± 0.03 (10)
RD	0.69 ± 0.13 (3)	1.00 ± 0.00 (3)	0.86 ± 0.18 (3)	0.76 ± 0.06 (12)	0.95 ± 0.01 (2)	0.78 ± 0.06 (7)
RC	1.71 ± 0.20 (4)	1.78 ± 0.24 (3)	1.89 ± 0.22 (3)	0.63 ± 0.09 (11)	1.96 ± 0.06 (2)	0.63 ± 0.09 (7)

Note: Values in μm and represented by ± 1 standard deviation. In parentheses is represented the number of micrographs taken the dimensions. HL = head length, TL = tail length, ESL = entire sperm length, MPL = midpiece length, AL = acrosome length, NBW = nucleus base width, NRL = nuclear rostrum length, DCL = distal centriole length, ETL = epinuclear lucent zone length, ETW = epinuclear lucent zone width, NSW = nuclear shoulders width, RD = ratio diameter of the principal piece diameter to midpiece diameter, and RC = ratio cytoplasm between fibrous sheath to principal diameter.

Characters	*Callopistes*	*Crocodilurus*	*Dracaena*	*Tupinambis*	*Cercosaura*
HL	16.81 ± 2.22 (12)	16.60 ± 2.38 (10)	18.08 ± 1.35 (8)	19.00 ± 1.28 (8)	14.75 ± 0.67 (12)
TL	85.56 ± 5.60 (9)	63.85 ± 2.08 (9)	66.66 ± 1.84 (6)	61.71 ± 3.48 (7)	50.57 ± 2.61 (13)
ESL	104.98 ± 5.72 (8)	84.98 ± 3.06 (9)	90.50 ± 3.41 (5)	86.00 ± 6.03 (7)	67.49 ± 2.67 (13)
MPL	1.82 ± 0.12 (19)	3.70 ± 0.30 (9)	3.82 ± 0.39 (5)	3.59 ± 0.14 (3)	2.18 ± 0.19 (9)
AL	2.99 ± 0.12 (11)	3.51 ± 0.22 (7)	3.15 ± 0.22 (5)	3.89 ± 0.42 (9)	2.83 ± 0.20 (9)
NBW	0.53 ± 0.04 (18)	0.51 ± 0.05 (19)	0.47 ± 0.05 (12)	0.51 ± 0.02 (3)	0.45 ± 0.06 (6)
NRL	0.65 ± 0.10 (12)	0.69 ± 0.04 (7)	0.72 ± 0.06 (10)	0.86 ± 0.07 (5)	0.57 ± 0.10 (5)
DCL	0.56 ± 0.06 (17)	1.04 ± 0.16 (14)	1.43 ± 0.12 (5)	1.10 ± 0.00 (2)	0.73 ± 0.04 (2)
ETL	0.01 ± 0.01 (4)	0.13 ± 0.04 (6)	0.12 ± 0.02 (3)	0.07 ± 0.03 (4)	0.11 ± 0.04 (6)
ETW	0.05 ± 0.01 (4)	0.06 ± 0.02 (4)	0.05 ± 0.01 (3)	0.06 ± 0.02 (4)	0.05 ± 0.00 (6)
NSW	0.34 ± 0.02 (10)	0.35 ± 0.03 (8)	0.33 ± 0.03 (9)	0.39 ± 0.03 (4)	0.33 ± 0.03 (3)
RD	0.75 ± 0.07 (19)	0.67 ± 0.08 (12)	0.56 ± 0.10 (8)	0.80 ± 0.04 (4)	0.66 ± 0.09 (5)
RC	1.52 ± 0.22 (19)	1.64 ± 0.20 (12)	1.78 ± 0.33 (4)	1.75 ± 0.12 (4)	0.48 ± 0.09 (2)

Note: Values in μm and represented by ± 1 standard deviation. In parentheses is represented the number of micrographs taken the dimensions. HL = head length, TL = tail length, ESL = entire sperm length, MPL = midpiece length, AL = acrosome length, NBW = nucleus base width, NRL = nuclear rostrum length, DCL = distal centriole length, ETL = epinuclear lucent zone length, ETW = epinuclear lucent zone width, NSW = nuclear shoulders width, RD = ratio diameter of the principal piece diameter to midpiece diameter, and RC = ratio cytoplasm between fibrous sheath to principal diameter.

FIGURE LEGENDS

FIG. 1.— Diagram of the general teiid spermatozoon, and corresponding transverse section. Scales of various components are only approximate. Scale bar 0.5 μm.

FIG. 2.— Diagrams of the anterior portion of sperm acrosome, showing the unilateral ridge on the acrosome surface. (0) absent, (1) present.

FIG. 3.—**A – C.** Diagrams of the anterior portion of sperm acrosome, showing the perforatorium base plate. **A.** Absence of perfotatorium base plate. **B.** Presence of perforatorium base plate with a stopper-like shape. **C.** Presence of a perforatorium base plate with a knoblike shape.

FIG. 4.—**A – C** Diagrams of the anterior portion of the sperm midpiece, showing the stratified laminar structure and the central densification within the proximal centriole. **A.** Stratified laminar structure: (0) poorly developed, (1) well developed. **B.** Stratified laminar structure projection: (0) unilateral, (1) bilateral. **C.** Electron dense structure inside the proximal centriole: (0) absent, (1) present.

FIG. 5.—Diagrams of the sperm midpiece, showing the adjacent peripheral fibers. (0) not grossly enlarged, (1) grossly enlarged.

FIG. 6.— Diagrams of the sperm midpiece, showing the number of sets of mitochondria and ring structures. (0) 3 sets, (1) 4 sets, (2) 5 sets, (3) 6 sets.

FIG. 7.—Diagrams of the sperm mitochondria, showing their shape in oblique section. (0) columnar, (1) slightly curved.

FIG. 8.— Diagrams of the sperm mitochondria, showing their end shape in longitudinal section section. (0) trapezoidal, (1) columnar mitochondria with rounded ends.

FIG. 9.—Diagrams of a region of the sperm midpiece, showing the dense bodies forming or not ring structures. (0) dense bodies not forming ring structures, (1) dense bodies, forming ring structures.

FIG. 10.— Diagrams of a region of the sperm midpiece, showing the dense bodies in the ring structures in oblique section. (0) fused dense bodies, forming compacted ring structures, (1) dense bodies not fused, forming descompacted ring structures.

FIG. 11.—Diagrams of the sperm midpiece in transverse section, showing the dense bodies position related to the fibrous sheath. (0) presence of mitochondria between the dense bodies and the fibrous sheath, (1) dense bodies juxtaposed to fibrous sheath.

FIG. 12.—Diagrams of the sperm midpiece, showing the beginning of the fibrous sheath. (0) fibrous sheath beginning at the third mitochondrial level, (1) fibrous sheath beginning at the second mitochondrial, (2) fibrous sheath beginning at the first mitochondrial level.

FIG. 13.—**A – C.** Diagrams of sperm dimensions, showing 3 quantitative sperm ultrastructrual characters. **A.** Ratio of head length to total sperm length. **B.** Ratio of acrosome length to head length. **C.** Ratio of midpiece length to flagellum lengh.

FIG. 14.— **A – B.** Diagrams of sperm dimensions, showing 2 quantitative sperm ultrastructrual characters. **A.** Ratio of distal centriole length to midpiece length. **B.** Ratio of mitochondrial tier length to midpiece length.

FIG. 15.—**A – B.** Diagrams of sperm dimensions, showing 2 quantitative sperm ultrastructrual characters. **A.** Ratio of ring structure tier length to midpiece length. **B.** Ratio of ring structure tier length to mitochondrial tier length.

FIG. 16.—**A – B.** Diagrams of sperm dimensions, showing 2 quantitative sperm ultrastructrual characters. **A.** Ratio of nuclear rostrum length to acrosome length. **B.** Ratio of electron lucent zone length to the electron lucent zone width.

FIG. 17.— **A – B.** Diagrams of sperm dimensions, showing 2 quantitative sperm ultrastructrual characters. **A.** Ratio of diameter of the anterior region of the principal

piece to diameter of the annulus region. **B.** Ratio of fibrous sheath width to principal piece width.

FIG. 18.— (A) Phylogenetic relationships of teiids lizards as postulated by this study, based in traditional morphological data. (B) Bootstrap 50% majority-rule consensus tree, based in the traditional morphological data.

FIG. 19.— (A) Phylogenetic relationships of teiids lizards as postulated by this study, based in sperm ultrastructural data. (B) Bootstrap 50% majority-rule consensus tree, based in the sperm ultrastructural data.

FIG. 20.— (A) Phylogenetic relationships of teiids lizards as postulated by this study, based in the combined data. (B) Bootstrap 50% majority-rule consensus tree, based in the combined data.

FIG. 21.— Bootstrap 50% majority-rule consensus tree, based in the undersampled traditional morphological data.

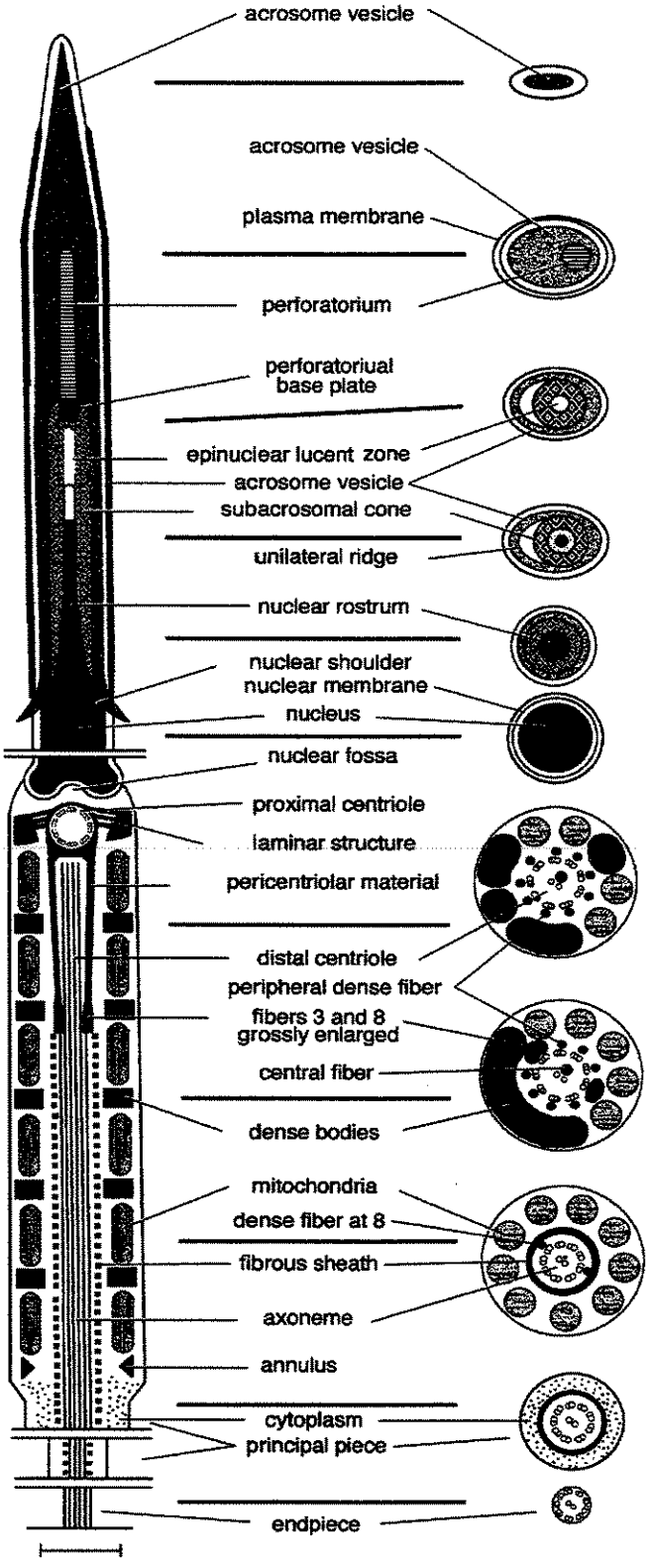
acrosome vesicle
acrosome vesicle
plasma membrane
perforatorium
perforatoriual base plate
epinuclear lucent zone
acrosome vesicle
subacrosomal cone
unilateral ridge
nuclear rostrum
nuclear shoulder
nuclear membrane
nucleus
nuclear fossa
proximal centriole
laminar structure
pericentriolar material
distal centriole
peripheral dense fiber
fibers 3 and 8 grossly enlarged
central fiber
dense bodies
mitochondria
dense fiber at 8
fibrous sheath
axoneme
annulus
cytoplasm
principal piece
endpiece

Fig. 2: Character 139

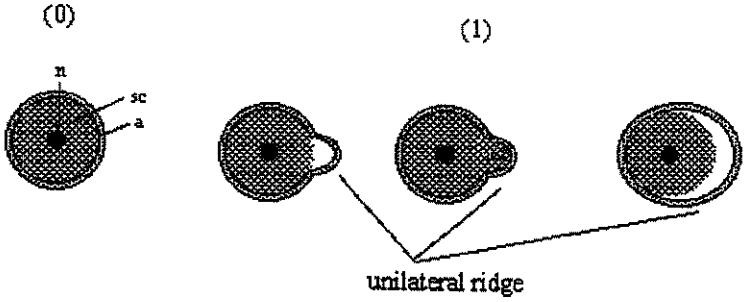

Fig. 3: Character 140 and 141

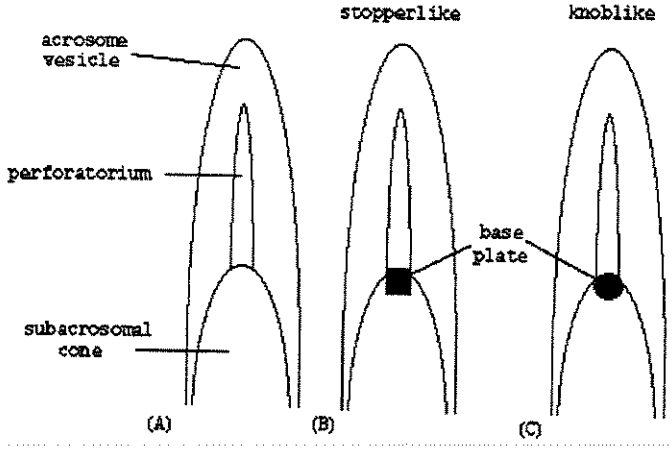

Fig. 4: Character 142, 143 and 144

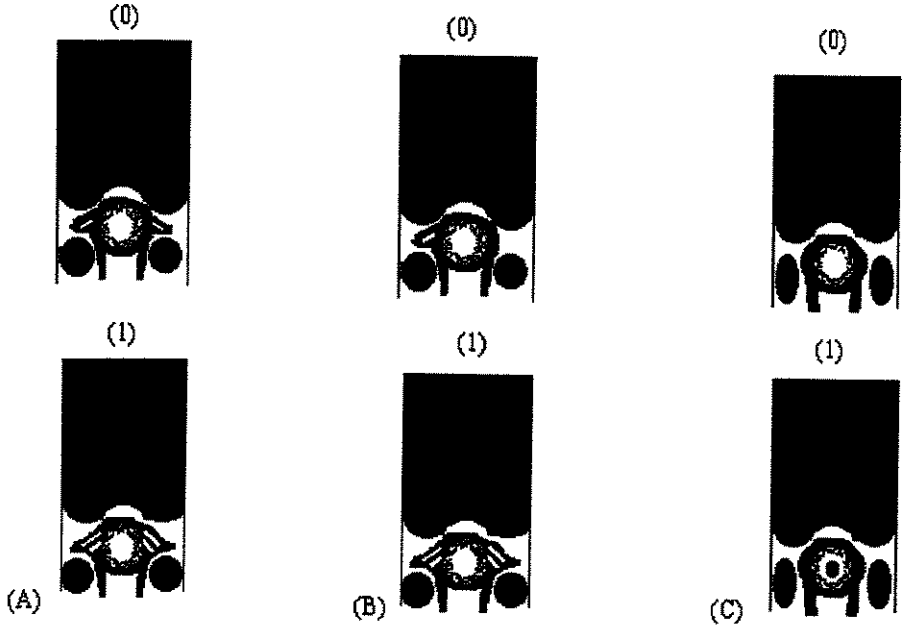

Fig. 5: Character 145

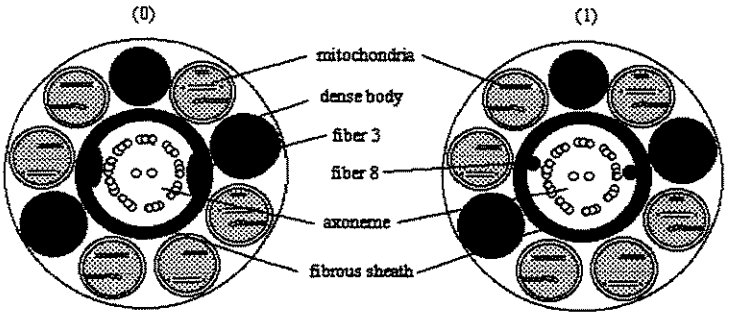

Fig. 6: Character 146

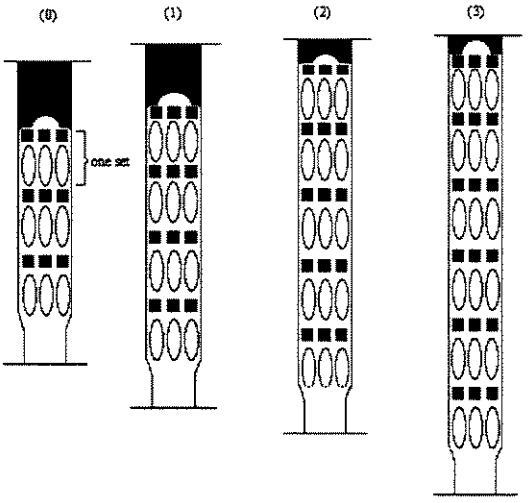

Fig. 7: Character 147

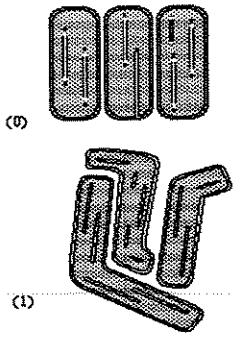

Fig. 8: Character 148

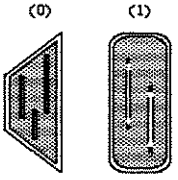

Fig. 9: Character 149

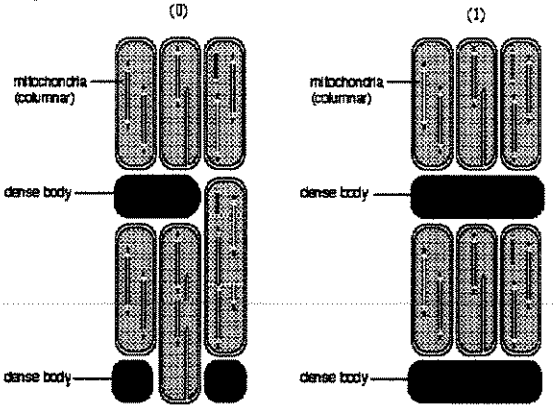

Fig. 10: Character 150

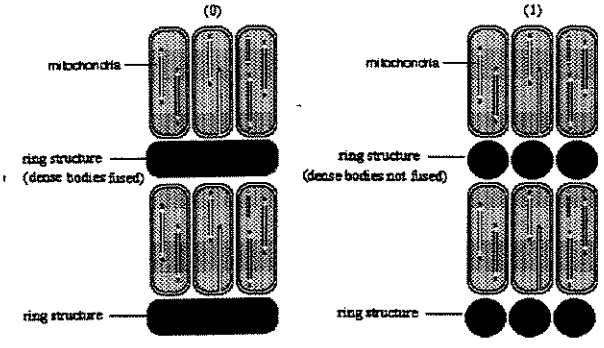

Fig. 11: Character 151

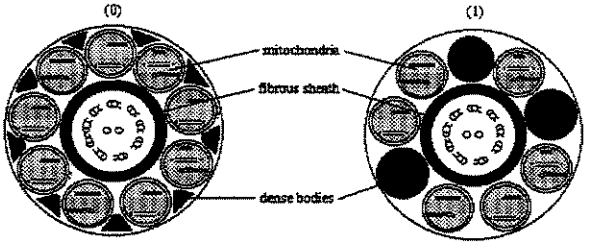

Fig. 12 : Character 152

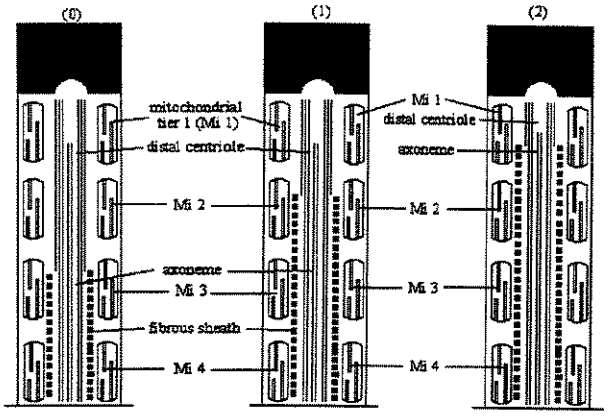

Fig. 13: Character 153

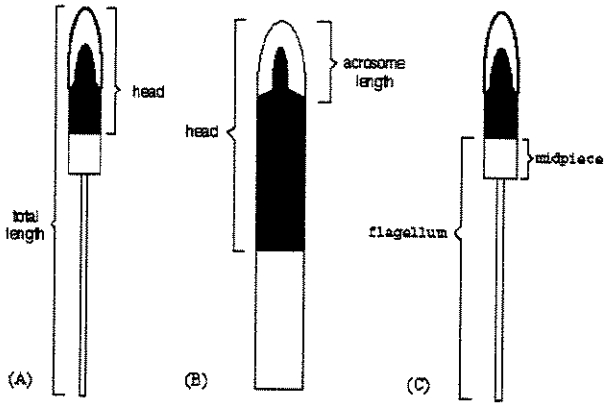

Fig. 14: Characters 156 and 157

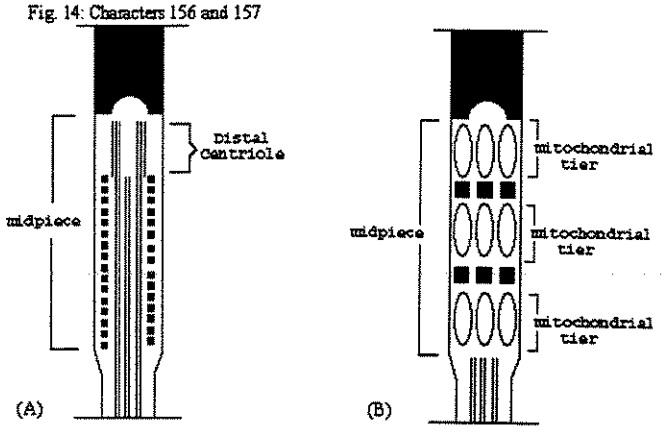

Fig. 15: Character 158 and 159

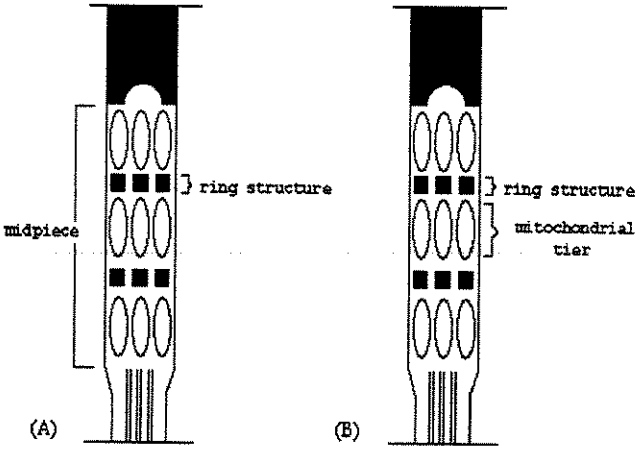

Fig. 16: Character 160 and 161

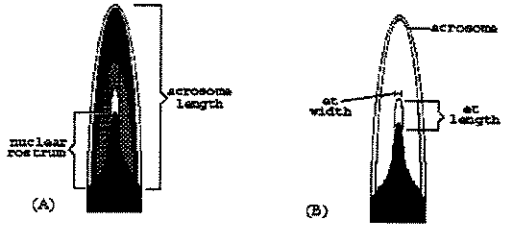

Fig. 17: Character 162 and 163

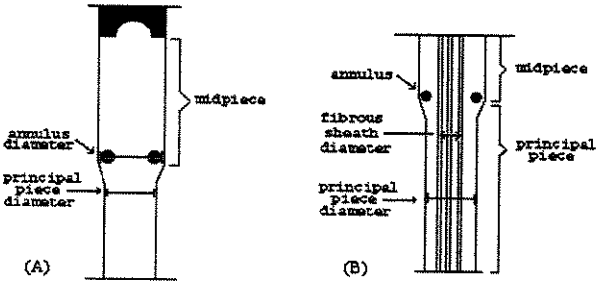

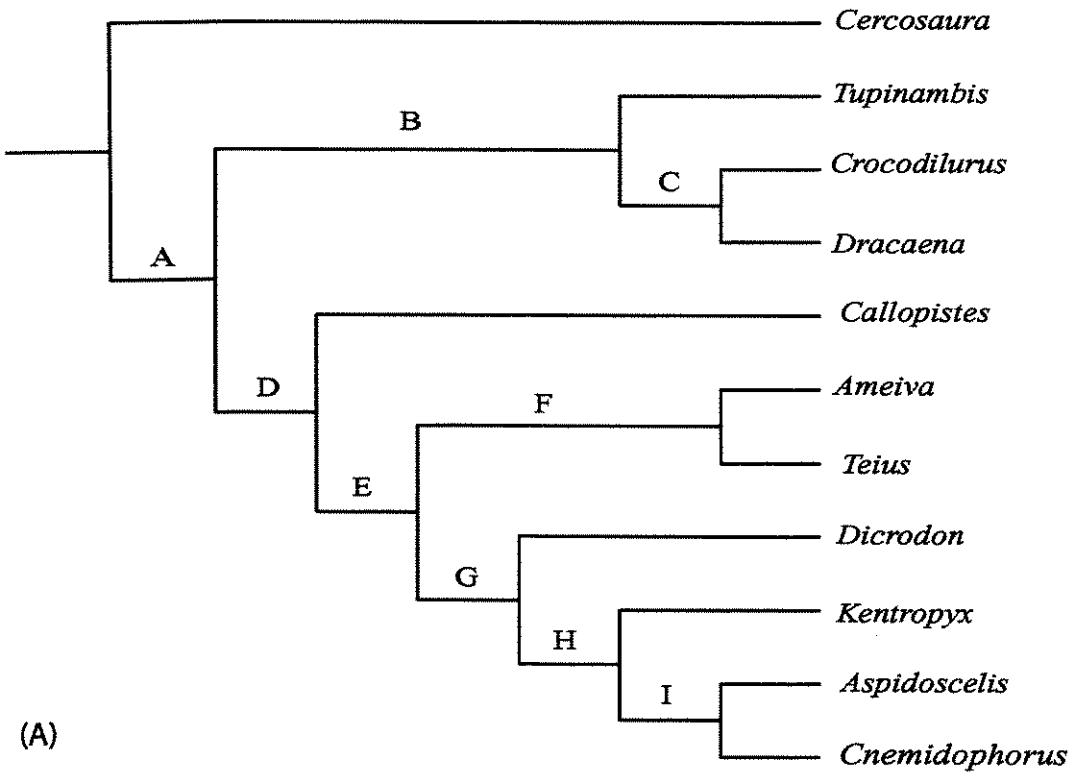

(A)

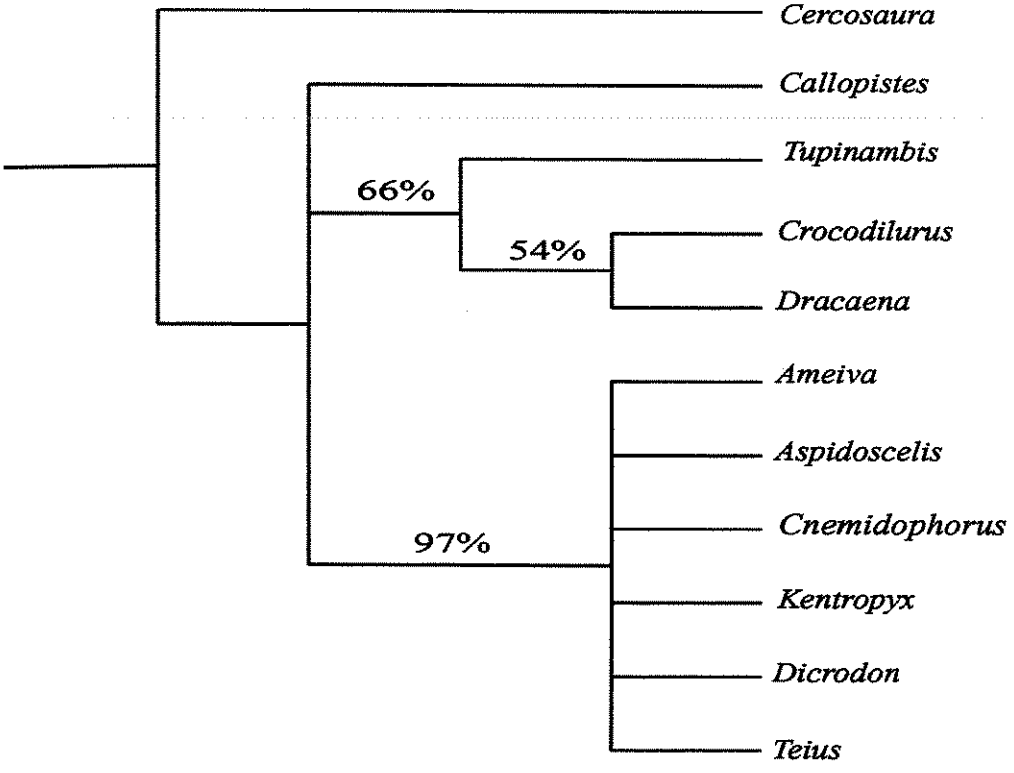

(B)

Fig. 18: Traditional morphological trees

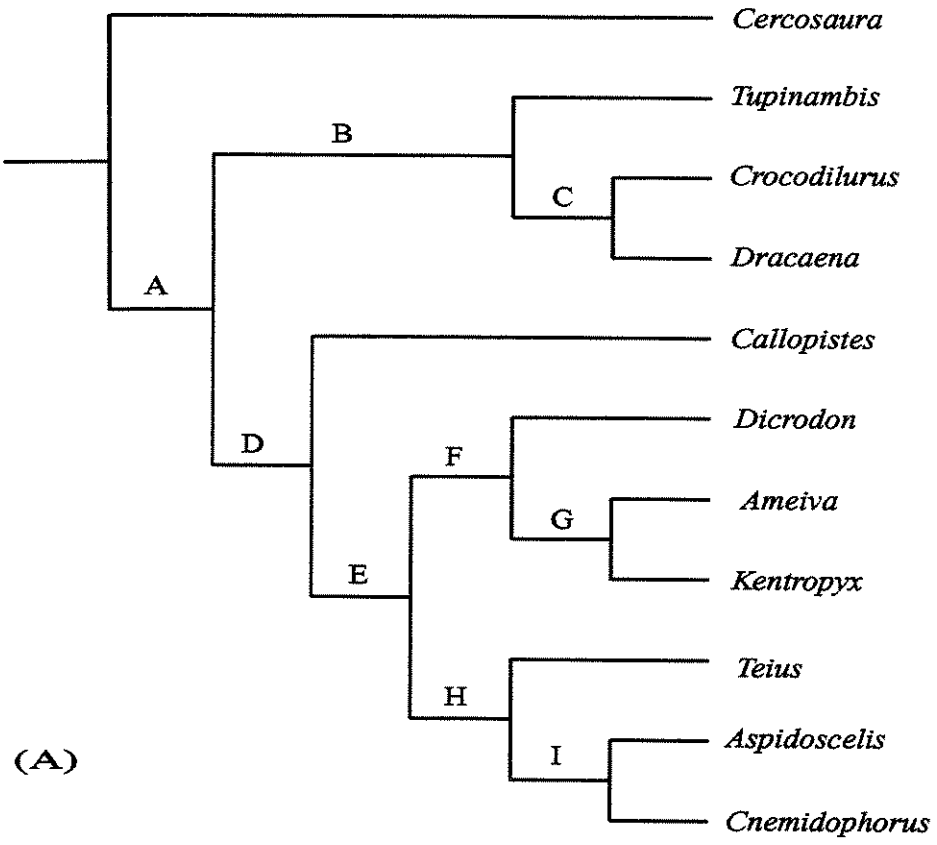

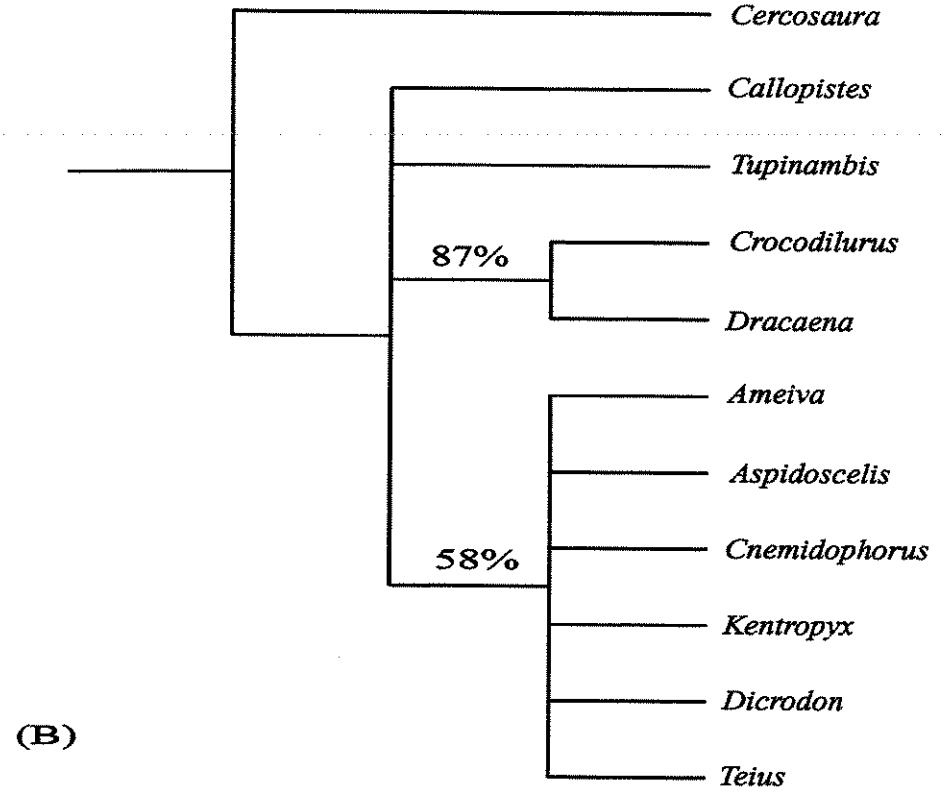

Fig. 19: Sperm ultrastructure trees

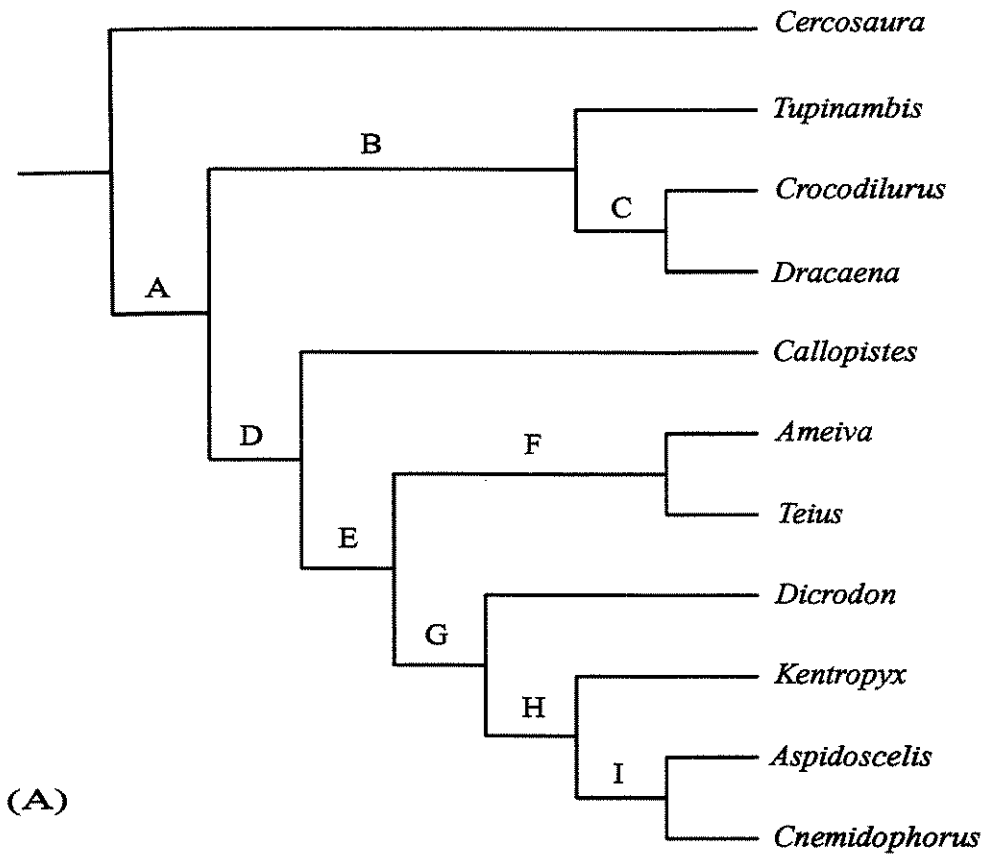

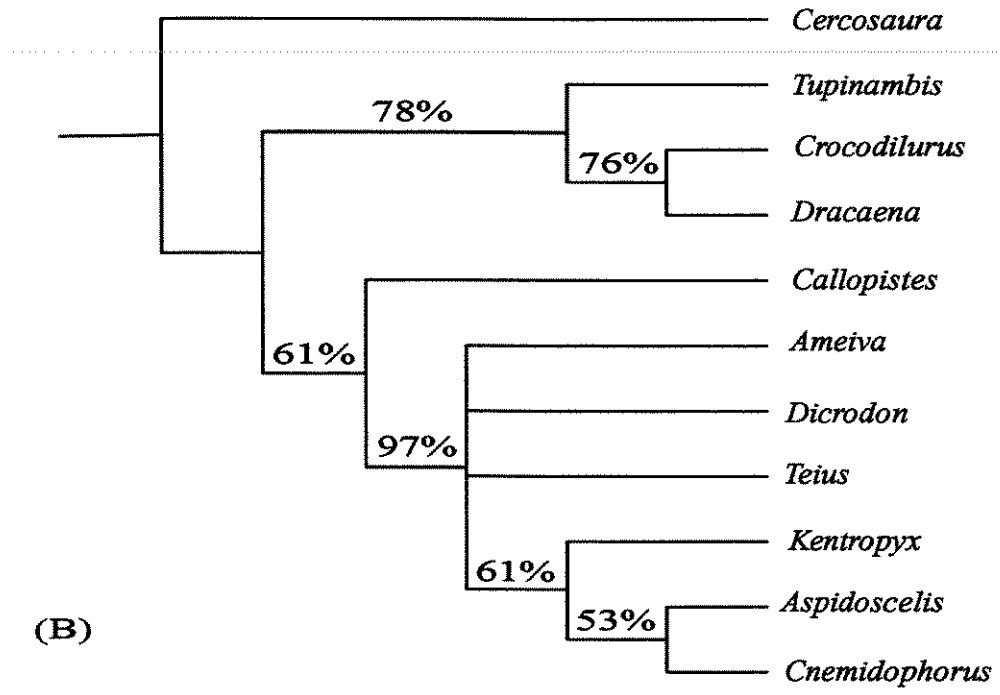

Fig. 20: Combined data trees

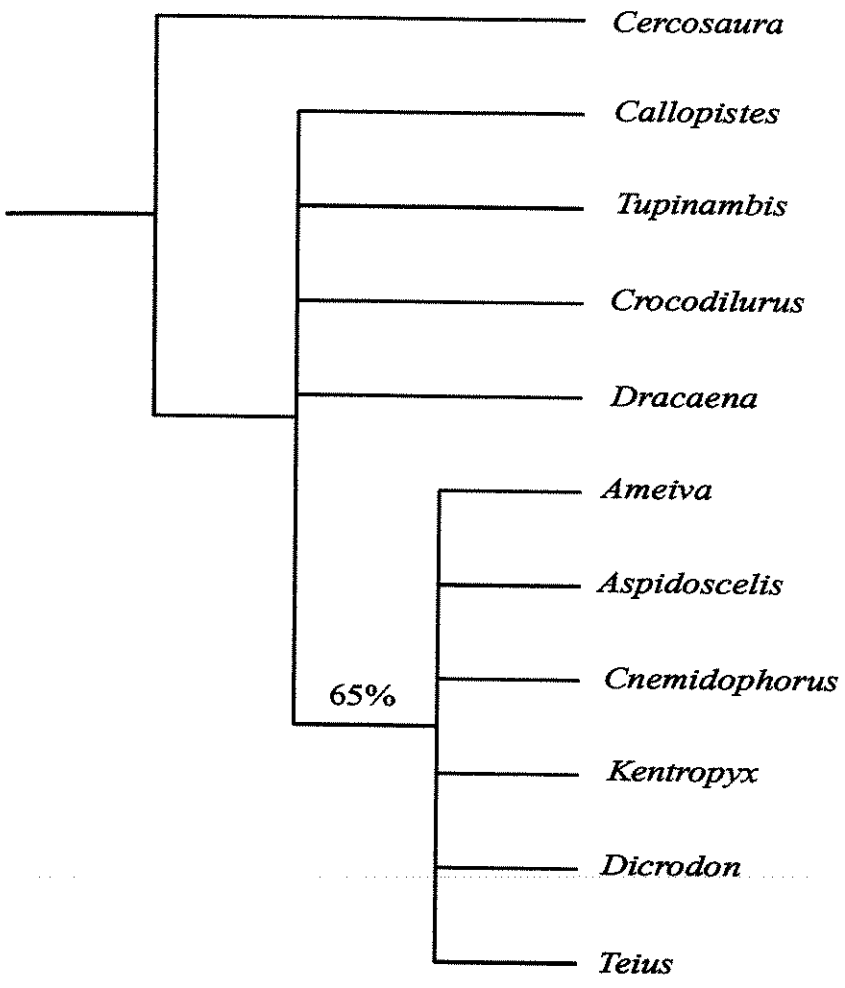

Fig. 21: Bootstrap 50% majority-rule consensus tree (undersampling traditional morphological data)

3 – CONCLUSÕES

3.1 – ESTUDO ULTRA-ESTRUTURAL DE ESPERMATOZÓIDE

Trabalho 1 – "Ultrastructure of spermatozoa of the lizard *Ameiva ameiva*, with considerations on polymorphism within the family teiidae (Squamata)"

O estudo comparativo da ultra-estrutura de espermatozóide de *Ameiva ameiva* e *Cnemidophorus sexlineatus* detectou altos níveis de variabilidade intergenéricos, indo de acordo com sugestões prévias feitas por Teixeira *et al.* (1999c, 1999d) de que a variabilidade intra-familial da ultra-estrutura de espermatozóide poderia ser maior do que era esperado.

Em estudos prévios, todas as famílias de Squamata, em que mais de uma espécie foi descrita Chamaeleonidae (Jamieson, 1995; Oliver *et al.*, 1996), Gekkonidae (Furieri, 1970; Phillips & Asa, 1993; Jamieson *et al.*, 1996), Lacertidae (Furieri, 1970; Butler & Gabri, 1984; Courtens & Depeiges, 1985), Phrynosomatidae (Scheltinga *et al.*, 2000), Polychrotidae (Furieri, 1974; Teixeira *et al.*, 1999a), Scincidae (Jamieson & Scheltinga, 1994; Jamieson, 1995; Jamieson *et al.*, 1996), e Tropiduridae (Furieri, 1974; Teixeira *et al.*, 1999d), mostraram características da ultra-estrutura de espermatozóide com altos níveis de variablilidade. Análises filogenéticas destas famílias, utilizando a ultra-estrutura de espermatozóide (Jamieson, 1995; Jamieson *et al.*, 1996; Teixeira *et al.*, 1999b, 1999c), produziram resultados insatisfatórios e incongruentes com filogenias baseadas em dados morfológicos tradicionais (Estes *et al.*, 1988; Lee, 1998; Caldwell, 1999). Estes resultados

podem ser causados pelos altos níveis de variabilidade na ultra-estrutura de espermatozóide e pelo fato dos táxons terminais serem família. Aparentemente, utilizando táxons de menores níveis taxonômicos, isto é, espécies ou gêneros como táxons terminais pode melhorar as estimativas das análises filogenéticas baseadas na ultra-estrutura de espermatozóide, podendo ser mais eficiente do que os métodos de codificação de caracteres polimórficos ou a exclusão destes caracteres (Wiens, 1998b). Desta forma, para a condução de análises no nível de família, seria de fundamental importância estudos adicionais que descrevessem a ultra-estrutura de espermatozóide do maior número possível de gêneros das famílias de Squamata. Descobrir o grau de variabilidade inter genérico pode melhorar as análises filogenéticas de Squamata no nível de família, assim como pode ajudar na determinação do melhor nível taxonômico para realizar análises filogenéticas utilizando a ultra-estrutura de espermatozóide.

Trabalho 2 – "Polymorphism in the sperm ultrastructure among four species of lizards in the genus *Tupinambis* (Squamata: Teiidae)"

Foi identificado variabilidade na ultra-estrutura de espermatozóide entre as espécies congenéricas de *Tupinambis duseni, T. merianae, T. quadrilineatus*, and *T. teguixin*, indicando que a variabilidade neste conjunto de dados também ocorre dentro de gêneros. As evidências indicam que a variabilidade na ultra-estrutura dessas espécies congenéricas está concentrada principalmente na região do complexo acrossomal (cabeça) e na peça intermediária (flagelo).

Em relação à causa da variabilidade na ultra-estrutura de espermatozóide pode-se inferir duas hipóteses: a variabilidade pode ser o produto de processos ao acaso, sem

nenhuma causa adaptativa relacionada à ecologia reprodutiva dos lagartos (Ridley, 1993) ou pode ser produto de processos evolutivos, em que o espermatozóide é adaptado ao modo de fertilização (Anderson & Personne, 1973). De acordo com Fitzgerald *et al.* (1993) e Herrera & Robinson (2000), os lagartos do gênero *Tupinambis* apresentam ecologias reprodutivas muito similares, o que leva a acreditar que a variabilidade na ultra-estrutura de espermatozóide entre as espécies de *Tupinambis* seja seletivamente neutra, não possuindo nenhuma base adaptativa.

A explicação das similaridades da ultra-estrutura de espermatozóide como produtos de herança comum (filogenia) ou de eventos evolutivos repetidos e independentes (convergências evolutivas), através do mapeamento dos caracteres em uma filogenia proposta para o gênero (Brooks & McLennan, 1991; Harvey & Pagel, 1991), revela que a ultra-estrutura de espermatozóide não é um bom indicador de filogenia para o grupo de *Tupinambis* estudados. A não identificação do mapeamento dos caracteres com a filogenia do grupo, indica que há uma forte influência de adaptação evolutiva nos caracteres (McCracken *et al.*, 1999; Wiens, 2000b), não tendo assim, as similaridades uma razão filogenética (Schwenk, 1993; Brown *et al.*, 2000). Isso mostra que as semelhanças nos caracteres da ultra-estrutura de espermatozóide não têm causas filogenéticas e sim adaptativas. No entanto, as semelhanças da ultra-estrutura (homoplasias) sendo convergências adaptativas, levam a diferenças na ecologia reprodutiva dos *Tupinambis*, o que não acontece. Desta forma, a variabilidade na ultra-estrutura não é um reflexo da história do grupo e nem consequência de adaptação, o que leva a concluir que a variabilidade é um produto de processos evolutivos ao acaso e seleção neutra.

Trabalho 3 – "A comparative ultrastructural study of spermatozoa of the teiid lizards, *Cnemidophorus gularis gularis*, *Cnemidophorus ocellifer* and *Kentropyx altamazonica* (Reptilia, Squamata, Teiidae)"

As comparações da ultra-estrutura de espermatozóide entre *Cnemidophorus ocellifer*, *Aspidoscelis gularis gularis*, *Kentropyx altamazonica* e *Ameiva ameiva*, sugerem que *Ameiva*, *Cnemidophorus* e *Aspidoscelis* são mais similares entre si do que com *Kentropyx altamazonica*. As análises estatísticas revelam diferenças significativas entre as dimensões dos espermatozóides de *Cnemidophorus*, *Aspidoceslis* e *Kentropyx*. Indicando variabilidade intergenérica na ultra-estrutura de espermatozóide.

Trabalho 4 – "Comparative study of sperm ultrastructure of five species of teiid lizards (Teiidae, Squamata), and *Cercosaura ocelata* (Gymnophthalmidae, Squamata)"

O estudo comparativo da ultra-estrutura de espermatozóide de espécies representantes de todos os gêneros da família Teiidae *Ameiva ameiva*, *Cnemidophorus ocellifer*, *Aspidoscelis gularis gularis*, *Kentropyx altamazonica*, *Tupinambis* teguixin, *Dracaena guianensis*, *Crocodilurus amazonicus*, *Callopistes flavipunctatus*, *Teius oculatus*, *Dicrodon guttulatum*, e do lagarto *Cercosaura ocellata*, representante da família Gymnophthalmidae, revela que a ultra-estrutura de espermatozóide dá suporte à existência das duas famílias de Teiioidea (Gymnophthalmidae e Teiidae), assim como das duas subfamílias de Teiidae (Teiinae e Tupinambinae). As análises estatísticas das 13 dimensões do espermatozóide mostram muitas diferenças significativas entre *Callopistes* e os gêneros pertencentes à subfamília Teiinae, distinguindo *Callopistes* dos gêneros de Teiinae. O

espermatozóide de *Crocodilurus* e *Dracaena* aparece similar em relação aos caracteres qualitativos e quantitativos, mostrando que de acordo com o espermatozóide, os dois gêneros são idênticos. Apesar da ultra-estrutura de espermatozóide de *Cnemidophorus* e *Aspidoscelis* ser similar, as análises estatísticas mostram diferenças significativas nas dimensões dos espermatozóide, distinguindo os dois gêneros. Esse resultado vai de acordo com as análises de Reeder et al (2002), em que *Cnemidophorus ocellifer* pertence ao grupo *leminiscatus* e ao gênero Cnemidophorus e *Aspidoscelis gularis gularis* ao grupo *Cnemidophorus* encontrado na América do Norte (*Aspidoscelis*).

Os resultados deste trabalho indicam altos níveis de variabilidade na ultra-estrutura de espermatozóide dos gêneros da família Teiidae.

Conclusão final sobre a ultra-estrutura de espermatozóide como um novo conjunto de dados

Os trabalhos indicam altos níveis de variabilidade intergenérica e intragenérica na ultra-estrutura de espermatozóide da família Teiidae. Apesar, dos caracteres ideais serem apenas aqueles que variam entre os táxons terminais e são fixos dentro deles (Thiele, 1993), é muito comum encontrar caracteres que variam nos táxons terminais (Poe & Wiens, 2000). Existem várias formas de lidar com esses caracteres variáveis: (1) utilizar o menor nível taxônomico, para que não haja variação, (2) excluir os caracteres variáveis, ou (3) utilizar diferentes tipos de métodos que lidam com a inclusão e codificação dos caracteres variáveis (Wiens & Servedio, 1997; Wiens, 1998b). Simulações e alguns dados empíricos (Wiens, 2000a) mostram que utilizar espécies como táxons terminais nas análises filogenéticas de

altos níveis taxonômicos (i.e. família), é mais eficiente na produção de resultados mais satisfatórios e de melhores estimativas sobre a filogenia do grupo do que excluir os caracteres variáveis ou utilizar os métodos de codificação para estes dados.

Enfim, analisar a ultra-estrutura de espermatozóide de um maior número possível de espécies de teiídeos e utilizar espécies como táxons terminais, podem tornar a ultra-estrutura de espermatozóide um bom conjunto de dados para as análises filogenéticas da família Teiidae.

3.2 – ANÁLISES FILOGENÉTICAS

Filogenias derivadas da ultra-estrutura de espermatozóide e dos dados morfológicos tradicionais

Ambas as topologias: (1) dividiram a família Teiidae nas duas subfamílias, Tupinambinae e Teiinae, encontradas nos estudos baseados em características externas (Vanzolini & Valencia, 1965), cromossomos (Gorman, 1970), dados osteológicos (Boulenger, 1885; Presch, 1974; Veronese & Krause, 1997), e dados miológicos (Rieppel, 1980), (2) colocaram *Callopistes* dentro da subfamília Teiinae, e (3) consideraram o par *Crocodilurus* and *Dracaena* bem aparentado.

No entanto, os conjuntos de dados produziram topologias com grau de suporte diferentes e algumas regiões de conflito dentro da subfamília Teiinae. A topologia derivada do conjunto de dados morfológicos tradicionais mostra (1) *Ameiva* e *Teius* bem aparentados, e (2) *Dicrodon* como grupo irmão de *Kentropyx* e do par *Aspidoscelis* – *Cnemidophorus*. Já, a topologia derivada da ultra-estrutura de espermatozóide mostra (1)

Ameiva e *Kentropyx* bem aparentados, (2) *Dicrodon* como grupo irmão de *Ameiva* e *Kentropyx*, e (3) Teius como grupo irmão do par *Aspidoscelis* – *Cnemidophorus*. Além disso, os clados da topologia de 50% da maioria do "Bootstrap", derivados da ultra-estrutura de espermatozóide, aparecem com pouco suporte. Os baixos valores do Bootstrap na topologia de espermatozóide podem ter duas razões possíveis: (1) altos níveis de homoplasia, que podem ter sido resultado de problemas na codificação, na plasticidade da ultra-estrutura de espermatozóide ou na evolução convergente, ou (2) o baixo número de caracteres utilizados, como já foi sugerido por Teixeira et al. (1999c). Comparações dos índices de consistência dos caracteres da ultra-estrutura de espermatozóide, mostram que os baixos valores do "Bootstrap" na topologia baseada nesses dados não são causados pelos caracteres homoplásicos, já que os caracteres da ultra-estrutura de espermatozóide e dos dados morfológicos tradicionais apresentam níveis homoplásicos semelhantes. O teste do efeito da subamostragem das análises baseadas nos dados morfológicos tradicionais nos valores do Bootstrap, indica que a redução do número de caracteres produz estimativas mal resolvidas e clados com pouco suporte do "Bootstrap".

Os resultados sugerem que a ultra-estrutura de espermatozóide é um bom indicador de filogenia, usando gêneros como táxons terminais por duas razões: (1) apresenta altos níveis de variabilidade intergenérico, ou seja, entre os táxons terminais, que de acordo com Thiele (1993) é o tipo de variabilidade ideal nos caracteres para ser utilizado nas análises, e (2) produz uma topologia com muitas áreas congruentes com a topologia derivada dos dados morfológicos tradicionais, apresentando poucas áreas de conflito com pouco suporte do "Boostrap". Desta forma, aumentar o número de caracteres da ultra-estrutura de

espermatozóide parece ser uma boa solução para o uso deste conjunto de dados não tradicionais nas análises filogenéticas no nível genérico.

Filogenia derivada dos conjuntos de dados combinados

De acordo com Teixeira et al (1999b), as incongruências entre as topologias derivadas dos dados morfológicos tradicionais e da ultra-estrutura de espermatozóide pode ter como causas as diferenças nas histórias evolutivas dos conjuntos de dados. No entanto, comparações das topologias produzidas mostram grandes áreas de congruência e pequenas incongruências com baixos valores de suporte do "Bootstrap". Esses resultados indicam que os conjuntos de dados morfológicos tradicionais e a ultra-estrutura de espermatozóide são conjuntos de dados dependentes e compatíveis como sugerido por Wiens (1998a).

Os dados combinados produzem uma filogenia semelhante a filogenia produzida pelos dados morfológicos tradicionais, com diferenças apenas no grau de suporte dos clados. O grau de suporte da topologia derivada dos dados combinados apresenta valores bem superiores aos encontrados nos clados produzidos pelos dados morfológicos tradicionais. Isso acontece devido ao aumento de caracteres nas análises combinadas, que produzem estimativas melhores que as análises derivadas de pequenos números de caracteres (Wiens, 1998a). Por esse motivo, as análises derivadas dos conjuntos de dados combinados contribuem para o aperfeiçoamento das relações filogenéticas da família Teiidae, refletindo melhores estimativas sobre a história evolutiva do grupo. De acordo com os resultados, a divisão da família em duas subfamílias Teiinae e Tupinambinae, e a relação entre *Crocodilurus* e *Dracaena* ficaram bem resolvidas e bem suportadas. No entanto, estudos adicionais, incluindo um maior número de espécies para cada gênero são

necessários para melhorar a resolução das relações entre os gêneros da subfamília Teiinae, que continuam mal resolvidas.

Comparações taxonômicos com estudos prévios

A divisão da família Teiidae em duas subfamílias, Teiinae e Tupinambinae, formalmente proposta por Presch (1974) foi corroborada pela filogenia baseada nos conjuntos de dados tradicionais (incluindo hemipênis, língua e escamas não utilizados em estudos prévios). As duas subfamílias foram também encontradas em estudos feitos por Vanzolini & Valencia (1965), Gorman (1970), Rieppel (1980), e Veronese & Valencia (1997).

Na filogenia derivada da combinação de conjuntos de dados morfológicos tradicionais e ultra-estrutura de espermatozóide, *Callopistes* pertence à subfamília Teiinae ao invés de Tupinambinae como sugerido pelas hipótese prévias. Dentro da subfamília Teiinae *Ameiva* aparece mais aparentado com *Teius, Cnemidophorus* mais aparentado com *Aspidoscelis, Kentropyx* como grupo irmão do par *Cnemidophorus – Aspidoscelis, Dicrodon* como grupo irmão de *Kentropyx, Cnemidophorus*, e *Aspidoscelis*, e *Callopistes* como grupo irmão de todos os outros gêneros de Teiinae. Dentro da subfamília Tupinambinae, a filogenia derivada de conjuntos de dados combinados sugeri *Dracaena – Crocodilurus* bem aparentados.

Análises baseadas em DNA mitocôndrial, morfologia e aloenzimas suportam a monofilia dos cnemidophirines, Ameiva, *Cnemidophorus*, e *Kentropyx*, no qual estão relacionados à linhagem mais basal de Teiinae, *Teius* and *Dicrodon* (Reeder *et al.*, 2002). De acordo com estudos baseados em características externas (Vanzolini & Valencia, 1965),

dentro de Teiinae, *Ameiva* é mais aparentado com *Cnemidophorus*, *Teius* mais aparentado com *Dicrodon*, e *Kentropyx* aparece como o gênero mais distinto da subfamília Teiinae, e *Dracaena* é mais aparentado com *Tupinambis* dentro de Tupinambinae. Estudos baseados em dados osteológicos, Presch (1974) considerou *Cnemidophorus* como sinônimo de *Ameiva*, e sugeriu *Ameiva/Cnemidophorus* mais aparentados com *Kentropyx*. Para Vanzolini & Valencia (1965) *Crocodilurus* é mais aparentado com *Callopistes* do que com o par *Tupinambis – Dracaena* como sugerido por Presch (1974). Análises baseadas em dados miológicos (Moro & Abdala, 2000) indicam que *Ameiva* é mais aparentado com *Teius* do que com *Cnemidophorus*, suportando a filogenia baseada na ultra-estrutura de espermatozóide e nos dados morfológicos combinados, *Callopistes* aparece mais aparentado com *Crocodilurus*, sendo congruente com os estudos miológicos de Rieppel (1980). Apesar da filogenia derivada dos conjuntos de dados morfológicos tradicionais e ultra-estruturais de espermatozóide ter apresentado incongruências com as hipótese prévias, a filogenia derivada dos dados combinados pode ser considerada a melhor estimativa das relações filogenéticas da família Teiidae. Isso deve-se por estar baseada em caracteres utilizados nas hipóteses prévias, combinados com caracteres morfológicos tradicionais novos não utilizados previamente (escamas, língua e hemipênis) e o novo conjunto de dados morfológicos não tradicionais (a ultra-estrutura de espermatozóide), aumentando o número de caracteres nas análises e consequentemente melhorando as estimativas das relações filogenéticas entre os gêneros da família Teiidae.

REFERÊNCIAS BIBLIOGRÁFICAS

ANDERSON, W. A.; PERSONNE, P. The form and function of spermatozoa: a comparative view. In: AFZELIUS, B. A. The Functional Anatomy of the Spermatozoon. Oxford: Pergamon Press, 1973. p. 3-14.

ARCHIE, J. W. Methods for coding variable morphological features for numeric taxonomic analysis. Syst Zool, v. 34, p. 326-345, 1985.

AVILA-PIRES, T. C. S. National Natuurhistorisch Museum. In:Lizards of Brazilian Amazonia. Alblasserdam:, 1995. p. 514-516.

BOULENGER, C. A. Catalogue of the Lizards in the British Museum (Natural History). London: British Museum of Natural History, 1885.

BROOKS, D. R.; MCLENNAN, D. A. Phylogeny, Ecology, and Behavior, a Research Program in Comparative Biology. Chicago: The University of Chicago Press, 1991. 434 p.

BROWN, B.; EMBERSON, R. M.;PATERSON, A. M. Morphological character evolution in hepialid moths (Lepidoptera: Hepialidae) from New Zealand. Biol J Linn Soc, v. 69, p. 383-397, 2000.

BULL, J. J.; HUELSENBECK, J. P.; CUNNINGHAM, C. W.; SWOFFORD, D. L.;WADDELL, P. J. Partitioning and combining data in phylogenetic analysis. Syst Biol, v. 42, p. 384-397, 1993.

BUTLER, R. D.; GABRI, M. S. Structure and development of the sperm head in the lizard *Podarcis* (=*Lacerta*) *taurica*. J Ultrastr Res, v. 88, p. 261-274, 1984.

CALDWELL, M. W. Squamate phylogeny and the relationships of snakes and mosasauroids. Zool J Linn Soc, v. 125, p. 115-147, 1999.

CAMPBELL, C. S. Phylogenetic reconstructions and two new varieties in the *Andropogon virginicus* complex (Poaceae: Andropogoneae). Syst Bot, v. 11, p. 280-291, 1986.

CARROL, R. L. Vertebrate Paleontology and Evolution. New York: W. H. Freeman and Company, 1988. 698 p.

CEI, J. M.; SCOLARO, J. A. Geographic distribution: *Tupinambis rufescens*. Herpetol Rev, v. 13, p. 26, 1982.

CHIPPINDALE, P. T.; WIENS, J. J. Weighting, partitioning, and combining characters in phylogenetic analysis. Sist Biol, v. 43, p. 278-287, 1994.

COLLESS, D. H. Congruence between morphological and allozyme data for Menidia species: a reappraisal. Syst Zool, v. 29, p. 288-299, 1980.

COURTENS, J. L.; DEPEIGES, A. Spermiogenesis of *Lacerta vivipara*. J Ultrastr Res, v. 90, p. 203-220, 1985.

DE QUEIROZ, A. For consensus (sometimes). Syst Biol, v. 42, p. 368-372, 1993.

DE QUEIROZ, A.; DONOGHUE, M. J.;KIM, J. Separate versus combined analysis of phylogenetic evidence. Annu Rev Ecol Syst, v. 26, p. 657-681, 1995.

DOYLE, J. J. Gene trees and species trees: Molecular systematics as one character taxonomy. Syst Bot, v. 17, p. 144-163, 1992.

ESTES, R.; DE QUEIROZ, K.;GAUTHIER, J. Phylogenetic relationships within Squamata. In: ESTES, R.; PREGILL, G. Phylogenetic Relationships of the Lizard Families Essays Commemorating Charles L Camp. Stanford, California: Stanford University Press, 1988. p. 119-281.

ESTES, R.; PREGILL, G. 1988. Phylogenetic Relationships of the Lizard Families. Essays Commemorating Charles L. Camp. Stanford, California, Stanford University Press. 631 p.

FITZGERALD, L. A.; CRUZ, F. B.;PEROTTI, G. The reproductive cycle and the size at maturity of *Tupinambis rufescens* (Sauria:Teiidae) in the dry Chaco of Argentina. J Herpetol, v. 27, p. 70-78, 1993.

FRANZÉN, A. Phylogenetic aspects of the morphology of spermatozoa and spermiogenesis. In: BACCETTI, B. Comparative Spermatology. New York: Academic Press, 1970. p. 29-46.

FURIERI, P. Sperm morphology of some reptiles: Squamata and Chelonia. In: BACCETTI, B. Comparative Spermatology. Rome, Italy: Accademia Nazionale dei Lincei, 1970. p. 115-131.

FURIERI, P. Spermi e spermatogenesi in alcuni iguanidi argentini. Riv Biol, v. 67, p. 233-279, 1974.

GALLAGHER JR., D. S.; DIXON, J. R.;SCHMIDLY, D. J. Geographic variation in the *Kentropyx calcarata* species group (Sauria: Teiidae): a possible example of morphological character displacement. J Herpetol, v. 20, p. 179-189, 1986.

GORMAN, G. C. Chromosomes and the systematics of the family Teiidae. Copeia, v. 1970, p. 230-245, 1970.

HARVEY, P. H.; PAGEL, M. D. The Comparative Method in Evolutionary Biology. New York: Oxford Univ. Press, 1991. 239 p.

HERRERA, E. A.; ROBINSON, M. D. Reproductive and fat body cycles of the tegu lizards, *Tupinambis teguixin*, in the llanos of Venezuela. J Herpetol, v. 34, p. 598-601, 2000.

HUELSENBECK, J. P.; BULL, J. J.;CUNNINGHAM, C. W. Combining data in phylogenetic analysis. Trends Ecol Evol, v. 11, p. 152-158, 1996.

HUEY, R. B.; BENNETT, A. F. Phylogenetic studies of co-adaptation: preferred temperatures versus optimal performance temperatures of lizards. Evolution, v. 41, p. 1098-1115, 1987.

JAMIESON, B. G. M. The ultrastructure of spermatozoa of the Squamata (Reptilia) with phylogenetic considerations. In: JAMIESON, B. G. M.; AUSIO, J.; JUSTINE, J. Advances in Spermatozoal Phylogeny and Taxonomy. Paris, France: Muséum National d'Histoire Naturelle, 1995. p. 359-383.

JAMIESON, B. G. M.; OLIVER, S. C.;SCHELTINGA, D. M. The ultrastructure of spermatozoa of Squamata. I. Scincidae, Gekkonidae and Pygopodidae (Reptilia). Acta Zool (Stockholm), v. 77, p. 85-100, 1996.

JAMIESON, B. G. M.; SCHELTINGA, D. M. The ultrastructure of spermatozoa of the Australian skinks, *Ctenotus taeniolatus*, *Carlia pectoralis* and *Tiliqua scincoides scincoides* (Scincidae, Reptilia). Mem Queensland Mus, v. 37, p. 181-193, 1994.

KITCHING, I. J.; FOREY, P. L.; HUMPHRIES, C. J.;WILLIAMS, D. M. Cladistics. The Theory and Practice of Parsimony Analysis. Oxford: Oxford University Press, 1998. 228 p.

KLUGE, A. G.; WOLF, A. J. Cladistics: What´s in a word? Cladistics, v. 9, p. 183-199, 1993.

LEE, M. S. Y. Convergent evolution and character correlation in burrowing reptiles: Towards a resolution of squamate relationships. Biol J Linn Soc, v. 65, p. 369-453, 1998.

MACLEAN, W. P. Feeding and locomotor mechanisms of teiid lizards: functional morphology and evolution. Pap Avul Zool, S Paulo, v. 27, p. 179-213, 1974.

MADDISON, W. P.; MADDISON, D. R. MacClade: Analysis of Phylogeny and Character Evolution. Sunderland, Massachusetts, Sinauer Associates, Inc. (1992)

MAGNUSSON, W. E. Economics, developing countries, and the captive propagation of crocodilians. Wildl Soc Bull, v. 12, p. 194-197, 1984.

MASSARY, J.; HOOGMOED, M. S. *Crocodilurus amazonicus* Spix, 1825: the valid name for *Crocodilurus lacertinus* auctorum (nec Daudin, 1802) (Squamata: Teiidae). J Herpetol, v. 35, p. 353-357, 2001.

MCCRACKEN, K. G.; HARSHMAN, J.; MCCLELLAN, D. A.;AFTON, A. D. Data set incongruence and correlated character evolution: an example of functional convergence in the hind-limbs of stifftail diving ducks. Syst Biol, v. 48, p. 683-714, 1999.

MICKEVICH, M. F.; JOHNSON, M. S. Congruence between morphological and allozyme data in evolutionary inference and character evolution. Syst Zool, v. 25, p. 260-270, 1976.

MIYAMOTO, M. M.; FITCH, W. M. Testing species phylogenies and phylogenetic methods with congruence. Syst Biol, v. 44, p. 64-76, 1995.

MORO, S.; ABDALA, V. Cladistic analysis of Teiidae (Squamata) based on myological characters. Rus J Herpetol, v. 7, p. 87-102, 2000.

OLIVER, S. C.; JAMIESON, B. G. M.;SCHELTINGA, D. M. The ultrastructure of spermatozoa of Squamata. II. Agamidae, Varanidae, Colubridae, Elapidae, and Boidae (Reptilia). Herpetologica, v. 52, p. 216-241, 1996.

PETERS, J. A.; OREJAS-MIRANDA, B. Catalogue of the Neotropical Squamata. Part II, Lizards and Amphisbaenians (Revised ed.). Washington, D.C.: Smithsonian Institution Press, 1986. 293 p.

PHILLIPS, D. M.; ASA, C. S. Strategies for formation of the midpiece. In: BACCETTI, B. Comparative Spermatology 20 Years After. New York: Raven Press, 1993. p. 997-1000.

PIMENTEL, R. A.; RIGGINS, R. The nature of cladistic data. Cladistics, v. 3, p. 275-289, 1987.

POE, S.; WIENS, J. J. Character selection and the methodology of morphological phylogenetics. In: WIENS, J. J. Phylogenetic analysis of morphological data. Washigton D. C.: Smithsonian Institution Press, 2000. p. 20-36.

POUGH, F. H.; HEISER, J. B.;MCFARLAND, W. N. A Vida dos Vertebrados. São Paulo, SP: Atheneu Editora São Paulo Ltda., 1993.

PRESCH, W. F., JR. The evolution of macroteiid lizards: an osteological interpretation. Los Angeles, CA, 1970.Ph.D. - University of Southern California.

PRESCH, W. F., JR. Evolutionary relationships and biogeography of the macroteiid lizards (Family Teiidae, Subfamily Teiinae). Bull So Calif Acad Sci, v. 73, p. 23-32, 1974.

RAND, A. S.; HUMPHREY, S. S. Interspecific competition in the tropical rain forest: ecological distribution among lizards at Belém, Pará. Proceedings of the United States Natural History Museum, v. 125, p. 1-17, 1968.

REEDER, T. W.; COLE, C. J.;DESSAUER, H. C. Phylogenetic relationships of whiptail lizards of the genus *Cnemidophorus* (Squamata: Teiidae): a test of monophyly, reevaluation of karyotypic evolution, and review of hybrid origins. American Museum Novitates, v. 3365, p. 1-61, 2002.

RIDLEY, M. Evolution. Boston: Blackwell Scientific Publications, 1993. 670 p.

RIEPPEL, O. The trigeminal jaw adductor musculature of *Tupinambis*, with comments on the phylogenetic relationships of the Teiidae (Reptilia, Lacertilia). Zool J Linn Soc, v. 69, p. 1-29, 1980.

RUIBAL, R. Revisionary studies of some South American Teiidae. Bull Mus Comp Zool, v. 106, p. 477-529, 1952.

RUSSEL, A. P. Limb muscles in relation to lizard systematics: a reappraisal. In: ESTES, R.; PREGILL, G. Phylogenetic Relationships of the Lizard Families Essays Commemorating Charles L Camp. Stanford, California, USA: Stanford University Press, 1988. p. 493-568.

SCHELTINGA, D. M.; JAMEISON, B. G. M.; TRAUTH, S. E.;MCALLISTER, C. T. Morphology of the spermatozoa of the iguanian lizards *Uta stansburiana* and *Urosaurus ornatus* (Squamata, Phrynosomatidae). J Submicr Cytol Pathol, v. 32, p. 261-271, 2000.

SCHWENK, K. Comparative morphology of the lepidosaur tongue and its relevance to squamate phylogeny. In: ESTES, R.; PREGILL, G. Phylogenetic Relationships of the Lizard Families Essays Commemorating Charles L Camp. Stanford, California: Stanford University Press, 1988. p. 569-598.

SCHWENK, K. The evolution of chemoreception in squamate reptiles: A phylogenetic approach. Brain Beh Evol, v. 41, p. 124-137., 1993.

SPIX, J. B. V. Animalia nova sive species novae Lacertarum, quas in intinere per brasilian annis MDCCCXVII-MDCCCXX jussu et auspiciis Maximiliani Josephi I. Bavariae regis suscepto collegit et descripsit Dr. J. B. de Spix, 1825.

SWOFFORD, D. L.; BERLOCHER, S. H. Inferring evolutionary trees from gene frequency data under the principle of maximum parsimony. Syst Zool, v. 36, p. 293-325, 1987.

SYSTEMATICS AGENDA 2000. Charting the Biosphere - Technical Report. American Society of Plant Taxonomists, Society of Systematic Biologists, Willi Hennig Society, and Association of Systematics Collections, 1994.

TEIXEIRA, R. D.; COLLI, G. R.;BÁO, S. N. The ultrastructure of spermatozoa of the lizard *Polychrus acutirostris* (Squamata, Polychrotidae). J Submicr Cytol Pathol, v. 31, p. 387-395, 1999a.

TEIXEIRA, R. D.; COLLI, G. R.;BÁO, S. N. The ultrastructure of the spermatozoa of the lizard *Micrablepharus maximiliani* (Squamata, Gymnophthalmidae), with considerations on the use of sperm ultrastructure characters in phylogenetic reconstruction. Acta Zool (Stockholm), v. 80, p. 47-59, 1999b.

TEIXEIRA, R. D.; COLLI, G. R.;BÁO, S. N. The ultrastructure of the spermatozoa of the worm-lizard *Amphisbaena alba* (Squamata, Amphisbaenidae), and the phylogenetic relationships of amphisbaenians. Can J Zool, v. 77, p. 1254-1264, 1999c.

TEIXEIRA, R. D.; VIEIRA, G. H. C.; COLLI, G. R.;BÁO, S. N. Ultrastructural study of spermatozoa of the neotropical lizards, *Tropidurus semitaeniatus* and *Tropidurus torquatus* (Squamata, Tropiduridae). Tissue & Cell, v. 31, p. 308-317, 1999d.

THIELE, K. The holy grail of the perfect character: the cladistic treatment of morphometric data. Cladistics, v. 9, p. 275-304, 1993.

THORPE, R. S. Coding morphometric characters for constructing distance Wagner networks. Evolution, v. 38, p. 244-355, 1984.

VANZOLINI, P. E. Notas bionômicas sobre *Dracaena guianensis* no Pará (Sauria:Teiidae). Pap Avul Dep Zool Secr Agric, S Paulo, v. 14, p. 237-241, 1961.

VANZOLINI, P. E.; VALENCIA, J. The genus *Dracaena*, with a brief consideration of macroteiid relationships (Sauria, Teiidae). Arq Zool, S Paulo, v. 13, p. 7-46, 1965.

VERONESE, L. B.; KRAUSE, L. Esqueleto pré-sacral e sacral dos lagartos teiídeos (Squamata, Teiidae). Revta bras Zool, v. 14, p. 15-34, 1997.

WIENS, J. J. Combining data sets with different phylogenetic histories. Syst Biol, v. 47, p. 568-581, 1998a.

WIENS, J. J. Testing phylogenetic methods with tree congruence: Phylogenetic analysis of polymorphic morphological characters in phrynosomatid lizards. Syst Biol, v. 47, p. 427-444., 1998b.

WIENS, J. J. Coding morphological variation within species and higher taxa for phylogenetic analysis. In: WIENS, J. J. Phylogenetic anaçysis of morphological data. Washington D.C.: Smithsonian Institution Press, 2000a. p. 115-145.

WIENS, J. J. Reconstructing phylogenies from allozyme data: testing method performance with congruence. Biol J Linn Soc, v. 70, p. 613-632, 2000b.

WIENS, J. J. Character analysis in morphological phylogenetics: problems and solutions. Syst Biol, v. 50, p. 689-699, 2001.

WIENS, J. J.; SERVEDIO, M. R. Accuracy of phylogenetic analysis including and excluding polymorphic characters. Syst Biol, v. 46, p. 332-345., 1997.

WRIGHT, J. W. Evolution of the lizards of the genus *Cnemidophorus*. In: WRIGHT, J. W.; VITT, L. J. Biology of Whiptail Lizards (Genus *Cnemidophorus*). Norman, Oklahoma, U.S.A.: The Oklahoma Museum of Natural History, 1993. p. 27-81.

ZELDITCH, M. L.; SWIDERSKI, D. L.;FINK, W. L. Discovery of phylogenetic characters in morphometric data. In: WIENS, J. J. Phylogenetic anaçysis of morphological data. Washington D.C.: Smithsonian Institution Press, 2000. p. 37-83.

ZUG, G. R.; VITT, L. J.; CALDWELL, J. P. Herpetology. An Introductory Biology of Amphibians and Reptiles (2nd ed.). San Diego, CA: Academic Press, 2001. 630 p.